



HAL
open science

Commande robuste et calibrage des systèmes de contrôle actif de vibrations

Tudor-Bogdan Airimitoiaie

► **To cite this version:**

Tudor-Bogdan Airimitoiaie. Commande robuste et calibrage des systèmes de contrôle actif de vibrations. Autre. Université de Grenoble; UNIVERSITE POLYTECHNIQUE DE BUCAREST, 2012. Français. NNT : 2012GRENT015 . tel-00767979

HAL Id: tel-00767979

<https://theses.hal.science/tel-00767979v1>

Submitted on 20 Dec 2012

HAL is a multi-disciplinary open access archive for the deposit and dissemination of scientific research documents, whether they are published or not. The documents may come from teaching and research institutions in France or abroad, or from public or private research centers.

L'archive ouverte pluridisciplinaire **HAL**, est destinée au dépôt et à la diffusion de documents scientifiques de niveau recherche, publiés ou non, émanant des établissements d'enseignement et de recherche français ou étrangers, des laboratoires publics ou privés.



THÈSE

Pour obtenir le grade de

DOCTEUR DE L'UNIVERSITÉ DE GRENOBLE

Spécialité : **Automatique-Productique**

Arrêté ministériel : 7 août 2006

Et de

**DOCTEUR DE L'UNIVERSITÉ "POLITEHNICA"
DE BUCAREST, ROUMANIE**

Spécialité : **Ingénierie des Systèmes**

Présentée par

Tudor-Bogdan AIRIMIȚOAI

Thèse dirigée par **Luc DUGARD**

codirigée par **Ioan Doré LANDAU**

et coencadrée par **Dumitru POPESCU**

préparée au sein du **Laboratoire GIPSA-Lab**

dans l'**École Doctorale Electronique, Electrotechnique, Automatique
et Traitement du Signal**

et de la **Faculté d'Automatique et Ordinateurs**

Commande robuste et calibrage des systèmes de contrôle actif de vibra- tions

Thèse soutenue publiquement le **28 juin 2012**,
devant le jury composé de :

M. Kouider Nacer M'SIRDI

Professeur, Aix-Marseille Université, France, Président

M. Raymond Arnoud DE CALLAFON

Professeur, Department of Mechanical and Aerospace Engineering, University of California, San Diego, Etats-Unis, Rapporteur

M. Alireza KARIMI

Maître d'enseignement et de recherche, EPFL, Lausanne, Suisse, Rapporteur

M. Dan ȘTEFĂNOIU

Professeur, Université "Politehnica" de Bucarest, Roumanie, Examineur

M. Luc DUGARD

Directeur de Recherche CNRS, Grenoble, France, Directeur de thèse

M. Ioan Doré LANDAU

Directeur de Recherche Emeritus CNRS, Grenoble, France, Co-Directeur de thèse

M. Dumitru POPESCU

Professeur, Université "Politehnica" de Bucarest, Roumanie, Co-Encadrant de thèse



To my parents and Valentina

ACKNOWLEDGMENTS

The work presented in this Ph.D. thesis has been done in the Control Systems Department of GIPSA-Lab, University of Grenoble, France, with the affiliation of the research team SLR (Systèmes Linéaires et Robustesse) and in the Faculty of Automatic Control and Computers, University “Politehnica” of Bucharest, Romania.

First of all, I would like to express my sincere gratitude to my Ph.D. advisors, M. Ioan Doré Landau, M. Luc Dugard, from the University of Grenoble, and M. Dumitru Popescu, from the University “Politehnica” of Bucharest, for their constant support and help during my years of study. I would also like to extend my thanks to M. Ioan Doré Landau, my main Ph.D. advisor, for having shared his expertise and having constantly encouraged me to pursue my goals in becoming a research scientist.

I would like to express my thanks to M. Kouider Nacer M’Sirdi, president of the examination committee, and M. Dan Ștefănoiu, member of the examination committee, for having accepted my invitation and having made the effort to come to Grenoble the day of my defence and also for their words of encouragement. None the less, I would like to express my gratitude to M. Raymond Arnoud de Callafon and M. Alireza Karimi for having accepted to review my manuscript and having made the effort of writing their conclusions with regard to my research work. I consider their remarks and suggestions as being very significant and helpful for my future research activities.

I express my gratitude also to M. Gabriel Buche and the entire technical team at GIPSA-Lab; their help and expertise in the development and maintenance of the test benches on Active Vibration Control have been of great importance in obtaining the results presented in this manuscript.

I would like to thank also Mme Alina Voda for her support and the trust that she had in me, during the last year of my thesis, when she allowed me to be a Teaching Assistant at the University Joseph Fourier of Grenoble. Also, I express my thanks to the teaching staff at the Polytechnic Institute of Grenoble for accepting me as part of their team.

My thanks also to M. Mathieu Noé, Engineer Specialist at Paulstra-Vibrachoc, for having accepted to collaborate on an Active Vibration Control project and share his knowledge with me.

I would like to express my thanks to B. Ciubotaru, V. Tanasă, A. Castellanos, M. Alma, I. Ahmad and all my friends in Bucharest and Grenoble for their advices and support.

Last but not least, I want to express my profound gratitude to my parents and to my dear Valentina for having always stood by my side and encouraged me even in the most difficult times.

Tudor-Bogdan Airimițoiaie

CONTENTS

Contents	9
List of figures	13
List of tables	15
Glossary	17
List of Publications	19
1 Introduction et Résumé Détaillé	21
1.1 Motivation	21
1.2 Description du Problème	22
1.2.1 Configuration du système de contrôle	23
1.2.2 Le problème de contrôle par action anticipatrice « feedforward » .	24
1.2.3 Le problème de contrôle par contre-réaction « feedback »	26
1.3 Revue de la Littérature	26
1.3.1 Méthodes de commande par action anticipatrice « feedforward » .	26
1.3.2 Méthodes de commande par contre-réaction « feedback » pour le rejet de perturbations bande étroite	30
1.4 Contributions	31
1.5 Plan du Manuscrit de Thèse	32
1.5.1 Description du système	32
1.5.2 Méthodes de compensation des vibrations par des structures hybrides	34
1.5.3 Méthodes de contrôle « feedforward » en utilisant la paramétrisa- tion de Youla-Kučera	38
1.5.4 Méthodes de contrôle par contre-réaction adaptatif	40
2 Introduction (english)	45
2.1 Motivation	45
2.2 Problem Description	46
2.2.1 Control system configurations	47
2.2.2 Feedforward control problem	48
2.2.3 Feedback regulation problem	49
2.3 Literature Overview	49
2.3.1 Feedforward control of vibrations	49
2.3.2 Feedback rejection of multiple narrow band disturbances	53
2.4 Contributions	54
2.5 Dissertation Outline	55

I	Adaptive Feedforward Disturbance Rejection	57
3	An AVC System Using an Inertial Actuator	59
3.1	System Description	59
3.2	Basic Equations and Notations	62
3.3	System Identification	65
3.4	Concluding Remarks	66
4	Adaptation Algorithms for Feedforward Compensation in AVC	67
4.1	Introduction	67
4.2	Development and Analysis of the Algorithms	69
4.3	Analysis of the Algorithms	72
4.3.1	Discussion of the algorithms	73
4.3.2	The stochastic case - perfect matching	73
4.3.3	The case of non-perfect matching	74
4.4	Relaxing the Positive Real Condition	76
4.5	Experimental Results	77
4.5.1	Broadband disturbance rejection with feedback controller and adaptation error filtering	77
4.5.2	Broadband disturbance rejection using only the feedforward adaptive filter	78
4.6	Concluding Remarks	81
5	General Youla-Kučera Parameterized Feedforward AVC	83
5.1	Introduction	83
5.2	Basic Equations and Notations	84
5.3	Development of the Algorithms	86
5.4	Analysis of the Algorithms	89
5.4.1	The deterministic case - perfect matching	89
5.4.2	The stochastic case - perfect matching	91
5.4.3	The case of non-perfect matching	92
5.4.4	Relaxing the positive real condition	93
5.4.5	Summary of the algorithms	94
5.5	Experimental Results	95
5.5.1	The Central Controllers	95
5.5.2	Broadband disturbance rejection using matrix adaptation gain	96
5.5.3	Broadband disturbance rejection using scalar adaptation gain	102
5.6	Comparison with Other Algorithms	104
5.7	Concluding Remarks	105
II	Adaptive Feedback Disturbance Compensation	107
6	Adaptive Indirect Regulation of Narrow Band Disturbances	109
6.1	Introduction	109
6.2	System Description	111
6.3	Frequency Estimation Using Adaptive Notch Filters	112
6.4	Indirect Adaptive Procedure Based on Band-stop Filters for Shaping the Sensitivity Function	113

6.5	Implementation Using the Youla-Kučera Parametrization	117
6.5.1	Stability Considerations	119
6.6	Experimental Results	120
6.6.1	An active vibration control system using an inertial actuator . . .	120
6.6.2	Attenuation of multi-sinusoidal disturbance	120
6.7	Concluding Remarks	122
7	Concluding Remarks and Future Work	125
7.1	Overall Conclusions	125
7.2	Future Work	126
A	Proofs for Chapter 4	127
A.1	Proof of the a posteriori adaptation error's asymptotic stability in Lemma 4.3.1	127
A.2	Proof of Lemma 4.4.1	129
A.3	Proof of Theorem 4.4.1	130
B	Proofs for Chapter 5	133
B.1	Proof of Lemma 5.3.1	133
B.2	Proof of Lemma 5.4.1	135
B.3	Changes to Lemma 5.3.1 when hypothesis $H2$ is not satisfied	135
B.4	Changes to the stability condition when hypothesis $H2$ is not satisfied . .	138
C	Adaptive Feedforward Compensation Algorithms for Active Vibration Control with Mechanical Coupling	141
D	Adaptive Feedforward Compensation Algorithms for AVC Systems in the Presence of a Feedback Controller	155
E	IIR Youla-Kucera Parameterized Adaptive Feedforward Compensators for Active Vibration Control with Mechanical Coupling	161
F	A Youla-Kucera Parametrized Adaptive Feedforward Compensator for Active Vibration Control with Mechanical Coupling	177
	Bibliography	185

LIST OF FIGURES

1.1	Réduction de bruit dans les casque - principe de fonctionnement.	22
1.2	Schéma de commande hybride « feedforward-feedback ».	23
1.3	Représentation générale d'un système de contrôle actif des vibrations (ou bruit).	24
1.4	Schéma bloc de la commande par action anticipatrice « feedforward ». . .	25
1.5	Schéma bloc du commande par contre-réaction « feedback ».	26
1.6	La représentation standard utilisée dans l'analyse des systèmes adaptatifs avec la théorie d'hyperstabilité.	28
1.7	Système de contrôle actif de vibrations utilisé pour les expérimentations.	33
1.8	Schéma du système de contrôle actif de vibrations utilisé pour les expérimentations.	33
1.9	Densités spectrales de puissance des filtres adaptatifs.	37
1.10	Phase de la fonction de transfert $H(z^{-1})$ estimé pour Algorithm <i>IIa</i> . . .	37
1.11	Résultats en temps réel avec Algorithme <i>IIa</i> avec adaptation scalaire « Intégral » (à gauche) et « Intégral + Proportionnel » (à droite).	38
1.12	Densités spectrales de puissance en boucle ouverte, avec IIRYK ($n_{B_Q} = 3$, $n_{A_Q} = 8$) et avec FIRYK ($n_Q = 31$) en utilisant le régulateur central H_∞ .	40
1.13	Fonction de sensibilité de la sortie avec régulateur nominal (gris), avec un régulateur basé sur le principe du modèle interne (noir) et avec un régulateur basé sur des filtres BSFs (gris en pointillés). Pour le contrôleur avec BSFs on a $\zeta_{d_i} = 0.04$ et $M_i = 60$ dB. Les atténuations sont introduits à 50, 70 et 90 Hz.	41
1.14	Schéma de l'algorithme adaptatif utilisant la paramétrisation de Youla-Kučera.	43
1.15	Comparaison des densités spectrales des puissances entre la mesure en boucle ouverte et les accélérations résiduelles obtenues avec deux régulateur adaptatifs (le premier avec filtres stop-bande et le deuxième avec le principe de modèle interne). L'entrée de la voie primaire est constituée par deux signaux sinusoïdaux à 63 Hz et à 88 Hz.	43
2.1	Outside noise reduction in headphones by use of ANC.	46
2.2	Block diagram representation of the combined feedforward-feedback control problem.	47
2.3	Generalized ANVC system representation.	48
2.4	Block diagram representation of the feedforward ANVC problem.	48
2.5	Block diagram representation of the feedback ANVC problem.	50
2.6	Standard representation used in the analysis of adaptive systems using hyperstability theory.	51

3.1	The AVC system used for experimentations - photo.	59
3.2	An AVC system using an adaptive feedforward and a fixed feedback compensation scheme.	60
3.3	Feedforward AVC: (a) in open loop and (b) with adaptive feedforward + fixed feedback compensator.	61
3.4	Frequency characteristics of the primary, secondary and reverse paths.	65
4.1	Equivalent feedback representation of the PAA with "Integral + Proportional" adaptation with constant integral adaptation gain.	77
4.2	Power spectral density of the open loop and when using the fixed feedback controller.	78
4.3	Real time results obtained with Algorithm <i>IIa</i> using "Integral" scalar adaptation gain.	79
4.4	Real time results obtained with Algorithm <i>IIa</i> using "Integral + Proportional" scalar adaptation gain.	79
4.5	Real time results obtained with Algorithm <i>IIb</i> using "Integral + Proportional" scalar adaptation gain and adaptation error filtering.	79
4.6	Power spectral density of the adaptive filters.	80
4.7	Phase of estimated $H(z^{-1})$ for Algorithm <i>IIa</i>	81
4.8	Real time results obtained with Algorithm <i>IIa</i> using "Integral" scalar adaptation gain (left) and "Integral + Proportional" scalar adaptation gain (right) over 1500s.	81
4.9	Real time results obtained with Algorithm <i>IIa</i> using "Integral" scalar adaptation gain (left) and "Integral + Proportional" scalar adaptation gain (right).	82
5.1	AVC block diagram with adaptive feedforward compensator using the YKIIR method.	85
5.2	Spectral densities of residual acceleration for the two central controllers (experimental).	96
5.3	Real time residual acceleration obtained with the IIR Youla-Kučera parametrization ($n_{B_Q} = 3, n_{A_Q} = 8$) using Algorithm <i>IIa</i> with matrix adaptation gain and the H_∞ central controller.	97
5.4	Real time residual acceleration obtained with the IIR Youla-Kučera parametrization ($n_{B_Q} = 3, n_{A_Q} = 8$) using Algorithm <i>III</i> with matrix adaptation gain and the H_∞ central controller.	97
5.5	Real time results obtained with the FIR Youla-Kučera parametrization ($n_Q = 31$) using Algorithm <i>III</i> with matrix adaptation gain and the H_∞ central controller.	98
5.6	Power spectral densities of the residual acceleration in open loop, with IIRYK ($n_{B_Q} = 3, n_{A_Q} = 8$) and with FIRYK ($n_Q = 31$) using the H_∞ central controller (experimental).	98
5.7	Evolution of the IIRYK parameters ($n_{B_Q} = 3, n_{A_Q} = 8$ and H_∞ central controller) for Algorithm <i>III</i> using matrix adaptation gain (experimental).	99
5.8	Evolution of the IIR parameters ($n_R = 9, n_S = 10$) for Algorithm <i>III</i> using matrix adaptation gain (experimental).	99
5.9	Power spectral densities of the residual acceleration when an additional sinusoidal disturbance is added (Disturbance = PRBS + sinusoid) and the adaptive IIRYK parametrization is used.	101

5.10	Power spectral densities of the residual acceleration when an additional sinusoidal disturbance is added (Disturbance = PRBS + sinusoid) and the adaptive FIRYK parametrization is used.	101
5.11	Power spectral densities of the residual acceleration when an additional sinusoidal disturbance is added (Disturbance = PRBS + sinusoid) and the direct adaptive IIR filter is used.	102
5.12	Real time residual acceleration obtained with the IIR Youla-Kučera parametrization ($n_{B_Q} = 3$, $n_{A_Q} = 8$) using Algorithm <i>III</i> with scalar adaptation gain and the H_∞ central controller.	103
5.13	Real time residual acceleration obtained with the FIR Youla-Kučera parametrization ($n_Q = 31$) using Algorithm <i>III</i> with scalar adaptation gain and the H_∞ central controller.	103
5.14	Power spectral densities of the residual acceleration in open loop, with IIRYK ($n_{B_Q} = 3$, $n_{A_Q} = 8$) and with FIRYK ($n_Q = 31$) using scalar adaptation gain and the H_∞ central controller (experimental).	104
6.1	Basic scheme for indirect adaptive control.	111
6.2	Output (upper) and input (lower) sensitivity functions with nominal controller (grey) and with controllers designed using BSFs (black) or the IMP (dotted grey). For the BSF controller, $\zeta_{d_i} = 0.04$ and $M_i = 60$ dB. The attenuations are introduced at 50, 70, and 90 Hz.	116
6.3	Youla-Kučera scheme for indirect adaptive control.	119
6.4	An AVC system using a feedback compensation - scheme.	120
6.5	Performance comparison in the presence of a two sine wave disturbance.	121
6.6	PSD comparison between the open loop measured disturbance and the residual accelerations obtained with the direct and the indirect compensators. In the upper figure, the PSDs are obtained with a 512 points window. In the lower one, the size of the window is 4096 points and therefore a better resolution is obtained. The input to the primary path of obtained by adding to sinusoidal signals of 63 Hz and 88 Hz.	122
6.7	Performance evaluation in the presence of 3 variable sinusoidal signals.	123
6.8	Three variable sinusoidal disturbances estimation using ANFs.	123
A.1	Equivalent feedback representation of the PAA with "Integral + Proportional" adaptation.	127
B.1	Equivalent system representation for Youla-Kučera parameterized feedforward compensators.	133
B.2	Equivalent system representation for Youla-Kučera parameterized feedforward compensators in the absence of hypothesis <i>H2</i>	136

LIST OF TABLES

5.1	Comparison of matrix gain algorithms for adaptive feedforward compensation in AVC with mechanical coupling.	94
5.2	Comparison of scalar gain algorithms for adaptive feedforward compensation in AVC with mechanical coupling.	95
5.3	Influence of the number of the IIRYK parameters upon the global attenuation.	100
5.4	Influence of the number of parameters upon the global attenuation for the FIRYK parametrization (lines 2 and 3) and for the IIR adaptive filter (line 4).	102

GLOSSARY

ANC	Active Noise Control
ANF	Adaptive Notch Filters
ANVC	Active Noise and Vibration Control
AVC	Active Vibration Control
BSF	Band-stop Filter
EFR	Equivalent Feedback Representation
FIR	Finite Impulse Response
FIRYK	Youla-Kučera parametrization using FIR adaptive filters
IIR	Infinite Impulse Response
IIRYK	Youla-Kučera parametrization using IIR adaptive filters
IMP	Internal Model Principle
PAA	Parameter Adaptation Algorithm
IP-PAA	“Integral + Proportional” Parameter Adaptation Algorithm
PSD	Power Spectral Density
RLS	Recursive Least Squares
Q	Youla-Kučera parameter
QFIR	FIR adaptive filter used in the Youla-Kučera parametrization
QIIR	IIR adaptive filter used in the Youla-Kučera parametrization
SPR	Strictly Positive Real
w.p.1	with probability one
w.r.t.	with respect to
YK	Youla-Kučera

LIST OF PUBLICATIONS

International Journals with Peer Review

- [J1] Adaptive feedforward compensation algorithms for active vibration control with mechanical coupling (Landau I.D., Alma M. and Airimițoaiu T.B.), *Automatica*, 47(10):2185 – 2196 ([Landau et al., 2011d]).
- [J2] Adaptive feedforward compensation algorithms for active vibration control systems in presence of a feedback controller (Alma M., Landau I.D. and Airimițoaiu T.B.), *Automatica*, 48(5):982 – 985 ([Alma et al., 2012a]).
- [J3] A Youla-Kučera parameterized adaptive feedforward compensator for active vibration control with mechanical coupling (Landau I.D., Airimițoaiu T.B. and Alma M.), *Automatica*, accepted for publication ([Landau et al., 2012b]).
- [J4] IIR Youla-Kučera parameterized adaptive feedforward compensators for active vibration control with mechanical coupling (Landau I.D., Airimițoaiu T.B. and Alma M.), *IEEE Transactions on Control Systems Technology*, accepted for publication ([Landau et al., 2012a]).
- [J5] Indirect Adaptive Attenuation of Multiple Narrow-band Disturbances Applied to Active Vibration Control (Airimițoaiu T.B. and Landau I.D.), submitted for review to the *IEEE Transactions on Control Systems Technology*.
- [J6] Improving adaptive feedforward vibration compensation by using "Integral + Proportional" adaptation (Landau I.D. and Airimițoaiu T.B.), submitted for review to *Automatica*.

International Conferences with Peer Review

- [C1] Advanced control and optimization for thermo-energetic installations (Airimițoaiu T.B., Popescu D. and Dimon C.), 5th International Symposium on Applied Computational Intelligence and Informatics, 2009 ([Airimițoaiu et al., 2009]).
- [C2] Comparison of two approaches for adaptive feedforward compensation in active vibration control with mechanical coupling (Landau I.D., Airimițoaiu T.B. and Alma M.), *Proceedings of the 19th Mediterranean Conference on Control and Automation*, 2011 ([Landau et al., 2011a]).
- [C3] Identification of mechanical structures in the presence of narrow band disturbances - Application to an active suspension (Airimițoaiu T.B., Landau I.D., Dugard L. and Popescu D.), *Proceedings of the 19th Mediterranean Conference on Control and Automation*, 2011 ([Airimițoaiu et al., 2011]).

- [C4] An adaptive feedforward compensation algorithm for active vibration control (Landau I.D., Airimițoaie T.B. and Alma M.), Proceedings of the 18th IFAC World Congress, Milano, Italy, 2011 ([Landau et al., 2011c]).
- [C5] Hybrid adaptive feedforward-feedback compensation algorithms for active vibration control systems (Alma M., Landau I.D. and Airimițoaie T.B.), Proceedings of the 50th IEEE Conference on Decision and Control, Atlanta, USA, 2011([Alma et al., 2011]).
- [C6] An IIR Youla-Kučera parameterized adaptive feedforward compensator for active vibration control with mechanical coupling (Landau I.D., Airimițoaie T.B. and Alma M.), Proceedings of the 50th IEEE Conference on Decision and Control, Atlanta, USA, 2011([Landau et al., 2011b]).
- [C7] Improving adaptive feedforward vibration compensation by using integral + proportional adaptation (Landau I.D. and Airimițoaie T.B.), submitted for review to the 51st IEEE Conference on Decision and Control, Maui, Hawaii, 2012.

CHAPTER 1

INTRODUCTION ET RÉSUMÉ DÉTAILLÉ

Ce chapitre introductif décrit les problèmes de base du contrôle actif de bruit (Active Noise Control, ANC) et du contrôle actif de vibrations (Active Vibration Control, AVC) qui ont motivé la recherche. Les structures de base utilisées pour le développement des algorithmes sont introduites et expliquées. Ensuite, un aperçu général des principaux résultats de la littérature et les directions de recherche sont présentés. Dans la dernière section, un résumé étendu des contributions originales de ce travail est fait et un aperçu de la thèse (Chapitres 3, 4, 5 et 6) est donné.

1.1 Motivation

Les principes de base du rejet actif de perturbations seront expliqués dans cette section. Quelques exemples seront utilisés pour indiquer d'une manière pratique ces problèmes de régulation et le contexte de ce travail sera également expliqué.

Le premier qui a mentionné le problème du contrôle actif du bruit (ANC) est Henri Coandă dans un brevet français ([Coanda, 1930]). Il a été suivi peu après par Paul Lueg ([Lueg, 1934]) et Harry F. Olson ([Olson and May, 1953]). Le problème abordé dans leurs ouvrages était celui de rejet de bruit provenant d'une source, en utilisant un microphone, un amplificateur et un haut-parleur. Il a été démontré que si l'ensemble capteur-régulateur-amplificateur-actionneur était capable de créer une onde sonore avec les mêmes caractéristiques en fréquence que le bruit source, mais avec un décalage de phase de 180^0 , il serait alors possible d'éliminer le bruit dans le domaine d'action des ondes sonores produites par le haut-parleur. Les réductions du bruit de moteur dans les avions et du bruit créé par différents types de machines à proximité de l'opérateur sont mentionnées comme applications possibles de ces techniques.

Dans la littérature scientifique, trois types de méthodes de contrôle ont été développés pour compenser des bruits ou des vibrations ([Fuller et al., 1997, Snyder, 2000]) : passifs, semi-actifs et actifs.

La solution classique est d'améliorer l'isolation ou d'ajouter des matériaux amortissants : c'est ce qu'on appelle l'approche passive car aucun algorithme de contrôle n'est nécessaire. Elle a l'avantage d'être simple et directe à utiliser et en même temps de fournir de solutions robustes, fiables et économiquement efficaces. L'utilisation de l'amortisseur passif est cependant limitée par l'impossibilité d'ajuster les forces de contrôle, la difficulté à cibler l'action de contrôle à des objectifs particuliers, la dépendance de la force de contrôle sur la dynamique du système naturel. Un bon exemple est le résonateur de Helmholtz décrit dans [Olson and May, 1953, Fleming et al., 2007].

Pour s'affranchir de ces défauts, différentes méthodes de contrôle qui permettent

l'utilisation de capteurs et d'actionneurs ont été employées. La plus simple est la méthode semi-active obtenue en utilisant des actionneurs qui se comportent comme des éléments passifs, permettant, par conséquent, seulement le stockage ou la dissipation d'énergie. Ils représentent encore une étape vers le contrôle actif parce que leurs propriétés mécaniques peuvent être ajustées par l'utilisation d'un signal provenant d'un contrôleur. Par exemple, les amortisseurs de certains véhicules ont un coefficient de frottement visqueux contrôlé par ordinateur. Comme dans le cas passif, il n'y a pas d'énergie injectée dans le système.

L'objectif de cette thèse concerne la troisième des solutions mentionnées ci-dessus, plus précisément le contrôle actif. La principale différence par rapport aux deux autres, c'est son aptitude à fournir une puissance mécanique au système et à cibler l'action de commande vers des objectifs spécifiques. Dans les applications de contrôle du bruit, la fréquence d'échantillonnage peut monter jusqu'à 40.000 Hz . Il est indiqué dans la littérature ([Olson and May, 1953, Fuller and von Flotow, 1995, Elliott, 2001]) que les techniques passives donnent généralement des résultats satisfaisants dans la bande des hautes fréquences (réductions de plus de 40 dB au-dessus de 500 Hz) et donc, au début, l'utilisation de méthodes actives est devenue intéressante pour les basses fréquences, en particulier d'un point de vue du contrôle adaptatif comme il sera montré plus tard. Il y a un grand nombre d'applications où les bruits extérieurs et les vibrations doivent être réduits. Un bon exemple est donné dans la Figure 1.1, qui montre comment fonctionnent les casques à réduction de bruit. Les écouteurs modernes sont conçus pour donner un son de bonne qualité, même dans les environnements bruyants. À cet effet, les perturbations extérieures sont mesurées par un microphone utilisé en tant que capteur et un algorithme de contrôle est développé pour annuler les perturbations en utilisant un haut-parleur intégré en tant qu'actionneur. Dans le cas idéal, le signal ajouté par l'actionneur devrait avoir une grandeur égale et avec un décalage de phase de 180° par rapport au bruit extérieur pour obtenir un rejet parfait. Une analyse globale est publiée dans les références suivantes: [Elliott and Nelson, 1993, Fuller and von Flotow, 1995, Guicking, 2007].

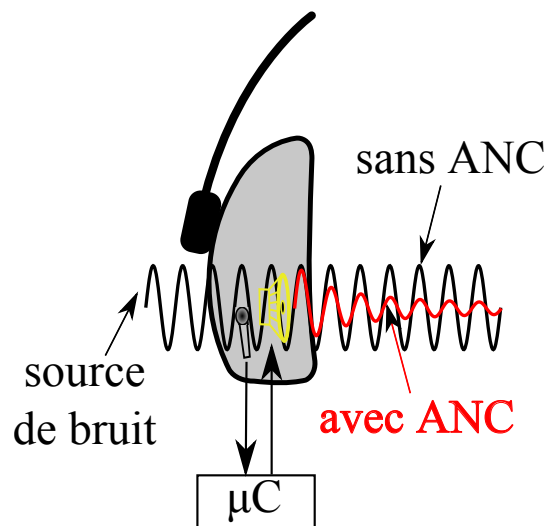


Figure 1.1: Réduction de bruit dans les casque - principe de fonctionnement.

1.2 Description du Problème

Cette section offre au lecteur une description succincte des problèmes de régulation adaptative qui seront traités dans les chapitres suivants. L'objectif principal est de réduire

le niveau des vibrations (ou des bruits) dans un endroit prédéfini tout en assurant la stabilité du système. Une présentation générale du système et des stratégies de contrôle sera faite dans les sections suivantes.

1.2.1 Configuration du système de contrôle

La Figure 2.2 représente un système de control actif des vibrations (ou des bruits) en utilisant un contrôleur généralisé « feedforward-feedback ». Le système a deux entrées et deux sorties. La première entrée est la perturbation $w(t)$, produite par une source inconnue $s(t)$ filtrée à travers un filtre de caractéristiques inconnues. La deuxième entrée est le signal de commande $u(t)$. La première sortie est la mesure de l'accélération résiduelle $e(t)$ (appelée aussi variable de performance). La deuxième sortie est un signal corrélé avec la perturbation inconnue, $y_1(t)$ dans la Figure 1.2. La *voie secondaire* caractérise les dynamiques entre le signal de commande et l'accélération résiduelle $e(t)$. La fonction de transfert entre le signal $w(t)$ qui caractérise l'image de la perturbation en l'absence des compensateurs et la mesure de l'accélération résiduelle $e(t)$, caractérise la *voie primaire*. Quand le système de compensation est actif, l'actionneur de contrôle agit sur l'accélération résiduelle, mais aussi sur la mesure de l'image de la perturbation. Le signal mesuré $y_1(t)$ est alors la somme de la mesure corrélée avec la perturbation $w(t)$, obtenue en l'absence de compensation en « feedforward », et l'effet de l'actionneur utilisé pour la compensation, sur cette mesure. Ce couplage entre le signal de commande et la mesure de l'image de la perturbation $y_1(t)$ via l'actionneur de compensation est appelé *voie inverse*. Ce retour positif non désiré peut poser plusieurs problèmes en pratique (source d'instabilités) et rend la synthèse et l'analyse des compensateurs plus difficiles.

L'objectif est de minimiser la variable de performance $e(t)$ par un contrôle $u(t)$ calculé en utilisant les variables mesurées $e(t)$ et $y_1(t)$.

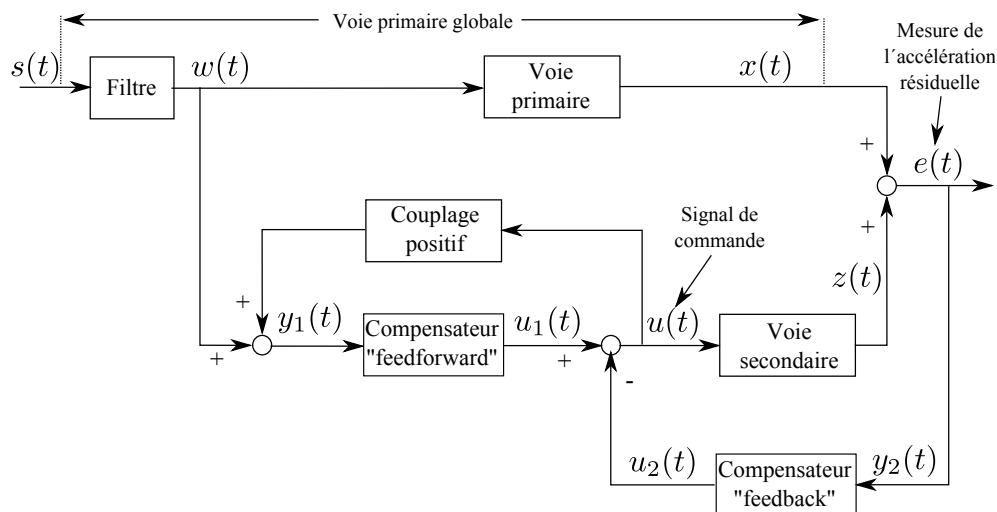


Figure 1.2: Schéma de commande hybride « feedforward-feedback ».

On peut remarquer que le signal de contrôle $u(t)$ est obtenu par la soustraction entre le signal de contrôle « feedforward », $u_1(t)$, et le signal de contrôle « feedback », $u_2(t)$. Le signal mesuré peut être décrit par $y(t) = [y_1(t), y_2(t)]^T$. En conséquence, le régulateur peut aussi être représenté par un vecteur $\kappa = [N, -K]^T$, où N et K représentent les compensateurs « feedforward » et « feedback » respectivement. Avec ces notations,

l'équation qui lie la mesure avec le signal de contrôle est donnée par

$$u(t) = u_1(t) - u_2(t) = N \cdot y_1(t) - K \cdot y_2(t) = \kappa^T \cdot y(t). \quad (1.1)$$

L'appellation « contrôleur feedforward » donnée à N est motivée par le fait que $y_1(t)$, appelé aussi « image corrélée avec la perturbation », est mesuré en amont de la variable de performance, en supposant en même temps que c'est physiquement possible d'obtenir une telle mesure. Dans les situations où il n'est pas possible d'installer un deuxième capteur comme décrit ci-dessus, seulement une approche par contrôle « feedback » peut être utilisée. Dans la littérature du contrôle actif des vibrations (ou bruits), la méthodologie de contrôle mixte « feedforward - feedback » est souvent appelée « contrôle hybride ».

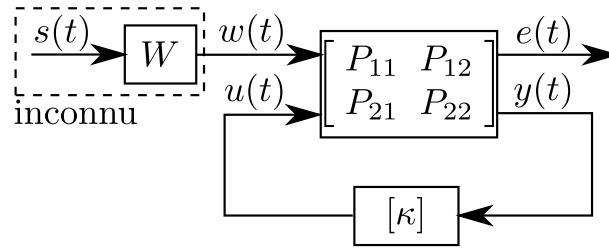


Figure 1.3: Représentation générale d'un système de contrôle actif des vibrations (ou bruit).

Une représentation standard sous la forme d'un système à 2 entrées et 2 sorties peut aussi être utilisée, comme indiqué dans la Figure 1.3. Cette représentation est très bien connue dans le contrôle robuste et optimal (voir aussi [Tay et al., 1997, Zhou et al., 1996]). Les équations du système associé à cette représentation avec contrôle par contre-réaction sont:

$$\begin{bmatrix} e(t) \\ y(t) \end{bmatrix} = \begin{bmatrix} P_{11} & P_{12} \\ P_{21} & P_{22} \end{bmatrix} \begin{bmatrix} w(t) \\ u(t) \end{bmatrix} = \left[\begin{array}{c|c} D & G \\ \hline 1 & M \\ D & G \end{array} \right] \begin{bmatrix} w(t) \\ u(t) \end{bmatrix}, \quad (1.2)$$

et la loi de commande est donnée par l'équation (1.1).

Deux cas particuliers, également proposés dans la thèse, seront présentés dans les sous-sections suivantes.

1.2.2 Le problème de contrôle par action anticipatrice « feedforward »

Une particularisation du problème général est d'atténuer les vibrations (ou bruits) par action anticipatrice « feedforward ». Une représentation schématique de cette situation est donnée dans la Figure 2.4. Une caractéristique importante de cette configuration est l'absence de régulateur à contre-réaction, $K = 0$. En regardant la Figure 2.4, on obtient $y(t) = y_1(t)$ et $u(t) = u_1(t)$. On suppose aussi, comme précisé ci-dessus, qu'on peut utiliser un deuxième capteur qui fournit une image corrélée avec la perturbation, installé en amont de la mesure de performance $e(t)$, ce qui permet d'utiliser la méthodologie présentée ci-après.

Cette méthode est importante dans les situations concrètes où des perturbations bande large doivent être réduites. Dans ces cas, une approche par contre-réaction serait limitée par les contraintes imposées par l'intégrale de Bode ([Hong and Bernstein, 1998]).

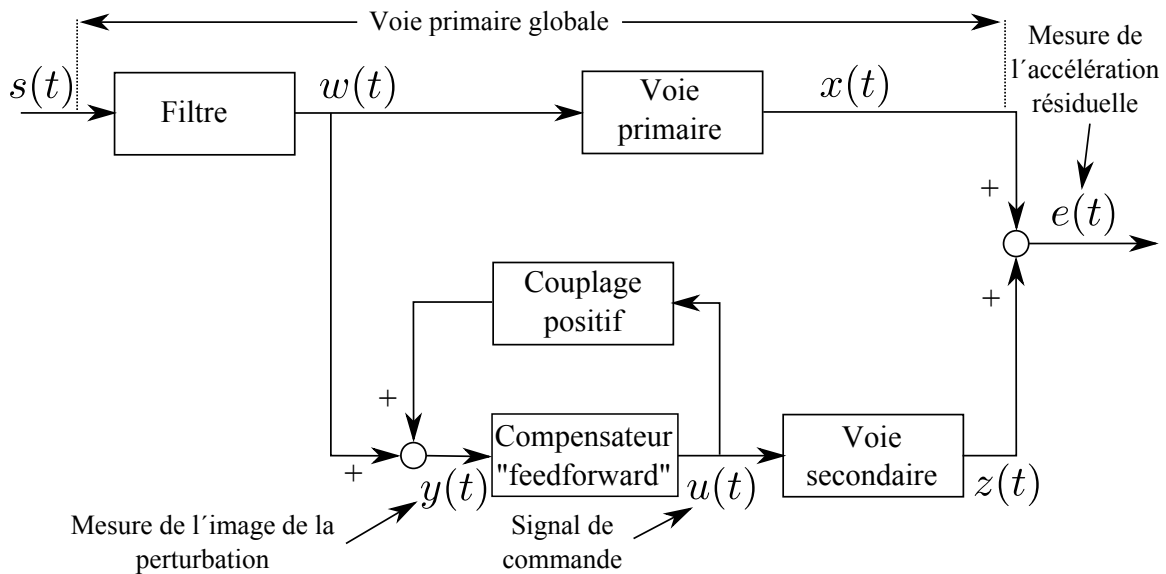


Figure 1.4: Schéma bloc de la commande par action anticipatrice « feedforward ».

Pour traiter le cas des perturbations à bande large, on peut utiliser le schéma de la Figure 1.4. Il peut être immédiatement observé de cette représentation que, quand le système de compensation est actif, l'actionneur n'agit pas seulement sur l'accélération résiduelle, mais aussi sur la mesure de l'image de la perturbation par la voie inverse. Ce retour positif non désiré complique la conception du contrôleur en posant plusieurs problèmes en pratique (source d'instabilités) et rend la synthèse et l'analyse des compensateurs plus difficiles.

Dans une première étape de développement des algorithmes pour résoudre ce problème, le couplage interne positif décrit ci-dessus n'a pas été pris en compte ([Widrow et al., 1975]), considérant que son influence peut être compensée ou qu'elle est trop faible pour poser des problèmes. Certaines techniques ont été proposées dans la littérature pour la compensation de l'effet du couplage positif, certaines étant de nature mécanique et d'autres étant plus liées à l'algorithme de contrôle. Par exemple pour la seconde, la méthode dite *de neutralisation du couplage positif*, a été décrite dans ([Kuo and Morgan, 1999, Nelson and Elliott, 1993]) et dépend d'une très bonne estimation de la voie inverse du système. Cependant, il est noté dans ([Nelson and Elliott, 1993, Mosquera et al., 1999]) que si l'estimation n'est pas exacte, alors la possibilité d'instabilité existe toujours.

Les algorithmes présentés dans cette thèse sont conçus pour fournir de bons résultats, même en présence du couplage interne positif et il n'y a donc pas besoin de la neutralisation.

L'utilisation du contrôle adaptatif est motivée par la prise en compte de l'éventualité que les caractéristiques de la perturbation peuvent varier ou que les modèles identifiés ne soient pas des représentations exactes des chemins du système. En outre, il y a aussi la possibilité que la perturbation ($d(t)$) change sa caractéristique fréquentielle pendant une expérimentation de longue durée.

1.2.3 Le problème de contrôle par contre-réaction « feedback »

Un autre cas trouvé dans la pratique est la régulation par contre-réaction « feedback ». Dans cette situation, on peut seulement réduire des perturbations à bande étroite. En général, on considère le problème de la réduction des vibrations issues de multiples sources de perturbation à bande étroite. Une représentation schématique de cette situation est donnée dans la Figure 1.5. On observe que dans ce cas $N = 0$. En conséquence, on obtient $y(t) = y_2(t)$ et $u(t) = u_2(t)$.

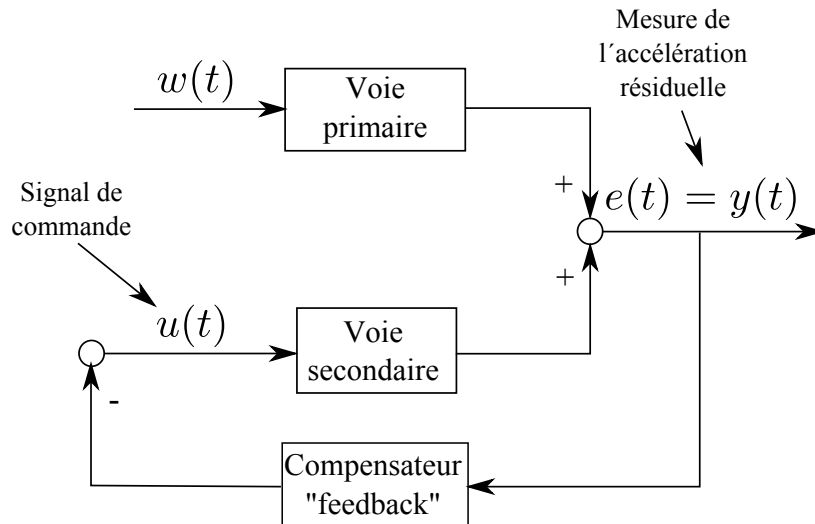


Figure 1.5: Schéma bloc du commande par contre-réaction « feedback ».

Dans les situations où on ne peut pas utiliser un deuxième capteur pour mesurer une image corrélée avec la perturbation parce que les caractéristiques physiques du système l'empêchent, une méthode de contrôle par contre-réaction doit être appliquée. Comme mentionné précédemment, les restrictions de l'intégrale de Bode ne permettent que la réduction ou le rejet des perturbations à bande étroite; dans cette partie de la thèse, l'objectif sera donc de développer des techniques uniquement pour la compensation des perturbations sinusoïdales multiples stationnaires ou variables.

1.3 Revue de la Littérature

Cette section présente un survol des contributions importantes dans la littérature du contrôle par action anticipatrice et par contre-réaction des bruits ou des vibrations.

1.3.1 Méthodes de commande par action anticipatrice « feedforward »

Les premiers résultats dans la littérature du contrôle par action anticipatrice « feedforward » pour la régulation des vibrations (ou des bruits) ont été obtenus en négligeant le couplage positif interne. La plupart des travaux faits dans ce domaine se concentrent autour de diverses modifications de la méthode de recherche par le gradient du Least Mean Square (LMS) (introduit dans [Widrow, 1971]). L'objectif de la méthode LMS est de trouver le point minimum de la surface de l'erreur quadratique moyenne (MSE) en mettant à jour les paramètres d'un filtre FIR (Finite Impulse Response) dans une direction qui est une estimation de la descente la plus rapide. A cet effet, l'algorithme

utilise l'échantillon actuel de l'erreur quadratique, qui est une approximation grossière de l'erreur quadratique moyenne.

Une des premiers progrès a été le LMS filtré sur l'entrée (appelé FxLMS), proposé indépendamment par [Burges, 1981] et [Widrow et al., 1981], qui ont utilisé une version filtrée des observations (mesures en corrélation avec la perturbation) dans l'algorithme d'adaptation. Les deux schémas d'adaptation étudiés par ces auteurs (contrôleur audio adaptatif dans la recherche de Burges et contrôle adaptatif inverse dans celle de Widrow) ont présenté un modèle de chemin secondaire qui influe sur la procédure d'adaptation. En conséquence, le filtrage du vecteur d'observation à travers le modèle du chemin secondaire a été proposé afin d'obtenir de meilleures performances. Les deux solutions proposées par ces auteurs ont utilisé l'adaptation d'un filtre FIR dans un schéma sans couplage positif interne.

Malgré la stabilité et la surface d'optimisation convexe pour les filtres FIR, il y a des situations où l'utilisation des filtres avec des pôles et des zéros, appelés filtres IIR, est particulièrement intéressante. Par exemple, pour obtenir de bonnes performances, avec des filtres FIR, on doit souvent utiliser un grand nombre de paramètres, tandis qu'avec les filtres IIR, il est possible d'obtenir des performances similaires avec un nombre considérablement réduit de paramètres. Une méthode d'adaptation des filtres IIR a été proposée par Feintuch dans [Feintuch, 1976]. Elle a été appelée LMS récursive (RLMS) et fournit une transformation de l'adaptation du filtre LMS basique à la structure IIR. Plus tard, l'algorithme a été amélioré en utilisant des observations filtrées de la même manière que cela est fait pour les FxLMS, fournissant l'algorithme Filtered-U LMS (FuLMS). Le FuLMS a d'abord été introduit dans [Eriksson et al., 1987] pour les applications de contrôle actif des bruits mais l'analyse de convergence et de stabilité n'a pas été donnée. Comme exemple d'application de cet algorithme : la réduction du bruit, à l'intérieur des avions à réaction, produit par les moteurs qui sont montés directement sur le fuselage est décrite dans [Billoud, 2001].

La famille des algorithmes LMS utilise une estimation approximative de la direction de descente maximale, obtenue en prenant le gradient de l'échantillon actuel de l'erreur quadratique au lieu du gradient de l'erreur quadratique moyenne. Une amélioration a été obtenue avec l'algorithme Filtered-v LMS (FvLMS) présenté dans [Crawford and Stewart, 1997] où le gradient exact est calculé. Néanmoins, en prenant en compte l'adaptation lente des paramètres, certaines approximations ont été faites pour réduire la complexité numérique de l'algorithme.

Un problème difficile pour les filtres adaptatifs IIR dans le cadre du contrôle des vibrations (ou bruits) concerne leur stabilité et l'analyse de leur convergence. Par rapport aux algorithmes d'erreur de sortie, présentés dans la littérature concernée avec l'identification des systèmes, ceci doit se faire en tenant compte de la structure particulière du système (surtout des voies secondaire et inverse, voir Section 1.2).

Une manière d'analyser la convergence, dans un environnement stochastique, est la méthode O.D.E. de Ljung ([Ljung and Söderström, 1983] - d'abord présentée dans [Ljung, 1977a] et appliquée dans l'analyse de la méthode erreur de sortie (voir [Landau, 1976]) pour l'estimation des paramètres dans [Ljung, 1977b]). Avec cette méthode, il a été possible d'analyser les propriétés de l'algorithme FuLMS. Dans [Wang and Ren, 2003, Fraanje et al., 1999], des conditions sont trouvées pour assurer la convergence avec une probabilité de 1, dans le cas avec retour interne positif, mais avec quelques conditions restrictives, parmi lesquelles deux sont résumées : le gain d'adaptation doit tendre vers zéro et la voie inverse ne doit pas déstabiliser le système.

Une autre méthode pour l'analyse de la stabilité et de la convergence des algorithmes adaptatifs est la théorie de l'*hyperstabilité*. Elle a été d'abord proposée dans les travaux de V.M. Popov et présentée dans les publications [Popov, 1960, Popov, 1966] et ensuite traduite dans [Popov, 1963, Popov, 1973]. Une des conséquences les plus importantes de cette théorie est son utilisation dans la synthèse des algorithmes adaptatifs en combinaison avec des systèmes positifs. Le cadre initial pour l'étude des systèmes adaptatifs en utilisant l'hyperstabilité a été mis en place dans [Landau and Silveira, 1979, Landau, 1979, Landau, 1980] et une analyse théorique complète peut être trouvée dans [Landau et al., 2011g]. Contrairement à l'approche de Lyapunov qui est limitée par la difficulté de trouver des fonctions de Lyapunov candidates appropriées, une grande famille de lois d'adaptation conduit à des algorithmes adaptatifs stables qui peuvent être conçus en utilisant la théorie d'hyperstabilité.

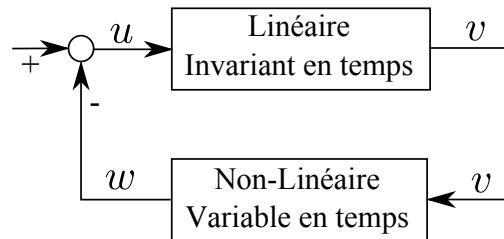


Figure 1.6: La représentation standard utilisée dans l'analyse des systèmes adaptatifs avec la théorie d'hyperstabilité.

L'hyperstabilité traite principalement la stabilité d'une classe de systèmes qui peuvent être représentés sous la forme donnée dans la Figure 1.6. Dans cette configuration, il est supposé que le bloc de réaction non-linéaire et / ou variable dans le temps satisfait une relation d'entrée-sortie de la forme

$$\sum_{t=0}^{t_1} v(t)w(t) \geq -\gamma^2 \text{ pour tout } t \geq 0. \quad (1.3)$$

Une des premières utilisations de l'hyperstabilité dans la synthèse d'algorithmes adaptatifs a été signalée dans [Treichler et al., 1978, Larimore et al., 1980]. L'algorithme SHARF (Simple Hyperstable Adaptive Recursive Filter) est convergent hyperstable uniquement pour un gain d'adaptation faible. En outre, la version plus complexe, HARF a été prouvée convergente sous des conditions significativement moins contraignantes ([Johnson, 1979]). Les deux algorithmes utilisent le filtrage de l'erreur d'estimation. La difficulté rencontrée dans ces algorithmes (celle qui les rend difficiles à utiliser dans des systèmes ANVC réels) est le choix du filtre qui assure la condition de Strict Positif Réel (SPR), en particulier en raison de l'existence des voies secondaires et inverses. En outre, ils ne sont pas proposés dans un contexte de contrôle actif des vibrations (ou des bruits), donc le couplage interne positif n'est pas pris en compte dans leur développement.

Une variante de l'algorithme HARF avec filtrage des observations et de l'erreur est proposée dans la recherche de [Mosquera et al., 1999]. La convergence est démontrée sur la base de la théorie développée précédemment. Une mise en œuvre sur un système de contrôle actif des bruits est testée en supposant le couplage interne positif nul (après utilisation d'un compensateur fixe spécialement conçu pour cette tâche), mais les résultats ne sont pas satisfaisants.

Comme pour les algorithmes (S)HARF, une méthode applicable dans le contrôle actif sans couplage interne positif est présentée dans [Snyder, 1994]. Contrairement aux

algorithmes (S)HARF, le filtrage se fait sur le vecteur d'observation, tandis que dans les algorithmes ci-dessus, il a été fait sur l'erreur d'estimation, et une façon de choisir le filtre est suggéré.

Une autre tentative d'élaborer un algorithme de contrôle actif des bruits par une méthode de stabilité a été proposée dans [Jacobson et al., 2001]. Néanmoins, les hypothèses spécifiques prises dans le développement restreignent l'application de cet algorithme à des cas spécifiques et, comme justifié dans [Landau et al., 2011d], il peut même devenir instable dans un problème plus général de contrôle actif des vibrations. Plus précisément, il a été supposé que la voie secondaire est une fonction de transfert réelle strictement positive mais ce n'est pas toujours le cas.

En plus de ces directions de recherche, le travail a été fait également sur l'amélioration de l'efficacité numérique surtout dans le cas des algorithmes de type RLS. Des références relatives à ces méthodes peuvent être trouvées dans [Montazeri and Poshtan, 2010, Montazeri and Poshtan, 2011], mais le travail a été limité au cas sans couplage de contre-réaction positive.

Un algorithme à erreur d'équation a été présenté dans [Sun and Chen, 2002]. L'algorithme a une convergence globale dans le cas où le couplage positif interne n'est pas présent et où le bruit de mesure est égal à zéro. En présence de bruit de mesure, il est démontré que le résultat est biaisé. Aussi, lorsque la contre-réaction existe, un minimum local est atteint, au lieu de minimum global. Pour surmonter ces problèmes, un algorithme Steiglitz-McBride de type IIR a été proposé dans [Sun and Meng, 2004]. Des résultats de simulation sans couplage positif interne sont présentés. Un autre inconvénient de cet algorithme est que la stabilité est supposée *a priori*, mais, dans la pratique, les pôles du filtre adaptatif IIR peuvent se déplacer en dehors du cercle unité et l'instabilité peut se produire.

Une approche différente est considérée dans [Zeng and de Callafon, 2006], où la conception est basée sur un modèle (Model Based Design - MBD) en utilisant une paramétrisation Youla-Kučera de tous les contrôleurs stabilisants avec une mise en œuvre pour un problème de rejet de bruit. Tout d'abord le filtre à action anticipatrice « feedforward » est identifié à partir des données obtenues en boucle ouverte, puis une fonction de base orthonormée est conçue sur la base de la théorie décrite dans [Heuberger et al., 1995]. Une autre différence de ce qui a été fait dans les recherches précédemment mentionnées, c'est que l'adaptation des paramètres ne se fait pas à chaque période d'échantillonnage, mais à certains intervalles au cours desquels le système fonctionne avec les dernières valeurs calculées pour le filtre adaptatif. Aucune analyse de la stabilité n'a été réalisée.

Pour conclure sur la revue des diverses méthodes développées dans le domaine du contrôle actif des vibrations et des bruits, il est nécessaire de mentionner également les compensateurs H_∞ et H_2 développés sur la base des modèles estimés. Cette approche a été prise en compte dans [Bai and H.H.Lin, 1997, Rotunno and de Callafon, 2003, Alma et al., 2012b]. Toutefois, le compensateur résultant n'a pas les capacités d'adaptation et sa performance n'est pas forcément très bonne. Sous la condition que la grande dimension du compensateur résultant peut être réduite, il peut constituer une valeur « initiale » pour les paramètres d'un compensateur adaptatif. Dans [Bai and H.H.Lin, 1997] il est démontré expérimentalement que les résultats obtenus avec la méthode H_∞ sont meilleurs que ceux obtenus en utilisant l'algorithme d'adaptation très populaire FULMS (pour une perturbation dont on connaît les caractéristiques spectrales). Une comparaison similaire réalisée expérimentalement dans le cadre de cette thèse et publiée dans [Landau et al., 2011d] confirme ce fait. Toutefois, ce n'est plus

vrai lorsque l'on compare les résultats obtenus avec un régulateur H_∞ aux algorithmes adaptatifs présentés dans cette thèse.

Il est important de remarquer que toutes ces contributions (sauf [Alma et al., 2012b]) ont été réalisées dans le cadre du contrôle actif de bruit. Bien que les algorithmes pour le contrôle actif de bruit puissent être utilisés dans le contrôle actif des vibrations, il faut prendre en compte la spécificité de ces systèmes qui disposent de nombreux modes de vibration faiblement amortis (résonance) et aussi des zéros complexes faiblement amortis (antirésonance).

1.3.2 Méthodes de commande par contre-réaction « feedback » pour le rejet de perturbations bande étroite

Souvent, dans la pratique, il n'est pas possible d'utiliser un deuxième capteur pour mesurer une image de la perturbation. Dans ces situations, une approche par commande à contre-réaction « feedback » doit être considérée. Tenant compte de la restriction de l'intégrale de Bode ([Åström and Murray, 2008, Zhou et al., 1996]), nous pouvons conclure que seulement des perturbations sur une bande de fréquences étroite peuvent être atténuées. Par conséquent, cette partie de la thèse concerne le rejet de plusieurs perturbations sinusoïdales variables dans le temps. Une analyse comparative de la commande par rétro-action « feedback » et par action anticipatrice « feedforward » est donnée dans [Elliott and Sutton, 1996].

Une présentation des méthodes existantes pour le rejet des perturbations bande étroite est donnée ci-dessous. Pour commencer, la différence entre les paradigmes « régulation adaptative » et « contrôle adaptatif » a été soulignée dans un article récent (voir [Landau et al., 2011f]). Il est alors mentionné que dans le contrôle adaptatif classique l'objectif est le suivi de la consigne ou/et l'atténuation des perturbations dans le cadre des systèmes (voie secondaire) à paramètres inconnus et variables dans le temps. Ainsi, l'objectif du contrôle adaptatif est centré sur l'adaptation par rapport aux variations dans les paramètres du système. Le modèle de la perturbation est supposé être connu et invariant dans le temps.

En revanche, la « régulation adaptative » fait référence à la suppression (ou atténuation) asymptotique de l'effet des perturbations inconnues et variables dans le temps. Il est également supposé que le modèle du système est connu et que des principes de contrôle robuste peuvent s'appliquer pour traiter d'éventuelles petites variations des paramètres. Par conséquent, aucun effort n'est mis dans l'estimation en temps réel du modèle du système. Un aspect important est que la perturbation devrait être située dans la région de fréquence où le système a assez de gain.

L'objectif de cette thèse étant le rejet des perturbations, le problème de la « régulation adaptative » sera pris en considération. Le cadre commun est l'hypothèse que la perturbation est le résultat d'un bruit blanc (ou une impulsion de Dirac) passé à travers le « modèle de la perturbation ». Pour rejeter son influence, différentes solutions ont été proposées. L'une d'entre elles fait appel au principe du modèle interne (IMP) présenté dans [Amara et al., 1999a, Amara et al., 1999b, Gouraud et al., 1997, Hillerstrom and Sternby, 1994, Valentinotti, 2001, Valentinotti et al., 2003]. Utiliser cette méthode suppose l'intégration du modèle de la perturbation dans le contrôleur ([Bengtsson, 1977, Francis and Wonham, 1976, Johnson, 1976, Tsytkin, 1997]). Ses paramètres doivent donc être estimés en permanence pour être en mesure de répondre à d'éventuelles modifications dans les caractéristiques de la perturbation. Cela conduira

à un algorithme indirect de commande adaptative. Toutefois, il a été montré dans [Landau et al., 2005] que l'adaptation directe est utilisable si on utilise la paramétrisation de Youla-Kučera pour tous les contrôleurs stabilisants.

Une autre idée qui a été utilisée est celle de construire un observateur adaptatif et de l'incorporer dans le contrôleur [Ding, 2003, Marino et al., 2003, Serrani, 2006, Marino and Tomei, 2007]. Toutefois, l'approche semble se concentrer sur des perturbations qui agissent sur l'entrée du système. Des hypothèses supplémentaires doivent être prises en compte avant de l'appliquer à des perturbations sur la sortie. On peut noter que, même si le principe du modèle interne n'est pas explicitement pris en considération dans ce schéma, incorporer l'observateur dans le contrôleur signifie que cette approche est semblable à la première.

Une approche directe pour le rejet de perturbations sinusoïdales de fréquences inconnues, basée sur l'intégration d'une boucle « phase-locked » pour la commande en contre-réaction adaptative avec un modèle de procédé connu, est présentée dans [Bodson and Douglas, 1997] et des résultats expérimentaux sont donnés dans [Bodson, 2005]. L'estimation de la fréquence de la perturbation et son élimination se font simultanément utilisant un seul signal d'erreur. La connaissance de la réponse fréquentielle du procédé dans la région fréquentielle considérée est nécessaire.

1.4 Contributions

Dans cette thèse, les objectifs principaux ont été de développer, analyser et tester sur les plateformes disponibles au sein du département Automatique du laboratoire GIPSA-Lab, des algorithmes pour le rejet (ou l'atténuation) des vibrations bande étroite ou bande large. Tenant compte des caractéristiques des perturbations, nous avons proposé soit des méthodes de contrôle par action anticipatrice « feedforward » pour les perturbations bande large, soit par contre-réaction « feedback » pour les perturbations bande étroite.

La Partie I de la thèse est consacrée aux méthodes « feedforward ». Les contributions les plus significatives sont :

1. Développement des algorithmes généralisés qui utilisent un filtrage sur l'erreur *a posteriori* et aussi un filtrage du vecteur d'observations. Les algorithmes ont été conçus en tenant compte du couplage interne positif existant dans les systèmes de contrôle actif de vibrations. La stabilité et la convergence sont vérifiées et des expérimentations sont faites pour confirmer l'analyse théorique.
2. Une solution est aussi proposée pour l'assouplissement de la condition de réelle positivité. L'idée est d'utiliser un Algorithme d'Adaptation Paramétrique « Intégral + Proportionnel ».
3. Développement et analyse des algorithmes paramétrés Youla-Kučera utilisant des filtres adaptatifs FIR ou IIR.

Les contributions de la Partie II de la thèse sont :

1. Développement d'un nouvel algorithme de contrôle par contre-réaction pour l'atténuation de perturbations bande étroite. L'algorithme est conçu en utilisant des filtres stop-bande pour calibrer la fonction de sensibilité avec un minimum d'influence en dehors des fréquences d'atténuation.

2. Utilisation des « Filtres Adaptatifs à Encoche » pour estimer les fréquences des perturbations dans un contexte de contrôle actif de vibrations.
3. Mise en œuvre avec la paramétrisation de Youla-Kučera pour diminuer la complexité de l'algorithme.

1.5 Plan du Manuscrit de Thèse

Les principaux objectifs de la thèse ont été le développement, l'analyse et l'évaluation expérimentale des algorithmes adaptatifs pour le rejet de perturbations sur les systèmes de contrôle actif de vibrations. Selon les caractéristiques de la perturbation et les contraintes du système, nous avons développé, soit des régulateurs par contre-réaction « feedback » soit des approches par action anticipatrice « feedforward ». La régulation par contre-réaction a été utilisée pour l'atténuation de perturbations bande étroite. Par contre, la compensation des perturbations bande large a été réalisée en utilisant un régulateur à action anticipatrice et en profitant d'un deuxième dispositif de mesure capable d'offrir une image de la perturbation.

Les Chapitres 3 - 6 présentent des différentes solutions pour le problème de contrôle abordé dans cette thèse. Les conclusions et les directions de recherches futures sont indiquées dans le Chapitre 7. Les preuves des lemmes, corolaires et théorèmes énoncés dans les chapitres précédents de la thèse sont données en annexes (**Appendices A** et **B**).

Les sections suivantes présentent un résumé de la thèse.

1.5.1 Description du système

La **Partie I** présente des algorithmes de contrôle par action anticipatrice « feedforward ». Tout d'abord, le **Chapitre 3** présente le système réel sur lequel les algorithmes proposés dans cette thèse ont été testés. La structure utilisée a été réalisée en collaboration avec le centre de recherche Vibrachoc, et s'est inspirée de problèmes de rejet de perturbations vibratoires dans le domaine industriel. Une image de ce système est donnée dans la Figure 1.7 et le schéma correspondant dans la Figure 1.8. Le système consiste en cinq plaques métalliques, reliées par des ressorts. Les plaques supérieure et inférieure sont reliées entre elles d'une manière rigide par quatre vis. Les trois plaques au centre seront dénotées M1, M2 et M3 dans les Figures 1.7 et 1.8. Les plaques métalliques mobiles M1 et M3 sont équipées d'actionneurs inertiels. Celui d'en haut, placé sur M1, sert de générateur de perturbations (actionneur inertiel I dans les Figures 1.7 et 1.8), et celui d'en bas, placé sur M3, sert à la compensation de ces perturbations (actionneur inertiel II dans les Figures 1.7 et 1.8). Le système est équipé avec une mesure de l'accélération résiduelle sur la plaque M3, comme sortie du procédé, et d'une mesure de l'image de la perturbation produite par un accéléromètre placé sur la plaque M1.

Les voies primaire (D), secondaire (G), et inverse (M) représentées dans la Figure 3.3(b) sont caractérisées par les fonctions de transfert :

$$X(q^{-1}) = \frac{B_X(q^{-1})}{A_X(q^{-1})} = \frac{b_1^X q^{-1} + \dots + b_{n_{B_X}}^X q^{-n_{B_X}}}{1 + a_1^X q^{-1} + \dots + a_{n_{A_X}}^X q^{-n_{A_X}}}, \quad (1.4)$$

avec $B_X = q^{-1}B_X^*$ et $A_X = 1 + q^{-1}A_X^*$ pour tout $X \in \{D, G, M\}$. $\hat{G} = \frac{\hat{B}_G}{\hat{A}_G}$, $\hat{M} = \frac{\hat{B}_M}{\hat{A}_M}$ et $\hat{D} = \frac{\hat{B}_D}{\hat{A}_D}$ représentent les modèles identifiés pour les voies secondaire, inverse et primaire.

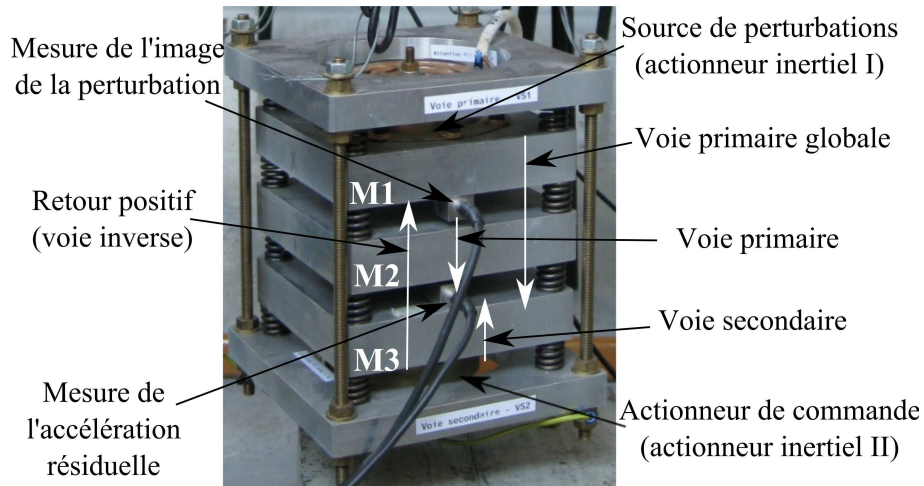


Figure 1.7: Système de contrôle actif de vibrations utilisé pour les expérimentations.

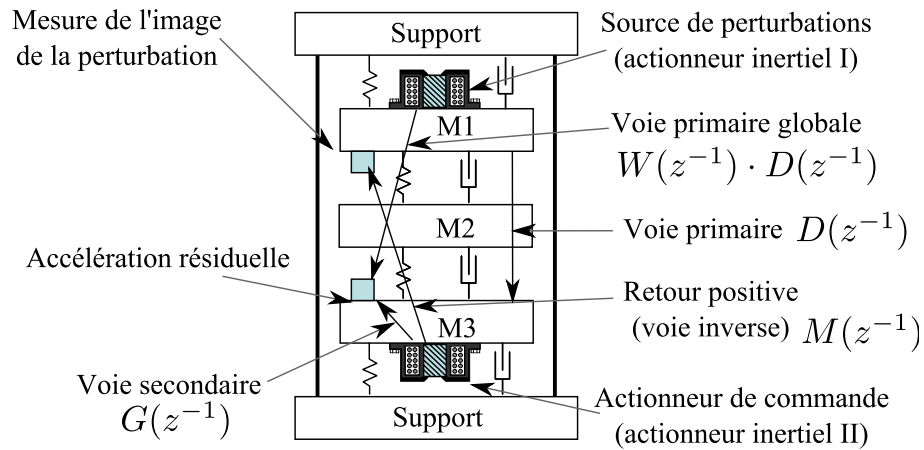


Figure 1.8: Schéma du système de contrôle actif de vibrations utilisé pour les expérimentations.

Dans la première partie de la thèse, des méthodes de commande par action anticipatrice sont proposées et étudiées en tenant compte de l'existence d'un couplage positif entre le signal de commande et la mesure de l'image de la perturbation, qui peut déstabiliser le système. Le filtre « feedforward » est représenté par

$$N(q^{-1}) = \frac{R(q^{-1})}{S(q^{-1})}, \quad (1.5)$$

où

$$R(q^{-1}) = r_0 + r_1 q^{-1} + \dots + r_{n_R} q^{-n_R}, \quad (1.6)$$

$$S(q^{-1}) = 1 + s_1 q^{-1} + \dots + s_{n_S} q^{-n_S} = 1 + q^{-1} S^*(q^{-1}). \quad (1.7)$$

Le filtre « feedforward » estimé est représenté par

$$\hat{N}(q^{-1}) = \frac{\hat{R}(q^{-1})}{\hat{S}(q^{-1})}. \quad (1.8)$$

Le vecteur des paramètres optimaux est

$$\theta^T = [s_1, \dots, s_{n_S}, r_0, \dots, r_{n_R}]^T \quad (1.9)$$

et le vecteur des paramètres estimés est

$$\hat{\theta}^T(t) = [\hat{s}_1(t), \dots, \hat{s}_{n_S}(t), \hat{r}_0(t), \dots, \hat{r}_{n_R}(t)]. \quad (1.10)$$

Les algorithmes développés ci-après en tenant compte de la théorie de l'hyperstabilité de Popov sont analysés dans différents contextes, tout d'abord en supposant qu'une condition de poursuite parfaite est satisfaite (*i.e.*, le nombre exact de paramètres du filtre optimal est connu et on l'utilise pour le filtre mis en œuvre); et ensuite sous des hypothèses moins restrictives.

Bien que développés pour un système de contrôle actif de vibrations, les algorithmes sont également applicables pour les systèmes de contrôle actif du bruit.

1.5.2 Méthodes de compensation des vibrations par des structures hybrides

Dans le **Chapitre 4**, une méthode d'adaptation directe des filtres IIR en utilisant un Algorithme d'Adaptation Paramétrique (AAP) généralisé « Intégral + Proportionnel » (IP-PAA) est présentée et analysée en présence d'un filtre à contre-réaction fixe. La méthode de compensation adaptative des vibrations présentée dans ce chapitre est une généralisation de celles proposées dans [Landau et al., 2011d, Alma et al., 2012a]. Le régulateur en contre-réaction de type RS, ci-après appelé K , est défini par

$$K(q^{-1}) = \frac{B_K(q^{-1})}{A_K(q^{-1})}. \quad (1.11)$$

L'algorithme de compensation feedforward adaptative sera développé sous les hypothèses suivantes :

H1) Le signal $w(t)$ est borné, *i.e.*,

$$|w(t)| \leq \alpha \quad \forall t \quad (0 \leq \alpha < \infty). \quad (1.12)$$

H2) Condition de poursuite parfaite - Il existe un filtre $N(q^{-1})$ de dimension finie de telle sorte que

$$\frac{N(z^{-1})}{1 - N(z^{-1})M(z^{-1})}G(z^{-1}) = -D(z^{-1}) \quad (1.13)$$

et les polynômes suivants:

- de la boucle interne

$$P(z^{-1}) = A_M(z^{-1})S(z^{-1}) - B_M(z^{-1})R(z^{-1}), \quad (1.14)$$

- de la boucle (G-K)

$$P_d(z^{-1}) = A_G(z^{-1})A_K(z^{-1}) + B_G(z^{-1})B_K(z^{-1}), \quad (1.15)$$

- du système

$$P_{fb-ff} = A_M S[A_G A_K + B_G B_K] - B_M R A_K A_G \quad (1.16)$$

sont stables.

H3) Contexte déterministe - L'effet du bruit de mesure sur l'erreur résiduelle est négligé.

H4) Le modèle de la voie primaire $D(z^{-1})$ est inconnu et invariant.

La première étape pour le développement des algorithmes est d'établir une relation entre les erreurs d'estimation des paramètres du filtre « feedforward » et l'accélération résiduelle mesurée. Ceci est donné par l'équation suivante :

$$\varepsilon(t+1) = \frac{A_M(q^{-1})A_G(q^{-1})A_K(q^{-1})G(q^{-1})}{P_{fb-ff}(q^{-1})} [\theta - \hat{\theta}]^T \phi(t), \quad (1.17)$$

où

$$\begin{aligned} \phi^T(t) &= [-\hat{u}_1(t), \dots, -\hat{u}_1(t-n_S+1), \hat{y}_1(t+1), \dots, \hat{y}_1(t-n_R+1)] \\ &= [\phi_{\hat{u}_1}^T(t), \phi_{\hat{y}_1}^T(t)], \end{aligned} \quad (1.18)$$

est le vecteur d'observations.

En filtrant le vecteur $\phi(t)$ par le filtre asymptotiquement stable $L(q^{-1}) = \frac{B_L}{A_L}$, l'éq. (1.17), pour $\hat{\theta}$ constant, devient

$$\varepsilon(t+1) = \frac{A_M(q^{-1})A_G(q^{-1})A_K(q^{-1})G(q^{-1})}{P_{fb-ff}(q^{-1})L(q^{-1})} [\theta - \hat{\theta}]^T \phi_f(t) \quad (1.19)$$

avec

$$\phi_f(t) = L(q^{-1})\phi(t). \quad (1.20)$$

L'éq. (1.19) sera utilisée pour le développement des algorithmes d'adaptation en négligeant pour l'instant la non-commutativité des opérateurs quand $\hat{\theta}$ est variant dans le temps. En remplaçant les paramètres estimés fixes par les paramètres estimés à l'instant courant, l'éq. (1.19) devient l'équation de l'erreur d'adaptation *a posteriori* non-filtrée (qui est calculée)

$$\varepsilon(t+1) = \frac{A_M(q^{-1})A_G(q^{-1})A_K(q^{-1})}{P_{fb-ff}(q^{-1})L(q^{-1})} G(q^{-1}) [\theta - \hat{\theta}(t+1)]^T \phi_f(t). \quad (1.21)$$

L'éq. (1.21) possède la forme standard d'une erreur d'adaptation *a posteriori* ([Landau et al., 2011g]), ce qui suggère l'utilisation de l'algorithme d'adaptation paramétrique « Intégral + Proportionnel » (IP-PAA) suivant

$$\hat{\theta}_I(t+1) = \hat{\theta}_I(t) + \xi(t)F_I(t)\Phi(t)\nu(t+1) \quad (1.22a)$$

$$\hat{\theta}_P(t+1) = F_P(t)\Phi(t)\nu(t+1) \quad (1.22b)$$

$$\varepsilon(t+1) = \frac{\varepsilon^0(t+1)}{1 + \Phi^T(t)(\xi(t)F_I(t) + F_P(t))\Phi(t)} \quad (1.22c)$$

$$\nu(t+1) = \varepsilon(t+1) + \sum_{i=1}^{n_1} v_i^B q^{-i} \varepsilon(t+1-i) - \sum_{i=1}^{n_2} v_i^A q^{-i} \nu(t+1-i) \quad (1.22d)$$

$$F_I(t+1) = \frac{1}{\lambda_1(t)} \left[F_I(t) - \frac{F_I(t)\Phi(t)\Phi^T(t)F_I(t)}{\frac{\lambda_1(t)}{\lambda_2(t)} + \Phi^T(t)F_I(t)\Phi(t)} \right] \quad (1.22e)$$

$$F_P(t) = \alpha(t)F_I(t), \quad \alpha(t) > -0.5 \quad (1.22f)$$

$$F(t) = \xi(t)F_I(t) + F_P(t) \quad (1.22g)$$

$$\xi(t) = 1 + \frac{\lambda_2(t)}{\lambda_1(t)} \Phi^T(t)F_P(t)\Phi(t); \quad (1.22h)$$

$$\hat{\theta}(t+1) = \hat{\theta}_I(t+1) + \hat{\theta}_P(t+1) \quad (1.22i)$$

$$1 \geq \lambda_1(t) > 0, \quad 0 \leq \lambda_2(t) < 2, \quad F_I(0) > 0 \quad (1.22j)$$

$$\Phi(t) = \phi_f(t), \quad (1.22k)$$

où $\nu(t+1)$ est l'erreur d'adaptation *a posteriori* généralisée.

La stabilité du système sera assurée si la fonction de transfert donnée par

$$H' = H - \frac{\lambda_2}{2} = \frac{A_M A_G A_K}{P_{fb-ff}} \frac{GV}{L} - \frac{\lambda_2}{2} \quad (1.23)$$

est SPR. Ceci est une condition suffisante pour la stabilité du système en boucle fermée.

Plusieurs algorithmes seront considérés en tenant compte des filtres V et L :

Algorithme <i>I</i>	$L = G, V = 1$	
Algorithme <i>IIa</i>	$L = \hat{G}, V = 1$	
Algorithme <i>IIb</i>	$L = \hat{G}, V \neq 1$	
Algorithme <i>IIc</i>	$L = \frac{\hat{G}}{1 + \hat{G}K}, V = 1$	
Algorithme <i>IId</i>	$L = \frac{\hat{G}}{1 + \hat{G}K}, V \neq 1$	
Algorithme <i>III</i>	$L = \frac{\hat{A}_M \hat{A}_G A_K}{\hat{P}_{fb-ff}} \hat{G}, V = 1$	(1.24)

où

$$\hat{P}_{fb-ff} = \hat{A}_M \hat{S} [\hat{A}_G A_K + \hat{B}_G B_K] - \hat{B}_M \hat{R} A_K \hat{A}_G \quad (1.25)$$

est une estimation du polynôme caractéristique du système.

Quand la condition de poursuite parfaite n'est pas satisfaite, une analyse de la distribution des biais des paramètres montre que de bonnes estimations sont obtenues dans les régions des fréquences qui sont les plus importantes d'un point de vue du contrôle (là où le gain de la voie secondaire et la distribution spectrale de la perturbation sont importants). Il est également montré, en utilisant la théorie des moyennes développée dans [Anderson et al., 1986] (voir aussi [Landau et al., 2011g]), que la condition SPR peut être relaxée en tenant compte du contenu spectral de la perturbation. Cela signifie que la condition SPR ne doit pas être nécessairement satisfaite sur toute la plage de fréquences. Il suffit, en gros, qu'elle soit satisfaite dans une bande fréquentielle limitée, si cette bande couvre le contenu spectral le plus important de la perturbation.

On propose dans ce chapitre une autre façon d'assouplir la condition SPR. Les avantages de l'adaptation IP-PAA sont mis en évidence par une analyse théorique et on constate que l'utilisation de cette adaptation a une influence bénéfique sur la stabilité et sur les performances de filtre adaptatif.

Des résultats expérimentaux confirment les conclusions théoriques. Premièrement, l'amélioration des performances par l'utilisation de l'adaptation IP-PAA est démontrée avec des résultats expérimentaux. La Figure 1.9 présente une comparaison des différents résultats obtenu en boucle ouverte et avec contrôle adaptatif sans et avec IP-PAA.

Deuxièmement, pour le cas du contrôle sans contre-réaction fixe, on cherche à améliorer la condition SPR en utilisant l'adaptation IP-PAA. La Figure 1.10 présente une estimation de la fonction $H(z^{-1})$ pour l'Algorithme *IIa* (voir aussi l'éq. (1.23)). On observe que cela n'est pas SPR dans des régions de fréquence où la perturbation est aussi importante (à comparer avec la densité spectrale de puissance obtenue en boucle ouverte dans la Figure 1.9). En utilisant l'adaptation IP-PAA on obtient tout de même une amélioration des performances comme montré dans la Figure 1.11.

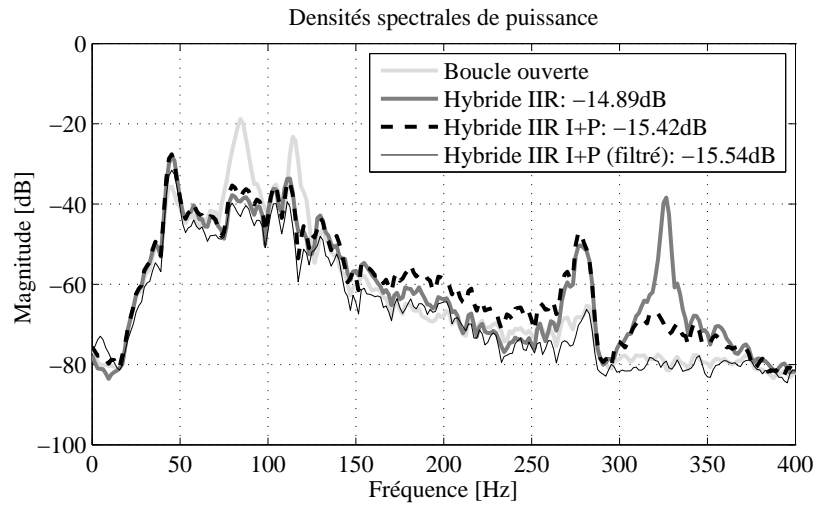
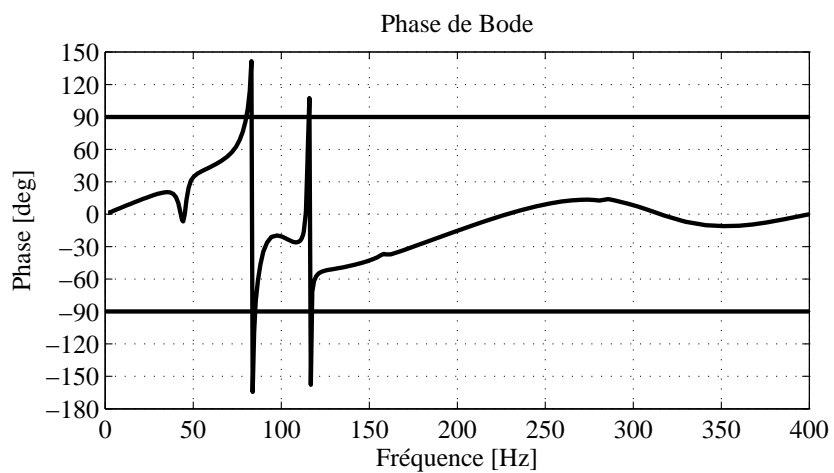


Figure 1.9: Densités spectrales de puissance des filtres adaptatifs.

Figure 1.10: Phase de la fonction de transfert $H(z^{-1})$ estimée pour l'algorithme *IIa*.

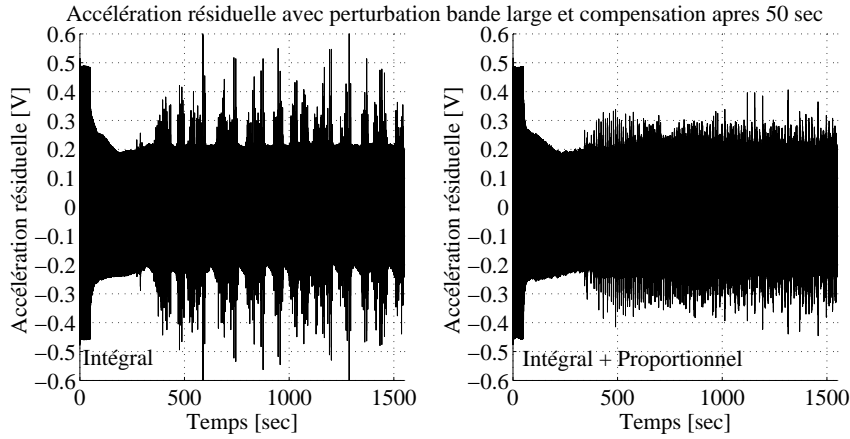


Figure 1.11: Résultats en temps réel avec l'algorithme *IIa* avec adaptation scalaire « Intégral » (à gauche) et « Intégral + Proportionnel » (à droite).

1.5.3 Méthodes de contrôle « feedforward » en utilisant la paramétrisation de Youla-Kučera

Ensuite, les avantages de la paramétrisation de Youla-Kučera sont exposés et une méthode basée sur elle est proposée dans le **Chapitre 5**. Dans ce chapitre, des algorithmes qui s'appuient sur la paramétrisation de Youla-Kučera sont développés autour de filtres adaptatifs de structure FIR ainsi qu'avec des filtres adaptatifs de structure IIR. Le principal avantage de cette paramétrisation est la possibilité de garantir la stabilité de la boucle interne positive. Ceci est toujours assuré si on utilise une structure FIR mais non plus si on utilise une structure IIR. Bien que cette dernière perde cet avantage, on constate une réduction du nombre de paramètres à adapter pour obtenir les mêmes performances, ce qui est très important dans le contrôle actif de bruit. En plus, contrairement aux filtres adaptatifs IIR directs, pour les filtres adaptatifs IIRYK, on observe l'avantage d'un contrôle de la stabilité beaucoup plus facile. Les algorithmes proposés sont analysés dans des conditions similaires à celles du Chapitre 4 et vérifiés en pratique sur le système décrit précédemment.

Dans le cas général des paramètres Youla-Kučera IIR, les polynômes du filtre adaptatif « feedforward » deviennent

$$R(q^{-1}) = A_Q(q^{-1})R_0(q^{-1}) - B_Q(q^{-1})A_M(q^{-1}), \quad (1.26)$$

$$S(q^{-1}) = A_Q(q^{-1})S_0(q^{-1}) - B_Q(q^{-1})B_M(q^{-1}), \quad (1.27)$$

où $S_0(q^{-1})$ et $R_0(q^{-1})$ représentent le dénominateur et le numérateur du régulateur central et $A_Q(q^{-1})$, $B_Q(q^{-1})$ sont le dénominateur et le numérateur du paramètre Youla-Kučera optimal

$$Q(q^{-1}) = \frac{B_Q(q^{-1})}{A_Q(q^{-1})} = \frac{b_0^Q + b_1^Q q^{-1} + \dots + b_{n_{BQ}}^Q q^{-n_{BQ}}}{1 + a_1^Q q^{-1} + \dots + a_{n_{AQ}}^Q q^{-n_{AQ}}}. \quad (1.28)$$

Le filtre QIIR estimé est

$$\hat{Q}(q^{-1}) = \frac{\hat{B}_Q(q^{-1})}{\hat{A}_Q(q^{-1})} = \frac{\hat{b}_0^Q + \hat{b}_1^Q q^{-1} + \dots + \hat{b}_{n_{BQ}}^Q q^{-n_{BQ}}}{1 + \hat{a}_1^Q q^{-1} + \dots + \hat{a}_{n_{AQ}}^Q q^{-n_{AQ}}} \quad (1.29)$$

et le vecteur de ces paramètres est

$$\hat{\theta}^T = [\hat{b}_0^Q, \dots, \hat{b}_{n_{B_Q}}^Q, \hat{a}_1^Q, \dots, \hat{a}_{n_{A_Q}}^Q] = [\hat{\theta}_{B_Q}^T, \hat{\theta}_{A_Q}^T]. \quad (1.30)$$

Deux régulateurs centraux sont utilisés dans ce schéma d'adaptation. Le premier (PP) a été obtenu par placement des pôles. Le deuxième (H_∞) est un régulateur de type H_∞ d'ordre réduit ([Alma et al., 2012b]).

Quelques observations s'imposent :

- La condition de poursuite parfaite devient

$$\frac{G \cdot A_M(R_0 A_Q - A_M B_Q)}{A_Q(A_M S_0 - B_M R_0)} = -D. \quad (1.31)$$

- Le polynôme caractéristique du système de contrôle actif de vibrations devient

$$P(z^{-1}) = A_Q(z^{-1}) (A_M(z^{-1})S_0(z^{-1}) - B_M(z^{-1})R_0(z^{-1})). \quad (1.32)$$

Suivant la même procédure que dans la sous-section précédente, on obtient l'équation de l'erreur d'adaptation *a posteriori*

$$\nu(t+1) = \frac{A_M(q^{-1})G(q^{-1})}{A_Q(q^{-1})P_0(q^{-1})L(q^{-1})} [\theta - \hat{\theta}(t+1)]^T \phi_f(t). \quad (1.33)$$

avec

$$\begin{aligned} \phi_f(t) &= L(q^{-1})\phi(t) \\ &= [\alpha_f(t+1), \dots, \alpha_f(t-n_{B_Q}+1), -\beta_f(t), \dots, -\beta_f(t-n_{A_Q})], \end{aligned} \quad (1.34)$$

où

$$\begin{aligned} \alpha_f(t+1) &= L(q^{-1})\alpha(t+1) \\ \beta_f(t) &= L(q^{-1})\beta(t) \end{aligned} \quad (1.35)$$

et¹

$$\alpha(t+1) = B_M \hat{u}(t+1) - A_M \hat{y}(t+1) = B_M^* \hat{u}(t) - A_M \hat{y}(t+1) \quad (1.36)$$

$$\beta(t) = S_0 \hat{u}(t) - R_0 \hat{y}(t). \quad (1.37)$$

On observe que la paramétrisation FIRYK est un cas particulier de la paramétrisation IIRYK obtenu en remplaçant A_Q par 1.

Les différents choix des filtres L conduisent aux algorithmes suivants :

Algorithme <i>I</i>	$L = G$	
Algorithme <i>IIa</i>	$L = \hat{G}$	
Algorithme <i>IIb</i>	$L = \frac{\hat{A}_M}{\hat{P}_0} \hat{G}$	(1.38)

Algorithme <i>III</i>	$L = \frac{\hat{A}_M}{\hat{P}} \hat{G}$	(1.39)
-----------------------	---	--------

Des résultats expérimentaux sont également donnés pour mettre en évidence l'analyse théorique. Dans la Figure 1.12 les densités spectrales de puissance pour les filtres adaptatifs utilisant des paramètres QFIR et QIIR sont comparées. On observe des résultats similaires obtenus avec QIIR même si le nombre des paramètres est plus que 2 fois plus petit.

¹En absence du contre-réaction fixe, on a $u(t) = u_1(t)$ et $y(t) = y_1(t)$.

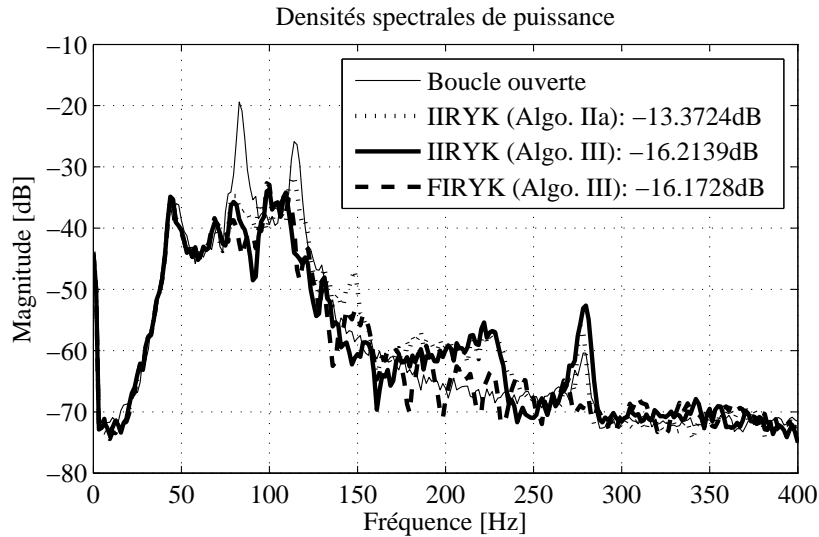


Figure 1.12: Densités spectrales de puissance en boucle ouverte, avec IIRYK ($n_{B_Q} = 3$, $n_{A_Q} = 8$) et avec FIRYK ($n_Q = 31$) en utilisant le régulateur central H_∞ .

1.5.4 Méthodes de contrôle par contre-réaction adaptatif

Dans la **Partie II, Chapitre 6**, la régulation par contre-réaction « feedback » adaptative des perturbations bande étroite est discutée et un algorithme indirect pour réduire des perturbations bande étroite, basé sur des filtres stop-bande (Band-stop Filter, BSF) pour le calibrage de la fonction de sensibilité est présenté. Par ailleurs, une comparaison expérimentale avec l'algorithme de régulation adaptative directe présenté dans [Landau et al., 2011e] est réalisée. Il est montré que la méthode proposée possède des propriétés intéressantes données par les BSFs. Plus précisément, il est possible de régler le niveau de l'atténuation et de réduire les effets sur les fréquences avoisinantes afin de préserver de bonnes marges de robustesse.

La procédure indirecte comprend l'estimation des fréquences des perturbations bande étroite par un observateur, le calcul des filtres stop-bande comme décrit dans [Landau and Zito, 2005] et les modifications des paramètres du régulateur en trouvant la solution d'une équation de Bezout.

L'estimation des fréquences des perturbations est faite en utilisant des Filtres Adaptatifs à Encoche (ANF)

$$H_f(z^{-1}) = \frac{A_f(z^{-1})}{A_f(\rho z^{-1})}, \quad (1.40)$$

où

$$A_f(z^{-1}) = 1 + a_1^f z^{-1} + \dots + a_n^f z^{-n} + \dots + a_1^f z^{-2n+1} + z^{-2n}. \quad (1.41)$$

On suppose que la perturbation a la forme

$$\hat{p}(t) = \sum_{i=1}^n c_i \sin(\omega_i \cdot t + \beta_i) + v(t) \quad (1.42)$$

et on utilise les filtres ANF pour estimer les fréquences ω_i . Le nombre des sinusoides qui constituent la perturbation est supposé connu. Des procédures d'analyse spectrale peuvent être utilisées pour résoudre ce problème.

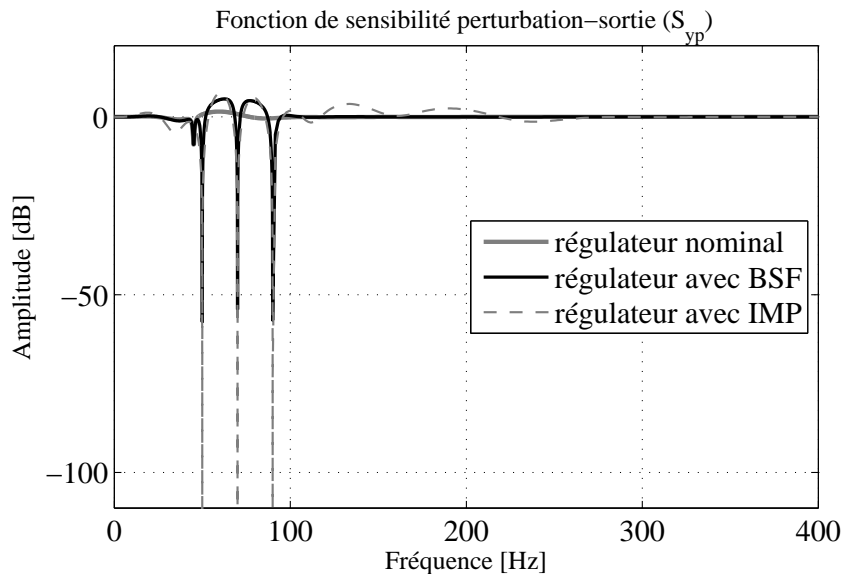


Figure 1.13: Fonction de sensibilité de la sortie avec régulateur nominal (gris), avec un régulateur basé sur le principe du modèle interne (noir) et avec un régulateur basé sur des filtres BSFs (gris en pointillés). Pour le contrôleur avec BSFs on a $\zeta_{d_i} = 0.04$ et $M_i = 60$ dB. Les atténuations sont introduits à 50, 70 et 90 Hz.

En utilisant les fréquences estimées, on peut calculer un filtre stop-bande

$$\frac{S_{BSF_i}(z^{-1})}{P_{BSF_i}(z^{-1})} = \frac{1 + \beta_1^i z^{-1} + \beta_2^i z^{-2}}{1 + \alpha_1^i z^{-1} + \alpha_2^i z^{-2}}. \quad (1.43)$$

qui résulte de la discrétisation du filtre continu (voir aussi [Procházka and Landau, 2003, Landau and Zito, 2005])

$$F_i(s) = \frac{s^2 + 2\zeta_{n_i}\omega_i s + \omega_i^2}{s^2 + 2\zeta_{d_i}\omega_i s + \omega_i^2} \quad (1.44)$$

avec la transformation bilinéaire. Ce filtre introduit une atténuation

$$M_i = -20 \cdot \log_{10} \left(\frac{\zeta_{n_i}}{\zeta_{d_i}} \right) \quad (1.45)$$

à la fréquence ω_i . Les valeurs positives de M_i signifient des atténuations ($\zeta_{n_i} < \zeta_{d_i}$) et les valeurs négatives signifient des amplifications ($\zeta_{n_i} > \zeta_{d_i}$).

Les filtres stop-bande sont utilisés pour calibrer la fonction de sensibilité perturbation-sortie. Leur numérateur, $S_{BSF_i}(z^{-1})$, fera partie du dénominateur du régulateur et leur dénominateur fera partie du polynôme caractéristique de la boucle fermée. L'influence du compensateur en dehors des fréquences des perturbations peut être minimisée en utilisant des valeurs ζ_{d_i} suffisamment petites. La Figure 1.13 présente la comparaison des fonctions de sensibilité perturbation-sortie entre un régulateur central qui n'est pas réalisé pour rejeter des perturbations, un régulateur contenant des filtres stop-bande pour rejeter les perturbations et un régulateur basé sur le principe du modèle interne pour rejeter les perturbations. On observe que pour les amortissements ζ_{d_i} utilisés pour le régulateur avec BSF dans la Figure 1.13, l'influence en dehors des fréquences des perturbations est visiblement moins importante que pour le régulateur avec IMP.

La difficulté est d'introduire le dénominateur des filtres BSF dans le polynôme caractéristique de la boucle fermée. La méthode la plus directe est de calculer le régulateur comme solution de l'équation de Bezout (placement des pôles)

$$P(z^{-1}) = P_0(z^{-1})P_{BSF}(z^{-1}) = A(z^{-1})H_S(z^{-1})S'(z^{-1}) + z^{-d}B(z^{-1})H_{R_1}(z^{-1})R'(z^{-1}). \quad (1.46)$$

$$H_S(z^{-1}) = S_{BSF}(z^{-1})H_{S_1}(z^{-1}) \quad (1.47)$$

Dans les éqs. (1.46) et (1.47), P_{BSF} et S_{BSF} représentent le dénominateur et le numérateur des BSFs, P_0 sont des pôles imposés pour satisfaire certaines conditions de robustesse, A et B sont le dénominateur et le numérateur du modèle, H_{R_1} et H_{S_1} sont les parties fixes du régulateur central et S' et R' doivent être calculés.

Ensuite, la paramétrisation de Youla-Kučera est utilisée pour réduire la complexité de l'équation matricielle qui doit être résolue à chaque période d'échantillonnage pour trouver les paramètres du régulateur. La schéma de la Figure 1.14 décrit cette technique. On utilise la factorisation des polynômes du régulateur :

$$R(z^{-1}) = R_0(z^{-1})P_{BSF}(z^{-1}) + A(z^{-1})H_{R_1}(z^{-1})H_{S_1}(z^{-1})Q(z^{-1}), \quad (1.48)$$

$$S(z^{-1}) = S_0(z^{-1})P_{BSF}(z^{-1}) - z^{-d}B(z^{-1})H_{R_1}(z^{-1})H_{S_1}(z^{-1})Q(z^{-1}), \quad (1.49)$$

Ceci permet de respecter les objectifs de la régulation et de réduire la taille de l'équation matricielle à résoudre. La nouvelle équation de Bezout est

$$S''P_{BSF} = S_{BSF}S' + q^{-d}BH_{R_1}Q. \quad (1.50)$$

Dans la dernière équation, S'' fait partie du dénominateur du régulateur central et on est intéressé à obtenir Q . La dimension de la nouvelle équation matricielle est $n_{BezYK} \times n_{BezYK}$, dont

$$n_{BezYK} = n_B + d + n_{H_{R_1}} + 2 \cdot n - 1. \quad (1.51)$$

Pour comparaison, la dimension de l'équation de Bezout initiale était $n_{Bez} \times n_{Bez}$, dont

$$n_{Bez} = n_A + n_B + d + n_{H_{S_1}} + n_{H_{R_1}} + 2 \cdot n - 1. \quad (1.52)$$

n_A , n_B et d sont les ordres et le retard du modèle, $n_{H_{S_1}}$ et $n_{H_{R_1}}$ sont les ordres des parties fixes du régulateur central et n est le nombre des perturbations sinusoïdales supposé connu.

La Figure 1.15 présente la densité spectrale de puissance obtenue en boucle ouverte, avec le régulateur adaptatif avec filtres stop-bande et avec un régulateur adaptatif basé sur le principe du modèle interne. On constate une influence importante du régulateur basé sur le principe de modèle interne en dehors de la zone fréquentielle d'atténuation. Par contre, pour le régulateur avec filtres stop-bande, l'influence est négligeable.

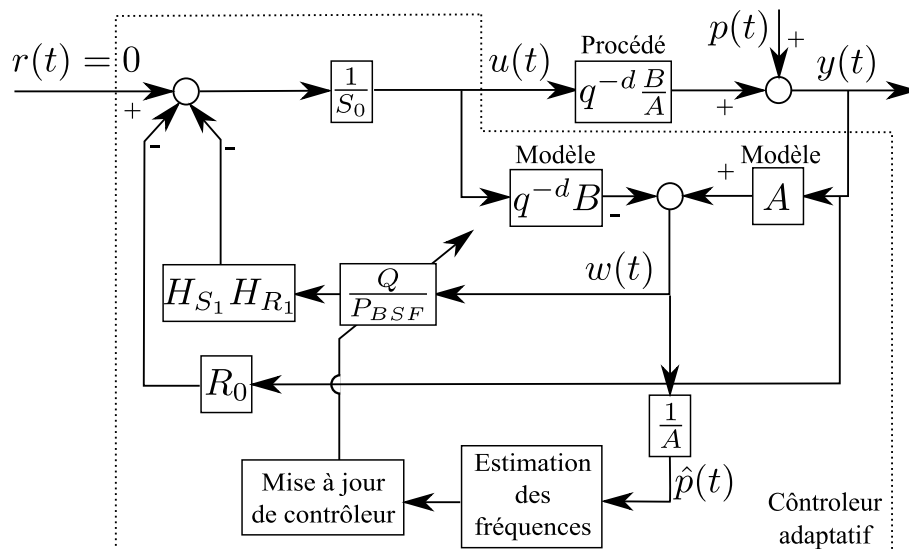


Figure 1.14: Schéma de l'algorithme adaptatif utilisant la paramétrisation de Youla-Kučera.

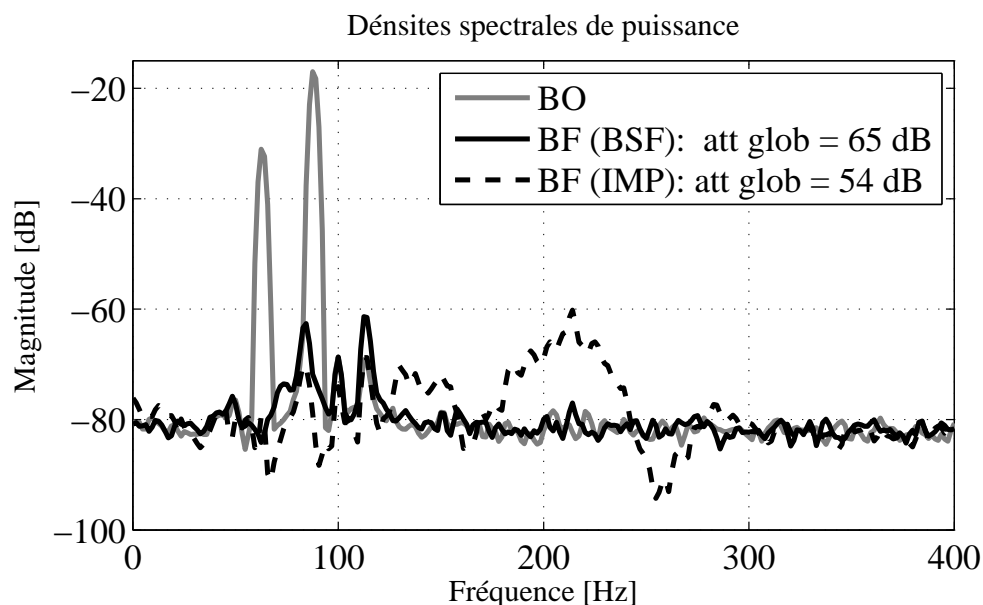


Figure 1.15: Comparaison des densités spectrales des puissances entre la mesure en boule ouverte et les accélérations résiduelles obtenues avec deux régulateur adaptatifs (le premier avec filtres stop-bande et le deuxième avec le principe de modèle interne). L'entrée de la voie primaire est constituée par deux signaux sinusoidaux à 63 Hz et à 88 Hz .

CHAPTER 2

INTRODUCTION (ENGLISH)

This introductory chapter describes the basic problems of Active Noise Control (ANC) and Active Vibration Control (AVC) that have motivated the research and gives an overview of the main results in the literature. In the last two sections of the chapter, the original contributions of this work are summarized and an outline of the dissertation is given.

2.1 Motivation

The basic principles of Active Noise and Vibration Control (ANVC) will be explained in this section. Some examples will be used to state the control problem associated with ANVC, and the context of this work will be presented.

Henri Coandă is probably the first one to have mentioned the Active Noise Control (ANC) problem in a French patent ([Coanda, 1930]). He was followed shortly after by Paul Lueg ([Lueg, 1934]) and Harry F. Olson [Olson and May, 1953]. The problem addressed in their works was that of silencing noise coming from a source by the use of a microphone, an amplifier and a loudspeaker. It is shown that if the silencing ensemble would be capable of creating a sound wave of same frequency characteristics as the noise source but with a 180° shift in the phase, then it would be possible to eliminate the noise in the field of action of the sound waves produced by the loudspeaker. The reduction of engine sound in airplanes and of the noise created by different types of machinery in the vicinity of the operator are mentioned as possible applications of these techniques.

In the scientific literature, three different types of control methods have been considered for compensating noises or vibrations ([Fuller et al., 1997, Snyder, 2000]): passive, semi-active and active.

The classical solution is that of adding insulation or damping materials and this is called passive because no control algorithm is needed. It has the advantages of being simple and straightforward to use, and in the same time, providing robust, reliable, and economically efficient solutions. The usage of the passive absorber is however limited by the impossibility to adjust the control forces, the difficulty in targeting the control action at particular objectives, and the dependence of the control force on the natural system's dynamics. One such example is the Helmholtz resonator described in [Olson and May, 1953, Fleming et al., 2007].

To solve these shortcomings, different control methods that permit the use of sensors and actuators have been employed. The simplest one is the semi-active approach which is obtained by using actuators that behave as passive elements, consequently allowing only storage or dissipation of energy. Still, they represent a step towards active control as their

mechanical properties can be adjusted by the use of a signal stemming from a controller. As an example, the shock-absorbers in some vehicles have a computer controlled viscous damping coefficient. As in the passive case, no energy is injected into the system.

This thesis focuses on the third of the aforementioned solutions, more precisely on the active control. The main difference with the other two ones is its ability to supply mechanical power to the system and to target the control action towards specific objectives. In noise control applications, the frequencies of interest range from 20 *Hz* to 20,000 *Hz*. It is stated in the literature ([Olson and May, 1953, Fuller and von Flotow, 1995, Elliott, 2001]) that passive techniques usually give satisfactory results in the high frequency band (reductions of more than 40 *dB* above 500 *Hz*); therefore it is in the low frequencies that the use of active methods first became interesting, and in particular, from an adaptive control point of view as it will be latter shown. There is a large number of applications where outside noises/vibrations need to be reduced. One such example is given in Fig. 2.1, which shows how head-phones with noise reduction capabilities work. Modern head-phones are designed to give good quality sound even in noisy environments. For this purpose, they measure outside disturbances by the use of a microphone as a transducer and cancel out these disturbances using a control algorithm and the built-in speaker as an actuator. In the ideal case, the added signal should be of equal magnitude and of 180° phase shift (negative) so as to completely cancel the disturbing noise. Further background analysis can be found in the survey papers of [Elliott and Nelson, 1993, Fuller and von Flotow, 1995, Guicking, 2007].

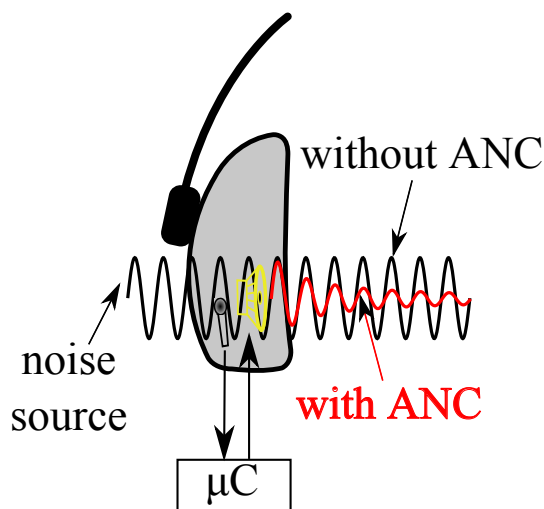


Figure 2.1: Outside noise reduction in headphones by use of ANC.

2.2 Problem Description

This section provides the reader with a brief description of the Active Noise and Vibration Control problems that will be treated in the later chapters of this thesis. The main objective is that of reducing the level of vibration (or noise) at a predefined location of interest. A general presentation of the system and the strategies of control will be given in the next subsections.

2.2.1 Control system configurations

Figure 2.2 represents an ANVC system using both feedforward and feedback compensators. The system has two inputs and two outputs. The first input is the *disturbance* $w(t)$ which is generated by the unknown disturbance source $s(t)$ passed through a filter with unknown characteristics. The second input is the *control signal*, $u(t)$. The first output is the measurement of the *residual acceleration*, $e(t)$ (also called the *performance variable*) and the second output is a *signal correlated with the unknown disturbance*, $y_1(t)$ in Figure 2.2. This correlation is a result of the physical characteristics of the system. As shown in Figure 2.2, the path that transmits the filtered disturbance, $w(t)$, to the residual acceleration is called the *primary path*. The control signal, on the other hand, is transmitted to the residual acceleration through the *secondary path*. The residual acceleration is formed by addition between the output of the primary path, denoted $x(t)$, and the output of the secondary path, denoted $z(t)$. ANVC systems present in general also a coupling between the control signal and the measured $y_1(t)$, as previously stated, which is shown in Figure 2.2 as the *positive coupling path* (also called *reverse path*). This results in an internal positive feedback which can destabilize the ANVC system if not taken into account.

The objective is that of minimizing the performance variable, $e(t)$, by computing an appropriate control, $u(t)$, based on the measurements $e(t)$ and $y_1(t)$.

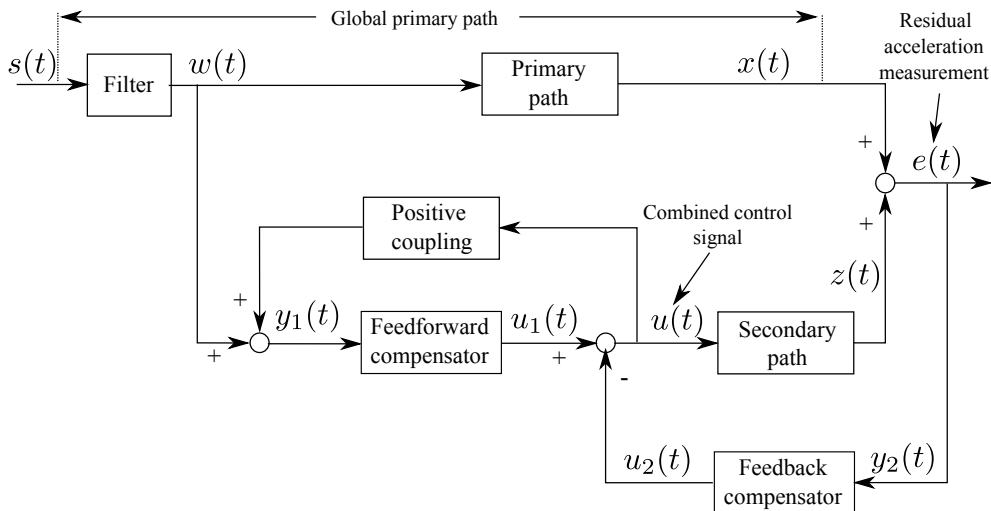


Figure 2.2: Block diagram representation of the combined feedforward-feedback control problem.

One can see that, in the control system architecture presented in Figure 2.2, the control signal $u(t)$ is obtained by the subtraction between the *feedforward control*, $u_1(t)$, and the *feedback control*, $u_2(t)$. The measurement obtained from the system can be put into a vector form as $y(t) = [y_1(t), y_2(t)]^T = [y_1(t), e(t)]^T$. As a consequence, the controller also has a vector representation $\kappa = [N, -K]^T$, where N and K denote respectively the *feedforward* and the *feedback* compensators. With these notations, the equation relating the measurements to the control signal is given by

$$u(t) = u_1(t) - u_2(t) = N \cdot y_1(t) - K \cdot y_2(t) = \kappa^T \cdot y(t). \quad (2.1)$$

The feedforward controller denomination attributed to N is motivated by the fact that $y_1(t)$, also called *correlated image of the disturbance*, is measured upstream of the

performance variable. This assumes also that it is physically possible to obtain such a measurement. The situations where this is not possible constitute feedback control problems, while the others are more generally addressed in the literature as hybrid control.

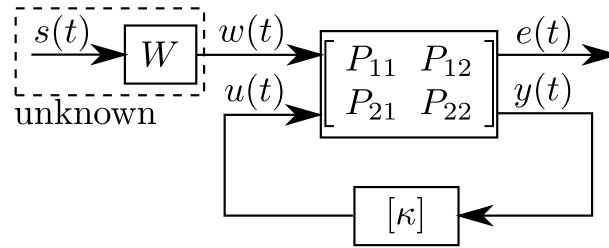


Figure 2.3: Generalized ANVC system representation.

A standard feedback representation in the form of a 2 input - 2 output system can also be considered as shown in Figure 2.3. This representation is very well known in robust and optimal control (see also [Tay et al., 1997, Zhou et al., 1996]). The equations associated with the feedback system representation are

$$\begin{bmatrix} e(t) \\ y(t) \end{bmatrix} = \begin{bmatrix} P_{11} & P_{12} \\ P_{21} & P_{22} \end{bmatrix} \begin{bmatrix} w(t) \\ u(t) \end{bmatrix} = \begin{bmatrix} D & G \\ 1 & M \\ D & G \end{bmatrix} \begin{bmatrix} w(t) \\ u(t) \end{bmatrix}, \quad (2.2)$$

and the control is given by (2.1).

Two special cases of this problem will be discussed next.

2.2.2 Feedforward control problem

One particular problem is that of the feedforward vibration (or noise) compensation. A schematic representation of this situation is given in Figure 2.4. As it can be observed, $K = 0$ in Figure 2.4. Therefore, in this situation we obtain $y(t) = y_1(t)$ and $u(t) = u_1(t)$. As mentioned earlier, it is supposed that a transducer can be used that provides a correlated image of the disturbance upstream of the performance variable $e(t)$, therefore allowing a feedforward regulation approach to be implemented.

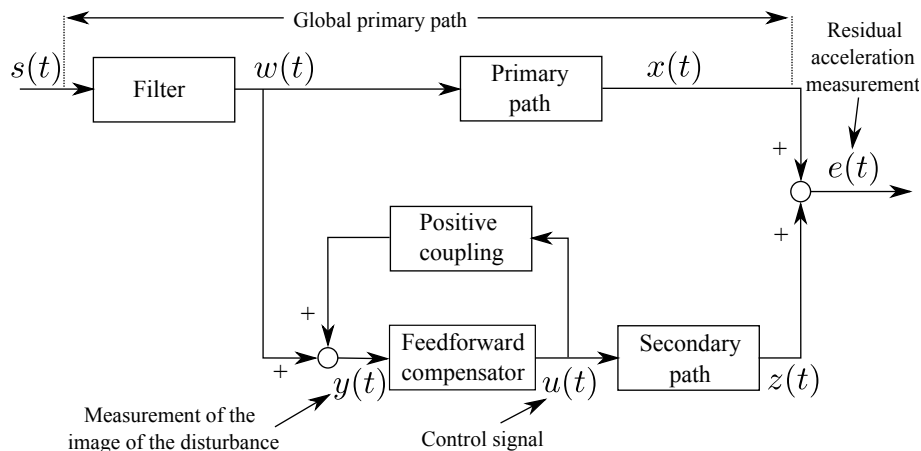


Figure 2.4: Block diagram representation of the feedforward ANVC problem.

This method is used in practical situations where large band perturbations need to be reduced. In these cases, a pure feedback approach would be hindered by the limitations

imposed through the Bode integral ([Hong and Bernstein, 1998]) and only narrow band disturbances could be compensated (as it will be shown in the next section).

To deal with large band disturbances, the scheme in Figure 2.4 can be used. It can be immediately observed from this representation that the measured correlated image of the disturbance will not only contain the significant information from the disturbance source but it will also be contaminated by the control signal transmitted through the positive coupling path. The presence of this intrinsic positive feedback complicates the controller design because it can cause instability.

In many of the research studies that began to propose solutions for this problem, the influence of the positive feedback coupling was not taken into account ([Widrow et al., 1975]), because it was either considered that its influence could be compensated or that it was too weak to raise any problems. Several techniques have been reported in the literature for the compensation of the positive feedback coupling's effect, some being of mechanical nature and other being more related to the control algorithm. One example concerning the second technique, called feedback neutralization, has been described in [Kuo and Morgan, 1999, Nelson and Elliott, 1993] and relies on a very good estimation of the feedback path's model. However, it has been reported in [Nelson and Elliott, 1993, Mosquera et al., 1999] that if the estimation is not exact, then the possibility for instability still exists.

The algorithms presented in this dissertation are designed to provide good results in the presence of the feedback coupling path and therefore there is no need for positive feedback path cancelation.

The use of adaptive control is motivated by the fact that the characteristics of the disturbance can vary in time or that the identified models might not be exact representations of the system's paths.

2.2.3 Feedback regulation problem

The feedback regulation is another special case. For this, one can only provide a solution for reducing narrow band disturbances. In general, the disturbances will be supposed to represent vibrations coming from multiple narrow band disturbances sources. A schematic representation of this situation is given in Figure 2.5. It should be observed that in this context $N = 0$, and consequently, we will have $y(t) = y_2(t)$ and $u(t) = u_2(t)$.

In the situations where a second transducer to measure an image correlated with the disturbance cannot be used because the physical characteristics of the process prevent it, feedback control techniques have to be applied. As discussed earlier, the Bode integral limitations permit only narrow band disturbances to be reduced or rejected; therefore, in this part of the dissertation, the objectives will be that of developing techniques for the compensation of multiple stationary or variable sinusoidal disturbances.

2.3 Literature Overview

In this section a review of the important contributions in the literature of feedforward and feedback regulation of noise or vibrations is presented.

2.3.1 Feedforward control of vibrations

The first attempts in the literature of adaptive feedforward active vibration (or noise) compensation have been done neglecting the positive feedback coupling. Most of the

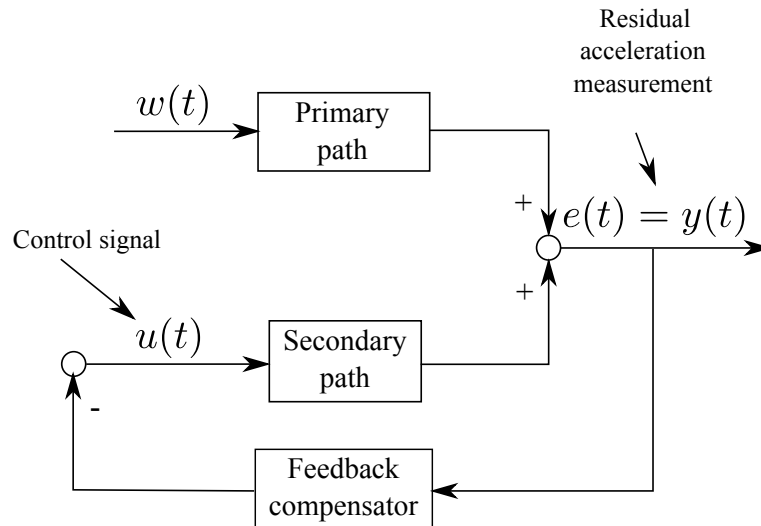


Figure 2.5: Block diagram representation of the feedback ANVC problem.

work that has been done in this field is centered around various developments of the Least Mean Squares (LMS) gradient search algorithm (introduced in [Widrow, 1971]). The objective of the LMS method is to find the minimum point on the Mean Square Error (MSE) surface by updating the parameters of a Finite Impulse Response (FIR) filter in a direction which is an estimate of the steepest descent. For this purpose, the algorithm uses the current sample of the squared error.

One of the first improvements was the Filtered-X LMS (FxLMS), proposed independently by [Burges, 1981] and [Widrow et al., 1981], which used a filtered version of the observations (measurements correlated with the disturbance) in the adaptation algorithm. Both adaptation schemes studied by these authors (adaptive sound controller in Burges's research and adaptive inverse control in Widrow's) presented a secondary path model that influenced the adaptation procedure. A filtering of the observation vector through the model of the secondary path had to be performed in order to obtain good estimations. Both problems addressed by these authors presented the adaptation of a FIR filter in a scheme without feedback coupling.

Despite the stability and the convex performance surface of the FIR filters, there are situations when the use of Infinite Impulse Response (IIR) filters is especially interesting (*e.g.*, to obtain good performances, one often has to use a large number of parameters for the FIR filter because of their all zero form, while with IIR filters, it is possible to obtain similar performances with a significantly reduced number of parameters). A method to adapt IIR filters was originally proposed by Feintuch in [Feintuch, 1976], called the Recursive LMS (RLMS), and provides a transformation of the basic LMS filter adaptation to the IIR structure. Later, the algorithm was improved by using filtered observations in the same way as was done in the FxLMS, providing the Filtered-U LMS (FuLMS) algorithm. The FuLMS was first introduced in [Eriksson et al., 1987] for ANVC applications but no convergence and stability analysis was provided. As an application example of this algorithm, the reduction of noise inside jet aircrafts, produced by the engines that are mounted directly on the fuselage is described in [Billoud, 2001].

The family of LMS algorithms uses an approximate estimate of the steepest descent direction, obtained by taking the gradient of the current sample of the squared error instead of the gradient of the mean squared error. An improvement has been obtained

in the Filtered-v LMS (FvLMS) algorithm presented in [Crawford and Stewart, 1997] where the full-gradient is calculated. Nevertheless, considering slow adaptation of the parameters, some approximations have been done to reduce the algorithm's numerical complexity.

A difficult problem for adaptive IIR filters in the context of ANVC is their stability and convergence analysis. Compared to the output error algorithms, this is complicated mainly by the secondary and feedback coupling paths.

One way of analyzing the convergence, in a stochastic environment, is the O.D.E. method of Ljung ([Ljung and Söderström, 1983] - first presented in [Ljung, 1977a] and applied in the analysis of the output error estimation method of [Landau, 1976] in [Ljung, 1977b]). Using this, it was possible to analyze the properties of the FuLMS algorithm and in [Wang and Ren, 2003, Fraanje et al., 1999]. Conditions are found so as to assure convergence w.p.1 in the case of positive feedback coupling but with some restricting conditions, two of them being that a vanishing adaptation gain has to be used and that the feedback path does not destabilize the system.

Another approach for the stability and convergence analysis of adaptive algorithms is the *hyperstability* theory. This was first proposed in the seminal work of V.M. Popov presented in the original publications [Popov, 1960, Popov, 1966] and then translated in [Popov, 1963, Popov, 1973]. One of the most important consequences of this theory is its use in the design of stable adaptive algorithms alongside positive dynamic systems. The initial framework for studying adaptive systems using the hyperstability was established in [Landau and Silveira, 1979, Landau, 1979, Landau, 1980] and a complete theoretical analysis can be found in [Landau et al., 2011g]. Unlike the Lyapunov approach which is limited by the difficulty in finding appropriate Lyapunov functions, a large family of adaptation laws leading to stable adaptive algorithms can be designed using the hyperstability theory.

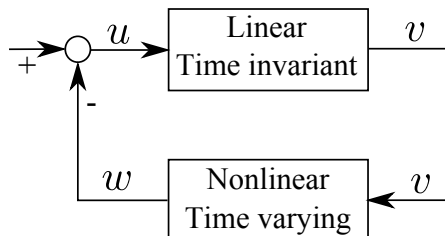


Figure 2.6: Standard representation used in the analysis of adaptive systems using hyperstability theory.

The hyperstability mainly deals with the stability of a class of systems that can be represented in the form given in Figure 2.6. In this configuration, it is supposed that the nonlinear and/or time-varying feedback block is such that it satisfies an input-output relation of the form

$$\sum_{t=0}^{t_1} v(t)w(t) \geq -\gamma^2 \text{ for all } t \geq 0 \quad (2.3)$$

One of the early uses of hyperstability in the synthesis of adaptive algorithms was reported in [Treichler et al., 1978, Larimore et al., 1980]. The Simple Hyperstable Adaptive Recursive Filter (SHARF) is convergent only for slow adaptation. The more complex HARF version has, instead, been proven convergent under less restrictive conditions

([Johnson, 1979]). Both algorithms use filtering of the estimation error. The challenge encountered in these algorithms and which makes them difficult to use in ANVC systems is the choice of the filter that assures the Strictly Positive Real (S.P.R.) condition, especially due to the existence of the secondary and reverse paths. Furthermore, they are not presented in an ANVC context, therefore the feedback coupling is not taken into account.

A filtered observations - filtered error variant of the HARF algorithm is presented in [Mosquera et al., 1999]. The convergence is concluded upon, based on the previously developed theory. An implementation on an ANC system is experimented using feedback cancellation but the results were not satisfactory.

Similarly to the (S)HARF algorithms, in [Snyder, 1994] a method applicable in active control without positive feedback coupling is formulated. In contrast to the (S)HARF algorithms, the filtering is done on the observation vector, whereas in the aforementioned algorithms it was done on the estimation error. A way of choosing the filtering is given.

Another attempt to use the stability approach to design an adaptive algorithm for ANC was proposed in [Jacobson et al., 2001]. However, specific assumptions taken in the development restrict the application of this algorithm to specific cases and, as shown in [Landau et al., 2011d]. The algorithm can even become unstable in a more general ANVC problem. More specifically, it was supposed that the secondary path is characterized by a SPR transfer function which is seldom true.

In addition to these directions of research, much work was done also on improving the numerical efficiency, especially in the case of RLS type algorithms and references pertaining to these methods can be found in [Montazeri and Poshtan, 2010, Montazeri and Poshtan, 2011], but it has been limited to the case without positive feedback coupling.

An equation error algorithm has been presented in [Sun and Chen, 2002]. The algorithm is globally convergent when the feedback coupling is not present and the measurement noise is zero. In the presence of measurement noise, it is shown that the result is biased. Also when feedback exists, a local minimum is attained instead of a global one. To overcome these problems, a Steiglitz-Mcbride type IIR algorithm has been published in [Sun and Meng, 2004]. Simulation results without feedback coupling are presented. One other drawback of this algorithm is that stability is assumed before hand but, in practice, the poles of the IIR filter may move outside the unit circle and instability may then occur.

A different approach is considered in [Zeng and de Callafon, 2006], where a Model Based Design (MBD) controller obtained using the Youla-Kučera parametrization of all stabilizing controllers is implemented for a noise cancellation problem. The feedforward filter is first identified from open loop data and then an orthonormal basis function is designed, based on the method presented in [Heuberger et al., 1995]. A further difference with previously mentioned research results is that the parameters' adaptation is not done continuously but at certain intervals during which the system operates based on the last computed values. No stability analysis has been performed.

To conclude on the review of the various methods developed in the field of ANVC, it is necessary to mention also the H_∞ and H_2 MBD compensators. This approach has been considered in [Bai and H.H.Lin, 1997, Rotunno and de Callafon, 2003, Alma et al., 2012b]. However, the resulting compensator does not have adaptation capabilities and its performance is not necessarily very good. Provided that the high dimension of the resulting compensator can be reduced, it may constitute an "initial" value for the parameters of an adaptive or self-tuning feedforward compensator. In

[Bai and H.H.Lin, 1997], it is shown experimentally that the results obtained with the H_∞ approach are better than those obtained using the very popular FULMS adaptation algorithm (for a disturbance with known spectral characteristics). A similar comparison done experimentally during the work for this thesis and published in [Landau et al., 2011d] confirms this fact. However, this is no more true when comparing the H_∞ design with the new adaptive algorithms introduced in this thesis.

It is important to remark that all these contributions (except [Alma et al., 2012b]) have been done in the context of ANC. While the algorithms for ANC can be used in AVC, one has to take into account the specificity of these latter systems which feature many low damped vibration modes (resonance) and low damped complex zeros (anti-resonance).

2.3.2 Feedback rejection of multiple narrow band disturbances

Often in practice, it is not possible to use a second transducer to measure the image of a disturbance. In these situations, a feedback control approach has to be considered. Taking into account the Bode integral restriction ([Åström and Murray, 2008, Zhou et al., 1996]) we can conclude that only disturbances on a finite band of frequencies can be attenuated. Consequently, this part of the dissertation is concerned with the rejection of multiple time-varying sinusoidal disturbances. A comparative analysis of feedback and feedforward disturbance rejection is given in [Elliott and Sutton, 1996].

A review of the existing methods for narrow band disturbance rejection is given hereafter. To begin with, the difference between the paradigms "adaptive regulation" and "adaptive control" was pointed out in a recent paper ([Landau et al., 2011f]). It is observed there that in classical "adaptive control" the objective is tracking/disturbance attenuation in the presence of unknown and time varying plant model parameters. Thus, the focus of adaptive control is put on the adaptation with respect to variations in the parameters of the plant's model. The model of the disturbance is assumed to be known and invariant.

Conversely, the "adaptive regulation" paradigm refers to asymptotically suppression (or attenuation) of the effect of unknown and time varying disturbances. It is also assumed that the plant model is known and that a robust control design can be applied to deal with possible small variations of its parameters. Thus no effort is put onto estimating in real time the model of the process. An important aspect is that the disturbance should be located in the frequency region where the plant model has enough gain.

The objective of this dissertation being disturbance rejection (or attenuation), the "adaptive regulation" problem will be considered. The common framework is the assumption that the disturbance is the result of a white noise or a Dirac impulse passed through the "model of the disturbance". To reject its influence, several solutions have been proposed. One of them is the Internal Model Principle (IMP) reported in [Amara et al., 1999a, Amara et al., 1999b, Gouraud et al., 1997, Hillerstrom and Sternby, 1994, Valentinotti, 2001, Valentinotti et al., 2003]. Using this method supposes that the model of the disturbance is incorporated in the controller ([Bengtsson, 1977, Francis and Wonham, 1976, Johnson, 1976, Tsytkin, 1997]). Its parameters should therefore be continuously estimated to be able to respond to possible changes in the disturbance's characteristics. This will lead to an indirect adaptive control algorithm. However, it has been shown in [Landau et al., 2005] that direct adaptation is possible if one uses the Youla-Kučera parametrization of all stable controllers.

Another idea that has been used is to build and incorporate an adaptive observer in the controller [Ding, 2003, Marino et al., 2003, Serrani, 2006, Marino and Tomei, 2007]. However, the approach seems to be mainly focused on disturbances acting on the input of the plant. Additional hypotheses should be taken into account before applying it to disturbances on the output (the plant should have stable zeros, which is seldom the case for discrete time plant models). It can be noted that, although the Internal Model Principle is not explicitly taken into consideration in this scheme, incorporating the observer into the controller means that the internal model principle is implicitly used.

A direct approach that uses the concept of a phase-locked loop is presented in [Bodson and Douglas, 1997] and experimental results are provided in [Bodson, 2005]. It can be applied to the rejection of sinusoidal disturbances with unknown frequencies. Disturbance frequency estimation and disturbance cancellation are performed simultaneously by using a single error signal. The frequency response of the plant in the frequency range of interest is needed.

2.4 Contributions

The main objective of the thesis has been the development of adaptive algorithms for vibration attenuation in mechanical systems. The algorithms have been extensively tested on the flexible structures available at the GIPSA-Lab of the University of Grenoble. Taking into consideration the characteristics of the disturbances, either feedforward control for large band disturbances or feedback control for narrow band disturbances has been used.

In Part I of the dissertation, feedforward control methods are proposed. The most significant contributions are:

1. Development of generalized feedforward compensation adaptive algorithms that take into account the existence of the positive feedback coupling inherent in AVC systems and using both filtering of the *a posteriori* error and of the observations vector. The stability and the convergence of the resulting algorithms are then analyzed and experiments are run on a real AVC system.
2. Relaxation of the SPR condition by use of “Integral + Proportional” Parametric Adaptation Algorithms.
3. Development and analysis of Youla-Kučera parameterized adaptive feedforward filters with either FIR or IIR parameters.

The contributions of Part II of this thesis are:

1. Development of new feedback control methods to reject narrow band disturbances based on Band-stop Filters with adjustable frequency bandwidths and attenuations to shape the output sensitivity function.
2. Use of Adaptive Notch Filters to estimate the central frequencies characterizing the narrow band disturbances in an active vibration control context.
3. Implementation using the Youla-Kučera parametrization to reduce the computational complexity of the algorithm.

Experimental results are shown and confirm the results of the theoretical analysis. Although developed for an Active Vibration Control system, the algorithms are also applicable to Active Noise Control.

2.5 Dissertation Outline

Depending on the characteristics of the disturbance and the constraints of the system, either feedback or feedforward approaches have been developed and the thesis will be structured accordingly.

In **Part I** of the thesis, feedforward control methods for compensating large band disturbances are proposed and studied, taking into account the existence of a positive feedback coupling between the control signal and the measurement of the image of the disturbance, which can destabilize the system. First of all, **Chapter 3** presents the AVC system on which the algorithms have been tested. The experimental system, built in collaboration with the Active Noise and Vibration Control, PAULSTRA SNC (Dept. VIBRACHOC) research center, is inspired by problems encountered in the industry. A special feature of this system is the presence of two measuring devices, therefore making it very well suited for experimenting feedforward adaptive control methods. In the next two chapters, the contributions in adaptive feedforward control are described, analyzed and tested. The algorithms are developed using Popov's Hyperstability Theory.

Chapters 4 and **5** present new ideas to solve the ANVC regulation problem. Firstly, a method for direct adaptation of IIR filters in the presence of a fixed feedback controller using a generalized "Integral + Proportional" PAA is presented (Chapter 4). Then the advantages of the Youla-Kučera parametrization are taken into consideration and methods based on it are presented in Chapter 5. The algorithms for adapting the parameters of FIR and IIR Youla-Kučera filters are developed and analyzed. It is shown that, although the FIRYK has some interesting stability properties, the reduced number of parameters needed for the IIRYK filter could be an important advantage in some applications.

The main difference of the proposed methods is the form of the adaptive filter: (i) direct IIR in Chapter 4, (ii) Youla-Kučera parameterized with FIR adaptive filter, and (iii) Youla-Kučera parameterized with IIR adaptive filter in Chapter 5.

An analysis of the algorithms is provided in each of the chapters, firstly assuming that a perfect matching condition is satisfied (*i.e.*, the exact number of parameters of the optimal filter is known and is used for the implemented filter), and then, using less restrictive assumptions. The satisfaction of a Strictly Positive Real (SPR) condition, required by the stability analysis, implies the use of an appropriate filtering either of the observation vector or of the residual acceleration. For non-perfect matching, an analysis of the parameters' bias distribution shows that good estimates are obtained in the frequency regions that are the most important from a control point of view (high gain of the secondary path and of the disturbance's spectral distribution). It is also shown, using the Averaging Theory ([Anderson et al., 1986, Landau et al., 2011g]), that the SPR condition can be relaxed by taking into consideration the spectral content of the disturbance. Another way of relaxing the SPR condition is the use of "Integral + Proportional" Parameter Adaptation Algorithms (IP-PAA) as shown in Chapter 4.

In **Part II**, the **Chapter 6** develops an indirect adaptive algorithm for the attenuation of multiple narrow band disturbances by shaping the output sensitivity function. The method is based on the introduction of Band-stop Filters (BSFs) in the output sensibility function. The indirect procedure is based on a first step of disturbances' frequencies estimation and a second step of controller updating. An experimental comparison with a direct adaptive regulation algorithm presented in [Landau et al., 2011e] is given. It is shown that the proposed method does have some interesting properties given by the

BSFs. More precisely, it is possible to adjust the level of the attenuation and to reduce the impact on neighboring frequencies in order to preserve good robustness performances.

Concluding remarks and directions for future research are given in **Chapter 7**. Finally, the thesis ends by detailing the proofs of the results presented in the previous chapters of the thesis (**Appendices A** and **B**).

Part I

Adaptive Feedforward Disturbance Rejection

CHAPTER 3

AN AVC SYSTEM USING AN INERTIAL ACTUATOR

This chapter gives a detailed presentation of the AVC system that will be used to test the adaptive algorithms proposed in this thesis (Section 3.1). Also, the basic equations which are common for the next chapters are given in Section 3.2. Finally, the procedure used for the identification of the various paths is described in Section 3.3.

3.1 System Description

Figures 3.1 and 3.2 show an AVC system using a measurement correlated with the disturbance and an inertial actuator used to reduce the residual acceleration. The structure is representative for a number of situations encountered in practice.

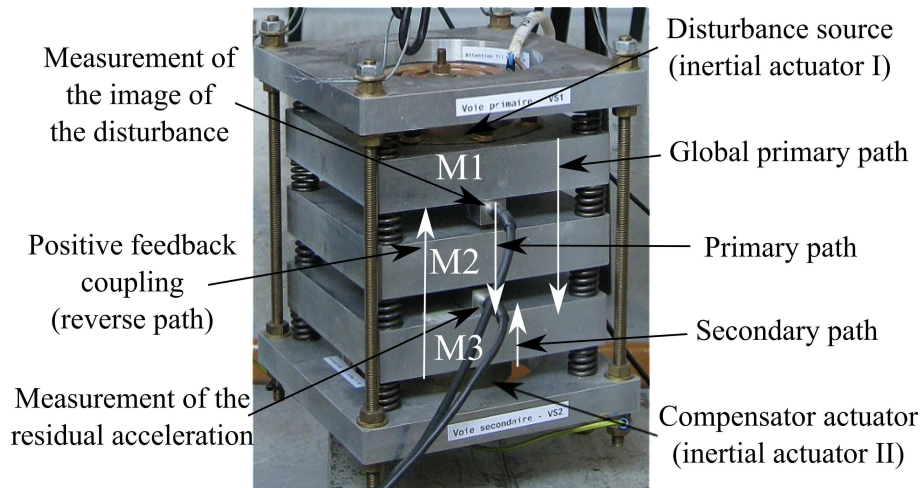


Figure 3.1: The AVC system used for experimentations - photo.

The system is composed of five metal plates (in dural of 1.8 *kg* each) interconnected by springs. The uppermost and lowermost ones are also rigidly linked together by four screws. The middle three plates will be labeled for easier referencing M1, M2 and M3 (see Figure 3.1). M1 and M3 are equipped with inertial actuators. The one on M1 is used as a disturbance generator (inertial actuator I in Figure 3.2), the one at the bottom is used for disturbance compensation (inertial actuator II in Figure 3.2). Inertial actuators use a principle similar as that of loudspeakers (see for example [Marcos, 2000, Landau et al., 2011e]). The measurement correlated with the disturbance (image of the

disturbance) is obtained from an accelerometer which is fixed on plate M1. Another sensor of the same type is fixed on plate M3 and is used to measure the residual acceleration (see Figure 3.2). The objective is to minimize the residual acceleration measured on plate M3.

The various paths described in Section 2.2 (and also 1.2) are indicated in Figures 3.1 and 3.2. The measured quantity $\hat{y}_1(t)$ will be the sum of the correlated disturbance measurement $w(t)$ obtained in the absence of the feedforward compensation (see Figure 3.3(a)) and of the effect of the actuator used for compensation.

The disturbance is the position of the mobile part of the inertial actuator (see Figures 3.1 and 3.2) located on the top of the structure. The input to the compensator system is the position of the mobile part of the inertial actuator located on the bottom of the structure. The input to the inertial actuators being a position, the global primary path, the secondary path and the reverse path have a double differentiator behavior (their respective output being measured by accelerometers). This structure is representative of various situations encountered in practice. Similar internal positive feedback coupling occurs also in feedforward active noise control ([Jacobson et al., 2001, Zeng and de Callafon, 2006]).

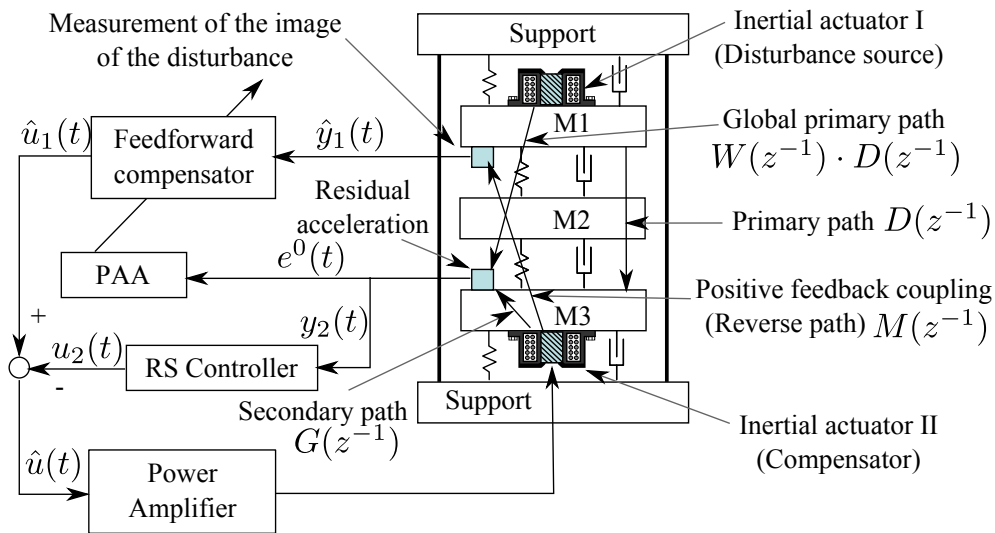


Figure 3.2: An AVC system using an adaptive feedforward and a fixed feedback compensation scheme.

The corresponding block diagrams, in open loop operation and with the compensator system, are shown in Figures 3.3(a) and 3.3(b), respectively. In Figure 3.3(b), $\hat{y}_1(t)$ denotes the effective output provided by the upstream measurement device and which will serve as input to the adaptive feedforward filter \hat{N} . The output of this filter is denoted by $\hat{u}_1(t)$. The feedback compensator has as input the performance variable¹ $y_2(t) = e^0(t)$ and its output is represented by $u_2(t)$ as described in Subsection 2.2.1. The control signal applied to the actuator through an amplifier is

$$\hat{u}(t) = \hat{u}_1(t) - u_2(t). \quad (3.1)$$

¹Here $e^0(t)$ denotes the *a priori* measured value of the residual acceleration (obtained with the parameters from time $t - 1$). In Figure 3.3(a), given that no adaptive filter is present, there is no point in differentiating between a *a priori* and a *a posteriori* values and the simplified notation $e(t)$ is used.

The transfer function G (the secondary path) characterizes the dynamics from the output of the compensator κ to the residual acceleration measurement (amplifier + actuator + dynamics of the mechanical system). The transfer function D between $w(t)$ and the measurement of the residual acceleration (in open loop operation) characterizes the primary path.

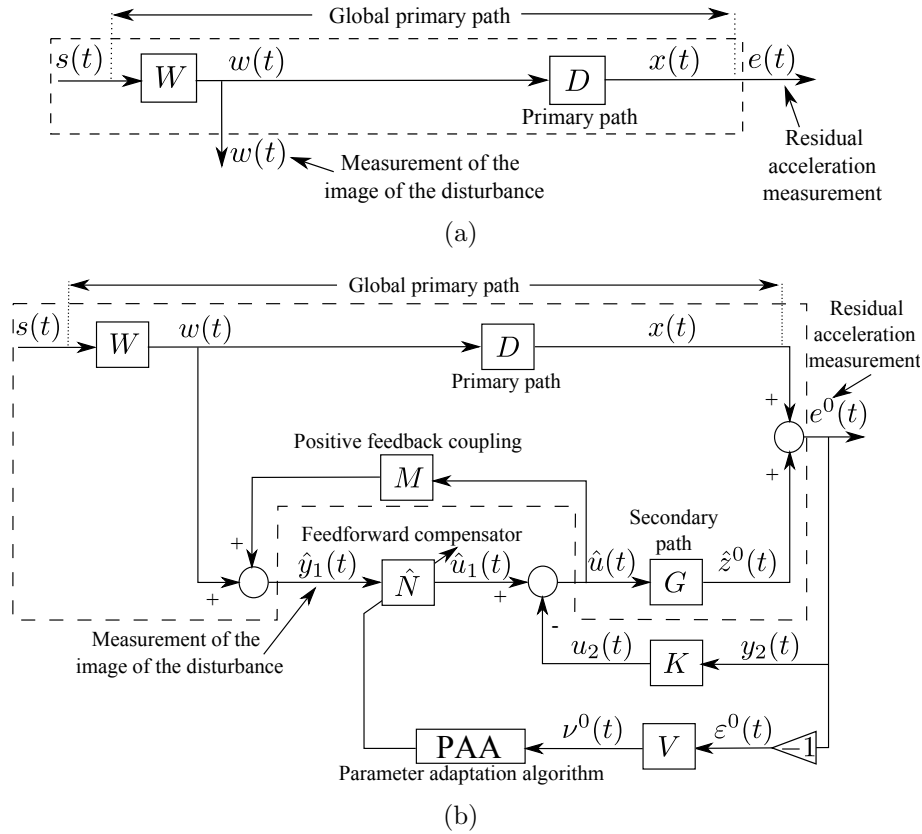


Figure 3.3: Feedforward AVC: (a) in open loop and (b) with adaptive feedforward + fixed feedback compensator.

The coupling between the output of the compensator, $\hat{u}(t)$, and the measurement $\hat{y}_1(t)$ is denoted by M . As indicated in Figure 3.3(b) this coupling is a "positive" feedback. This unwanted coupling raises problems in practice (source of instabilities) and makes the analysis of adaptive (estimation) algorithms more difficult.

At this stage it is important to make the following remarks, when there is no compensator (open loop operation):

- very reliable models for the secondary path and the "positive" feedback path can be identified by applying appropriate excitation on the actuator used for compensation;
- an initial estimation of the primary path transfer function can be obtained using the measured $w(t)$ as input and $e(t)$ as output (the compensator actuator being at rest);
- the design of a fixed model based stabilizing feedforward compensator requires the knowledge of the reverse path model only;
- the adaptation algorithms do not use informations concerning the primary path whose characteristics may be unknown or subject to change;
- the knowledge of the disturbance characteristics and of the primary path model, in addition to the secondary and reverse path models, is mandatory for the design

of an optimal fixed model based feedforward compensator ([Alma et al., 2012b, Rotunno and de Callafon, 2003]).

The objective is to develop stable recursive algorithms for online estimation and adaptation of the parameters of the feedforward filter such that the measured residual error (acceleration or force in AVC, noise in ANC) be minimized with respect to a certain criterion while simultaneously assuring the stability of the internal positive feedback loop. This has to be done for broadband disturbances $w(t)$ (or $s(t)$) with unknown and variable spectral characteristics and an unknown primary path model².

3.2 Basic Equations and Notations

The different blocks of the AVC system (Figure 3.3(b)) are described in this section. The primary path is characterized by the asymptotically stable transfer operator

$$D(q^{-1}) = \frac{B_D(q^{-1})}{A_D(q^{-1})}, \quad (3.2)$$

where³

$$B_D(q^{-1}) = b_1^D q^{-1} + \dots + b_{n_{BD}}^D q^{-n_{BD}} = q^{-1} B_D^*(q^{-1}), \quad (3.3)$$

$$A_D(q^{-1}) = 1 + a_1^D q^{-1} + \dots + a_{n_{AD}}^D q^{-n_{AD}}. \quad (3.4)$$

The unmeasurable value of the output of the primary path (when the compensation is active) is denoted $x(t)$.

The secondary path is characterized by the asymptotically stable transfer operator

$$G(q^{-1}) = \frac{B_G(q^{-1})}{A_G(q^{-1})}, \quad (3.5)$$

where

$$B_G(q^{-1}) = b_1^G q^{-1} + \dots + b_{n_{BG}}^G q^{-n_{BG}} = q^{-1} B_G^*(q^{-1}), \quad (3.6)$$

$$A_G(q^{-1}) = 1 + a_1^G q^{-1} + \dots + a_{n_{AG}}^G q^{-n_{AG}}. \quad (3.7)$$

The positive feedback coupling is characterized by the asymptotically stable transfer operator

$$M(q^{-1}) = \frac{B_M(q^{-1})}{A_M(q^{-1})}, \quad (3.8)$$

where

$$B_M(q^{-1}) = b_1^M q^{-1} + \dots + b_{n_{BM}}^M q^{-n_{BM}} = q^{-1} B_M^*(q^{-1}), \quad (3.9)$$

$$A_M(q^{-1}) = 1 + a_1^M q^{-1} + \dots + a_{n_{AM}}^M q^{-n_{AM}}. \quad (3.10)$$

B_G , B_M , and B_D have a one step discretization delay. The identified models of the secondary path and of the positive feedback coupling are denoted \hat{G} and \hat{M} , respectively, and their numerators and denominators \hat{B}_G , \hat{A}_G , \hat{B}_M and \hat{A}_M .

²Variations of the unknown model W , the transfer function between the disturbance $s(t)$ and $w(t)$ are equivalent to variations of the spectral characteristics of $s(t)$.

³Throughout the thesis, the notation $V(q^{-1}) = v_0 + q^{-1}V_D^*(q^{-1})$ will be used. Usually, v_0 will either be 1 or 0.

The optimal feedforward filter (unknown) is defined by

$$N(q^{-1}) = \frac{R(q^{-1})}{S(q^{-1})}, \quad (3.11)$$

where

$$R(q^{-1}) = r_0 + r_1 q^{-1} + \dots + r_{n_R} q^{-n_R}, \quad (3.12)$$

$$S(q^{-1}) = 1 + s_1 q^{-1} + \dots + s_{n_S} q^{-n_S} = 1 + q^{-1} S^*(q^{-1}). \quad (3.13)$$

The estimated feedforward filter is denoted by

$$\hat{N}(q^{-1}) = \frac{\hat{R}(q^{-1})}{\hat{S}(q^{-1})}. \quad (3.14)$$

The vector of optimal feedforward filter parameters is

$$\theta^T = [s_1, \dots, s_{n_S}, r_0, \dots, r_{n_R}]^T \quad (3.15)$$

and the vector of estimated feedforward filter coefficients is

$$\hat{\theta}^T(t) = [\hat{s}_1(t), \dots, \hat{s}_{n_S}(t), \hat{r}_0(t), \dots, \hat{r}_{n_R}(t)]^T. \quad (3.16)$$

The different representations concerning this feedforward controller will be presented in the following two chapters.

The fixed RS controller K , computed on the basis of the model \hat{G} to reject broadband disturbances on the output $e(t)$, is characterized by the asymptotically stable transfer function

$$K(q^{-1}) = \frac{B_K(q^{-1})}{A_K(q^{-1})}, \quad (3.17)$$

where

$$B_K(q^{-1}) = b_0^K + b_1^K q^{-1} + \dots + b_{n_{B_K}}^K q^{-n_{B_K}}, \quad (3.18)$$

$$A_K(q^{-1}) = 1 + a_1^K q^{-1} + \dots + a_{n_{A_K}}^K q^{-n_{A_K}}. \quad (3.19)$$

The input of the feedforward filter (called also reference) is denoted by $\hat{y}_1(t)$ and it corresponds to the measurement provided by the primary transducer (force or acceleration transducer in AVC or a microphone in ANC). In the absence of the compensation loop (open loop operation) $\hat{y}_1(t) = w(t)$. The output of the feedforward compensator is denoted by $\hat{u}_1(t+1) = \hat{u}_1(t+1|\hat{\theta}(t+1))$ (*a posteriori* output)⁴.

The measured input to the feedforward filter can also be written as

$$\hat{y}_1(t+1) = w(t+1) + \frac{B_M^*(q^{-1})}{A_M(q^{-1})} \hat{u}(t), \quad (3.20)$$

where

$$\hat{u} = \hat{u}_1(t) - u_2(t), \quad (3.21)$$

$\hat{u}_1(t)$ and $u_2(t)$ are the outputs given by the adaptive feedforward and the fixed feedback compensator, respectively. \hat{u} is the effective input sent to the control actuator.

⁴In adaptive control and estimation the predicted output at $t+1$ can be computed either on the basis of the previous parameter estimates (*a priori*, time t) or on the basis of the current parameter estimates (*a posteriori*, time $t+1$).

The *a priori* output of the estimated feedforward filter is given by

$$\begin{aligned}\hat{u}_1^0(t+1) &= \hat{u}_1(t+1|\hat{\theta}(t)) \\ &= -\hat{S}^*(t, q^{-1})\hat{u}_1(t) + \hat{R}(t, q^{-1})\hat{y}_1(t+1) \\ &= \hat{\theta}^T(t)\phi(t) = [\hat{\theta}_S^T(t), \hat{\theta}_R^T(t)] \begin{bmatrix} \phi_{\hat{y}_1}(t) \\ \phi_{\hat{u}_1}(t) \end{bmatrix}\end{aligned}\quad (3.22)$$

where $\hat{\theta}^T(t)$ has been given in (3.16) and

$$\begin{aligned}\phi^T(t) &= [-\hat{u}_1(t), \dots, -\hat{u}_1(t-n_S+1), \hat{y}_1(t+1), \hat{y}_1(t), \dots, \hat{y}_1(t-n_R+1)] \\ &= [\phi_{\hat{u}_1}^T(t), \phi_{\hat{y}}^T(t)]\end{aligned}\quad (3.23)$$

In the context of this thesis, fixed feedback compensators K will be considered. The input to the feedback compensator is given by the performance variable, therefore $y_2(t) = e(t)$. Its output will be $u_2(t) = K \cdot y_2(t)$.

The unmeasurable value of the output of the primary path (when the compensation is active) is denoted $x(t)$. The *a priori* output of the secondary path is denoted $\hat{z}^0(t+1) = \hat{z}(t+1|\hat{\theta}(t))$ while its input is $\hat{u}(t)$. One has

$$\hat{z}^0(t+1) = \frac{B_G^*(q^{-1})}{A_G(q^{-1})}\hat{u}(t) = \frac{B_G^*(q^{-1})}{A_G(q^{-1})}\hat{u}(t|\hat{\theta}(t)).\quad (3.24)$$

The measured residual acceleration (or force) satisfies the following equation

$$e^0(t+1) = x(t+1) + \hat{z}^0(t+1).\quad (3.25)$$

The filtered *a priori* adaptation error is defined as

$$\nu^0(t+1) = \nu(t+1|\hat{\theta}(t))\quad (3.26)$$

$$= \varepsilon^0(t+1) + \sum_{i=1}^{n_1} v_i^B \varepsilon(t+1-i) - \sum_{i=1}^{n_2} v_i^A \nu^0(t+1-i),\quad (3.27)$$

where

$$\varepsilon^0(t+1) = \varepsilon(t+1|\hat{\theta}(t)) = -e^0(t+1) = -x(t+1) - \hat{z}^0(t+1)\quad (3.28)$$

and

$$\varepsilon(t+1) = \varepsilon(t+1|\hat{\theta}(t+1)) = -e(t+1) = -x(t+1) - \hat{z}(t+1)\quad (3.29)$$

are also called, respectively, the *a priori* and the *a posteriori* unfiltered adaptation errors.

The coefficients v_i^X , $X \in \{B, A\}$, are the coefficients of an IIR filter, with all poles and zeros inside the unit circle, acting on the adaptation error

$$V(q^{-1}) = \frac{B_V(q^{-1})}{A_V(q^{-1})},\quad (3.30)$$

where

$$X_V(q^{-1}) = 1 + q^{-1}X_V^*(q^{-1}) = 1 + \sum_{i=1}^{n_j} v_i^X q^{-i}, \quad X \in \{B, A\}.\quad (3.31)$$

The filtered *a posteriori* unmeasurable (but computable) adaptation error is given by

$$\nu(t+1) = \nu(t+1|\hat{\theta}(t+1))\quad (3.32)$$

$$= \varepsilon(t+1) + \sum_{i=1}^{n_1} v_i^B \varepsilon(t+1-i) - \sum_{i=1}^{n_2} v_i^A \nu(t+1-i),\quad (3.33)$$

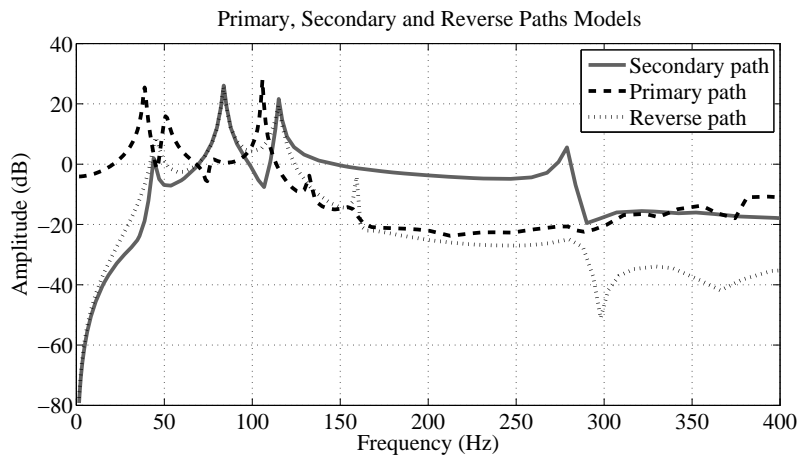


Figure 3.4: Frequency characteristics of the primary, secondary and reverse paths.

with $\varepsilon(t+1)$ given in (3.29).

The *a posteriori* value of the output of the secondary path $\hat{z}(t+1)$ (dummy variable) is given by

$$\hat{z}(t+1) = \hat{z}(t+1|\hat{\theta}(t+1)) = \frac{B_G^*(q^{-1})}{A_G(q^{-1})} \hat{u}(t|\hat{\theta}(t+1)). \quad (3.34)$$

For compensators with **constant** parameters $\nu^0(t) = \nu(t)$, $\varepsilon^0(t) = \varepsilon(t)$, $e^0(t) = e(t)$, $\hat{z}^0(t) = \hat{z}(t)$, $\hat{u}^0(t) = \hat{u}(t)$.

Remark: in Chapter 5, one has $V(q^{-1}) = 1$ (the adaptation error is not filtered) and, therefore, the *a priori* and the *a posteriori* adaptation errors will have respectively the forms

$$\nu^0(t+1) = \nu(t+1|\hat{\theta}(t)) = \varepsilon(t+1|\hat{\theta}(t)) = -e^0(t+1) = -x(t+1) - \hat{z}^0(t+1) \quad (3.35)$$

and

$$\nu(t+1) = \nu(t+1|\hat{\theta}(t+1)) = \varepsilon(t+1|\hat{\theta}(t+1)) = -e(t+1) = -x(t+1) - \hat{z}(t+1). \quad (3.36)$$

3.3 System Identification

This section describes the identification procedure for the mechanical structure's paths. The methodology used for parametric system identification is similar to that presented in [Landau et al., 2001b, Landau et al., 2001a, Landau et al., 2011d]. The sampling frequency is 800 Hz. The identification of the secondary and the reverse paths has been done in the absence of the compensator (see Figure 3.3(b)) using as an excitation signal a PRBS generated by a 10 bit shift register and a frequency divider⁵ $p = 4$ applied at the input of the inertial actuator II where the control signal $\hat{u}(t)$ is applied (see figures 3.1 and 3.2).

For the secondary path, $G(q^{-1})$, the output is the residual acceleration measurement, $e(t)$. For the reverse path, $M(q^{-1})$, the output is the signal delivered by the primary transducer (accelerometer) $\hat{y}_1(t)$. The estimated orders of the model for the secondary path are $n_{B_G} = 14$, $n_{A_G} = 14$. The best results, in terms of validation, have been obtained

⁵It was first verified with $p = 2$ that there are no significant dynamics around 200 Hz and then $p = 4$ has been chosen in order to enhance the power spectral density of the excitation in low frequencies while keeping a reasonable length for the experiment.

with the *Recursive Extended Least Square* method. The frequency characteristics of the secondary path is shown in Figure 3.4, solid line. It features several very low damped vibration modes. The first vibration mode is at 44 *Hz* with a damping of 0.0212, the second at 83.8 *Hz* with a damping of 0.00961 and the third one at 115 *Hz* with a damping of 0.00694. There is also a pair of low damped complex zeros at 108 *Hz* with a damping of 0.021. As a consequence of the double differentiator behavior, a double zero at $z = 1$ is also present.

For the reverse path $M(q^{-1})$, the model's complexity has been estimated to be $n_{B_M} = 13$, $n_{A_M} = 13$. The frequency characteristic of the reverse path is shown in Figure 3.4 (dotted line). There are several very low damped vibration modes at 45.1 *Hz* with a damping of 0.0331, at 83.6 *Hz* with a damping of 0.00967, at 115 *Hz* with a damping of 0.0107 and some additional modes in high frequencies. There are two zeros on the unit circle corresponding to the double differentiator behavior. The gain of the reverse path is of the same order of magnitude as the gain of the secondary path up to 150 *Hz*, indicating a strong feedback in this frequency zone.

The primary path has been also identified in the absence of the compensator using $w(t)$ as an input and measuring $e(t)$. The disturbance $s(t)$ was a PRBS sequence ($N = 9$, frequency divider $p = 2$). The estimated orders of the model are $n_{B_D} = 26$, $n_{A_D} = 26$. The frequency characteristic is presented in Figure 3.4 (dashed line) and may be used for simulations and detailed performance evaluation. Note that the primary path features a strong resonance at 108 *Hz*, exactly where the secondary path has a pair of low damped complex zeros (almost no gain). Therefore, one cannot expect a good attenuation around this frequency.

3.4 Concluding Remarks

This chapter concludes the description of the system and of the basic equations. The next ones will focus on presenting the adaptive control methods proposed in this thesis. Nevertheless, parts of this chapter will often be referenced.

CHAPTER 4

ADAPTATION ALGORITHMS FOR FEEDFORWARD COMPENSATION IN AVC

4.1 Introduction

Adaptive feedforward for broadband disturbance compensation is widely used when a well correlated signal with the disturbance (image of the disturbance) is available ([Elliott and Nelson, 1994, Elliott and Sutton, 1996, Kuo and Morgan, 1999, Zeng and de Callafon, 2006]). However, in many systems, there is a positive mechanical coupling between the feedforward compensation system and the measurement of the image of the disturbance. This often leads to the instability of the system.

In the context of this inherent "positive" feedback, the adaptive feedforward compensator should minimize the effect of the disturbance while simultaneously assuring the stability of the internal positive feedback loop.

An approach discussed in the literature is the analysis in this new context of existing algorithms for adaptive feedforward compensation developed for the case without feedback. An attempt is made in [Wang and Ren, 2003] where the asymptotic convergence in a stochastic environment of the so called "Filtered-U LMS" (FULMS) algorithm is discussed. Further results on the same direction can be found in [Fraanje et al., 1999]. The authors use the Ljung's ODE method ([Ljung and Söderström, 1983]) for the case of a scalar vanishing adaptation gain. Unfortunately this is not enough because nothing is said about the stability of the system with respect to initial conditions and when a non vanishing adaptation gain is used (to keep adaptation capabilities). The authors assume that the positive feedback does not destabilize the system.

A stability approach to develop appropriate adaptive algorithms in the context of internal positive feedback is discussed in [Jacobson et al., 2001] and [Landau et al., 2011d]. In [Landau et al., 2011d] there is also an experimental comparison of various algorithms for IIR adaptive compensators in the presence of the internal positive feedback.

Combining adaptive feedforward compensation with feedback control has been considered as an issue to further improve the performance of the adaptive feedforward compensation alone. Several references are available, like [de Callafon and Kinney, 2010, Ray et al., 2006, Esmailzadeh et al., 2002]. While various procedures for designing the fixed feedback controller can be considered, it is clear that an improvement of the global performance can be obtained. Unfortunately, there is a strong interaction between the presence of this local feedback controller and the stability conditions for the adaptive feedforward compensations algorithms.

All the research papers referenced this far use "Integral" PAAs. This means that the

equation for updating the parameters of the adaptive filter can be written as the output of an integrator, which has as input a vector obtained by multiplying a matrix (or scalar) adaptation gain, the observations' vector, and the *a posteriori* error.

Another important issue in adaptive feedforward compensation is the design of filters either on the observed variables of the feedforward compensator or on the residual acceleration in order to satisfy positive realness conditions on some transfer functions. In [Landau et al., 2011d] based on the work done by [Anderson et al., 1986], it was shown that for small adaptation gains (slow adaptation) the violation of the positive real conditions in some frequency regions is acceptable, provide that in the average, the input-output product associated with this transfer function is positive. It is in fact a signal dependent condition.

However, the problem of removing or relaxing the positive real condition can be also approached by adding a proportional adaptation to the widely used integral adaptation. While this approach is known in adaptive control [Landau et al., 2011g, Tomizuka, 1982], it has not been used apparently in the context of adaptive feedforward compensation. One other effect of the "Integral + Proportional" adaptation is that of speeding up the transients of the adaptation error while slowing down the convergence of the parameters.

A subject of debate in the context of adaptive feedforward compensation was the choice between filtering the data or filtering the residual acceleration (error) in order to satisfy the positive realness conditions required by the stability analysis (in the presence of the internal positive feedback or not). Some of the references discussing this issue are [Larimore et al., 1980, Montazeri and Poshtan, 2011, Sun and Chen, 2002, Sun and Meng, 2004]. As it will shown, the reason to use one of the two options is related to the criterion which is minimized and to the presence or not of unstable zeros in the secondary path. The filtering of the residual error will affect the PSD of the residual error. There are a number of situations where shaping the residual error in the frequency domain is very useful. A more detailed discussion on the various implications of both types of filtering will be done later in this chapter.

From the user point of view and taking into account the type of operation of adaptive disturbance compensation systems, one has to consider two modes of operation of the adaptive schemes:

- *Adaptive* operation. The adaptation is performed continuously with a non vanishing adaptation gain and the feedforward compensator is updated at each sampling.
- *Self-tuning* operation. The adaptation procedure starts either on demand or when the performance is unsatisfactory. A vanishing adaptation gain is used. The current controller is either updated at each sampling instant once adaptation starts or is frozen during the estimation/computation of the new controller parameters.

Scalar adaptation gains are used in some algorithms for adaptive feedforward compensation, but most of the recent algorithms use RLS type matrix adaptation gains able to cover both self tuning and adaptive operations. In the context of the absence of internal feedback, [Montazeri and Poshtan, 2011] gives a detailed comparison of the two types of adaptation gain. A quite similar comparison in the presence of the internal positive feedback can be found in [Landau et al., 2011d]. Although not detailed in this chapter, it is important to keep in mind that the time varying adaptation gains associated with RLS type algorithms require the use of a UD factorization for implementation in real time in order to avoid numerical errors due to round off errors [Bierman, 1977, Landau et al., 2011g]. The complexity of the algorithms has been one of the reasons why initially algorithms using a scalar adaptation gain have been used. It

turns out that using an array type implementation strongly reduced the complexity of algorithms using RLS type matrix adaptation gain. This is very pertinently shown in the context of adaptive feedforward compensation in [Montazeri and Poshtan, 2010].

The main contributions of this chapter are:

- Analysis of the interaction between the local feedback loop and the adaptive feedforward compensation in the presence of an internal positive feedback coupling;
- Development and analysis of a general algorithm for adaptive feedforward compensation in the presence of an internal positive coupling and a local feedback controller using both filtering of the observations and of the residual error and a IP-PAA (“Integral + Proportional” Parameter Adaptation Algorithm);
- Enhancement of the role of the desired performance criterion in the design of specific algorithms;
- Enhancement of the use of proportional adaptation to relax the positive real conditions;
- Comparison of the new algorithm with some existing algorithms;
- Application of the algorithms to an active vibration control system featuring internal positive mechanical coupling.

One of the important observations resulting from the analysis developed in this chapter, is that the stability conditions for the adaptive feedforward compensation are highly influenced by the design of the feedback loop. This interaction is further enhanced when the internal positive coupling is present. The major practical consequence is that the filters used in order to assure the stability conditions for the adaptive feedforward compensation will depend upon the elements of the feedback compensation loop built around the secondary path and upon the parameters of the positive internal feedback loop.

The chapter is organized as follows. The algorithms for adaptive feedforward compensation are developed in Section 4.2 and analyzed in Section 4.3. The problem of SPR relaxation is discussed in Section 4.4. Section 4.5 presents experimental results obtained on the AVC system.

4.2 Development and Analysis of the Algorithms

The description of the AVC system in the presence of an hybrid feedforward + feedback controller has been given in Sections 3.1 and 3.2.

The algorithms for adaptive feedforward compensation in the presence of RS feedback controller will be developed under the following hypotheses:

H1) The signal $w(t)$ is bounded, *i.e.*,

$$|w(t)| \leq \alpha, \quad \forall t \quad (0 \leq \alpha < \infty) \quad (4.1)$$

(which is equivalent to say that $s(t)$ is bounded and $W(q^{-1})$ in Figure 3.3 is asymptotically stable).

H2) Perfect matching condition - There exists a filter $N(q^{-1})$ of finite dimension such that

$$\frac{N(z^{-1})}{1 - N(z^{-1})M(z^{-1})}G(z^{-1}) = -D(z^{-1}) \quad (4.2)$$

and the characteristic polynomials:

- of the "internal" positive coupling loop

$$P(z^{-1}) = A_M(z^{-1})S(z^{-1}) - B_M(z^{-1})R(z^{-1}), \quad (4.3)$$

- of the closed loop (G-K)

$$P_d(z^{-1}) = A_G(z^{-1})A_K(z^{-1}) + B_G(z^{-1})B_K(z^{-1}), \quad (4.4)$$

- and of the coupled feedforward-feedback loop

$$P_{fb-ff} = A_M S[A_G A_K + B_G B_K] - B_M R A_K A_G \quad (4.5)$$

are Hurwitz polynomials.

H3) Deterministic context - The effect of the measurement noise upon the measured residual error is neglected.

H4) The primary path model $D(z^{-1})$ is unknown and constant.

Once the algorithms are developed under these hypotheses, H2 and H3 will be removed and the algorithms will be analyzed in this modified context.

A first step in the development of the algorithms is to establish a relation between the errors on the estimation of the parameters of the feedforward filter and the measured residual acceleration. This is summarized in the following lemma.

Lemma 4.2.1. *Let the system be described by eqs. (3.2) - (3.34). Under hypotheses H1, H2, H3, and H4, using a feedforward compensator \hat{N} with constant parameters, leads to*

$$\varepsilon(t+1) = \frac{A_M(q^{-1})A_G(q^{-1})A_K(q^{-1})G(q^{-1})}{P_{fb-ff}(q^{-1})} [\theta - \hat{\theta}]^T \phi(t), \quad (4.6)$$

where

$$\theta^T = [s_1, \dots, s_{n_S}, r_0, r_1, \dots, r_{n_R}] = [\theta_S^T, \theta_R^T] \quad (4.7)$$

is the vector of parameters of the optimal filter N assuring perfect matching,

$$\hat{\theta}^T = [\hat{s}_1, \dots, \hat{s}_{n_S}, \hat{r}_0, \dots, \hat{r}_{n_R}] = [\hat{\theta}_S^T, \hat{\theta}_R^T] \quad (4.8)$$

is the vector of constant estimated parameters of \hat{N} ,

$$\begin{aligned} \phi^T(t) &= [-\hat{u}_1(t), \dots, -\hat{u}_1(t - n_S + 1), \hat{y}_1(t+1), \dots, \hat{y}_1(t - n_R + 1)] \\ &= [\phi_{\hat{u}_1}^T(t), \phi_{\hat{y}_1}^T(t)], \end{aligned} \quad (4.9)$$

and $\hat{y}_1(t+1)$ is given by

$$\hat{y}_1(t+1) = w(t+1) + \frac{B_M^*(q^{-1})}{A_M(q^{-1})} \hat{u}(t). \quad (4.10)$$

The proof has been given in [Alma, 2011].

The results of Lemma 4.2.1 can be easily particularized to the case without internal positive feedback or without RS feedback controller (see also [Alma, 2011]).

Filtering the vector $\phi(t)$ with an asymptotically stable filter $L(q^{-1}) = \frac{B_L}{A_L}$, eq. (4.6) for $\hat{\theta} = \text{constant}$ leads to

$$\varepsilon(t+1) = \frac{A_M(q^{-1})A_G(q^{-1})A_K(q^{-1})G(q^{-1})}{P_{fb-ff}(q^{-1})L(q^{-1})} [\theta - \hat{\theta}]^T \phi_f(t) \quad (4.11)$$

with

$$\phi_f(t) = L(q^{-1})\phi(t). \quad (4.12)$$

Eq. (4.11) will be used to develop the adaptation algorithms, neglecting for the moment the non-commutativity of the operators when $\hat{\theta}$ is time varying (however an exact algorithm can be derived in such cases - see [Landau et al., 2011g]). Replacing the fixed estimated parameters by the current estimated parameters, equation (4.11) becomes the equation of the *a posteriori* residual unfiltered error $\varepsilon(t+1)$ (which is computed)

$$\varepsilon(t+1) = \frac{A_M(q^{-1})A_G(q^{-1})A_K(q^{-1})}{P_{fb-ff}(q^{-1})L(q^{-1})} G(q^{-1}) [\theta - \hat{\theta}(t+1)]^T \phi_f(t). \quad (4.13)$$

Eq. (4.13) has the standard form for an *a posteriori* adaptation error ([Landau et al., 2011g]), which suggests to use the following IP-PAA

$$\hat{\theta}_I(t+1) = \hat{\theta}_I(t) + \xi(t)F_I(t)\Phi(t)\nu(t+1) \quad (4.14a)$$

$$\hat{\theta}_P(t+1) = F_P(t)\Phi(t)\nu(t+1) \quad (4.14b)$$

$$\varepsilon(t+1) = \frac{\varepsilon^0(t+1)}{1 + \Phi^T(t)(\xi(t)F_I(t) + F_P(t))\Phi(t)} \quad (4.14c)$$

$$\nu(t+1) = \varepsilon(t+1) + \sum_{i=1}^{n_1} v_i^B \varepsilon(t+1-i) - \sum_{i=1}^{n_2} v_i^A \nu(t+1-i) \quad (4.14d)$$

$$F_I(t+1) = \frac{1}{\lambda_1(t)} \left[F_I(t) - \frac{F_I(t)\Phi(t)\Phi^T(t)F_I(t)}{\frac{\lambda_1(t)}{\lambda_2(t)} + \Phi^T(t)F_I(t)\Phi(t)} \right] \quad (4.14e)$$

$$F_P(t) = \alpha(t)F_I(t), \quad \alpha(t) > -0.5 \quad (4.14f)$$

$$F(t) = \xi(t)F_I(t) + F_P(t) \quad (4.14g)$$

$$\xi(t) = 1 + \frac{\lambda_2(t)}{\lambda_1(t)} \Phi^T(t)F_P(t)\Phi(t); \quad (4.14h)$$

$$\hat{\theta}(t+1) = \hat{\theta}_I(t+1) + \hat{\theta}_P(t+1) \quad (4.14i)$$

$$1 \geq \lambda_1(t) > 0, \quad 0 \leq \lambda_2(t) < 2, \quad F_I(0) > 0 \quad (4.14j)$$

$$\Phi(t) = \phi_f(t), \quad (4.14k)$$

where $\nu(t+1)$ is the generalized filtered adaptation error (see also Section 3.2 for more details), $\lambda_1(t)$ and $\lambda_2(t)$ allow to obtain various profiles for the matrix adaptation gain $F(t)$ ([Landau et al., 2011g]). By taking $\lambda_2(t) \equiv 0$ one obtains a constant adaptation gain matrix and choosing $F_I = \gamma I$, $\gamma > 0$ one gets a scalar adaptation gain). For $\alpha(t) \equiv 0$, one obtains the algorithm with integral adaptation gain introduced in [Landau et al., 2011d].

For the adaptive operation, a $F_I(t)$ with constant trace can be obtained by automatically computing $\lambda_1(t)$ and $\lambda_2(t)$ at each sampling period as a function of the newly computed trace of the ‘‘Integral’’ adaptation matrix, $\text{tr}(F_I(t))$, and the desired constant trace, $\text{tr}(F_{I_0})$. In this case, a design parameter $\alpha_F = \frac{\lambda_1(t)}{\lambda_2(t)}$ (chosen equal to 1 in Section 4.5) is also used. The equations are given below:

$$\lambda_1(t) = \frac{\text{tr}(F_I(t))}{\text{tr}(F_{I_0})}, \quad \lambda_2(t) = \frac{\lambda_1(t)}{\alpha_F}. \quad (4.15)$$

Note also that eq. (4.15) is obtained from

$$F_I^{-1}(t+1) = \lambda_1(t)F_I^{-1}(t) + \lambda_2(t)\Phi(t)\Phi^T(t), \quad (4.16)$$

using the matrix inversion lemma ([Landau et al., 2011g]).

4.3 Analysis of the Algorithms

The equation for the *a posteriori* adaptation error has the form

$$\nu(t+1) = H(q^{-1}) [\theta - \hat{\theta}(t+1)]^T \Phi(t) \quad (4.17)$$

where

$$H(q^{-1}) = \frac{A_M A_G A_K G V}{P_{fb-ff} L}, \quad \Phi = \phi_f. \quad (4.18)$$

Neglecting the non-commutativity of the time varying operators, one has the following result

Lemma 4.3.1. *Assuming that eq. (4.17) represents the evolution of the a posteriori adaptation error and that the IP-PAA (4.14) is used, one has:*

$$\lim_{t \rightarrow \infty} \nu(t+1) = 0 \quad (4.19)$$

$$\lim_{t \rightarrow \infty} \frac{[\nu^0(t+1)]^2}{1 + \Phi(t)^T F(t) \Phi(t)} = 0 \quad (4.20)$$

$$\|\Phi(t)\| \text{ is bounded} \quad (4.21)$$

$$\lim_{t \rightarrow \infty} \nu^0(t+1) = 0 \quad (4.22)$$

for any bounded initial conditions $\hat{\theta}(0), \nu^0(0), F(0)$, provided that

$$H'(z^{-1}) = H(z^{-1}) - \frac{\lambda_2}{2} \quad (4.23)$$

is a SPR transfer function.

The proof¹ of (4.19) is given in Appendix A.1. For (4.20), (4.21), and (4.22), the proof follows [Landau, 1980, Landau et al., 2011d] and is omitted.

It should be observed that the PAA with "Integral + Proportional" adaptation gain presented here, is a generalization of that given in Theorem 3.2 of [Landau et al., 2011d]. Note also that $P(t), Q(t), S(t)$, and $R(t)$ used in the proof of Appendix A.1 are generalized forms of those used in the proof of the theorem mentioned above for "Integral" PAA.

The proof of [Landau and Silveira, 1979] for "Integral + Proportional" adaptation with time varying integral adaptation gain is given for $\xi(t) = \frac{1}{\lambda_1(t)} + \frac{\lambda_2(t)}{\lambda_1(t)} \Phi^T(t) F_P(t) \Phi(t)$. To the knowledge of the authors, the proof for $\xi(t) = 1 + \frac{\lambda_2(t)}{\lambda_1(t)} \Phi^T(t) F_P(t) \Phi(t)$ is presented here for the first time.

¹ $\varepsilon^0(t+1)$ is computed using $\hat{\theta}(t) = \hat{\theta}_I(t)$.

4.3.1 Discussion of the algorithms

Below several versions of the algorithms particularized for various choices of V and L are given:

$$\begin{array}{ll}
\text{Algorithm I} & L = G, V = 1 \\
\text{Algorithm IIa} & L = \hat{G}, V = 1 \\
\text{Algorithm IIb} & L = \hat{G}, V \neq 1 \\
\text{Algorithm IIc} & L = \frac{\hat{G}}{1 + \hat{G}K}, V = 1 \\
\text{Algorithm IIId} & L = \frac{\hat{G}}{1 + \hat{G}K}, V \neq 1 \\
\text{Algorithm III} & L = \frac{\hat{A}_M \hat{A}_G A_K}{\hat{P}_{fb-ff}} \hat{G}, V = 1
\end{array} \tag{4.24}$$

where

$$\hat{P}_{fb-ff} = \hat{A}_M \hat{S} [\hat{A}_G A_K + \hat{B}_G B_K] - \hat{B}_M \hat{R} A_K \hat{A}_G \tag{4.25}$$

is an estimation of the characteristic polynomial of the coupled feedforward-feedback loop computed on the basis of available estimates of the parameters of the filter \hat{N} .

For the Algorithm III, several options for updating \hat{P}_{fb-ff} can be considered:

- Run one of the Algorithms II for a certain time to get estimates of \hat{R} and \hat{S} ;
- Run a simulation (using the identified models);
- Update \hat{P}_{fb-ff} at each sampling instant or from time to time using Algorithm III (after a short initialization horizon using one of the Algorithms II).

Remark: It should be noticed that in the adaptive control literature, adaptation error filtering as well as observation vector filtering have been reported (see also Subsection 2.3.1 for a more complete review). Even though the objective of both types of filtering is the same, satisfaction of the SPR condition, their effects are different. The filtering of the adaptation error introduces a frequency weighting on the performance criterion. On the other hand, special care has to be taken because satisfaction of the SPR condition (4.23) by adaptation error filtering alone ($V(q^{-1}) \neq 1$, $L(q^{-1}) = 1$) implies filtering by the inverse of the secondary path which in some cases is not of minimum phase thus its inverse is unstable. This problem is avoided when filtering the observation vector using $L(q^{-1})$.

4.3.2 The stochastic case - perfect matching

There are two sources of measurement noise, one acting on the primary transducer which gives the correlated measurement with the disturbance and the second acting on the measurement of the residual error (force, acceleration). For the primary transducer, the effect of the measurement noise is negligible since the signal to noise ratio is very high. The situation is different for the residual error where the effect of the noise can not be neglected.

In the presence of the measurement noise ($n(t)$), the equation of the *a posteriori* residual error becomes

$$\nu(t+1) = H(q^{-1}) [\theta - \hat{\theta}(t+1)]^T \Phi(t) + n(t+1). \tag{4.26}$$

The O.D.E. method [Ljung and Söderström, 1983] can be used to analyse the asymptotic behavior of the algorithm in the presence of noise. Taking into account the form of equation (4.26), one can directly use [Landau et al., 2011g, Theorem 4.1] or [Landau and Karimi, 1997, Theorem B1].

The following assumptions will be made:

1. $\lambda_1(t) = 1$ and $\lambda_2(t) = \lambda_2 > 0$;
2. $\hat{\theta}(t)$ generated by the algorithm belongs infinitely often to the domain D_S :

$$D_S \triangleq \{\hat{\theta} : \hat{P}(z^{-1}) = 0 \Rightarrow |z| < 1\}$$

for which stationary processes

$$\begin{aligned}\Phi(t, \hat{\theta}) &\triangleq \Phi(t)|_{\hat{\theta}(t)=\hat{\theta}=\text{const}} \\ \nu(t, \hat{\theta}) &= \nu(t)|_{\hat{\theta}(t)=\hat{\theta}=\text{const}}\end{aligned}$$

can be defined;

3. $n(t)$ is a zero mean stochastic process with finite moments and independent of the sequence $w(t)$.

From (4.26) for $\hat{\theta}(t) = \hat{\theta}$, one gets

$$e(t+1, \hat{\theta}) = H(q^{-1}) [\theta - \hat{\theta}]^T \Phi(t, \hat{\theta}) + n(t+1). \quad (4.27)$$

Since $\Phi(t, \hat{\theta})$ depends upon $w(t)$ only, one concludes that $\Phi(t, \hat{\theta})$ and $n(t+1)$ are independent. Therefore, using [Landau et al., 2011g, Theorem 4.1] it results that if

$$H'(z^{-1}) = \frac{A_M A_G A_K G V}{P_{fb-ff} L} - \frac{\lambda_2}{2} \quad (4.28)$$

is a SPR transfer function, one has $Prob\{\lim_{t \rightarrow \infty} \hat{\theta}(t) \in D_C\} = 1$, where $D_C = \{\hat{\theta} : \Phi^T(t, \hat{\theta})(\theta - \hat{\theta}) = 0\}$. If furthermore $\Phi^T(t, \hat{\theta})(\theta - \hat{\theta}) = 0$ has a unique solution (richness condition), the condition that $H'(z^{-1})$ be SPR implies that $Prob\{\lim_{t \rightarrow \infty} \hat{\theta}(t) = \theta\} = 1$.

4.3.3 The case of non-perfect matching

If $\hat{N}(t, q^{-1})$ does not have the appropriate dimension, there is no chance to satisfy the perfect matching condition. Two problems are of interest in this case:

1. The boundedness of the residual error
2. The bias distribution in the frequency domain

Boundedness of the residual error

Results from [Landau and Karimi, 1997, Landau et al., 2001b] can be used to analyze the boundedness of the residual error. The following assumptions are made:

1. There exists a reduced order filter \hat{N} , characterized by the unknown polynomials \hat{S} (of order n_S) and \hat{R} (of order n_R), for which the polynomials given in eqs. (4.3)-(4.5), where S and R have been replaced by \hat{S} and \hat{R} , are Hurwitz.
2. The output of the optimal filter satisfying the matching condition can be expressed as

$$\hat{u}_1(t+1) = - \left[\hat{S}^*(q^{-1})\hat{u}_1(t) - \hat{R}(q^{-1})\hat{y}_1(t+1) + \eta(t+1) \right], \quad (4.29)$$

where $\eta(t+1)$ is a norm bounded signal.

Using the results of [Landau and Karimi, 1997, Theorem 4.1, pp. 1505-1506] and assuming that $w(t)$ is norm bounded, it can be shown that all the signals are norm bounded under the passivity condition (4.23), where \hat{P}_{fb-ff} is computed now with the reduced order estimated filter.

Bias distribution

Using the Parseval's relation, the asymptotic bias distribution of the estimated parameters in the frequency domain can be obtained, starting from the expression of $\nu(t)$, by taking into account that the algorithm minimizes (almost) a criterion of the form $\lim_{N \rightarrow \infty} \frac{1}{N} \sum_{t=1}^N \nu^2(t)$.

The bias distribution (for Algorithm III) is given by

$$\hat{\theta}^* = \arg \min_{\hat{\theta}} \int_{-\pi}^{\pi} |V(e^{-j\omega})|^2 \cdot \left[\left| \frac{1 - \hat{N}(e^{-j\omega})M(e^{-j\omega})}{1 - \hat{N}(e^{-j\omega})M(e^{-j\omega}) + K(e^{-j\omega})G(e^{-j\omega})} \right|^2 \cdot \left| D(e^{-j\omega}) + \frac{\hat{N}(e^{-j\omega})G(e^{-j\omega})}{1 - \hat{N}(e^{-j\omega})M(e^{-j\omega})} \right|^2 \phi_w(\omega) + \phi_n(\omega) \right] d\omega \quad (4.30)$$

where ϕ_w and ϕ_n are the spectral densities of the disturbance $w(t)$ and of the measurement noise. Taking into account equation (4.2), one obtains

$$\hat{\theta}^* = \arg \min_{\hat{\theta}} \int_{-\pi}^{\pi} |V|^2 \cdot \left[|S_{NM}|^2 |N - \hat{N}|^2 \left| \frac{1}{1 - \hat{N}M + KG} \right|^2 |G|^2 \phi_w(\omega) + \phi_n(\omega) \right] d\omega \quad (4.31)$$

where $S_{NM} = \frac{1}{1-NM}$ is the output sensitivity function of the internal closed loop for the optimal controller.

From (4.30) and (4.31) one concludes that a good approximation of $N(q^{-1})$ will be obtained in the frequency region where ϕ_w is significant and where $G(q^{-1})$ has a high gain (usually $G(q^{-1})$ should have high gain in the frequency region where ϕ_w is significant in order to counteract the effect of $w(t)$). However, the quality of the estimated $\hat{N}(q^{-1})$ will be affected also by the output sensitivity function of the internal closed loop $N - M$. Clearly, the introduction of the filter $V(q^{-1})$ on the adaptation error will shape the frequency distribution of the error.

4.4 Relaxing the Positive Real Condition

The adaptive system formed by eq. (4.17) and the adaptation algorithm (4.14) admits an equivalent feedback representation (EFR) for $\lambda_1(t) \equiv 1$, $\lambda_2(t) \equiv 0$ (constant adaptation gain). The stability condition of eq. (4.23) (in this case $H'(z^{-1}) = H(z^{-1})$) is a direct consequence of the passivity of the equivalent feedback path, since if the feedback path is passive, it is enough that the equivalent linear feedforward path is SPR (see [Landau et al., 2011g]). However, this condition is only sufficient. There is an additional "excess" of passivity in the feedback path (which depends upon the adaptation gains and on the magnitude of $\Phi(t)$) which can be transferred to the linear feedforward block in order to relax the SPR condition. This idea was prompted out in the context of recursive identification by Tomizuka and results have been given for the case of integral adaptation and for the case when the equivalent linear feedforward path is characterized by an all poles (no zeros) transfer function (see [Tomizuka, 1982]). These results have been extended in [Landau et al., 2011g] for "Integral + Proportional" adaptation with constant adaptation gain.

In what follows, the results of [Tomizuka, 1982, Landau et al., 2011g] will be extended to the case of linear equivalent feedforward paths characterized by a poles-zeros transfer function and taking into account the presence of the proportional adaptation which increases significantly the reserve of passivity of the equivalent feedback path. One needs first the following result:

Lemma 4.4.1. *Given the discrete transfer function*

$$H(z^{-1}) = \frac{B(z^{-1})}{A(z^{-1})} = \frac{b_0 + b_1 z^{-1} + \dots + b_{n_B} z^{-n_B}}{1 + a_1 z^{-1} + \dots + a_{n_A} z^{-n_A}}, \quad (4.32)$$

under the hypotheses:

H5) $H(z^{-1})$ has all its zeros inside the unit circle,

H6) $b_0 \neq 0$,

there exists a positive scalar gain K such that $\frac{H}{1+KH}$ is SPR.

The proof of this lemma is presented in Appendix A.2.

Using the above property, the EFR of the adaptive feedback system given by the eqs. (4.14) and (4.17) for $\lambda_2(t) \equiv 0$, $\lambda_1(t) \equiv 1$ (constant adaptation gain) can be represented as in Figure 4.1, where K has been chosen such that $\frac{H}{1+KH}$ is SPR and

$$\tilde{\theta}_I(t) = \hat{\theta}_I(t) - \theta, \quad (4.33)$$

$$\nu(t+1) = -\frac{H(z^{-1})}{1+KH(z^{-1})} y_{e2}(t), \quad (4.34)$$

$$\tilde{\theta}_I(t+1) = \tilde{\theta}_I(t) + \xi(t) F_I \Phi(t) \nu(t+1), \quad (4.35)$$

$$y_{e2}(t) = \Phi^T(t) \tilde{\theta}_I(t) + (\Phi^T(t) F(t) \Phi(t) - K) \nu(t+1), \quad (4.36)$$

$$u_{e2}(t) = \nu(t+1) \quad (4.37)$$

For the stability, it remains to show that the new equivalent path is passive, *i.e.*, it satisfies the Popov inequality

$$\sum_{t=0}^{t_1} y_{e2}(t) u_{e2}(t) \geq -\gamma_0^2. \quad (4.38)$$

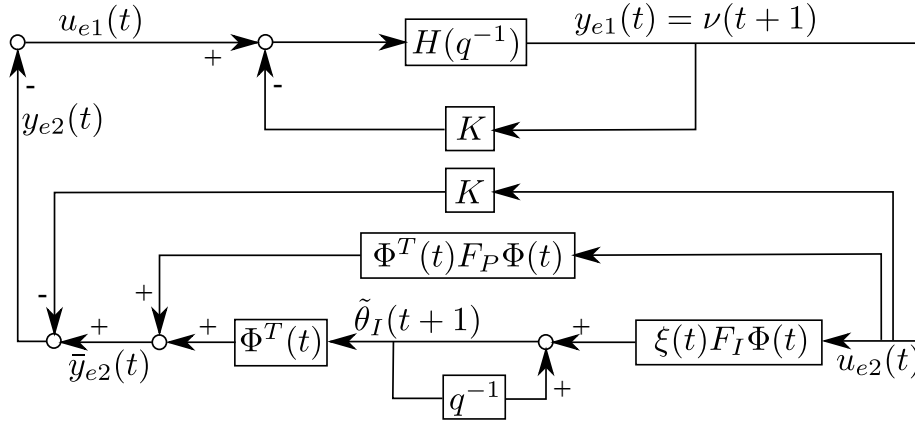


Figure 4.1: Equivalent feedback representation of the PAA with "Integral + Proportional" adaptation with constant integral adaptation gain.

Theorem 4.4.1. *The adaptive system described by eq. (4.17) and eqs. (4.14) for $\lambda_2(t) \equiv 0$ and $\lambda_1(t) \equiv 1$ is asymptotically stable provided that:*

T1) *There exists a gain K such that $\frac{H}{1+KH}$ is SPR,*

T2) *The adaptation gains F_I and $F_P(t)$ and the observation vector $\Phi(t)$ satisfy*

$$\sum_{t=0}^{t_1} \left[\Phi^T(t-1) \left(\frac{1}{2}F_I + F_P(t-1) \right) \Phi(t-1) - K \right] \nu^2(t) \geq 0 \quad (4.39)$$

for all $t_1 \geq 0$ or

$$\Phi^T(t) \left(\frac{1}{2}F_I + F_P(t) \right) \Phi(t) > K > 0, \quad (4.40)$$

for all $t \geq 0$.

The proof of this theorem is given in Appendix A.3.

4.5 Experimental Results

The advantages of using the feedforward adaptive compensator in the presence of the fixed feedback have been demonstrated in the thesis [Alma, 2011] and will not be recalled here. In Section 4.5.1, it will be shown that using an IP-PAA in addition to the above mentioned scheme can have a positive effect on the disturbance rejection performance. Section 4.5.2 will provide experimental results which highlight the relaxation of the SPR condition by use of IP-PAA. In both sections, scalar adaptations are experimented with.

4.5.1 Broadband disturbance rejection with feedback controller and adaptation error filtering

The adaptive feedforward filter structure for all of the experiments has been $n_R = 3$, $n_S = 4$ (total of 8 parameters). This complexity does not allow to verify the "perfect matching condition" (not enough parameters). A PRBS excitation on the global primary path will be considered as the disturbance.

Figure 4.2 shows the performance of the feedback controller with respect to the open loop. A 13 dB of global attenuation is obtained.

For the *adaptive* operation the Algorithm *IIa* and *IIb* have been used with scalar adaptation gain ($\lambda_1(t) = 1$, $\lambda_2(t) = 0$)². The experiments have been carried out by first applying the disturbance in open loop during 50 sec and after that, closing the loop with the adaptive feedforward algorithms in the presence of the fixed feedback controller. The experiments have been run over a 1500 sec time period.

Time domain results obtained on the AVC system with only an "Integral" PAA are shown in Figure 4.3. Figure 4.4 shows the time domain result obtained using the IP-PAA. The advantage of using an "Integral + Proportional" PAA is an overall improvement of the transient behavior. A variable $\alpha(t)$ in the PAA has been chosen, starting with an initial value of 200 and linearly decreasing to 100 (over a horizon of 25s).

In Figure 4.5, in addition to the IP-PAA a filtering of the adaptation error using $V(q^{-1}) = 1 - 0.9q^{-1}$ has been introduced (using Algorithm *IIb*). In this case, $\alpha(t)$ has been initialized at 200 and was linearly decreased to 10 over a horizon of 950 sec.

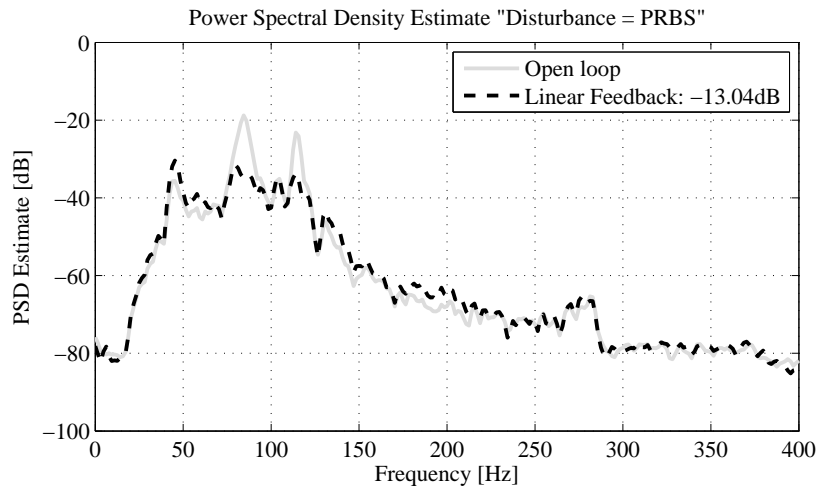


Figure 4.2: Power spectral density of the open loop and when using the fixed feedback controller.

A comparison of the power spectral densities obtained with the three adaptive algorithms is presented in Figure 4.6. One observes a very good attenuation obtained by the IP-PAA algorithm with adaptation error filtering and no degradation with respect to the open loop above at high frequencies, which is in congruence with the $V(q^{-1})$ filter that has been used. It has to be mentioned that for the PSDs only the last ten seconds of the 1500 sec experiments have been taken into account.

It is clear that "Integral + Proportional" adaptation gives better results than only "Integral" adaptation and that using a filtering of the adaptation error can also have a good effect.

4.5.2 Broadband disturbance rejection using only the feedforward adaptive filter

As it turns out, in the hybrid case, the positive real condition was satisfied even with Algorithm *IIa* in the frequency region from 0 to 300 Hz, which under the slow adaptation

²Note that Algorithm *IIa* uses the same filtering as FuLMS algorithm.

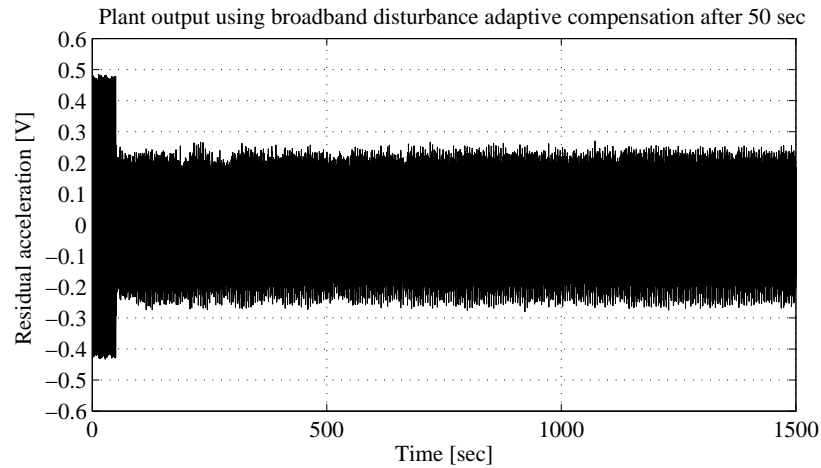


Figure 4.3: Real time results obtained with Algorithm *IIa* using "Integral" scalar adaptation gain.

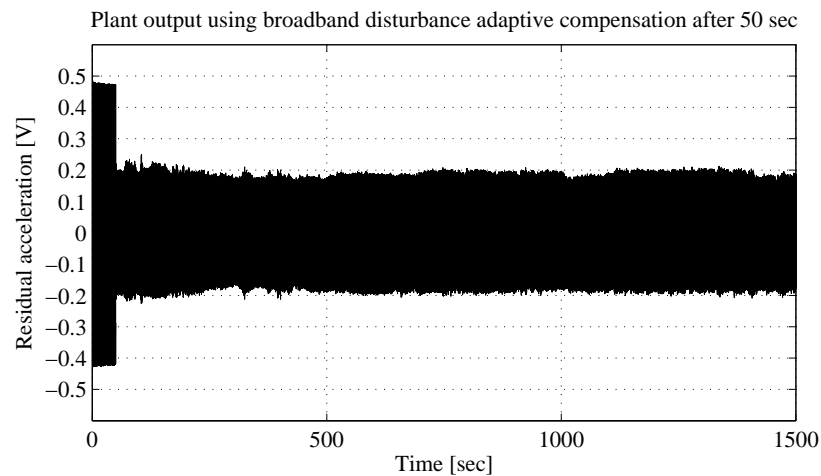


Figure 4.4: Real time results obtained with Algorithm *IIa* using "Integral + Proportional" scalar adaptation gain.

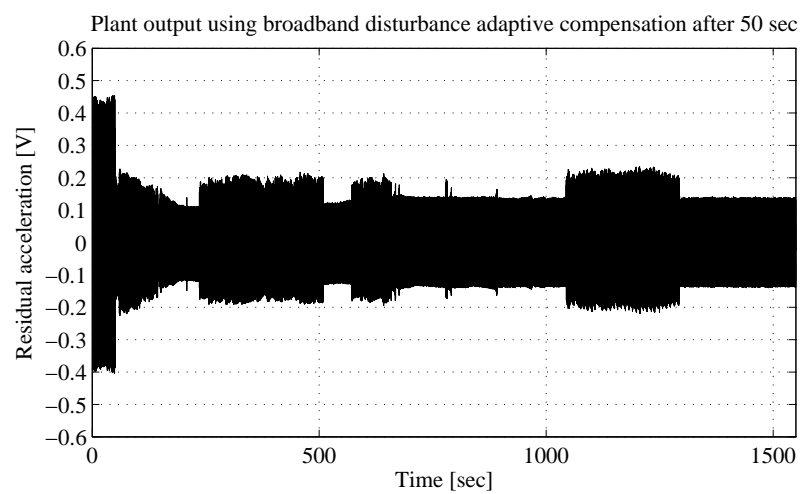


Figure 4.5: Real time results obtained with Algorithm *IIb* using "Integral + Proportional" scalar adaptation gain and adaptation error filtering.

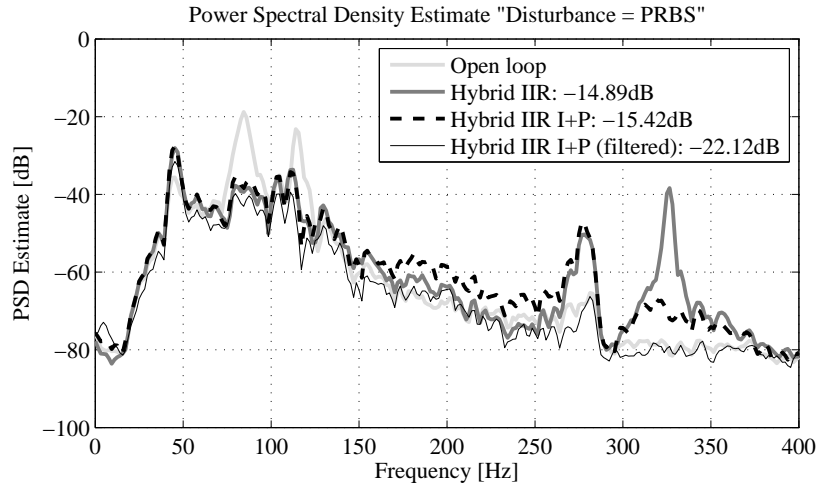


Figure 4.6: Power spectral density of the adaptive filters.

gain assumption is enough to guarantee the stability of the system taking also into consideration the frequency characteristics of the disturbance (Figure 4.6, open loop). In this subsection, the case without fixed feedback compensator is considered. The objective is to show that the SPR condition can be improved in a more general case when this is an issue.

In the absence of the feedback controller, $B_K(q^{-1}) = 0$ and $A_K(q^{-1}) = 1$, and with no filtering of the adaptation error, $V(q^{-1}) = 1$, eq. (4.18) for Algorithm *IIa* (or *IIb*) becomes

$$H(q^{-1}) = \frac{A_M G}{P \hat{G}}. \quad (4.41)$$

The advantage of using an "Integral + Proportional" PAA is an overall improvement of the transient behavior despite the fact that the SPR condition on $H(q^{-1})$ is not satisfied as shown in Figure 4.7 (the SPR condition is not satisfied around 83 Hz and around 116 Hz). Note that Figure 4.7 corresponds to an estimation of this transfer function assuming $\hat{G} = G$, $\hat{M} = M$ and $P = A_M \hat{S} - B_M \hat{R}$ in which the parameters of \hat{R} and \hat{S} have been obtained by running the adaptation algorithm for 1500s. A variable $\alpha(t)$ in the PAA has been chosen, starting with an initial value of 200 and linearly decreasing to 100 (over a horizon of 25s). To obtain this profile for $\alpha(t)$, different variations have been tried first, taking also into consideration the theoretical analysis given in Section 4.4, and the one giving the best results has been used in the end. The most important objective has been to improve the performance during the initial transient period, thus a large value for $\alpha(t)$ has been used at start decreasing to smaller values so that parameter variations could be reduced in the end, thus obtaining better global attenuations.

Time domain results obtained on the AVC system are shown in Figure 4.9. Figure 4.8 shows the comparison between "Integral" and "Integral + Proportional" adaptation over an horizon of 1500s (Figure 4.9 is a zoom of Figure 4.8 covering only the first 30s after the introduction of the adaptive feedforward compensator). It is clear that "Integral + Proportional" adaptation gives better results on a long run. The effect in the initial phase of the adaptation, Figure 4.9, is an acceleration of transients. It can be observed that the adaptation error is limited to the interval $[-0.3, 0.3]$ 10 seconds sooner when using IP-PAA than when using basic integral adaptation.

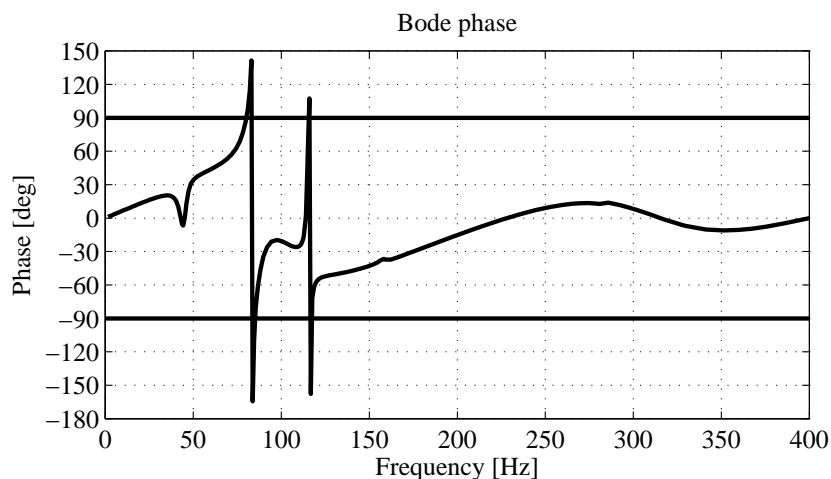


Figure 4.7: Phase of estimated $H(z^{-1})$ for Algorithm *IIa*.

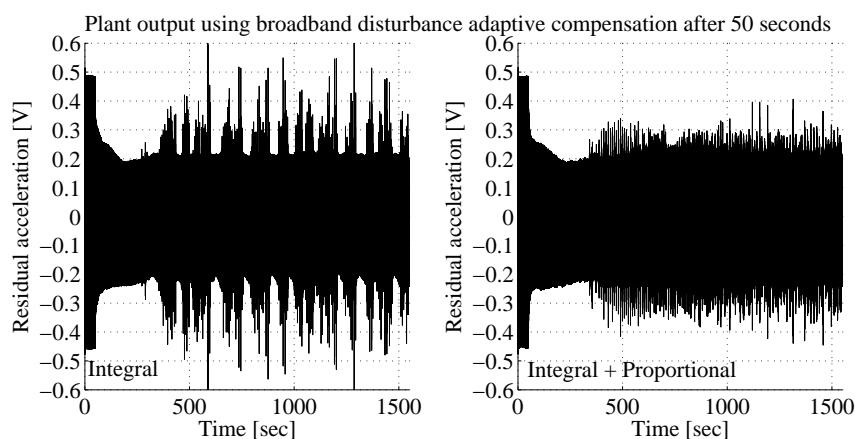


Figure 4.8: Real time results obtained with Algorithm *IIa* using "Integral" scalar adaptation gain (left) and "Integral + Proportional" scalar adaptation gain (right) over 1500s.

4.6 Concluding Remarks

In this chapter it has been shown that the "Integral + Proportional" adaptation algorithms presented are useful in the context of adaptive feedforward vibration (or noise) compensation. Theoretical development shows that the SPR condition can be relaxed and an improvement of the adaptation transients is obtained. Furthermore, the introduction of a feedback controller on one hand modifies the stability conditions and on the other hand improves significantly the performances of the adaptive feedforward compensation schemes.

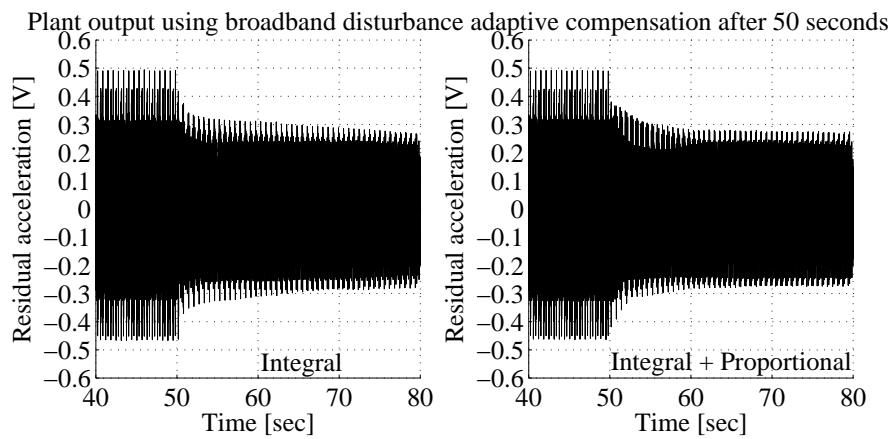


Figure 4.9: Real time results obtained with Algorithm *IIa* using "Integral" scalar adaptation gain (left) and "Integral + Proportional" scalar adaptation gain (right).

CHAPTER 5

GENERAL YOULA-KUČERA PARAMETERIZED FEEDFORWARD AVC

5.1 Introduction

The importance of designing feedforward adaptive algorithms for AVC systems taking into account the inherent "positive" feedback has been highlighted in the previous chapter. Here, a different approach to the development of feedforward algorithms is taken by use of the Youla-Kučera parametrization.

In [Zeng and de Callafon, 2006], the idea of using a Youla-Kučera parametrization¹ of the feedforward compensator is illustrated in the context of active noise control. Based on the identification of the system, a stabilizing Youla-Kučera controller using an orthonormal basis filter is designed. The Youla-Kučera parameters weighting the orthonormal basis filters are then updated by using a two time scale indirect procedure: (1) estimation of the Q-filter's parameters over a certain horizon, (2) updating of the controller. No stability proof for the tuning procedure is provided.

In the control literature the use of Youla-Kučera type controllers has been extensively discussed, see [Anderson, 1998, Tay et al., 1997] and related references [de Callafon and Kinney, 2010, Ficocelli and Ben Amara, 2009]².

The objectives of this chapter are:

- to develop, to analyze and to evaluate experimentally new recursive algorithms for online estimation and adaptation of the Q-parameters of IIR Youla-Kučera (subsequently called *QIIR*) parameterized feedforward compensators for broadband disturbances with unknown and variable spectral characteristics;
- to evaluate comparatively these algorithms with respect to existing algorithms from theoretical, implementation and experimental points of view.

As it will be seen, this chapter focuses on the IIR Youla-Kučera parametrization. The main reason is that the FIR Youla-Kučera is a special case of the former, more general one. Discussions on the simplifications that arise when passing from IIR to FIR Youla-Kučera parameters will be given at the different stages of the development and the analysis.

The main contributions of this chapter with respect to [Zeng and de Callafon, 2006] are:

¹Throughout the chapter the *Youla-Kučera parametrization* will also be called *Q* (or *YK*) - *parametrization*.

²To the best knowledge of the author, the specific problem considered in this chapter is not covered in the existing literature.

- the development of new real time recursive adaptation algorithms for the Q-parameters of FIR/IIR Youla-Kučera feedforward compensators and the analysis of the stability of the resulting system;
- the application of the algorithms to an active vibration control system;
- the experimental comparison with adaptive IIR feedforward compensators;
- the significant reduction of the number of parameters to be adapted for the same level of performance when using adaptive IIR Youla-Kučera feedforward compensators instead of adaptive FIR Youla-Kučera feedforward compensators.

In the context of this chapter, it is assumed that:

- the characteristics of the wide band disturbance acting on the system are unknown and they may vary;
- the internal positive feedback can not be neglected;
- the dynamic models of the AVC are constant and a good estimation of these models is available (these models can be estimated from experimental data).

From the user point of view and taking into account the type of operation of adaptive disturbance compensation systems, one has to consider two modes of operation of the adaptive schemes:

- *Adaptive* operation. The adaptation is performed continuously with a non vanishing adaptation gain.
- *Self-tuning* operation. The adaptation procedure starts either on demand or when the performance is unsatisfactory. A vanishing adaptation gain is used.

From the implementation point of view, the chapter will explore the comparative performances of adaptation algorithms with matrix adaptation gain and with scalar adaptation gain. While the algorithms have been developed and tested in the context of AVC, the results are certainly applicable to ANC (Active Noise Control) systems since they feature the same type of internal positive feedback.

The chapter is organized as follows. The system representation and the IIR Youla-Kučera feedforward compensator structure are given in Section 5.2. The algorithms for adaptive feedforward compensation are developed in Section 5.3 and analyzed in Section 5.4. Section 5.5 presents experimental results obtained on the active vibration control system with the algorithms introduced in this chapter, as well as an experimental comparison with those given in [Landau et al., 2011c, Landau et al., 2011d]. Section 5.6 summarizes the comparison with other algorithms.

5.2 Basic Equations and Notations

For the purpose of this chapter, an IIR Youla-Kučera parametrization of the optimal feedforward filter, Figure 2.4, is considered (see [Anderson, 1998] for more detailed informations on the Youla-Kučera parametrization). Taking into account the fact that in the present chapter there is no feedback compensator ($K \equiv 0$), the measured signal and the control are as described in Subsection 2.2.2 ($u(t) = u_1(t)$ and $y(t) = y_1(t)$). The block diagram representing this method is given in Figure 5.1. In this case, the filter polynomials $R(q^{-1})$ and $S(q^{-1})$, from eq. 3.11, become

$$R(q^{-1}) = A_Q(q^{-1})R_0(q^{-1}) - B_Q(q^{-1})\hat{A}_M(q^{-1}), \quad (5.1)$$

$$S(q^{-1}) = A_Q(q^{-1})S_0(q^{-1}) - B_Q(q^{-1})\hat{B}_M(q^{-1}), \quad (5.2)$$

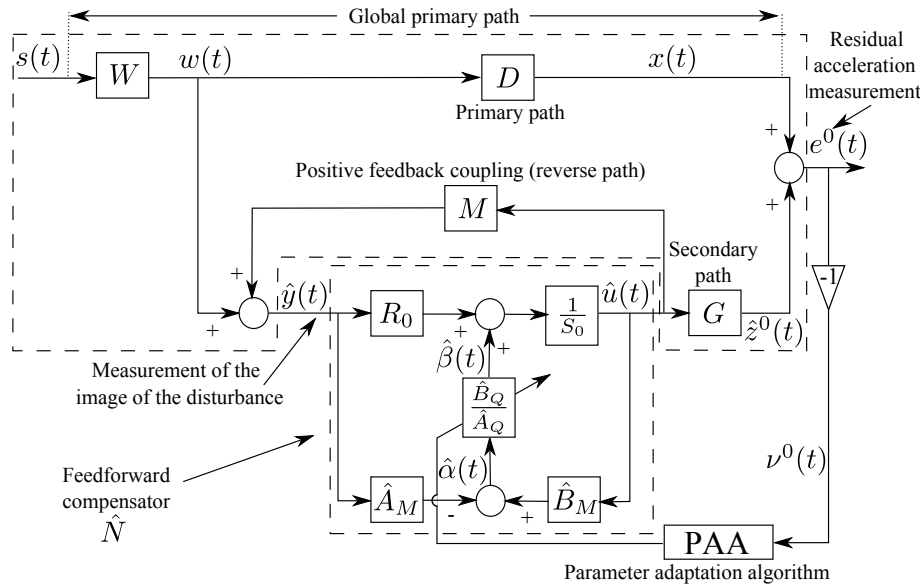


Figure 5.1: AVC block diagram with adaptive feedforward compensator using the YKIIR method.

where $S_0(q^{-1})$ and $R_0(q^{-1})$ denote respectively the denominator and numerator of a central (stabilizing) controller (see Section 5.5.1) and $A_Q(q^{-1})$ and $B_Q(q^{-1})$ are the denominator and the numerator of the optimal $QIIR$ filter

$$Q(q^{-1}) = \frac{B_Q(q^{-1})}{A_Q(q^{-1})} = \frac{b_0^Q + b_1^Q q^{-1} + \dots + b_{n_{BQ}}^Q q^{-n_{BQ}}}{1 + a_1^Q q^{-1} + \dots + a_{n_{AQ}}^Q q^{-n_{AQ}}}. \quad (5.3)$$

The estimated $QIIR$ filter is denoted by $\hat{Q}(q^{-1})$ or $\hat{Q}(\hat{\theta}, q^{-1})$ when it is a linear filter with constant coefficients or $\hat{Q}(t, q^{-1})$ during the estimation (adaptation) stage. The vector of parameters of the optimal $QIIR$ filter assuring perfect matching will be denoted by

$$\theta^T = [b_0^Q, \dots, b_{n_{BQ}}^Q, a_1^Q, \dots, a_{n_{AQ}}^Q] = [\theta_{BQ}^T, \theta_{AQ}^T]. \quad (5.4)$$

The vector of parameters for the estimated $QIIR$ filter

$$\hat{Q}(q^{-1}) = \frac{\hat{B}_Q(q^{-1})}{\hat{A}_Q(q^{-1})} = \frac{\hat{b}_0^Q + \hat{b}_1^Q q^{-1} + \dots + \hat{b}_{n_{BQ}}^Q q^{-n_{BQ}}}{1 + \hat{a}_1^Q q^{-1} + \dots + \hat{a}_{n_{AQ}}^Q q^{-n_{AQ}}} \quad (5.5)$$

is denoted by

$$\hat{\theta}^T = [\hat{b}_0^Q, \dots, \hat{b}_{n_{BQ}}^Q, \hat{a}_1^Q, \dots, \hat{a}_{n_{AQ}}^Q] = [\hat{\theta}_{BQ}^T, \hat{\theta}_{AQ}^T]. \quad (5.6)$$

The *a priori* output of the estimated feedforward compensator using an IIRYK parametrization for the case of time varying parameter estimates is given by (using eq. (3.11) and taking into consideration that the adaptation error is not filtered in the present context, $V(q^{-1}) = 1$)

$$\begin{aligned} \hat{u}^0(t+1) &= \hat{u}(t+1|\hat{\theta}(t)) = -\hat{S}^*(t, q^{-1})\hat{u}(t) + \hat{R}(t, q^{-1})\hat{y}(t+1) \\ &= -((\hat{A}_Q(t, q^{-1})S_0(q^{-1}))^* - \hat{B}_Q(t, q^{-1})\hat{B}_M^*(q^{-1}))\hat{u}(t) \\ &\quad + (\hat{A}_Q(t, q^{-1})R_0(q^{-1}) - \hat{B}_Q(t, q^{-1})\hat{A}_M(q^{-1}))\hat{y}(t+1) \end{aligned} \quad (5.7)$$

$$\begin{aligned} &= -(\hat{A}_Q(t, q^{-1})S_0(q^{-1}))^*\hat{u}(t) + \hat{A}_Q(t, q^{-1})R_0(q^{-1})\hat{y}(t+1) \\ &\quad + \hat{B}_Q(t, q^{-1})\left(\hat{B}_M^*(q^{-1})\hat{u}(t) - \hat{A}_M(q^{-1})\hat{y}(t+1)\right), \end{aligned} \quad (5.8)$$

where

$$\begin{aligned} \hat{u}(t+1) = & -(\hat{A}_Q(t+1, q^{-1})S_0(q^{-1}))^* \hat{u}(t) + \hat{A}_Q(t+1, q^{-1})R_0(q^{-1})\hat{y}(t+1) \\ & + \hat{B}_Q(t+1, q^{-1}) \left(\hat{B}_M^*(q^{-1})\hat{u}(t) - \hat{A}_M(q^{-1})\hat{y}(t+1) \right). \end{aligned} \quad (5.9)$$

Notice that eqs. (5.1), (5.2), (5.3), (5.8) and (5.9) can be easily particularized for the case of a FIR Youla-Kučera parametrization by taking $\hat{A}_Q(t, q^{-1}) \equiv 1$.

5.3 Development of the Algorithms

The algorithms for adaptive feedforward IIRYK compensators will be developed under the following hypotheses:

- H1) The signal $w(t)$ is bounded (which is equivalent to $s(t)$ is bounded and $W(q^{-1})$ in Figures 3.3 and 5.1 is asymptotically stable).
- H2) The estimated model for the reverse path is identical to the true model ($\hat{A}_M \equiv A_M$ and $\hat{B}_M \equiv B_M$).
- H3) There exists a central feedforward compensator N_0 (R_0, S_0) which stabilizes the inner positive feedback loop formed by N_0 and M and a *QIIR* filter (B_Q, A_Q) such that the characteristic polynomial of the closed loop³

$$P(q^{-1}) = A_Q(q^{-1}) \left(A_M(q^{-1})S_0(q^{-1}) - B_M(q^{-1})R_0(q^{-1}) \right) = A_Q(q^{-1})P_0(q^{-1}) \quad (5.10)$$

is a Hurwitz polynomial.

- H4) Perfect matching condition - There exists a value of the Q parameters such that

$$\frac{G \cdot A_M(R_0A_Q - A_MB_Q)}{A_Q(A_MS_0 - B_MR_0)} = -D. \quad (5.11)$$

- H5) Deterministic context - The effect of the measurement noise upon the measurement of the residual acceleration is neglected.

- H6) The primary path model $D(z^{-1})$ is unknown and constant.

Once the algorithms will be developed under these hypotheses, *H2*, *H4*, and *H5* will be removed and the algorithm will be analyzed in this modified context.

A first step in the development of the algorithms is to establish, for a fixed estimated compensator, a relation between the error on the Q-parameters (with respect to the optimal values) and the adaptation error ν . This is summarized in the following lemma.

Lemma 5.3.1. *Under the hypotheses H1 - H6 for the system described by eqs. 3.2 - (3.34) (with $K \equiv 0$) using an estimated IIR Youla-Kučera parameterized feedforward compensator with constant parameters $\hat{\theta}$, one has*

$$\nu(t+1) = \frac{A_M(q^{-1})G(q^{-1})}{A_Q(q^{-1})P_0(q^{-1})} [\theta - \hat{\theta}]^T \phi(t), \quad (5.12)$$

³The parenthesis (q^{-1}) will be omitted in some of the following equations to make them more compact.

where $\phi(t)$ is given by

$$\phi^T(t) = [\alpha(t+1), \dots, \alpha(t-n_{B_Q}+1), -\beta(t), \dots, -\beta(t-n_{A_Q})]. \quad (5.13)$$

and

$$\alpha(t+1) = \hat{B}_M \hat{u}(t+1) - \hat{A}_M \hat{y}(t+1) = \hat{B}_M^* \hat{u}(t) - \hat{A}_M \hat{y}(t+1) \quad (5.14a)$$

$$\beta(t) = S_0 \hat{u}(t) - R_0 \hat{y}(t) \quad (5.14b)$$

The proof of this lemma is given in Appendix B.1.

Corollary 5.3.1. *Under the hypotheses H1 - H6 for the system described by eqs. (3.2) - (3.34) using an estimated FIR Youla-Kučera parameterized feedforward compensator with constant parameters $\hat{\theta}$, one has*

$$\nu(t+1) = \frac{A_M(q^{-1})G(q^{-1})}{P_0(q^{-1})} [\theta - \hat{\theta}]^T \phi(t), \quad (5.15)$$

where

$$\theta^T = [b_0^Q, \dots, b_{n_{B_Q}}^Q] = [\theta_{B_Q}^T] \quad (5.16)$$

is the vector of parameters of the optimal QFIR filter assuring perfect matching,

$$\hat{\theta}^T = [\hat{b}_0^Q, \dots, \hat{b}_{n_{B_Q}}^Q] = [\hat{\theta}_{B_Q}^T] \quad (5.17)$$

is the vector of parameters for the estimated \hat{Q} FIR filter

$$\hat{Q}(q^{-1}) = \hat{B}_Q(q^{-1}) = \hat{b}_0^Q + \hat{b}_1^Q q^{-1} + \dots + \hat{b}_{n_{B_Q}}^Q q^{-n_{B_Q}}, \quad (5.18)$$

and $\phi^T(t)$ is given by

$$\phi^T(t) = [\alpha(t+1), \alpha(t), \dots, \alpha(t-n_{B_Q}+1)]. \quad (5.19)$$

where $\alpha(t+1)$ is given in eq. (5.14a).

Proof. This result can be straightforwardly obtained by making $\hat{A}_Q(q^{-1}) = 1$ and $A_Q(q^{-1}) = 1$ in Lemma 5.3.1. \square

Throughout the remainder of this section and the next one, unless stated differently, the Youla-Kučera parametrization with a QIIR filter will be discussed. It should be observed that the results for the case of QFIR polynomials can be obtained by imposing $A_Q(q^{-1}) = 1$ and $\hat{A}_Q(q^{-1}) = 1$. Further comments will be made when appropriate.

As it will be shown later on, it is convenient, for assuring the stability of the system, to filter the observation vector $\phi(t)$. Filtering the vector $\phi(t)$ with an asymptotically stable filter $L(q^{-1}) = \frac{B_L}{A_L}$, eq. (5.12) for a constant $\hat{\theta}$ becomes

$$\nu(t+1) = \frac{A_M(q^{-1})G(q^{-1})}{A_Q(q^{-1})P_0(q^{-1})L(q^{-1})} [\theta - \hat{\theta}]^T \phi_f(t) \quad (5.20)$$

with

$$\begin{aligned} \phi_f(t) &= L(q^{-1})\phi(t) \\ &= [\alpha_f(t+1), \dots, \alpha_f(t-n_{B_Q}+1), -\beta_f(t), \dots, -\beta_f(t-n_{A_Q})], \end{aligned} \quad (5.21)$$

where

$$\begin{aligned}\alpha_f(t+1) &= L(q^{-1})\alpha(t+1) \\ \beta_f(t) &= L(q^{-1})\beta(t).\end{aligned}\tag{5.22}$$

Eq. (5.20) will be used to develop the adaptation algorithms. When the parameters of \hat{Q} are time-varying and neglecting the non-commutativity of the time-varying operators (which implies slow adaptation (see [Anderson et al., 1986]), *i.e.*, a limited value for the adaptation gain), eq. (5.20) transforms into⁴

$$\nu(t+1) = \frac{A_M(q^{-1})G(q^{-1})}{A_Q(q^{-1})P_0(q^{-1})L(q^{-1})}[\theta - \hat{\theta}(t+1)]^T \phi_f(t).\tag{5.23}$$

Eq. (5.23) has the standard form for an *a posteriori* adaptation error ([Landau et al., 2011g]), which immediately suggests to use the following PAA

$$\hat{\theta}(t+1) = \hat{\theta}(t) + F(t)\psi(t)\nu(t+1)\tag{5.24a}$$

$$\nu(t+1) = \frac{\nu^0(t+1)}{1 + \psi^T(t)F(t)\psi(t)}\tag{5.24b}$$

$$F(t+1) = \frac{1}{\lambda_1(t)} \left[F(t) - \frac{F(t)\psi(t)\psi^T(t)F(t)}{\lambda_2(t) + \psi^T(t)F(t)\psi(t)} \right]\tag{5.24c}$$

$$1 \geq \lambda_1(t) > 0, \quad 0 \leq \lambda_2(t) < 2, \quad F(0) > 0\tag{5.24d}$$

$$\psi(t) = \phi_f(t),\tag{5.24e}$$

where $\lambda_1(t)$ and $\lambda_2(t)$ allow to obtain various profiles for the matrix adaptation gain $F(t)$ (see Section 5.5 and [Landau et al., 2011g]). By taking $\lambda_2(t) \equiv 0$ and $\lambda_1(t) \equiv 1$, one gets a constant adaptation gain matrix (or a scalar adaptation gain by choosing $F = \gamma I$, $\gamma > 0$).

Several choices for the filter L will be considered, leading to different algorithms:

$$\begin{aligned}\text{Algorithm } I & & L &= G \\ \text{Algorithm } IIa & & L &= \hat{G} \\ \text{Algorithm } IIb & & L &= \frac{\hat{A}_M}{\hat{P}_0} \hat{G}\end{aligned}\tag{5.25}$$

$$\text{Algorithm } III & & L &= \frac{\hat{A}_M}{\hat{P}} \hat{G}\tag{5.26}$$

with

$$\hat{P} = \hat{A}_Q(\hat{A}_M S_0 - \hat{B}_M R_0) = \hat{A}_Q \hat{P}_0,\tag{5.27}$$

where \hat{A}_Q is an estimation of the denominator of the ideal *QIIR* filter computed on the basis of available estimates of the parameters of the filter \hat{Q} . For the Algorithm *III* several options for updating \hat{A}_Q can be considered:

- Run Algorithm *IIa* or *IIb* during a certain time to get an estimate of \hat{A}_Q .
- Run a simulation (using the identified models).

⁴However, exact algorithms can be developed taking into account the non-commutativity of the time varying operators - see [Landau et al., 2011g].

- Update \hat{A}_Q at each sampling instant or from time to time using Algorithm *III* (after a short initialization horizon using Algorithm *IIa* or *IIb*).

The following procedure is applied at each sampling time for *adaptive* or *self-tuning* operation:

1. Get the measured image of the disturbance $\hat{y}(t+1)$, the measured residual error $e^0(t+1)$ and compute $\nu^0(t+1) = -e^0(t+1)$.
2. Compute $\phi(t)$ and $\phi_f(t)$ using (5.13) and (5.21).
3. Estimate the parameter vector $\hat{\theta}(t+1)$ using the PAA of (5.24a) - (5.24e).
4. Compute (using (5.9)) and apply the control.

5.4 Analysis of the Algorithms

5.4.1 The deterministic case - perfect matching

For Algorithms *I*, *IIa*, *IIb* and *III* the equation for the *a posteriori* adaptation error has the form

$$\nu(t+1) = H(q^{-1}) [\theta - \hat{\theta}(t+1)]^T \psi(t), \quad (5.28)$$

where

$$H(q^{-1}) = \frac{A_M(q^{-1})G(q^{-1})}{A_Q(q^{-1})P_0(q^{-1})L(q^{-1})}, \psi = \phi_f. \quad (5.29)$$

Neglecting the non-commutativity of time varying operators, one has the following result:

Lemma 5.4.1. *Assuming that eq. (5.28) represents the evolution of the a posteriori adaptation error when using an IIR Youla-Kučera adaptive feedforward compensator and that the PAA (5.24a) - (5.24e) is used, one has:*

$$\lim_{t \rightarrow \infty} \nu(t+1) = 0 \quad (5.30)$$

$$\lim_{t \rightarrow \infty} \psi^T(t) [\theta - \hat{\theta}(t+1)] = 0 \quad (5.31)$$

$$\lim_{t \rightarrow \infty} \frac{[\nu^0(t+1)]^2}{1 + \psi(t)^T F(t) \psi(t)} = 0 \quad (5.32)$$

$$\|\psi(t)\| \text{ is bounded} \quad (5.33)$$

$$\lim_{t \rightarrow \infty} \nu^0(t+1) = 0 \quad (5.34)$$

for any initial conditions $\hat{\theta}(0)$, $\nu^0(0)$, $F(0)$, provided that

$$H'(z^{-1}) = H(z^{-1}) - \frac{\lambda_2}{2}, \max_t [\lambda_2(t)] \leq \lambda_2 < 2 \quad (5.35)$$

is a strictly positive real transfer function.

The proof of this lemma is given in Appendix B.2. This result can be particularized for the case of FIR Youla-Kučera adaptive compensators by using the following corollary:

Corollary 5.4.1. *Assuming that eq. (5.28) represents the evolution of the a posteriori adaptation error for FIR Youla - Kučera adaptive feedforward compensators, where*

$$H(q^{-1}) = \frac{A_M(q^{-1})G(q^{-1})}{P_0(q^{-1})L(q^{-1})}, \psi = \phi_f, \quad (5.36)$$

$$\phi_f(t) = L(q^{-1})\phi(t) = [\alpha_f(t+1), \dots, \alpha_f(t - n_{B_Q} + 1)],$$

and that the PAA (5.24a) - (5.24e) is used with $\hat{\theta}(t)$ given by (5.17), then (5.30), (5.32), (5.34) and (5.34) hold for any initial conditions $\hat{\theta}(0)$, $\nu^0(0)$, $F(0)$, provided that

$$H'(z^{-1}) = H(z^{-1}) - \frac{\lambda_2}{2}, \max_t [\lambda_2(t)] \leq \lambda_2 < 2 \quad (5.37)$$

is a SPR transfer function.

The proof is similar to that of Lemma 5.4.1 and will be omitted.

Remark 1: Using Algorithm III and taking into account eq. (5.26), the stability condition for $\lambda_2 = 1$ can be transformed into ([Ljung and Söderström, 1983, Ljung, 1977b]):

$$\left| \left(\frac{A_M}{\hat{A}_M} \cdot \frac{\hat{A}_Q}{A_Q} \cdot \frac{\hat{P}_0}{P_0} \cdot \frac{G}{\hat{G}} \right)^{-1} - 1 \right| < 1 \quad (5.38)$$

for all ω . This roughly means that it always holds provided that the estimates of A_M , A_Q , P_0 , and G are close to the true values (*i.e.*, $H(e^{-j\omega})$ in this case is close to a unit transfer function).

Remark 2: For the case of constant adaptation gain ($F = \alpha I = \text{const.}$) and using Algorithm III, eq. (5.24a) can be viewed as an approximation of the gradient algorithm. For constant adaptation gain $\lambda_2(t) \equiv 0$, the strict positive realness on $H'(z^{-1})$ implies at all the frequencies

$$-90^\circ < \angle \frac{A_M(e^{-j\omega})G(e^{-j\omega})}{A_Q(e^{-j\omega})P_0(e^{-j\omega})} - \angle \frac{\hat{A}_M(e^{-j\omega})\hat{G}(e^{-j\omega})}{\hat{A}_Q(e^{-j\omega})\hat{P}_0(e^{-j\omega})} < 90^\circ. \quad (5.39)$$

Therefore, the interpretation of the SPR condition of Lemma 5.4.1 is that the angle between the direction of adaptation and the direction of the inverse of the true gradient (not computable) should be less than 90° . For time-varying adaptation gains, the condition is sharper since in this case $\text{Re}\{H(e^{-j\omega})\}$ should be larger than $\frac{\lambda_2}{2}$ at all frequencies.

Remark 3: Eq. (5.31) indicates that the estimated parameters of the feedforward compensator converge toward the domain $D_C = \{\hat{\theta} : \psi^T(t, \hat{\theta})(\theta - \hat{\theta}) = 0\}$. If furthermore $\psi^T(t, \hat{\theta})(\theta - \hat{\theta}) = 0$ has a unique solution (richness condition), then $\lim_{t \rightarrow \infty} \hat{\theta}(t) = \theta$.

Remark 4: The poles of the estimated Q filter (the roots of \hat{A}_Q), which are also poles of the internal positive closed loop, will be asymptotically inside the unit circle, if the SPR condition is satisfied. However, transiently, they may be outside the unit circle. It is possible to force these poles to remain inside of the unit circle during transient periods using adaptive algorithms with projection (see [Landau et al., 2011g]). However, the SPR condition remains the same.

5.4.2 The stochastic case - perfect matching

There are two sources of measurement noise, one acting on the primary transducer which gives the correlated measurement with the disturbance and the second acting on the measurement of the residual error (force, acceleration). For the primary transducer the effect of the measurement noise is negligible since the signal to noise ratio is very high. The situation is different for the residual since the effect of the noise can not be neglected.

In the presence of the measurement noise ($n(t)$), the equation of the *a posteriori* residual error becomes

$$\nu(t+1) = H(q^{-1}) [\theta - \hat{\theta}(t+1)]^T \psi(t) + n(t+1). \quad (5.40)$$

In this context, we should analyze the asymptotic behavior of the adaptation algorithms (*i.e.*, the convergence points in the parameter space). The O.D.E. method [Ljung and Söderström, 1983, Ljung, 1977b] can be used to analyse the asymptotic behavior of the algorithm in the presence of noise. Taking into account the form of eq. (5.40), one can directly use Theorem 4.1 of [Landau et al., 2011g] or Theorem B1 of [Landau and Karimi, 1997].

The following assumptions will be made:

1. $\lambda_1(t) = 1$ and $\lambda_2(t) = \lambda_2 > 0$
2. $\hat{\theta}(t)$ generated by the algorithm belongs infinitely often to the domain D_S :

$$D_S \triangleq \{\hat{\theta} : \hat{P}(z^{-1}) = 0 \Rightarrow |z| < 1\}$$

for which the stationary processes:

$$\begin{aligned} \psi(t, \hat{\theta}) &\triangleq \psi(t)|_{\hat{\theta}(t)=\hat{\theta}=\text{const}} \\ \nu(t, \hat{\theta}) &= \nu(t)|_{\hat{\theta}(t)=\hat{\theta}=\text{const}} \end{aligned}$$

can be defined.

3. $n(t)$ is a zero mean stochastic process with finite moments and independent of the sequence $w(t)$.

From (5.40) for $\hat{\theta}(t) = \hat{\theta}$, one gets

$$\nu(t+1, \hat{\theta}) = H(q^{-1}) [\theta - \hat{\theta}]^T \psi(t, \hat{\theta}) + n(t+1). \quad (5.41)$$

Since $\psi(t, \hat{\theta})$ depends upon $w(t)$ only, one concludes that $\psi(t, \hat{\theta})$ and $n(t+1, \hat{\theta})$ are independent. Therefore, using Theorem 4.1 from [Landau et al., 2011g], it results that if

$$H'(z^{-1}) = \frac{A_M(z^{-1})G(z^{-1})}{A_Q(z^{-1})P_0(z^{-1})L(z^{-1})} - \frac{\lambda_2}{2} \quad (5.42)$$

is a SPR transfer function, one has $\text{Prob}\{\lim_{t \rightarrow \infty} \hat{\theta}(t) \in D_C\} = 1$ where $D_C = \{\hat{\theta} : \psi^T(t, \hat{\theta})(\theta - \hat{\theta}) = 0\}$. If furthermore $\psi^T(t, \hat{\theta})(\theta - \hat{\theta}) = 0$ has a unique solution (richness condition), the condition that $H'(z^{-1})$ be strictly positive real implies that: $\text{Prob}\{\lim_{t \rightarrow \infty} \hat{\theta}(t) = \theta\} = 1$.

5.4.3 The case of non-perfect matching

If $\hat{Q}(t, q^{-1})$ does not have the appropriate dimension there is no chance to satisfy the perfect matching condition. Two important questions arise in this case:

1. The boundedness of the residual error
2. The bias distribution in the frequency domain

Boundedness of the residual error

The analysis of the boundedness of the residual error can be done using [Landau and Karimi, 1997, Landau et al., 2001b]. The following assumptions are made:

1. There exists a reduced order filter \hat{N} characterized by the unknown polynomials \hat{A}_Q (of order n_{A_Q}) and \hat{B}_Q (of order n_{B_Q}) as described in eqs. (5.2) and (5.1), for which the closed loop formed by \hat{N} and M is asymptotically stable, *i.e.*, $\hat{A}_Q(A_M S_0 - B_M R_0)$ is a Hurwitz polynomial.
2. The output of the optimal filter satisfying the matching condition can be expressed as:

$$\hat{u}(t+1) = - \left[\hat{S}^*(q^{-1})\hat{u}(t) - \hat{R}(q^{-1})\hat{y}(t+1) + \eta(t+1) \right] \quad (5.43)$$

where $\eta(t+1)$ is a norm bounded signal.

Using the results of [Landau and Karimi, 1997] (Theorem 4.1, pages 1505-1506) and assuming that $w(t)$ is norm bounded, it can be shown that all the signals are norm bounded under the passivity condition (5.35), where P is computed now with the reduced order estimated filter.

Bias distribution

Using the Parseval's relation, the asymptotic bias distribution of the estimated parameters in the frequency domain can be obtained starting from the expression of $\nu(t)$, by taking into account the fact that the algorithm minimizes (almost) a criterion of the form $\lim_{N \rightarrow \infty} \frac{1}{N} \sum_{t=1}^N \nu^2(t)$.

Using eq. (5.11), the bias distribution (for Algorithm III) is given by

$$\hat{\theta}^* = \arg \min_{\hat{\theta}} \int_{-\pi}^{\pi} \left[\left| D(e^{-j\omega}) + \frac{\hat{N}(e^{-j\omega})G(e^{-j\omega})}{1 - \hat{N}(e^{-j\omega})M(e^{-j\omega})} \right|^2 \phi_w(\omega) + \phi_n(\omega) \right] d\omega \quad (5.44)$$

where ϕ_w and ϕ_n are the spectral densities of the disturbance $w(t)$ and of the measurement noise $n(t)$. Taking into account eq. (5.11), one obtains

$$\hat{\theta}^* = \arg \min_{\hat{\theta}} \int_{-\pi}^{\pi} \left[\left| \frac{GA_M^2}{P_0} \right|^2 \left| \frac{B_Q}{A_Q} - \frac{\hat{B}_Q}{\hat{A}_Q} \right|^2 \phi_w(\omega) + \phi_n(\omega) \right] d\omega. \quad (5.45)$$

From (5.45) one concludes that a good approximation of the Q filter will be obtained in the frequency region where ϕ_w is significant and where G has a high gain (usually G should have high gain in the frequency region where ϕ_w is significant in order to counteract

the effect of $w(t)$). However, the quality of the estimated \hat{Q} filter will also depend on the transfer function $\frac{A_M^2}{P_0}$.

A similar result is obtained for FIRYK parameters by replacing $A_Q \equiv 1$ and $\hat{A}_Q \equiv 1$ in eq. (5.45).

5.4.4 Relaxing the positive real condition

It is possible to relax the SPR conditions taking into account the fact that:

1. The disturbance (input to the system) is a broadband signal
2. Most of the adaptation algorithms work with a low adaptation gain.

Under these two assumptions, the behavior of the algorithms can be well described by the "averaging theory" developed in [Anderson et al., 1986] and [Ljung and Söderström, 1983] (see also [Landau et al., 2011g]).

When using the averaging approach, the basic assumption of a slow adaptation holds for small adaptation gains (constant and scalar in [Anderson et al., 1986], *i.e.*, $\lambda_2(t) \equiv 0$, $\lambda_1(t) = 1$; matrix and time decreasing asymptotically in [Ljung and Söderström, 1983, Landau et al., 2011g] *i.e.* $\lim_{t \rightarrow \infty} \lambda_1(t) = 1$, $\lambda_2(t) = \lambda_2 > 0$ or scalar and time decreasing).

In the context of averaging, the basic condition for stability is that:

$$\lim_{N \rightarrow \infty} \frac{1}{N} \sum_{t=1}^N \psi(t) H'(q^{-1}) \psi^T(t) = \frac{1}{2} \int_{-\pi}^{\pi} \Psi(e^{j\omega}) [H'(e^{j\omega}) + H'(e^{-j\omega})] \Psi^T(e^{-j\omega}) d\omega > 0 \quad (5.46)$$

is a positive definite matrix, where $\Psi(e^{j\omega})$ is the Fourier transform of $\psi(t)$.

One can view (5.46) as the weighted energy of the observation vector ψ . Of course, the SPR sufficient condition upon $H'(z^{-1})$ (see eq. (5.35)) allows to satisfy this condition. However, in the averaging context, it is only needed that (5.46) is true which allows that H' may be non positive real in a limited frequency band. Expression (5.46) can be re-written as follows ([Landau et al., 2011d]):

$$\begin{aligned} & \int_{-\pi}^{\pi} \psi(e^{j\omega}) [H' + H'^*] \psi^T(e^{-j\omega}) d\omega = \\ & \sum_{i=1}^r \int_{\alpha_i}^{\alpha_i + \Delta_i} \psi(e^{j\omega}) [H' + H'^*] \psi^T(e^{-j\omega}) d\omega - \\ & \sum_{j=1}^p \int_{\beta_j}^{\beta_j + \Delta_j} \psi(e^{j\omega}) [\bar{H}' + \bar{H}'^*] \psi^T(e^{-j\omega}) d\omega > 0 \end{aligned} \quad (5.47)$$

where H' is SPR in the frequency intervals $[\alpha_i, \alpha_i + \Delta_i]$ and $\bar{H}' = -H'$ is positive real in the frequency intervals $[\beta_j, \beta_j + \Delta_j]$ (H'^* denotes the complex conjugate of H'). The conclusion is that H' does not need to be SPR. It is enough that the "positive" weighted energy exceeds the "negative" weighted energy. This explains why Algorithms I, IIa and IIb will work in practice, in most of the cases. It is however important to remark that if the disturbance is a single sinusoid (which violates the hypothesis of broadband disturbance) located in the frequency region where H' is not SPR, the algorithm may diverge (see [Anderson et al., 1986, Ljung and Söderström, 1983]). It was observed that despite the satisfaction of condition (5.47) which will assure the stability of the system,

attenuation is not very good in the frequency regions where the positive real condition (5.37) is violated.

Without any doubt, the best approach for relaxing the SPR conditions is to use the Algorithm III (given in eq. (5.26)) instead of Algorithm IIa or IIb. This is motivated by equation (5.38). As it will be shown experimentally, this algorithm gives the best results.

5.4.5 Summary of the algorithms

Tables 5.1 and 5.2 summarize the structure of the algorithms as well as the stability and convergence conditions for the algorithms developed in this chapter with matrix and scalar adaptation gain for IIR Youla-Kučera feedforward compensators, for FIR Youla-Kučera feedforward compensators, and for IIR adaptive feedforward compensators introduced in [Landau et al., 2011d]. These two references take also into account the internal positive feedback. Concerning algorithms for IIR adaptive feedforward compensators, the algorithms introduced in [Jacobson et al., 2001] and the FULMS algorithms ([Wang and Ren, 2003]) can be viewed as particular cases of those introduced in [Landau et al., 2011d].

It was not possible to give in Tables 5.1 and 5.2 all the options for the adaptation gain. However, basic characteristics for adaptive operation (non vanishing adaptation gain) and self-tuning operation (vanishing adaptation gain) have been provided⁵.

Table 5.1: Comparison of matrix gain algorithms for adaptive feedforward compensation in AVC with mechanical coupling.

	IIRYK	FIRYK	[Landau et al., 2011d]
$\hat{\theta}(t+1) =$	$\hat{\theta}(t) + F(t)\psi(t)\frac{\nu^0(t+1)}{1+\psi^T(t)F(t)\psi(t)}$		
Adapt. gain	$F(t+1)^{-1} = \lambda_1(t)F(t) + \lambda_2(t)\psi(t)\psi^T(t)$ $0 \leq \lambda_1(t) < 1, 0 \leq \lambda_2(t) < 2, F(0) > 0$		
Adaptive	Decr. gain and const. trace		
Self tuning	$\lambda_2 = const., \lim_{t \rightarrow \infty} \lambda_1(t) = 1$		
$\hat{\theta}(t) =$	$[\hat{b}_0^Q, \dots, \hat{a}_1^Q, \dots]$	$[\hat{b}_0^Q, \dots]$	$[-\hat{s}_1(t), \dots, \hat{r}_0(t), \dots]$
$\phi^T(t) =$	$[\alpha(t+1), \dots, -\beta(t), \dots]$ $\alpha(t) = \hat{B}_M \hat{u}(t) - \hat{A}_M \hat{y}(t)$ $\beta(t) = S_0 \hat{u}(t) - R_0 \hat{y}(t)$	$[\alpha(t+1), \dots]$ $\alpha(t) = \hat{B}_M \hat{u}(t) - \hat{A}_M \hat{y}(t)$	$[-\hat{u}(t), \dots, \hat{y}(t+1), \dots]$
$\hat{P} =$	$\hat{A}_Q(\hat{A}_M S_0 - \hat{B}_M R_0)$	$\hat{A}_M S_0 - \hat{B}_M R_0$	$\hat{A}_M \hat{S} - \hat{B}_M \hat{R}$
$P =$	$A_Q(A_M S_0 - B_M R_0)$	$A_M S_0 - B_M R_0$	$A_M \hat{S} - B_M \hat{R}$
$\psi(t) =$	$L\phi(t); L_2 = \hat{G}; L_3 = \frac{\hat{A}_M}{\hat{P}}\hat{G}$		
Stability condition	$\frac{A_M G}{P L} - \frac{\lambda}{2} = SPR \quad (\lambda = \max \lambda_2(t))$		
Conv. condition	$\frac{A_M G}{P L} - \frac{\lambda}{2} = SPR \quad (\lambda = \lambda_2)$		

⁵Convergence analysis can be applied only for vanishing adaptation gains.

Table 5.2: Comparison of scalar gain algorithms for adaptive feedforward compensation in AVC with mechanical coupling.

	IIRYK	FIRYK	[Landau et al., 2011d]
	Scalar gain		
$\hat{\theta}(t+1) =$	$\hat{\theta}(t) + \gamma(t)\psi(t)\frac{\nu^0(t+1)}{1+\gamma(t)\psi^T(t)\psi(t)}$		
Adapt. gain	$\gamma(t) > 0$		
Adaptive	$\gamma(t) = \gamma = \text{const}$		
Self tuning	$\sum_{t=1}^{\infty} \gamma(t) = \infty, \quad \lim_{t \rightarrow \infty} \gamma(t) = 0$		
$\hat{\theta}(t) =$	$[\hat{b}_0^Q, \dots, \hat{a}_1^Q, \dots]$	$[\hat{b}_0^Q, \dots]$	$[-\hat{s}_1(t), \dots, \hat{r}_0(t), \dots]$
$\phi^T(t) =$	$[\alpha(t+1), \dots, -\beta(t), \dots]$ $\alpha(t) = \hat{B}_M \hat{u}(t) - \hat{A}_M \hat{y}(t)$ $\beta(t) = S_0 \hat{u}(t) - R_0 \hat{y}(t)$	$[\alpha(t+1), \dots]$ $\alpha(t) = \hat{B}_M \hat{u}(t) - \hat{A}_M \hat{y}(t)$	$[-\hat{u}(t), \dots, \hat{y}(t+1), \dots]$
$\hat{P} =$	$\hat{A}_Q(\hat{A}_M S_0 - \hat{B}_M R_0)$	$\hat{A}_M S_0 - \hat{B}_M R_0$	$\hat{A}_M \hat{S} - \hat{B}_M \hat{R}$
$P =$	$A_Q(A_M S_0 - B_M R_0)$	$A_M S_0 - B_M R_0$	$A_M \hat{S} - B_M \hat{R}$
$\psi(t) =$	$L\phi(t); \quad L_2 = \hat{G}; \quad L_3 = \frac{\hat{A}_M}{\hat{P}}\hat{G}$		
Stability condition	$\frac{A_M G}{P L} = SPR$		
Conv. condition	$\frac{A_M G}{P L} = SPR$		

5.5 Experimental Results

The detailed description of the system used for the experiments has been given in Section 3.1 and a picture of the mechanical structure is shown in Figure 3.1. The identification procedure is the one described in Section 3.3.

This section presents first the central controllers (Subsection 5.5.1) and then experimental results obtained either using matrix adaptation (Subsection 5.5.2) or scalar adaptation (Subsection 5.5.3).

5.5.1 The Central Controllers

Two central controllers have been used to test the Youla-Kučera parameterized adaptive feedforward compensators. The first (PP) has been designed using a pole placement method adapted for the case of positive feedback systems. Its main objective is to stabilize the internal positive feedback loop. The end result was a controller of orders $n_{R_0} = 15$ and $n_{S_0} = 17$. The second is a reduced order H_∞ controller with $n_{R_0} = 19$ and $n_{S_0} = 20$ from [Alma et al., 2012b]⁶. For the design of the H_∞ controller, the knowledge of the primary path is mandatory (which is not necessary for the PP controller). Figure 5.2 shows a comparison of the performances obtained with these controllers. One observes that H_∞ already provides a good attenuation (14.70 dB).

⁶The orders of the initial H_∞ controller were: $n_{R_{H_\infty}} = 70$ and $n_{S_{H_\infty}} = 70$

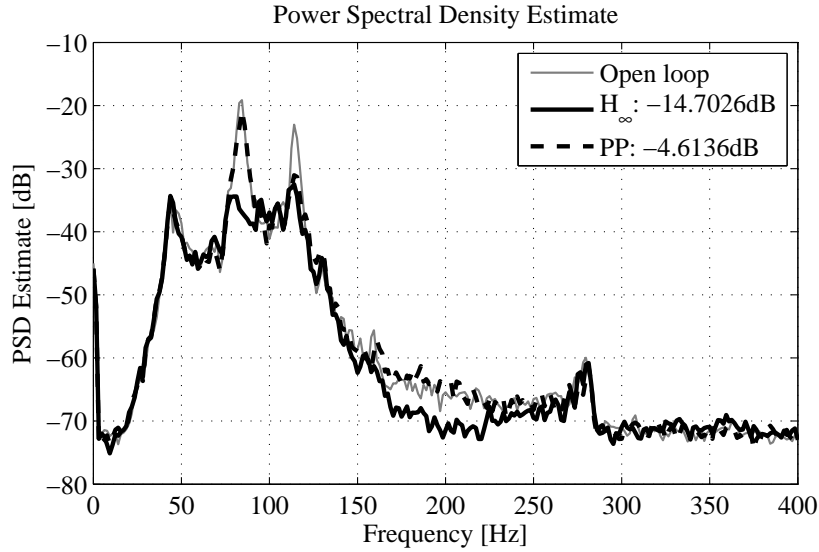


Figure 5.2: Spectral densities of residual acceleration for the two central controllers (experimental).

5.5.2 Broadband disturbance rejection using matrix adaptation gain

Broadband disturbance rejection capabilities using the two Youla-Kučera parameterizations with IIR and FIR filters described in columns 2 and 3 of Table 5.1 are evaluated in this subsection and some observations regarding how they compare to the algorithm of column 4 (see also [Landau et al., 2011d]) are made. For most of the experiments, the complexity of the IIRYK filter was $n_{BQ} = 3$ and $n_{AQ} = 8$, leading to 12 parameters in the adaptation algorithm according to eq. (5.3). For the FIRYK parametrization, an adaptive filter of order $n_Q = 31$ (32 parameters) has been used. These values do not allow to satisfy the “perfect matching condition”.

A PRBS excitation on the global primary path is considered as the disturbance. Two modes of operation can be considered, depending on the particular choices taken in eq. (5.24c):

- For adaptive operation, Algorithms *IIa* and *III* have been used with *decreasing adaptation gain* ($\lambda_1(t) = 1$, $\lambda_2(t) = 1$) combined with a *constant trace* adaptation gain. The adaptation is started at an initial high value of the adaptation gain matrix. While the decreasing adaptation gain algorithm is active, the trace of $F(t)$ decreases towards zero. When the trace of the adaptation matrix is below a given value, the decreasing adaptation gain algorithm is replaced by the constant trace algorithm. The constant trace gain updating modifies the values of $\lambda_1(t)$ and $\lambda_2(t)$ so that the trace of $F(t)$ is kept constant. This assures the evolution of the PAA in the optimal direction but the step size does not go to zero, therefore maintaining adaptation capabilities for eventual changes in disturbance or variations of the primary path model.
- In self-tuning operation, a decreasing adaptation gain $F(t)$ is used and the step size goes to zero. Then, if a degradation of the performance is observed, as a consequence of a change of the disturbance characteristics, the PAA is re-started.

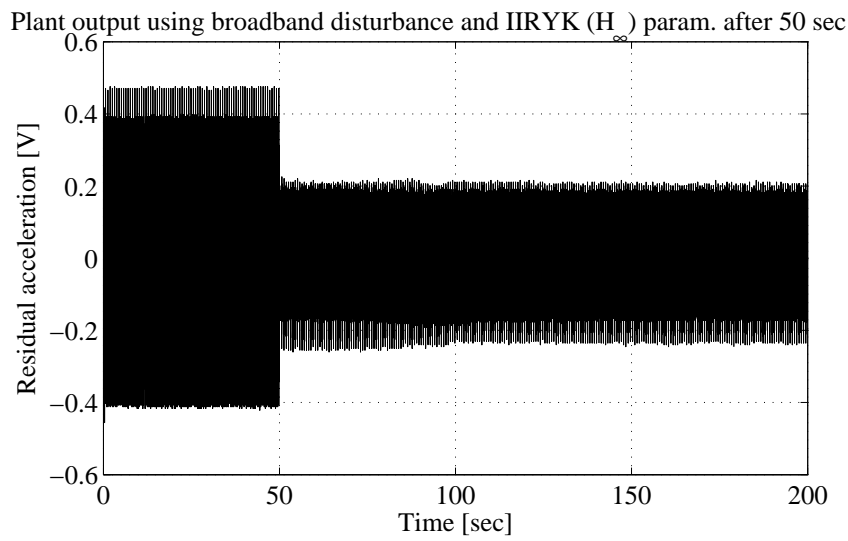


Figure 5.3: Real time residual acceleration obtained with the IIR Youla-Kučera parametrization ($n_{B_Q} = 3$, $n_{A_Q} = 8$) using Algorithm *IIa* with matrix adaptation gain and the H_∞ central controller.

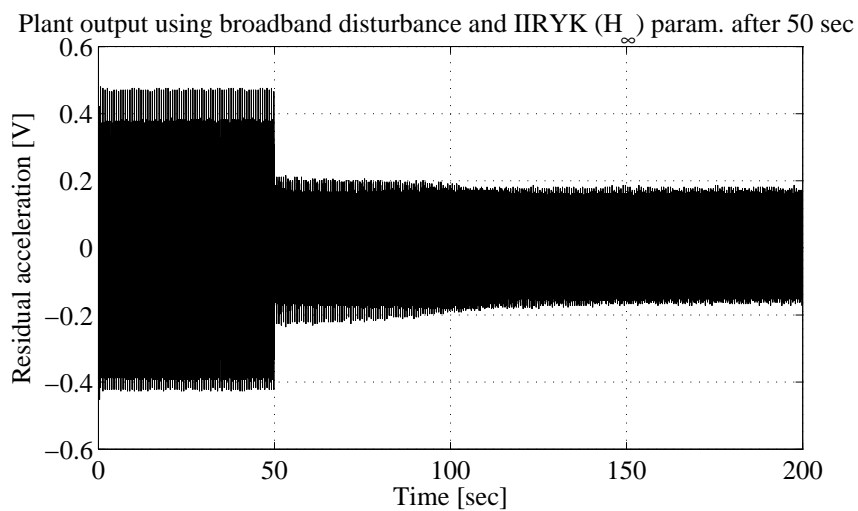


Figure 5.4: Real time residual acceleration obtained with the IIR Youla-Kučera parametrization ($n_{B_Q} = 3$, $n_{A_Q} = 8$) using Algorithm *III* with matrix adaptation gain and the H_∞ central controller.

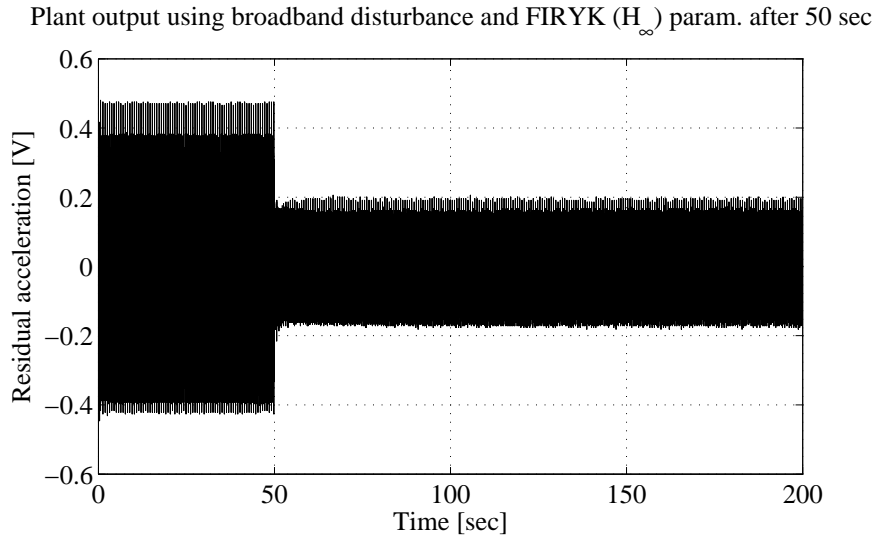


Figure 5.5: Real time results obtained with the FIR Youla-Kučera parametrization ($n_Q = 31$) using Algorithm *III* with matrix adaptation gain and the H_∞ central controller.

The PAAs have been implemented using the UD factorization [Landau et al., 2011g]⁷. For the reason of space, only the experimental results in adaptive operation will be presented. For IIRYK the adaptation has been done starting with an initial gain of 0.02 (initial trace = initial gain \times number of adjustable parameters, thus 0.24) and using a constant trace of 0.02. For FIRYK an initial gain of 0.05 (initial trace $0.05 \times 32 = 1.6$) and constant trace 0.1 have been used.

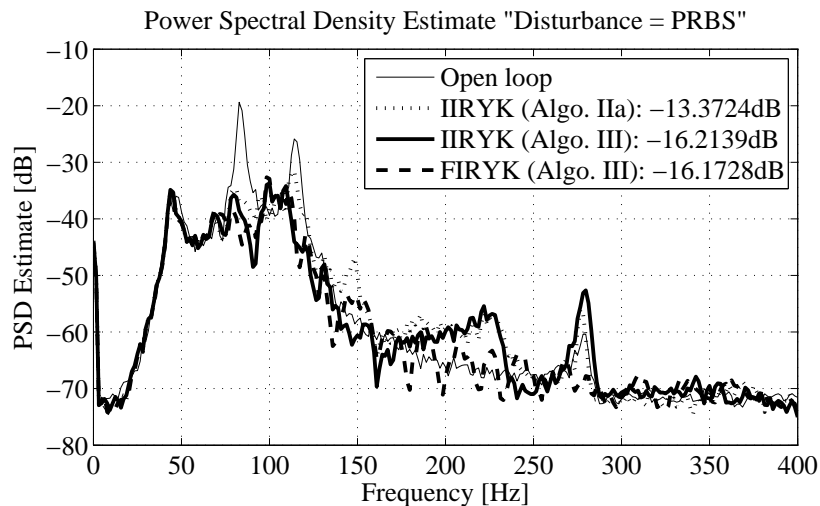


Figure 5.6: Power spectral densities of the residual acceleration in open loop, with IIRYK ($n_{B_Q} = 3$, $n_{A_Q} = 8$) and with FIRYK ($n_Q = 31$) using the H_∞ central controller (experimental).

The experiments have been carried out by first applying the disturbance and then starting the adaptive feedforward compensation after 50 seconds using the FIR or the IIR Youla-Kučera parametrization. If not otherwise specified, the results which will be

⁷An array implementation as in [Montazeri and Poshtan, 2010] can also be considered.

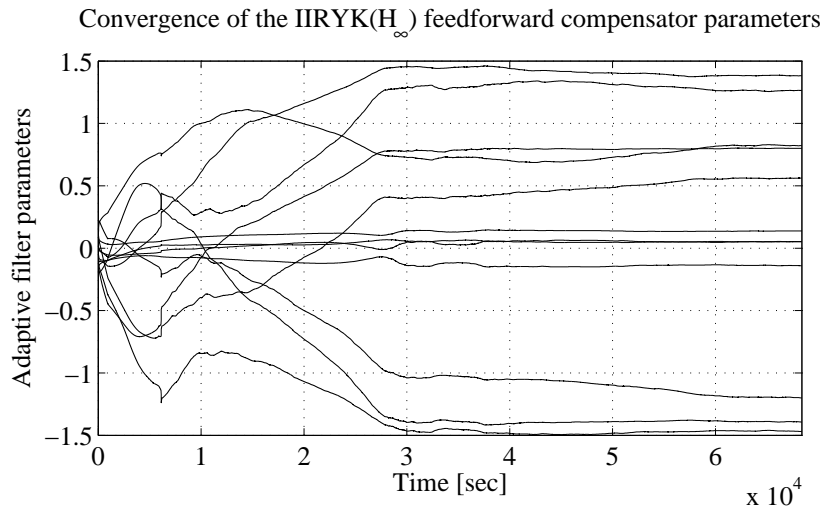


Figure 5.7: Evolution of the IIRYK parameters ($n_{B_Q} = 3$, $n_{A_Q} = 8$ and H_∞ central controller) for Algorithm *III* using matrix adaptation gain (experimental).

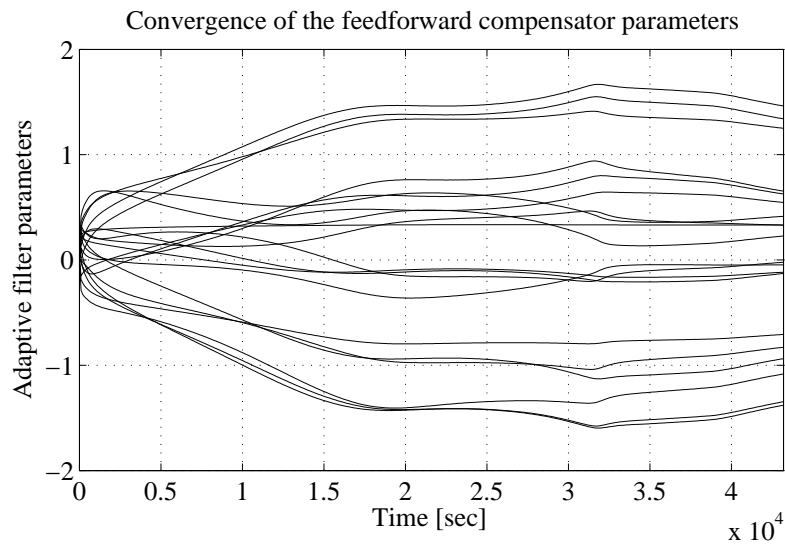


Figure 5.8: Evolution of the IIR parameters ($n_R = 9$, $n_S = 10$) for Algorithm *III* using matrix adaptation gain (experimental).

presented have been obtained with the H_∞ central controller. In the case of the IIRYK parametrization using Algorithm *III*, the filtering by the denominator of the *QIIR* filter used in eq. (5.27) is done adaptively by using the last stable estimation of $A_Q(q^{-1})$. Time domain results using IIRYK with Algorithms *Ia* and *III* are shown in Figures 5.3 and 5.4 respectively. It can be seen that Algorithm *III* provides a better performance than Algorithm *Ia* and this can be explained by a better approximation of the positive real condition (see discussion in Subsection 5.4.4). Figure 5.5 shows the evolution of the residual acceleration with the FIRYK adaptive compensator using Algorithm *III* of [Landau et al., 2011c]. The final attenuation given by IIRYK using Algorithm *III* (16.21dB) is better than that provided by IIRYK using Algorithm *Ia* (13.37dB) and slightly better than that provided by using FIRYK with Algorithm *III* (16.17dB) which uses significantly more adjustable parameters (32 instead of 12). However, the adaption transient is slightly more rapid for FIRYK.

The power spectral density of the residual acceleration (after the adaptation transient period) for the considered algorithms are shown in Fig. 5.6.

Figure 5.7 shows the convergence of the parameters for the IIRYK feedforward adaptive compensator using Algorithm *III*. The experiment has been carried out over an horizon of 13 hours. Parameters take approximatively 8 hours to almost settle. However, this does not impair the performance (the transient duration on the residual acceleration for Algorithm *III* is about 50 s). This result can be compared to that obtained with the direct adaptive IIR filter shown in Figure 5.8.

An evaluation of the influence of the number of parameters upon the global attenuation of the IIRYK parametrization is shown in Table 5.3. The results are grouped on two lines corresponding to the two central controllers used, and the given attenuations are measured in *dB*. The column headers give the number of numerator coefficients followed by the number of denominator coefficients. It can be observed that a larger order of the denominator is better than a larger order of the numerator.

Total no. param.	0	8	12			16		
No. param. of num/den	0/0	4/4	8/4	4/8	6/6	10/6	6/10	8/8
H_∞ (db)	14.7	15.96	15.56	16.21	16.31	15.67	16.5	16.47
PP (db)	4.61	15.52	16.25	16.02	16.24	15.57	15.72	16.21

Table 5.3: Influence of the number of the IIRYK parameters upon the global attenuation.

A similar analysis for the FIRYK feedforward adaptive compensators is given in Table 5.4. Comparing the two tables, one can say that a reduction of adjustable parameters by a factor of (at least) 2 is obtained in the case of IIRYK with respect to FIRYK for approximatively the same level of performance (compare IIRYK with 8 parameters with the FIRYK with 16 and the IIRYK with 6/6 parameters with the FIRYK with 32 parameters). It can be noticed that the IIRYK is less sensitive than FIRYK with respect to the performances of the model based central controller. Table 5.4 gives also comparative results for the IIR adaptive feedforward compensators. The IIRYK structure seems to allow a slight reduction of the number of parameters with respect to the IIR structure for the same level of performance (compare the results of IIRYK with 16 adjustable parameters (6/10) with the IIR using 20 adjustable parameters).

To verify the adaptive capabilities of the two parameterizations, a narrow band disturbance has been added after 1400 seconds of experimentation. This has been made

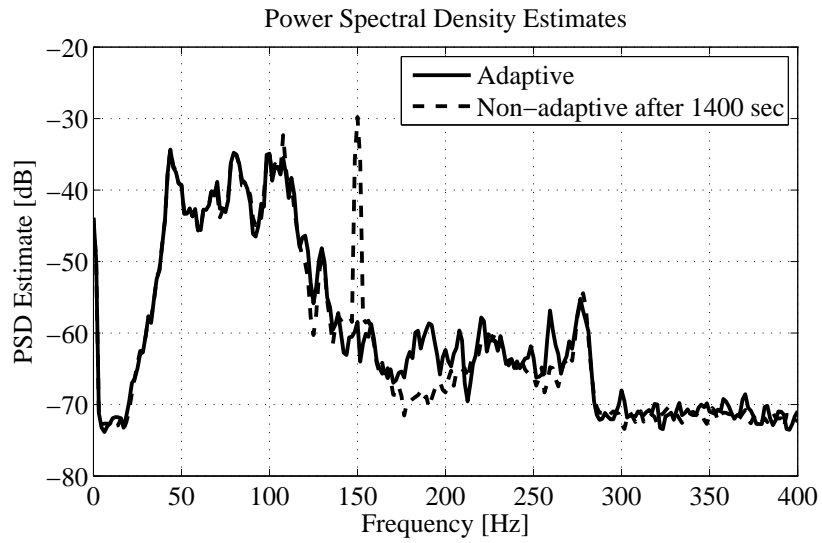


Figure 5.9: Power spectral densities of the residual acceleration when an additional sinusoidal disturbance is added (Disturbance = PRBS + sinusoid) and the adaptive IIRYK parametrization is used.

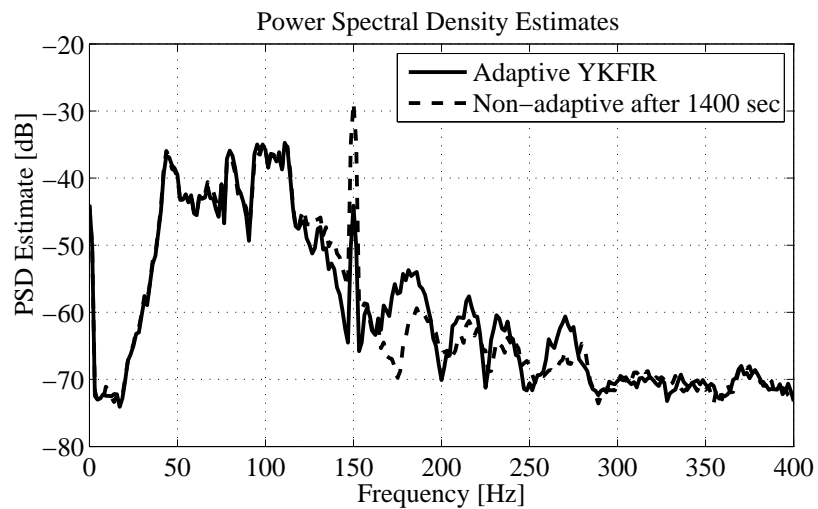


Figure 5.10: Power spectral densities of the residual acceleration when an additional sinusoidal disturbance is added (Disturbance = PRBS + sinusoid) and the adaptive FIRYK parametrization is used.

No. param.	0	8	16	20	32	40
H_∞ (db)	14.7	15.4	15.6	-	16.17	16.03
PP (db)	4.61	14.69	15.89	-	15.7	15.33
IIR (db)		-	-	16.23	16.49	16.89

Table 5.4: Influence of the number of parameters upon the global attenuation for the FIRYK parametrization (lines 2 and 3) and for the IIR adaptive filter (line 4).

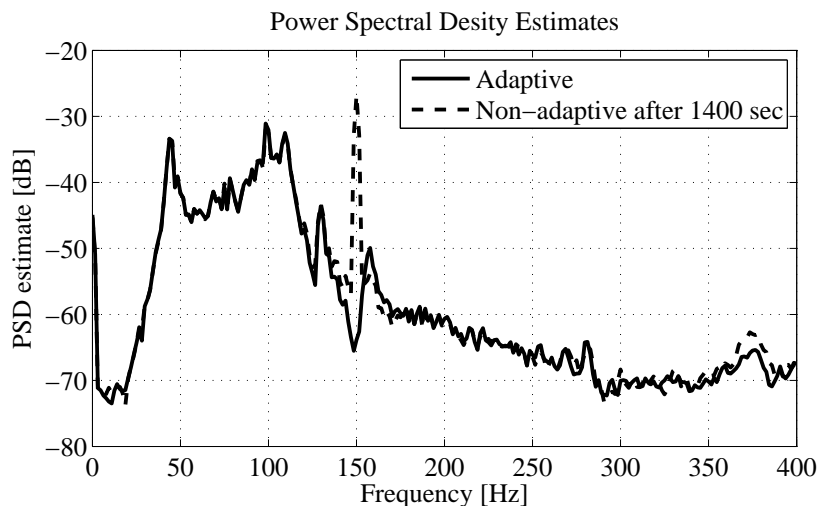


Figure 5.11: Power spectral densities of the residual acceleration when an additional sinusoidal disturbance is added (Disturbance = PRBS + sinusoid) and the direct adaptive IIR filter is used.

by using a sinusoidal signal of 150 Hz . Power spectral density estimates are shown in Fig. 5.9 for the IIRYK parametrization and Fig. 5.10 for the FIRYK parametrization. Better results are obtained with the IIRYK parametrization and they are comparable with those obtained for IIR adaptive feedforward compensators, shown in Fig. 5.11.

5.5.3 Broadband disturbance rejection using scalar adaptation gain

The scalar adaptation gain algorithms of columns 5 and 6 from Table 5.2 have been also tested on the AVC system.

In the *adaptation* regime, as opposed to the matrix cases, a constant adaptation gain of 0.001 has been used for both parameterizations, as in [Landau et al., 2011d] (see also table 5.2). This corresponds to a constant trace of 0.012 for the IIRYK and 0.032 for the FIRYK (taking in account the number of adapted parameters). Figure 5.12 shows the adaptation transient for the scalar version of the IIRYK parametrization using Algorithm III. Surprisingly, the performances are close to those obtained with a matrix adaptation gain (a similar observation has been made in [Landau et al., 2011d, Figure 14]). Figure 5.13 shows the adaptation transient for the FIRYK parametrization using a scalar adaptation gain. It can be seen that the transient performances are a little better for the IIRYK. In Figure 5.14, power spectral densities and the corresponding global attenuations are given for both parameterizations. It can be observed that

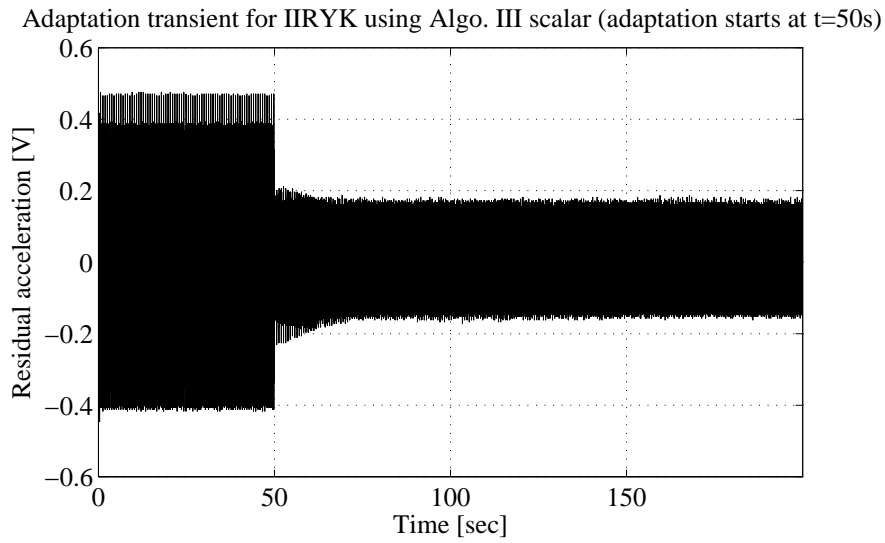


Figure 5.12: Real time residual acceleration obtained with the IIR Youla-Kučera parametrization ($n_{B_Q} = 3$, $n_{A_Q} = 8$) using Algorithm III with scalar adaptation gain and the H_∞ central controller.

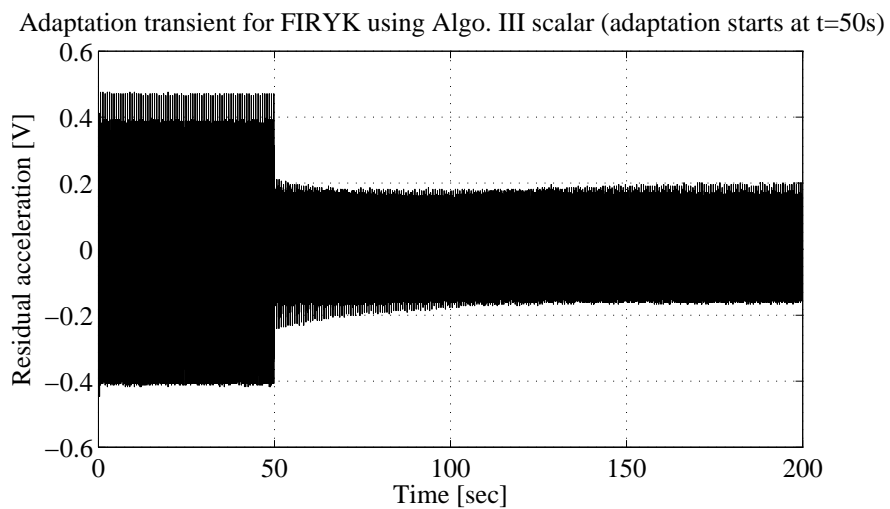


Figure 5.13: Real time residual acceleration obtained with the FIR Youla-Kučera parametrization ($n_Q = 31$) using Algorithm III with scalar adaptation gain and the H_∞ central controller.

IIRYK parametrization with 12 adjustable parameters gives a slightly better attenuation (additional 0.5 dB) with respect to a FIRYK parametrization with 32 parameters.

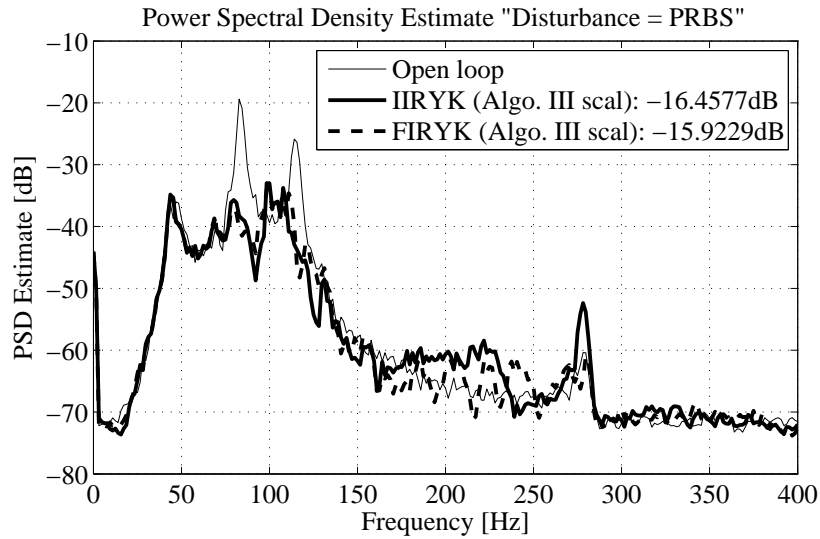


Figure 5.14: Power spectral densities of the residual acceleration in open loop, with IIRYK ($n_{B_Q} = 3$, $n_{A_Q} = 8$) and with FIRYK ($n_Q = 31$) using scalar adaptation gain and the H_∞ central controller (experimental).

5.6 Comparison with Other Algorithms

The algorithms developed in this chapter with matrix and scalar adaptation gains for IIR Youla-Kučera feedforward compensators have been compared with the FIR Youla-Kučera parameterized feedforward compensators from [Landau et al., 2011c] and the direct IIR adaptive algorithm of [Landau et al., 2011d] (see Tables 5.2 and 5.1). This section summarizes the observations made in Subsection 5.4.5 and in Section 5.5 based on experimental results.

Remark 1 - The number of adjustable parameters. The main advantage of the IIRYK adaptive feedforward compensators introduced in this chapter compared with FIRYK adaptive compensators is that they require a significantly lower number of adjustable parameters for a given level of performance (a reduction by a factor of 2 in the application presented). This is, without any doubt, a major practical advantage in terms of implementation complexity. A slight reduction of the number of adjustable parameters is also obtained with respect to IIR adaptive feedforward compensators.

Remark 2 - The poles of the internal positive closed loop. For IIR adaptive feedforward compensators, provided that the SPR condition for stability is satisfied, the poles of the internal "positive" loop will be asymptotically stable but they can be very close to the unit circle. For FIRYK, the poles of the internal positive feedback loop are assigned by the central stabilizing controller and they remain unchanged under the effect of adaptation. For IIRYK, some of the poles of the internal positive feedback loop are assigned by the central stabilizing controller but there are additional poles corresponding to \hat{A}_Q . These poles will be inside the unit circle if the positive real condition for stability is satisfied but they can be very close to the unit circle (at least theoretically). However, if one wants to impose that these poles lie inside a circle of a certain radius, this can be easily achieved by using PAAs with "projections" ([Goodwin and Sin, 1984, Landau et al., 2011g]).

Remark 3 - Implementation of the filter for Algorithm III. For IIRYK adaptive compensator, one has to run first Algorithm *IIa* or *IIb* over a short horizon in order to get an estimate of \hat{A}_Q for implementing the appropriate filter. A similar procedure has to be used also for IIR adaptive compensators (See [Landau et al., 2011d]). For the IIRYK the filter can be continuously improved by updating at each step the estimation of \hat{A}_Q in the filter. Such a procedure is more difficult to apply to the IIR structure since the estimated closed loop poles have to be computed at each step based on current estimates of the feedforward compensator's parameters and the knowledge of the reverse path $M(q^{-1})$. For FIRYK, this initialization procedure is not necessary since the poles of the internal positive feedback loop remain unchanged under the effect of adaptation and a good estimation is provided by the knowledge of the central stabilizing compensator and of the model of the reverse path.

Remark 4 - Initial model based design compensator. Since the system as well as the initial characteristics of the disturbance can be identified, a model based design of an initial feedforward compensator can be done. Unfortunately this information can not be easily used to efficiently initialize the parameters of the IIR adaptive compensator because the model based design (like H_∞) will lead in general to a controller with a larger number of parameters than the number of those used in the adaptive IIR filter (the number of the adjustable parameters should be the same as the number of the parameters of the model based controller). When using a FIRYK or an IIRYK feedforward compensator, any model based designed compensator can be used as the central controller (no matter what is its dimension). Its performances will be enhanced by the adaptation of the Q-parameters.

Remark 5 - Influence of the initial stabilizing controller. The performances of the IIRYK adaptive compensator are less sensitive than those of the FIRYK adaptive compensator with respect to the performances of the initial model based stabilizing controller (at least for a reduced number of adjustable parameters).

5.7 Concluding Remarks

The chapter has presented an adaptive IIR Youla-Kučera parametrized feedforward compensator built around a stabilizing filter for the internal "positive" feedback loop occurring in AVC and ANC systems. Experimental results on an active vibration control system featuring an internal "positive" feedback have illustrated the potential of the approach. It has been shown that the use of the IIR Youla-Kučera filters allows to reduce significantly the number of parameters to be adapted with respect to the FIR Youla-Kučera filters for the same level of performance.

Part II

Adaptive Feedback Disturbance Compensation

CHAPTER 6

ADAPTIVE INDIRECT REGULATION OF NARROW BAND DISTURBANCES

6.1 Introduction

An important problem in active vibration (or noise) control is the compensation of disturbances without measuring them. In this case, a feedback approach is considered for disturbance attenuation. In general, one considers the disturbances as being a white noise or a Dirac impulse passed through a filter which characterizes the model of the disturbance¹. To be more specific, the disturbances considered can be defined as "finite band disturbances". This includes single or multiple narrow band disturbances or sinusoidal signals. For the purpose of this chapter, the disturbances are considered to be time varying, in other words, their model has time varying coefficients. This motivates the use of an adaptive regulation approach since the objective is the attenuation of unknown disturbances without measuring them.

The potential advantage of adaptive regulation versus adaptive feedforward disturbance compensation [Beranek and Ver, 1992, Fuller et al., 1997, Landau et al., 2011d] is the elimination of the need for a second transducer used for obtaining an image of the disturbance (a correlated measurement with the disturbance).

A popular methodology for this regulation problem is the design of a controller that incorporates the model of the disturbance (internal model principle). This technique has been described in [Francis and Wonham, 1976, Bengtsson, 1977, Landau et al., 2005, Landau et al., 2011e]. The main problem using the IMP principle is that complete rejection of the disturbances is attempted (asymptotically) and this may have a strong influence upon the sensitivity functions outside the frequency band in which attenuation is achieved. As long as rejection of a single narrow band disturbance is considered ([Landau et al., 2005, Landau et al., 2011e]), the influence upon the output sensitivity functions does in general not pose problems. However, application of this (IMP) approach for the case of multiple narrow band disturbances may lead to unacceptable profiles of the output sensitivity functions in terms of robustness and unacceptable amplification of the residual noise in certain frequency regions. Also, the IMP approach may lead to actuator saturation. In addition, in many applications, only a level of attenuation is required (IMP does too much!).

In this chapter, a different solution is proposed. Instead of complete cancelation of the disturbances, only a chosen attenuation is introduced by

¹Throughout the chapter, it is assumed that the number of multiple narrow band disturbances is known (it can be estimated from data if necessary) but not their frequency characteristics.

shaping the output sensitivity function with band-stop filters (BSF) (see also [Landau and Zito, 2005, Procházka and Landau, 2003]) at those frequencies corresponding to spikes in the spectrum of the disturbance². In order to implement the algorithm, one needs to estimate in real time the frequency spikes contained in the disturbance. System identification techniques can be used to estimate the model of the disturbance ([Airimițoiaie et al., 2011, Landau et al., 2011e]). Unfortunately, to find the frequencies of the spikes requires the computation in real time of the roots of an equation of order $2 \cdot n$, where n is the number of spikes. Therefore, this approach is applicable in the case of one eventually two narrow band disturbances. What is needed is an algorithm which can directly estimate the frequencies of the various spikes of the disturbance. Several methods have been proposed in the signal processing community to solve this issue ([Tichavský and Nehorai, 1997]). One approach which has been reported to give very good results ([Stoica and Nehorai, 1988, M'Sirdi et al., 1988]) is based on the use of ANFs ([Rao and Kung, 1984, Nehorai, 1985, Chen et al., 1992, Li, 1997]).

Based on the current estimation of the frequencies of the spikes at each sampling time, one has to solve a Bezout equation in order to find the parameters of the controller. As it will be shown, using a Youla-Kučera parametrization of the controller ([Tsypkin, 1997, de Callafon and Kinney, 2010, Landau et al., 2005, Tay et al., 1997]) the dimension of the matrix equation that has to be solved is reduced significantly and therefore the computation load will be much lower. The other advantage that motivates the use of the Youla-Kučera parametrization is the fact that a nominal controller is always present in order to stabilize and to assure the nominal performances of the closed loop system in the absence of the disturbance (*e.g.*, damping of vibration modes in the system).

In the present framework, the hypothesis of constant dynamic characteristics of the AVC system is made (like in [Landau et al., 2011e]). Furthermore, the corresponding control model is supposed to be accurately identified from input/output data.

In [Landau et al., 2005] the direct adaptive regulation of narrow band disturbances using IMP and the Youla-Kučera parametrization is described and analyzed and extended in [Landau et al., 2011e] for multiple disturbances. Another method for narrow band disturbances rejection by feedback is based on the use of a disturbance observer ([Nakao et al., 1987, Huang and Messner, 1998, Chen and Tomizuka, 2012]). However, this method is different with respect to that proposed in this chapter, since an adaptive Q filter, that is not part of the controller parametrization, is used to extract the narrow band disturbances. The rejection is then obtained by subtracting the predicted disturbance out of the control signal, taking into consideration the fact that the disturbance is supposed to act at the input of the process.

The main contributions of this chapter are:

- the development of new algorithms based on Band-stop Filters with adjustable frequency bandwidths and attenuations for shaping the output sensitivity function with minimal influences outside the attenuation frequency regions;
- the use of Adaptive Notch Filters for estimation of the central frequencies characterizing the narrow band disturbances;
- the reduction of the computation complexity of the indirect adaptive controllers by using a Youla-Kučera parametrization of the adjustable controller.

This chapter is organized as follows. In Section 6.2 the main notations and equations for the indirect adaptive system are given. The estimation method used for tracking

²The numerators of these filters will be implemented in the controller while the denominators will define additional desired close-loop poles.

the variations of the disturbances' frequencies is briefly described in Section 6.3. The indirect adaptive regulation method based on BSFs is presented in Section 6.4. A reduced complexity implementation of this method using the Youla-Kučera parametrization is then given in Section 6.5. In Section 6.6, an experimental performance evaluation and comparison with the method of [Landau et al., 2011e] are presented. Some concluding remarks are given in Section 6.7.

6.2 System Description

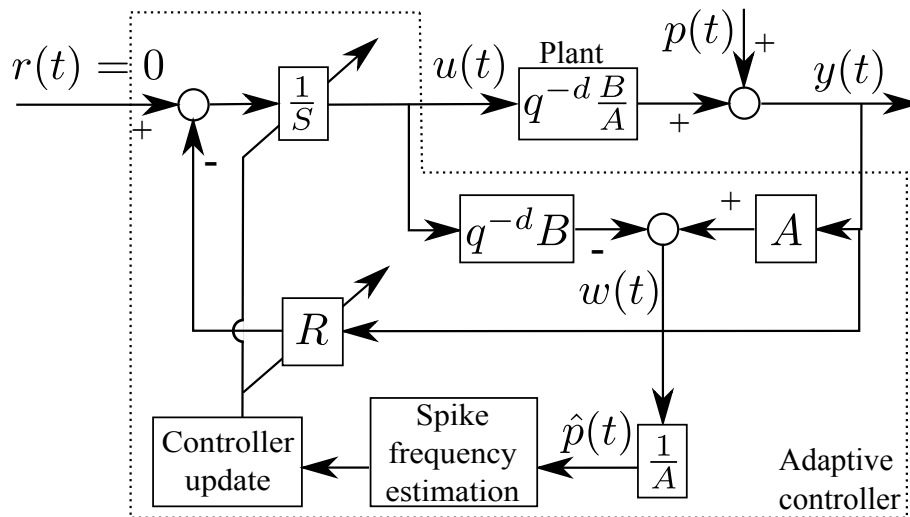


Figure 6.1: Basic scheme for indirect adaptive control.

The basic indirect adaptive control block diagram used is shown in Figure 6.1. The process output can be written as³

$$y(t) = G(q^{-1}) \cdot u(t) + p(t), \quad (6.1)$$

where

$$G(q^{-1}) = q^{-d} \frac{B(q^{-1})}{A(q^{-1})} \quad (6.2)$$

is called the secondary path of the system and $p(t)$ is the effect of the disturbances on the measured output.

As specified in Section 6.1, the hypothesis of constant dynamic characteristics of the AVC system is considered (similar to [Landau et al., 2005, Landau et al., 2011e]). The denominator of the secondary path model is given by

$$A(q^{-1}) = 1 + a_1 q^{-1} + \dots + a_{n_A} q^{-n_A}, \quad (6.3)$$

the numerator is given by

$$B(q^{-1}) = b_1 q^{-1} + \dots + b_{n_B} q^{-n_B} = q^{-1} B^*(q^{-1}) \quad (6.4)$$

and d is the integer delay (number of sampling periods)⁴.

³The complex variable z^{-1} will be used to characterize the system's behavior in the frequency domain and the delay operator q^{-1} will be used for the time domain analysis.

⁴As indicated earlier, it is assumed that a reliable model identification is achieved and therefore the estimated model is assumed to be equal to the true model.

The control signal is given by

$$u(t) = -R(q^{-1}) \cdot y(t) - S^*(q^{-1}) \cdot u(t-1), \quad (6.5)$$

with

$$\begin{aligned} S(q^{-1}) &= 1 + q^{-1}S^*(q^{-1}) = 1 + s_1q^{-1} + \dots + s_{n_S}q^{-n_S} \\ &= S'(q^{-1}) \cdot H_S(q^{-1}), \end{aligned} \quad (6.6)$$

$$\begin{aligned} R(q^{-1}) &= r_0 + r_1q^{-1} + \dots + r_{n_R}q^{-n_R} \\ &= R'(q^{-1}) \cdot H_R(q^{-1}), \end{aligned} \quad (6.7)$$

where $H_S(q^{-1})$ and $H_R(q^{-1})$ represent fixed (imposed) parts in the controller and $S'(q^{-1})$ and $R'(q^{-1})$ are computed. Under the hypothesis that the plant model parameters are constant and that an accurate identification experiment can be run, a reliable estimate $\hat{p}(t)$ of the disturbance signal can be obtained by using the following disturbance observer

$$\hat{p}(t+1) = y(t+1) - q^{-d} \frac{B(q^{-1})}{A(q^{-1})} u(t+1) \quad (6.8)$$

$$= y(t+1) - q^{-d} \frac{B^*(q^{-1})}{A(q^{-1})} u(t) \quad (6.9)$$

as shown in Figure 6.1. The disturbance estimator ($\hat{p}(t)$) is followed by a block which estimates spikes' frequencies and computes in real time the controller parameters.

6.3 Frequency Estimation Using Adaptive Notch Filters

The indirect adaptive regulation methodology presented here is based on the knowledge of the spikes frequencies in the spectrum of the disturbance. In the framework of narrow band disturbance rejection, it is usually supposed that the disturbances are in fact sinusoidal signals with variable frequencies. In most of the situations encountered in practice, these frequencies are not known, thus the need for adaptive estimation arises. As specified in the introduction, the hypothesis of known number of multiple narrow band disturbances is assumed (similar to [Landau et al., 2005, Landau et al., 2011e, Chen and Tomizuka, 2012]). A technique based on ANFs will be used to estimate the frequencies of the sinusoidal signals in the disturbance (details can be found in [Nehorai, 1985, M'Sirdi et al., 1988]).

The general form of an ANF is

$$H_f(z^{-1}) = \frac{A_f(z^{-1})}{A_f(\rho z^{-1})}, \quad (6.10)$$

where the polynomial $A_f(z^{-1})$ is such that the zeros of the transfer function $H_f(z^{-1})$ lie on the unit circle. A necessary condition for a monic polynomial to satisfy this property is that its coefficients have a mirror symmetric form

$$A_f(z^{-1}) = 1 + a_1^f z^{-1} + \dots + a_n^f z^{-n} + \dots + a_1^f z^{-2n+1} + z^{-2n}. \quad (6.11)$$

Another requirement is that the poles of the ANF should be on the same radial lines as those of the zeros but slightly closer to the origin of the unit circle. Using filter denominators of the general form $A_f(\rho z^{-1})$ with ρ a positive real number smaller but

close to 1, the poles have the desired property and are in fact located on a circle of radius ρ ([Nehorai, 1985]).

The estimation algorithm will be detailed next. It is considered that the disturbance signal (or a good estimation) is available.

A cascade construction of second order ANF filters is considered. Their number is given by the number of narrow band signals whose frequencies have to be estimated. The main idea behind this algorithm is to consider the signal $\hat{p}(t)$ as having the form

$$\hat{p}(t) = \sum_{i=1}^n c_i \sin(\omega_i \cdot t + \beta_i) + v(t), \quad (6.12)$$

where $v(t)$ is a noise affecting the measurement and n is the number of narrow band signals with different frequencies.

The ANF cascade form will be given by (this is an equivalent representation of eqs. (6.10) and (6.11))

$$H_f(z^{-1}) = \prod_{i=1}^n H_f^i(z^{-1}) = \prod_{i=1}^n \frac{1 + a^{f_i} z^{-1} + z^{-2}}{1 + \rho a^{f_i} z^{-1} + \rho^2 z^{-2}}. \quad (6.13)$$

Next, the estimation of one spike's frequency is considered, assuming convergence of the other $(n-1)$ \hat{a}^{f_i} (estimations of the true a^{f_i}) to a^{f_i} , which can thus be filtered out of the estimated disturbance signal, $\hat{p}(t)$, by applying

$$\hat{p}^j(t) = \prod_{\substack{i=1 \\ i \neq j}}^n \frac{1 + a^{f_i} z^{-1} + z^{-2}}{1 + \rho a^{f_i} z^{-1} + \rho^2 z^{-2}} \hat{p}(t). \quad (6.14)$$

The prediction error is obtained from

$$\epsilon(t) = H_f(z^{-1}) \hat{p}(t) \quad (6.15)$$

and can be computed based on one of the $\hat{p}^j(t)$ to reduce the computation complexity. Each cell can be adapted independently after prefiltering the signal by the others. Following the Recursive Prediction Error (RPE) technique, the gradient is obtained as

$$\Psi^j(t) = -\frac{\partial \epsilon(t)}{\partial a^{f_j}} = \frac{(1-\rho)(1-\rho z^{-2})}{1 + \rho a^{f_j} z^{-1} + \rho^2 z^{-2}} \hat{p}^j(t). \quad (6.16)$$

The parametric adaptation algorithm can be summarized as

$$\hat{a}^{f_j}(t) = \hat{a}^{f_j}(t-1) + F(t-1) \cdot \Psi^j(t) \cdot \epsilon(t) \quad (6.17)$$

$$F(t) = \frac{F(t-1)}{\lambda + F(t-1) \Psi^j(t)^2}, \quad (6.18)$$

where \hat{a}^{f_j} are estimations of the true a^{f_j} , which are connected to the narrow band signals' frequencies by $\omega_{f_j} = \arccos(-\frac{a^{f_j}}{2})$.

6.4 Indirect Adaptive Procedure Based on Band-stop Filters for Shaping the Sensitivity Function

This section presents a technique of output sensitivity function shaping for narrow band disturbance compensation. It will be used to compute the parameters of the adjustable

controller. Here the controller's parameters computation procedure considering constant and known frequencies of the narrow band disturbances is presented. The design uses BSFs to shape the output sensitivity functions. Following [Landau and Zito, 2005, Procházka and Landau, 2003], there exists a digital filter $\frac{H_{S_i}}{P_{F_i}}$ which, if used in the design of the controller, will assure the desired attenuation of a narrow band disturbance (index $i \in \{1, \dots, n\}$). The numerator of the filter is directly included in the controller. The denominator will specify a factor in the desired closed loop characteristic polynomial.

It is important to remark that one should only reject disturbances located in frequency regions where the plant model has enough gain. The reason for this can be better understood by looking at the transfer function from the disturbance to the controller output. Perfect disturbance rejection at a certain frequency ω_0 means having $S_{yp}(e^{-j\omega_0}) = 0$. Taking into consideration the form of the output sensitivity function,

$$S_{yp}(z^{-1}) = \frac{A(z^{-1})S(z^{-1})}{A(z^{-1})S(z^{-1}) + z^{-d}B(z^{-1})R(z^{-1})}, \quad (6.19)$$

and keeping in mind that $A(z^{-1})$ and $B(z^{-1})$ are fixed, it is easy to see that perfect rejection can only be obtained if $S_{yp}(e^{-j\omega_0}) = 0$. For the input sensitivity function,

$$S_{up}(z^{-1}) = -\frac{A(z^{-1})R(z^{-1})}{A(z^{-1})S(z^{-1}) + z^{-d}B(z^{-1})R(z^{-1})}, \quad (6.20)$$

this means that $S_{up}(e^{-j\omega_0}) = \frac{A(e^{-j\omega_0})}{B(e^{-j\omega_0})}$. Therefore, if the gain of the model is too small at the frequency ω_0 , the disturbance will be amplified to a value that could saturate or damage the actuator (in addition this can lead to a lack of robustness with respect to additive plant uncertainties).

The purpose of this method is to allow the possibility of choosing the desired attenuation and bandwidth of attenuation for each of the estimated narrow band disturbances. This is the main advantage with respect to classical internal model methods which, in the case of several narrow band disturbances, as a consequence of complete cancellation of the disturbances, may lead to unacceptable values of the modulus of the output sensitivity function outside the attenuation regions. Choosing the level of attenuation and the bandwidth allows to preserve the sensitivity functions outside the attenuation bands and this is very useful in the case of multiple narrow band disturbances' regulation.

As mentioned before, the algorithm makes use of the estimated frequencies of the narrow band disturbances. These are needed to shape the output sensitivity function using BSFs which have the following structure

$$\frac{S_{BSF_i}(z^{-1})}{P_{BSF_i}(z^{-1})} = \frac{1 + \beta_1^i z^{-1} + \beta_2^i z^{-2}}{1 + \alpha_1^i z^{-1} + \alpha_2^i z^{-2}} \quad (6.21)$$

resulting from the discretization of a continuous filter (see also [Procházka and Landau, 2003, Landau and Zito, 2005])

$$F_i(s) = \frac{s^2 + 2\zeta_{n_i}\omega_i s + \omega_i^2}{s^2 + 2\zeta_{d_i}\omega_i s + \omega_i^2} \quad (6.22)$$

using the bilinear transformation. This filter introduces an attenuation of

$$M_i = -20 \cdot \log_{10} \left(\frac{\zeta_{n_i}}{\zeta_{d_i}} \right) \quad (6.23)$$

at the frequency ω_i . Positive values of M_i denote attenuations ($\zeta_{n_i} < \zeta_{d_i}$) and negative values denote amplifications ($\zeta_{n_i} > \zeta_{d_i}$)⁵.

Remark: the design parameters for each BSF are the desired attenuation (M_i), the central frequency of the filter (ω_i) and the damping of the denominator (ζ_{d_i}). The denominator damping is used to adjust the frequency bandwidth of the BSF. For very small values of the frequency bandwidth, the influence of the filters on frequencies other than those defined by ω_i is negligible. Therefore, the number of BSFs and subsequently that of the narrow band disturbances that can be compensated, can be as large as necessary. However, for fast varying narrow band signals, it is recommended to use larger values for the denominators' dampings. In this situation, care has to be taken for the constraint imposed by the Bode integral of the output sensitivity function.

In Figure 6.2, a comparison of the sensitivity functions of a nominal controller (which does not attenuate disturbances) and two controllers that attenuate disturbances (one using the IMP and the other one using BSFs) is shown. The method which uses BSFs, for $\zeta_{d_i} = 0.04$ and an attenuation of -60 dB, $\forall i \in \{1, 2, 3\}$ (a level large enough in most of the applications), introduces less alteration into the characteristics of the nominal controller outside the attenuation band than the IMP controller. It can be concluded from the input sensitivity function that the IMP controller might amplify the measurement noise to a level that could saturate the system's input⁶. Note that for the design of the IMP controller, 3 pairs of poles close to the disturbances' frequencies with damping 0.2 have been added to improve its robustness.

For n narrow band disturbances, n band-stop filters will be used

$$\frac{S_{BSF}(z^{-1})}{P_{BSF}(z^{-1})} = \frac{\prod_{i=1}^n S_{BSF_i}(z^{-1})}{\prod_{i=1}^n P_{BSF_i}(z^{-1})}. \quad (6.24)$$

As stated before, the objective is that of shaping the output sensitivity function. The characteristic polynomial

$$P(z^{-1}) = A(z^{-1})S(z^{-1}) + z^{-d}B(z^{-1})R(z^{-1}) \quad (6.25)$$

can be rewritten, considering (6.6), (6.7), the factorizations of $S(z^{-1})$ and $R(z^{-1})$:

$$S(z^{-1}) = H_S(z^{-1})S'(z^{-1}), \quad (6.26)$$

$$R(z^{-1}) = H_R(z^{-1})R'(z^{-1}), \quad (6.27)$$

and a factorization of $P(z^{-1})$, as

$$P(z^{-1}) = P_0(z^{-1})P_{BSF}(z^{-1}) = A(z^{-1})H_S(z^{-1})S'(z^{-1}) + z^{-d}B(z^{-1})H_{R_1}(z^{-1})R'(z^{-1}). \quad (6.28)$$

In the last equation, P_{BSF} is the combined denominator of all the band-stop filters, (6.24), and P_0 are other imposed poles of the closed loop system (usually for satisfying robustness conditions). It is easy to see that the output sensitivity function becomes

$$S_{yp}(z^{-1}) = \frac{A(z^{-1})S(z^{-1})}{P_0(z^{-1})P_{BSF}(z^{-1})}. \quad (6.29)$$

⁵For frequencies below $0.17f_S$ (f_S is the sampling frequency) the design can be done with a very good precision directly in discrete time ([Landau and Zito, 2005]).

⁶The optimal design of the nominal controller when using IMP in order to minimize the effect of the output sensitivity function outside the attenuation bands is still an open problem.

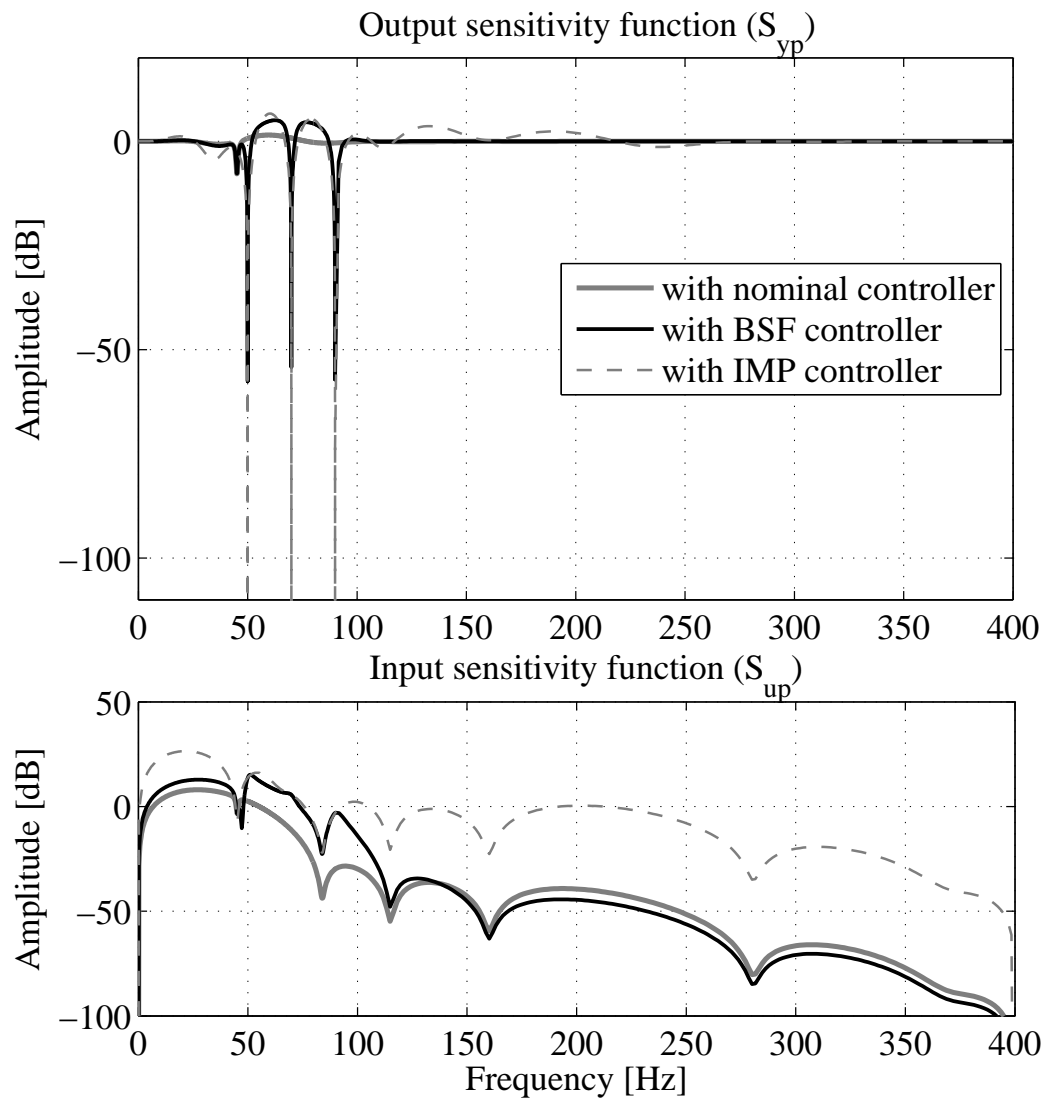


Figure 6.2: Output (upper) and input (lower) sensitivity functions with nominal controller (grey) and with controllers designed using BSFs (black) or the IMP (dotted grey). For the BSF controller, $\zeta_{d_i} = 0.04$ and $M_i = 60$ dB. The attenuations are introduced at 50, 70, and 90 Hz.

The fixed part of the controller denominator H_S is in turn factorized into

$$H_S(z^{-1}) = S_{BSF}(z^{-1})H_{S_1}(z^{-1}), \quad (6.30)$$

where S_{BSF} is the combined numerator of the band-stop filters, (6.24), and H_{S_1} can be used if necessary to satisfy other control specifications (in Section 6.6 it is equal to 1). H_{R_1} is similar to H_{S_1} allowing to introduce fixed parts in the controller's numerator if needed (like opening the loop at certain frequencies). Equation (6.28) is called the Bezout (or Diophantine) equation. The unknowns S' and R' can be computed by putting (6.28) into matrix form (see also [Landau and Zito, 2005]). Thus, the inclusion of the band-stop filter in the output sensitivity function is achieved. The size of the matrix equation that needs to be solved is $n_{Bez} \times n_{Bez}$, where

$$n_{Bez} = n_A + n_B + d + n_{H_{S_1}} + n_{H_{R_1}} + 2 \cdot n - 1. \quad (6.31)$$

n_A , n_B , and d are respectively the order of the plant's model denominator, numerator, and delay (given in (6.3) and (6.4)), $n_{H_{S_1}}$ and $n_{H_{R_1}}$ are the orders of $H_{S_1}(z^{-1})$ and $H_{R_1}(z^{-1})$ respectively and n is the number of narrow band disturbances. Eq. (6.28) has a unique minimal degree solution for S' and R' , if

$$n_P \leq n_{Bez}, \quad (6.32)$$

where n_P is the order of the pre-specified characteristic polynomial $P(q^{-1})$. Also, it can be seen from (6.28) and (6.30) that the minimal orders of S' and R' will be

$$n_{S'} = n_B + d + n_{H_{R_1}} - 1, \quad (6.33)$$

$$n_{R'} = n_A + n_{H_{S_1}} + 2 \cdot n - 1. \quad (6.34)$$

Note that for real time applications, the Diophantine equation has to be solved either at each sampling time (adaptive operation) or each time when a change in the narrow band disturbances' frequencies occurs (self-tuning operation).

6.5 Implementation Using the Youla-Kučera Parametrization

The computational complexity related to the Bezout equation (6.28) is significant. In this section, we show how the computation load of the algorithm can be reduced by the use of the Youla-Kučera parametrization.

As before, a multiple band-stop filter

$$H_{BSF}(z^{-1}) = \frac{S_{BSF}(z^{-1})}{P_{BSF}(z^{-1})} = \frac{\prod_{i=1}^n S_{BSF_i}(z^{-1})}{\prod_{i=1}^n P_{BSF_i}(z^{-1})} \quad (6.35)$$

should be continuously calculated based on the estimated frequencies of the multiple narrow band signal. The objective is to implement the design method described in Section 6.4 using a Youla-Kučera parametrization of the controller.

Suppose that a nominal controller

$$R_0(z^{-1}) = H_{R_1}(z^{-1})R''(z^{-1}), \quad (6.36)$$

$$S_0(z^{-1}) = H_{S_1}(z^{-1})S''(z^{-1}) \quad (6.37)$$

is available, that assures nominal performances for the closed loop system in the absence of narrow band disturbances. This controller satisfies the Bezout equation

$$P_0(z^{-1}) = A(z^{-1})S_0(z^{-1}) + z^{-d}B(z^{-1})R_0(z^{-1}). \quad (6.38)$$

A Youla-Kučera parametrization can offer the desired characteristics for disturbance rejection, maintaining also the fixed parts of the nominal controller ($H_{R_1}(z^{-1})$ and $H_{S_1}(z^{-1})$) and is consequently used. For this purpose, the controller polynomials are factorized as

$$R(z^{-1}) = R_0(z^{-1})P_{BSF}(z^{-1}) + A(z^{-1})H_{R_1}(z^{-1})H_{S_1}(z^{-1})Q(z^{-1}), \quad (6.39)$$

$$S(z^{-1}) = S_0(z^{-1})P_{BSF}(z^{-1}) - z^{-d}B(z^{-1})H_{R_1}(z^{-1})H_{S_1}(z^{-1})Q(z^{-1}), \quad (6.40)$$

where $Q(z^{-1})$ is a FIR filter computed in order to satisfy

$$P(z^{-1}) = P_0(z^{-1})P_{BSF}(z^{-1}), \quad (6.41)$$

for $P(z^{-1})$ in (6.25). $R_0(z^{-1})$, $S_0(z^{-1})$ are given by (6.36) and (6.37) respectively.

Taking into account (6.25), (6.28), and (6.30), it remains to compute $Q(z^{-1})$ such that

$$S(z^{-1}) = S_{BSF}(z^{-1})H_{S_1}(z^{-1})S'(z^{-1}). \quad (6.42)$$

Turning back to eq. (6.40) one obtains⁷

$$S_0P_{BSF} = S_{BSF}H_{S_1}S' + z^{-d}BH_{R_1}H_{S_1}Q. \quad (6.43)$$

and taking into consideration also (6.37) it results that

$$S''P_{BSF} = S_{BSF}S' + q^{-d}BH_{R_1}Q. \quad (6.44)$$

In the last equation, the left side of the equal sign is known and on its right side only $S'(z^{-1})$ and $Q(z^{-1})$ are unknown. This is also a Bezout equation which can be solved by finding the solution to a matrix equation of dimension $n_{BezYK} \times n_{BezYK}$, where

$$n_{BezYK} = n_B + d + n_{H_{R_1}} + 2 \cdot n - 1. \quad (6.45)$$

As it can be observed, the size of the new Bezout equation is reduced in comparison to (6.31) by $n_A + n_{H_{S_1}}$. For systems with large dimensions, this has a significant influence on the computation time (in Section 6.6, $n_A = 14$, $n_B = 14$, the number of sinusoids is $n \in \{2, 3\}$, $n_{H_{R_1}} = 2$, $n_{H_{S_1}} = 0$, and $d = 0$). The nominal controller, being a unique and minimal degree solution to a Bezout equation, satisfies

$$n_{S''} = n_B + d + n_{H_{R_1}} - 1. \quad (6.46)$$

By adding $2 \cdot n$ in both sides of the last equation, one obtains

$$n_{S''} + 2 \cdot n = 2 \cdot n + n_B + d + n_{H_{R_1}} - 1 \quad (6.47)$$

which proves that the solution of the simplified Bezout equation is unique and of minimal degree. Furthermore, the order of the Q FIR filter is equal to $2 \cdot n$.

Figure 6.3 summarizes the implementation of the Youla-Kučera parameterized indirect adaptive controller described in this section. The Youla-Kučera parameter in Figure 6.3

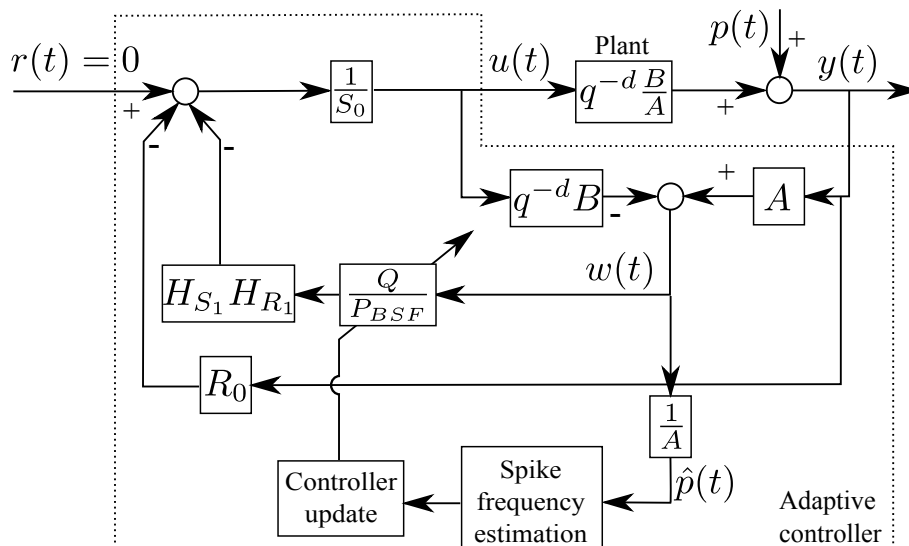


Figure 6.3: Youla-Kučera scheme for indirect adaptive control.

is of the IIR filter type and it satisfies the controller factorization given by eqs. (6.39) and (6.40).

The design parameters that need to be provided to the algorithm are: the number of narrow band spikes in the disturbance (n), the desired attenuations and dampings of the BSFs, either as unique values ($M_i = M$, $\zeta_{d_i} = \zeta_d$, $\forall i \in \{1, \dots, n\}$) or as individual values for each of the spikes (M_i and ζ_{d_i}), and the nominal controller (R_0 , S_0) together with its fixed parts (H_{R_1} , H_{S_1}). The control signal is computed by applying the following procedure at each sampling time:

- Get the measured output $y(t+1)$ and the applied control $u(t)$ to compute the estimated disturbance signal $\hat{p}(t+1)$ as in (6.9).
- Estimate the disturbances' frequencies using adaptive notch filters, eqs. (6.14)-(6.18).
- Calculate $S_{BSF}(z^{-1})$ and $P_{BSF}(z^{-1})$ as in (6.21) - (6.24).
- Find $Q(z^{-1})$ by solving the reduced order Bezout equation (6.44).
- Compute and apply the control using (6.5) with R and S given respectively by (6.39) and (6.40).

6.5.1 Stability Considerations

The stability analysis of the algorithm for adapting the notch filters has been done in [Stoica and Nehorai, 1988] and will not be recalled here.

The stability of the closed loop for the case of known constant narrow band disturbances with the indirect adaptive controller is satisfied as the poles of the system are given by those of the nominal controller and the poles of the band-stop filters, which are always stable.

A complete stability analysis of the full adaptive control scheme remains to be done and will be the subject of a future research.

⁷The argument (z^{-1}) has been dropped to simplify the writing of the equation.

6.6 Experimental Results

6.6.1 An active vibration control system using an inertial actuator

The detailed system's description has been given in Section 3. While the real system remains unchanged, in this chapter only feedback control is experimented. This implies that the measurement of the image of the disturbance obtained by the use of the accelerometer positioned on plate M1 in Figure 3.1 is no longer necessary. Figure 6.4 presents the adaptive scheme in the context of feedback control. The disturbance $p(t)$ represents here the output of the global primary path (also called $x(t)$ in Section 2.2).

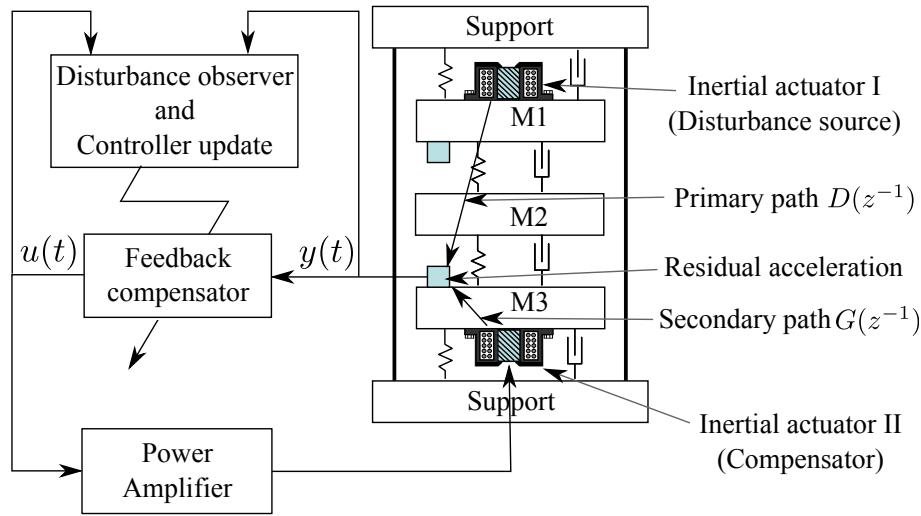


Figure 6.4: An AVC system using a feedback compensation - scheme.

As before, a sampling frequency of 800 Hz is been used.

6.6.2 Attenuation of multi-sinusoidal disturbance

An experimental comparison of the proposed algorithm with the direct adaptive controller of [Landau et al., 2011e] is presented. A multi-sinusoidal signal has been used as disturbance (input of the primary path).

The main advantage of the proposed method is that the BSFs can be adjusted in order to satisfy the desired regulation objectives and, in the same time, to modify as little as possible the closed loop characteristics outside the frequency regions of attenuation. This can be done by choosing very small denominator dampings for the BSFs (in Figure 6.2, $\zeta_d = 0.04$ has been chosen). On the other hand, the direct adaptive algorithm of [Landau et al., 2011e] has a strong influence outside the attenuation region when several disturbances have to be rejected (as shown in Figure 6.2). Due to the time-varying nature of the disturbance, in all of the following experiments, ζ_d has been chosen equal to 0.04. Also, a 60 dB attenuation has been imposed on all of the BSFs. The nominal controller's characteristic polynomial, $P_0(z^{-1})$, contains all the undamped poles of the secondary path and 15 additional real poles at 0.42 for robustness.

The results and their interpretations are given next. In this test, the sine signals change their frequencies at given times. Two experiments have been run. 2 sine signals have been used in the first (Figure 6.5) with a magnitude of 0.1 each and

3 sine signals in the second (Figures 6.7 and 6.8) with a magnitude of 0.04 each in order to avoid saturation of the control input with the direct adaptive controller of [Landau et al., 2011e]. In Figures 6.5 and 6.7, the curves on top represent the effect of the disturbance upon the residual acceleration in open loop operation, the ones in the middle are the residual accelerations in closed loop with the proposed algorithm and the ones on the bottom are the residual accelerations obtained with the direct adaptive regulator of [Landau et al., 2011e]. Three sequences of multi-sinusoidal disturbances have been applied to the primary path. Their corresponding frequencies are given in the figures. The first sequence starts at 3 sec and the duration of each one is of 10 sec.

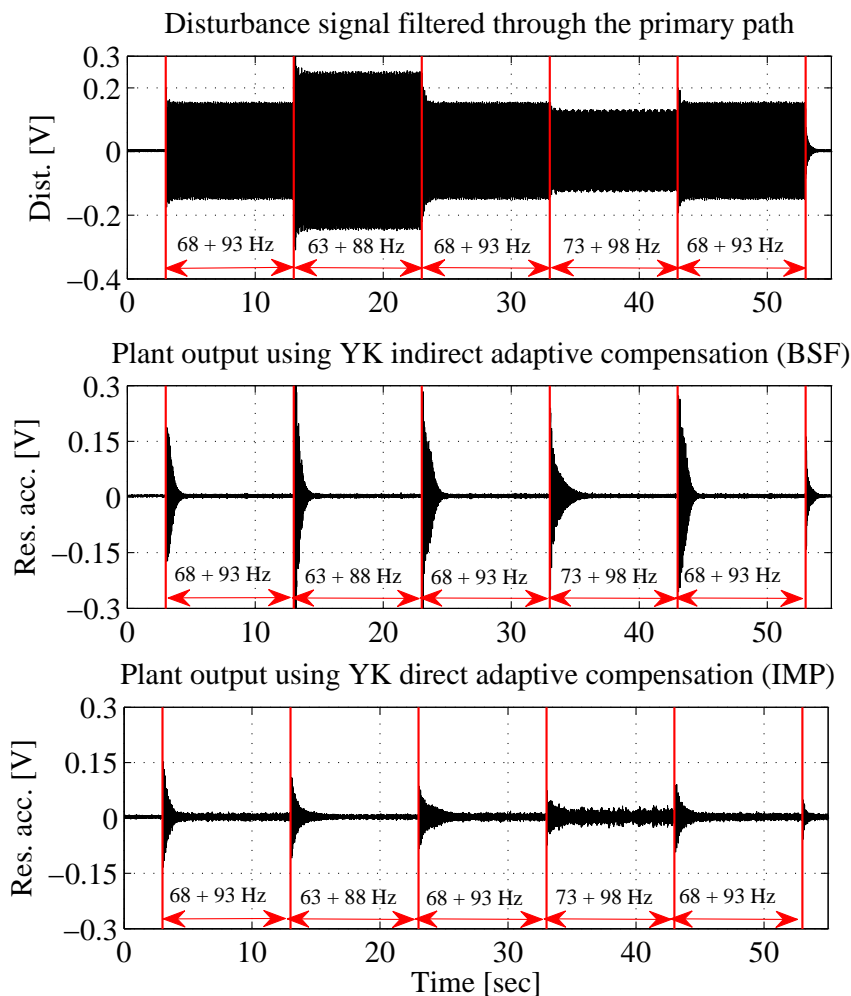


Figure 6.5: Performance comparison in the presence of a two sine wave disturbance.

It should be observed that the proposed algorithm has very good stationary disturbance rejection properties but the one of [Landau et al., 2011e] is better with regard to the transient behavior. As seen from Figure 6.8, the transient behavior of the proposed method is mainly due to the ANFs frequency estimation. For 3 sines, the BSF outperforms the IMP controller.

Remark: for the rejection of 3 sines with the adaptive IMP algorithm, 3 pairs of poles close to the disturbances' frequencies with damping 0.2 have been added to the nominal closed loop to improve its robustness outside the attenuation band removing, for the minimality of the solution, 6 real poles with respect to the nominal characteristic

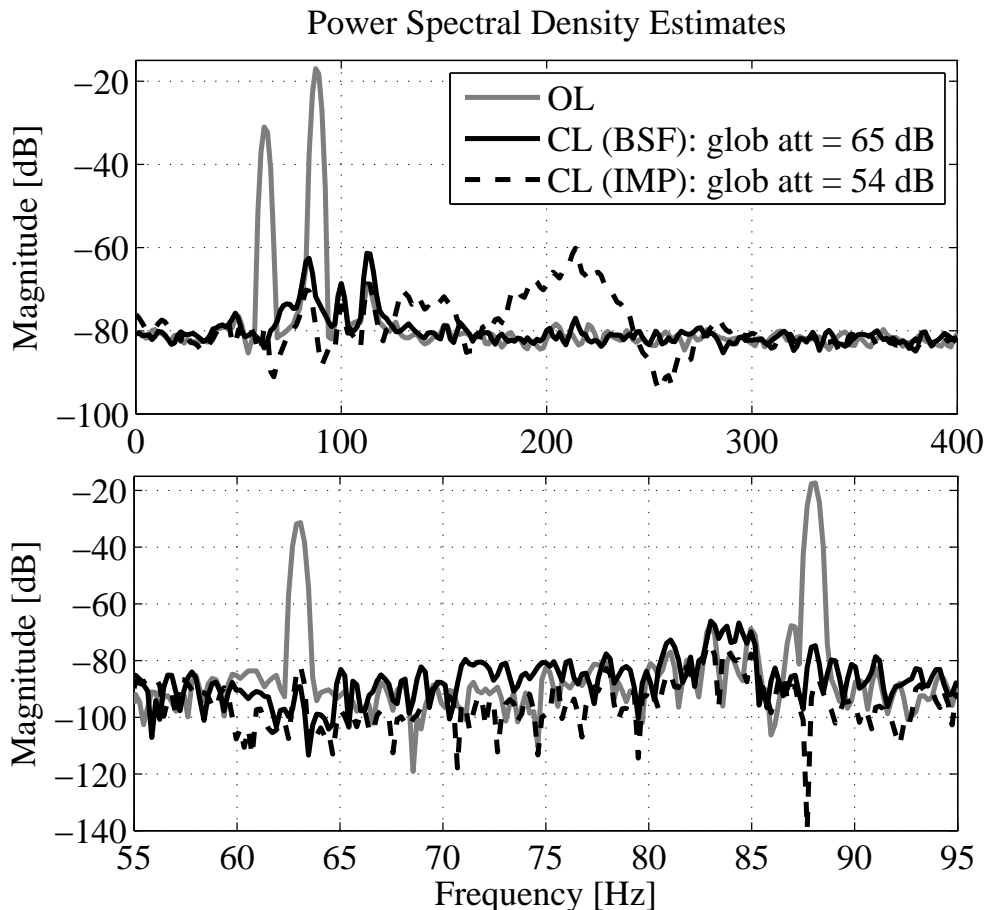


Figure 6.6: PSD comparison between the open loop measured disturbance and the residual accelerations obtained with the direct and the indirect compensators. In the upper figure, the PSDs are obtained with a 512 points window. In the lower one, the size of the window is 4096 points and therefore a better resolution is obtained. The input to the primary path of obtained by adding to sinusoidal signals of 63 Hz and 88 Hz .

polynomial described earlier.

Further analysis can be done by looking at the power spectral density (PSD) estimates (computed after the adaptation process has converged toward an almost constant controller). In Figure 6.6, the PSD for 63 and 88 Hz disturbance are shown first with a complete view and after that with a detailed view on the frequency region where the attenuation is introduced. It should be observed that the direct adaptive algorithm of [Landau et al., 2011e] introduces a significant amplification of the residual acceleration between 190 Hz and 240 Hz (17db with respect to the open loop). This influences the global attenuation of the algorithm. A better global attenuation is obtained by the proposed algorithm (65 dB) in comparison to the direct adaptive algorithm of [Landau et al., 2011e] (54 dB).

6.7 Concluding Remarks

The technique of BSF to shape the output sensitivity function [Procházka and Landau, 2003] is very appropriate for the attenuation of multiple narrow band disturbances in an adaptive procedure. This design method has been transformed into an adaptive

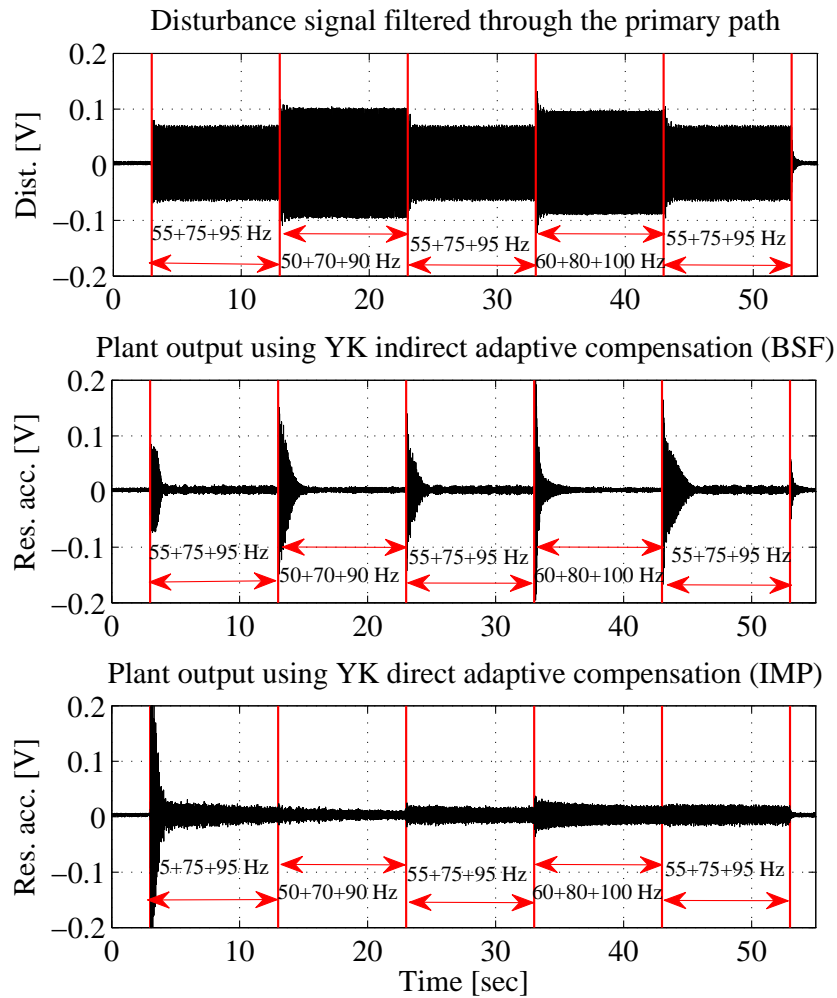


Figure 6.7: Performance evaluation in the presence of 3 variable sinusoidal signals.

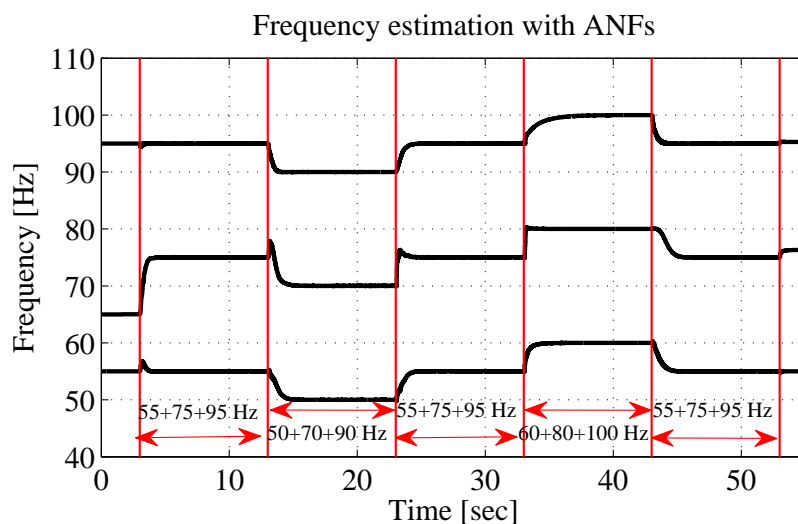


Figure 6.8: Three variable sinusoidal disturbances estimation using ANFs.

procedure by adding an estimator of the spikes' frequencies characterizing unknown time varying multiple narrow band disturbances. The experimental results show the potential

of this approach to solve practical problems related to the attenuation of narrow band disturbances. Future work will include stability analysis and possible development of a direct adaptation algorithm to solve this adaptive regulation problem.

It should be pointed out that the ideas of this chapter provide also a way for improving the robustness of the direct adaptive regulation of narrow band disturbances proposed in [Landau et al., 2011e, Landau et al., 2005]. As explained before, the IMP method shows robustness problems when trying to compensate a large number of disturbances. However, the robustness can be improved by considering the scheme of Figure 6.3 in which only the poles P_{BSF} are now computed using the ANF estimation and the BSFs given in Section 6.4 while the polynomial Q is updated using the direct adaptation algorithm proposed in [Landau et al., 2011e, Section V]. Choosing a denominator damping (for the BSFs) close to or smaller than 0.2 for the BSFs will compensate for the loss of robustness due to the use of the IMP. Furthermore, as it turns out, the direct estimated Q 's parameters will be close to those of the BSF's numerator (for sufficiently small values of the denominator damping). One can consider this method also as a replacement of the Bezout equation solving that has been proposed in this chapter.

CHAPTER 7

CONCLUDING REMARKS AND FUTURE WORK

7.1 Overall Conclusions

To conclude this work, a classification of the control strategies and their main objectives and advantages is drawn.

Adaptive feedforward vibration compensation

The main concern of this thesis was the control of active vibration systems. Adaptive and robust algorithms have been presented and tested on an experimental configuration. A Strictly Positive Real condition has been found to provide the necessary stability and convergence properties. Two different approaches have been followed.

The first algorithm is based on direct adaptation of the parameters of an IIR regulator in the presence of a fixed feedback controller. The analysis has shown that, if the SPR condition is satisfied, the algorithm is stable and parameter convergence can be obtained even in the stochastic case, provided that a richness condition on the observation vector is true. To relax the SPR condition, an “Integral + Proportional” Parameter Adaptation Algorithm has been introduced and analyzed.

The second class of algorithms is based on the use of the Youla-Kučera parametrization. This representation of the controller has been analyzed in the context of Active Vibration Control. At first a FIR adaptive filter is used inside the Youla-Kučera parametrization. Their main advantage is that the poles of the internal positive loop remain unchanged as specified by the central controller. Nevertheless, a reduction of the number of coefficients is obtained if one uses an IIR filter as Youla-Kučera parameter. Although this scheme introduces new poles in the internal positive loop, these are the poles of the QIIR filter and therefore their stability is easier to verify than for direct adaptive IIR schemes. The analysis of the adaptation algorithm is done in a similar manner as for the direct adaptive IIR filter in the presence of internal positive feedback and an analogous SPR condition is found.

Adaptive feedback vibrations compensation

The focus of this part of the thesis was set on adaptive feedback regulation. A new method for adaptive indirect rejection of narrow band disturbances has been proposed. This is done by first identifying the frequency characteristics of the disturbance using Adaptive Notch Filters and then using adjustable Band-stop Filters to remove the influence of the

perturbations. The advantage of this method is that it allows to adjust the attenuation at each frequency and minimize the effect of the adaptive controller at neighboring frequencies. In consequence, it is easier to obtain robust controllers than with methods that use IMP where perfect cancellation is achieved.

7.2 Future Work

The algorithms have been presented in the context of Active Vibration Control systems but they are also applicable to Active Noise Control systems. Taking into considerations that in ANC systems the sampling frequencies are usually around 20,000 Hz , it is intended that in the future fast-array type versions of the algorithms should be implemented.

Another perspective of future research is the introduction of an adaptive feedforward + adaptive feedback algorithm. It has been shown that a non-adaptive negative feedback from the residual acceleration to the input of the secondary path can significantly improve the global attenuation of the AVC system. Adapting also the feedback controller's parameters in the hybrid approach should improve on these results even further.

A different path of research is to analyze the influence of the Youla-Kučera parametrization and the possible benefits of using it in the hybrid approach. In Chapter 4, the direct IIR has been analyzed in this context. A combination of YK and direct adaptive regulators can also be considered.

A very important hypothesis for the development of the algorithms has been that the plant model's parameters do not change over time. This is not always true and, in future, methods have to be proposed for obtaining similarly good results in a more general, time varying context.

Another direction for future research is the development of multi variable control algorithms for ANVC systems. In a number of situations (*e.g.*, adaptive optics, multistage active vibration isolation systems) a multi variable approach has to be considered. Therefore, another direction of research is the development of control algorithms for systems with more than one input and one output. One of the problems that arise in this context is the computational complexity of the algorithms which should be taken into account especially for very large systems.

APPENDIX A

PROOFS FOR CHAPTER 4

A.1 Proof of the a posteriori adaptation error's asymptotic stability in Lemma 4.3.1

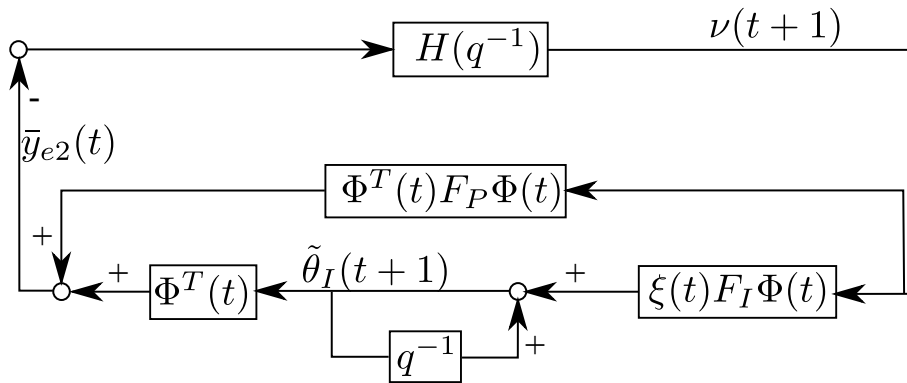


Figure A.1: Equivalent feedback representation of the PAA with "Integral + Proportional" adaptation.

Before going into the details of the proof, [Landau and Silveira, 1979, Theorem 1] and [Landau and Silveira, 1979, Lemma 2] will be recalled (note that in [Landau and Silveira, 1979] the variable k has been used instead of t).

Theorem A.1.1. ([Landau and Silveira, 1979, Theorem 1]) *A discrete linear time-invariant system belonging to the class $L(\Lambda)$ in feedback connection with a discrete linear time-varying system belonging to the class $N(\Gamma)$ is globally asymptotically stable if*

$$\Lambda - \Gamma(t) \geq 0, \forall t \geq t_0. \quad (\text{A.1})$$

Lemma A.1.1. ([Landau and Silveira, 1979, Lemma 2]) *The discrete linear time-varying system described by*

$$x(t+1) = A(t)x(t) + B(t)u(t) \quad (\text{A.2})$$

$$y(t) = C(t)x(t) + D(t)u(t) \quad (\text{A.3})$$

belongs to the class $N(\Gamma)$ if there exist three sequences of positive (or semipositive) definite matrices $P(t)$, $Q(t)$, and $R(t)$, a matrix sequence $S(t)$, and a sequence of symmetric

matrices $\Gamma(t)$ such that the following system of equations is satisfied:

$$A^T(t)P(t+1)A(t) - P(t) = -Q(t) + C^T(t)\Gamma(t)C(t) \quad (\text{A.4})$$

$$B^T(t)P(t+1)A(t) + S^T(t) = C(t) + D^T(t)\Gamma(t)C(t) \quad (\text{A.5})$$

$$R(t) - D^T(t)\Gamma(t)D(t) = D(t) + D^T(t) - B^T(t)P(t+1)B(t) \quad (\text{A.6})$$

and

$$M(t) = \begin{bmatrix} Q(t) & S(t) \\ S^T(t) & R(t) \end{bmatrix} \geq 0 \quad (\text{A.7})$$

with $P(0)$ being bounded.

The proof of Lemma 4.3.1 is given next.

Proof. This result can be directly obtained by applying [Landau and Silveira, 1979, Theorem 1]. The linear feedforward block belongs to the class $L(\lambda_2)$ as it can be concluded from the condition that $H'(z^{-1})$ given in eq. (4.23) is SPR.

It remains to show that the feedback block belongs to the class $N(\gamma)$, for $\gamma(t) = \lambda_2(t)$. One can directly verify Lemma 2 of [Landau and Silveira, 1979] by considering an equivalent feedback representation (EFR) of the adaptive feedback system given by the eqs. (4.14a) - (4.14k) and (4.17) (Fig. A.1)

$$\tilde{\theta}_I(t) = \hat{\theta}_I(t) - \theta, \quad (\text{A.8})$$

$$\nu(t+1) = -H(z^{-1})\Phi^T(t)\tilde{\theta}(t+1) \quad (\text{A.9})$$

$$\tilde{\theta}_I(t+1) = \tilde{\theta}_I(t) + \xi(t)F_I(t)\Phi(t)\nu(t+1), \quad (\text{A.10})$$

$$\bar{y}_{e2}(t) = \Phi^T(t)\tilde{\theta}_I(t) + \Phi^T(t)F(t)\Phi(t)\nu(t+1), \quad (\text{A.11})$$

In order to use Lemma 2 of [Landau and Silveira, 1979], one has to consider the following change of notations:

$$A(t) = I, \quad (\text{A.12})$$

$$B(t) = \xi(t)F_I(t)\Phi(t), \quad (\text{A.13})$$

$$C(t) = \Phi^T(t), \quad (\text{A.14})$$

$$D(t) = \Phi^T(t)F(t)\Phi(t). \quad (\text{A.15})$$

Then, eqs. (2.16)-(2.18) of [Landau and Silveira, 1979] are satisfied for

$$P(t) = F_I^{-1}(t), \quad (\text{A.16})$$

$$Q(t) = [1 - \lambda_1(t)]F_I^{-1}(t), \quad (\text{A.17})$$

$$S(t) = [1 - \lambda_1(t)]\Phi(t), \quad (\text{A.18})$$

$$f_{F_I}(t) \stackrel{\text{def}}{=} \Phi^T(t)F_I(t)\Phi(t), \quad (\text{A.19})$$

$$f_{F_P}(t) \stackrel{\text{def}}{=} \Phi^T(t)F_P(t)\Phi(t), \quad (\text{A.20})$$

$$\begin{aligned} R(t) &= [2 - \lambda_1(t)]f_{F_I}(t) + \frac{\lambda_2^2(t)}{\lambda_1(t)}f_{F_I}(t)f_{F_P}^2(t) \\ &\quad + \lambda_2(t)f_{F_P}^2(t) + 2\frac{\lambda_2(t)}{\lambda_1(t)}f_{F_I}(t)f_{F_P}(t) + 2f_{F_P}(t). \end{aligned} \quad (\text{A.21})$$

Finally, condition (2.21) of [Landau and Silveira, 1979] is assured by the choice of $\gamma(t) = \lambda_2(t)$ and the fact that the feedforward path is of the class $L(\lambda_2)$, where $\lambda_2 \geq \lambda_2(t)$ from eq. (4.23).

Thus the conditions of Theorem 1 given in [Landau and Silveira, 1979] are satisfied and the time-varying feedback system is asymptotically stable, which implies eq. (4.19). \square

A.2 Proof of Lemma 4.4.1

Proof. To analyse the strict positive realness of this transfer function, one has to check first that it's real part is strictly positive. We then have:

$$\begin{aligned} \operatorname{Re}\left\{\frac{H(z^{-1})}{1 + K \cdot H(z^{-1})}\right\} &= \operatorname{Re}\left\{\frac{\operatorname{Re}\{H\} + j\operatorname{Im}\{H\}}{1 + K \cdot \operatorname{Re}\{H\} + jK \cdot \operatorname{Im}\{H\}}\right\} \\ &= \operatorname{Re}\left\{\frac{(\operatorname{Re}\{H\} + j\operatorname{Im}\{H\}) \cdot (1 + K \cdot \operatorname{Re}\{H\} - jK \cdot \operatorname{Im}\{H\})}{(1 + K \cdot \operatorname{Re}\{H\})^2 + (K \cdot \operatorname{Im}\{H\})^2}\right\} \\ &= \frac{K \cdot \operatorname{Re}\{H\}^2 + \operatorname{Re}\{H\} + K \cdot \operatorname{Im}\{H\}^2}{(1 + K \cdot \operatorname{Re}\{H\})^2 + (K \cdot \operatorname{Im}\{H\})^2}. \end{aligned} \quad (\text{A.22})$$

In eq. (A.22), the denominator is always strictly positive. Thus, the strict positive realness is satisfied if K is chosen such that the numerator of eq. (A.22) is also strictly positive. This is always true if K satisfies the relation

$$\begin{aligned} K &> -\frac{\operatorname{Re}\{H(e^{-j\omega})\}}{\operatorname{Re}\{H(e^{-j\omega})\}^2 + \operatorname{Im}\{H(e^{-j\omega})\}^2}, \\ 0 &\leq \omega \leq \pi \cdot f_s, \end{aligned} \quad (\text{A.23})$$

f_s being the sampling frequency.

Next, the stability of the direct path is analyzed. Under hypothesis H6, the direct path becomes:

$$\frac{H(q^{-1})}{1 + K \cdot H(q^{-1})} = \frac{\sum_{m=0}^{n_B} b_m q^{-m}}{1 + \sum_{p=1}^{n_A} a_p q^{-p}} \quad (\text{A.24})$$

$$= \frac{\sum_{m=0}^{n_B} b_m q^{-m}}{1 + K b_0 + \sum_{p=1}^{n_A} a_p q^{-p} + K \sum_{m=1}^{n_B} b_m q^{-m}} \quad (\text{A.25})$$

$$= \frac{\frac{1}{1+Kb_0} \sum_{m=0}^{n_B} b_m q^{-m}}{1 + \frac{\sum_{p=1}^{n_A} a_p q^{-p} + K \sum_{m=1}^{n_B} b_m q^{-m}}{1+Kb_0}}. \quad (\text{A.26})$$

The poles of the direct path are thus given by the roots of the polynomial

$$P(q^{-1}) = 1 + \frac{\sum_{p=1}^{n_A} a_p q^{-p} + K \sum_{m=1}^{n_B} b_m q^{-m}}{1 + K b_0} \quad (\text{A.27})$$

and assuming K large enough such that $K b_m \gg a_p, \forall m \in \{1, \dots, n_B\}, p \in \{1, \dots, n_A\}$,

$$P(q^{-1}) \cong \begin{cases} 1 + \sum_{m=1}^{n_B} \frac{b_m}{b_0} q^{-m}, & \text{if } n_B \geq n_A, \\ 1 + \sum_{m=1}^{n_B} \frac{b_m}{b_0} q^{-m} + \sum_{p=n_B+1}^{n_A} \frac{a_p}{1+Kb_0} q^{-p}, & \text{if } n_B < n_A. \end{cases} \quad (\text{A.28})$$

Thus for $n_B \geq n_A$, the poles and the zeros of the direct path become identical when $K \rightarrow \infty$. For $n_B < n_A$, in addition to the poles identical to the zeros of $B(q^{-1})$, there appear $n_A - n_B$ poles that go to zero as $K \rightarrow \infty$.

It is now obvious that hypothesis H5 has been introduced to assure the stability of the direct path when H6 is satisfied.

The necessity of hypothesis H6 is shown with the use of a counterexample. Let suppose that $b_0 = 0$. Then the direct path's transfer function becomes

$$\frac{H(q^{-1})}{1 + K \cdot H(q^{-1})} = \frac{\sum_{m=1}^{n_B} b_m q^{-m}}{1 + \sum_{p=1}^{n_A} a_p q^{-p} + K \sum_{m=1}^{n_B} b_m q^{-m}}. \quad (\text{A.29})$$

Taking a first order system as an example, $H(q^{-1}) = \frac{b_1 q^{-1}}{1 + a_1 q^{-1}}$, it is evident that the poles will be the zeros of $1 + (a_1 + K b_1) q^{-1} = 0$ and thus the direct path becomes unstable for large enough K . \square

A.3 Proof of Theorem 4.4.1

Proof. The proof is similar to that of [Landau et al., 2011g, Theorem 3.3, pp. 109] where Lemma 3.3 (pp. 110) is replaced by Lemma 4.4.1 of this paper. However, the details of the proof of Theorem 3.3 in [Landau et al., 2011g] are not given. For the sake of completeness, the details of the proof of Theorem 4.4.1 are given next.

The proof is done by using [Landau and Silveira, 1979, Theorem 1]. The adaptive system can be rearranged into the one given in Fig. 4.1. Under condition T1, the linear feedforward block from $u_{e1}(t)$ to $\nu(t+1)$ belongs to the class $L(0)$.

Given the choice in adaptation gain ($\lambda_2(t) \equiv 0$, $\lambda_1(t) \equiv 1$), the necessary condition for asymptotic stability is only that the time-varying feedback block belongs to the class $N(0)$ and, therefore, its input-output product verifies Popov's inequality (4.38),

$$\sum_{t=0}^{t_1} y_{e2}(t) u_{e2}(t) = \sum_{t=0}^{t_1} \bar{y}_{e2}(t) u_{e2}(t) - K \sum_{t=0}^{t_1} u_{e2}^2(t) \geq -\gamma_0^2. \quad (\text{A.30})$$

It should be observed that with the current choice of $\lambda_2(t) \equiv 0$, $\lambda_1(t) \equiv 1$, one obtains $\xi(t) = 1$ from eq. (4.14h).

Taking into consideration eqs. (A.10) and (A.11)

$$\begin{aligned} \bar{y}_{e2}(t) u_{e2}(t) &= \bar{y}_{e2}(t) \nu(t+1) = \tilde{\theta}_I^T(t+1) \Phi(t) \nu(t+1) + \\ &\quad + \Phi^T(t) F_P(t) \Phi(t) \nu^2(t+1). \end{aligned} \quad (\text{A.31})$$

The first term in the right hand side can be further expressed as (see also Lemma 3.2 of [Landau et al., 2011g])

$$\tilde{\theta}_I^T(t+1) \Phi(t) \nu(t+1) = \tilde{\theta}_I^T(t+1) F_I^{-1} \tilde{\theta}_I(t+1) - \tilde{\theta}_I^T(t+1) F_I^{-1} \tilde{\theta}_I(t). \quad (\text{A.32})$$

On the other hand

$$\begin{aligned} [\tilde{\theta}_I(t+1) - \tilde{\theta}_I(t)]^T F_I^{-1} [\tilde{\theta}_I(t+1) - \tilde{\theta}_I(t)] &= \tilde{\theta}_I^T(t+1) F_I^{-1} \tilde{\theta}_I(t+1) + \tilde{\theta}_I^T(t) F_I^{-1} \tilde{\theta}_I(t) - \\ &\quad - 2 \tilde{\theta}_I^T(t+1) F_I^{-1} \tilde{\theta}_I(t) \geq 0, \end{aligned} \quad (\text{A.33})$$

from which, using (4.16) and (A.10), results

$$\begin{aligned}\tilde{\theta}_I^T(t+1)F_I^{-1}\tilde{\theta}_I(t) &= \frac{1}{2}\tilde{\theta}_I^T(t+1)F_I^{-1}\tilde{\theta}_I(t+1)+ \\ &+ \frac{1}{2}\tilde{\theta}_I^T(t)F_I^{-1}\tilde{\theta}_I(t) - \frac{1}{2}\Phi^T(t)F_I\Phi(t)\nu^2(t+1).\end{aligned}\quad (\text{A.34})$$

Substituting the last equation back into (A.32) and using (4.16)

$$\begin{aligned}\tilde{\theta}_I^T(t+1)\Phi(t)\nu(t+1) &= \frac{1}{2}\tilde{\theta}_I^T(t+1)F_I^{-1}\tilde{\theta}_I(t+1)- \\ &- \frac{1}{2}\tilde{\theta}_I^T(t)F_I^{-1}\tilde{\theta}_I(t) + \frac{1}{2}\Phi^T(t)F_I\Phi(t)\nu^2(t+1),\end{aligned}\quad (\text{A.35})$$

and summing up from $t = 0$ to t_1 , one gets

$$\begin{aligned}\sum_{t=0}^{t_1} y_{e2}(t)\nu(t+1) &= \frac{1}{2}\tilde{\theta}_I^T(t_1+1)F_I^{-1}\tilde{\theta}_I(t_1+1)+ \\ &+ \sum_{t=0}^{t_1} \Phi^T(t) \left(\frac{1}{2}F_I + F_P(t) \right) \Phi(t)\nu^2(t+1)- \\ &- K \sum_{t=0}^{t_1} \nu^2(t+1) - \frac{1}{2}\tilde{\theta}_I^T(0)F_I^{-1}\tilde{\theta}_I(0).\end{aligned}\quad (\text{A.36})$$

From eq. (A.36) and the fact that F_I is positive definite concludes that

$$\sum_{t=0}^{t_1} y_{e2}(t)u_{e2}(t) \geq -\frac{1}{2}\tilde{\theta}_I^T(0)F_I^{-1}\tilde{\theta}_I(0)\quad (\text{A.37})$$

as long as K satisfies condition T2 of the theorem, thus Popov's inequality is satisfied and the adaptive system is asymptotically stable. \square

APPENDIX B

PROOFS FOR CHAPTER 5

B.1 Proof of Lemma 5.3.1

Proof. Using hypotheses *H2* and *H4* (perfect matching condition), one can construct an equivalent closed loop system for the primary path as in Figure B.1.

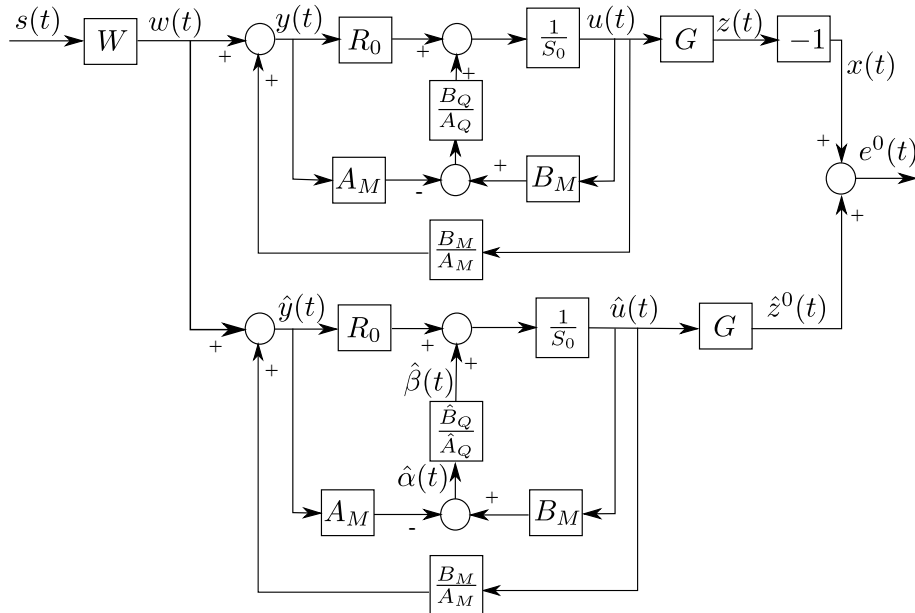


Figure B.1: Equivalent system representation for Youla-Kučera parameterized feedforward compensators.

Considering a $Q(q^{-1})$ filter as in eq. (5.3), the polynomial $S(q^{-1})$ given in eq. (3.13) can be rewritten as

$$S(q^{-1}) = 1 + q^{-1}S^* = 1 + q^{-1}((A_Q S_0)^* - B_Q B_M^*). \quad (\text{B.1})$$

Under hypothesis *H4*, the output of the primary path can be expressed as

$$x(t) = -z(t) = -G(q^{-1})u(t) \quad (\text{B.2})$$

and the input of the Youla-Kučera scheme as

$$y(t+1) = w(t+1) + \frac{B_M}{A_M}u(t+1), \quad (\text{B.3})$$

where $u(t)$ is a dummy variable given by

$$\begin{aligned} u(t+1) &= -S^*u(t) + Ry(t+1) \\ &= -((A_Q S_0)^* - B_Q B_M^*)u(t) + (A_Q R_0 - B_Q A_M)y(t+1) \\ &= -(A_Q S_0)^*u(t) + A_Q R_0 y(t+1) + B_Q (B_M^* u(t) - A_M y(t+1)). \end{aligned} \quad (\text{B.4})$$

Similarly, the output of the adaptive feedforward filter (for a **fixed** \hat{Q}) is given by

$$\hat{u}(t+1) = -(\hat{A}_Q S_0)^* \hat{u}(t) + \hat{A}_Q R_0 \hat{y}(t+1) + \hat{B}_Q (B_M^* \hat{u}(t) - A_M \hat{y}(t+1)). \quad (\text{B.5})$$

The output of the secondary path is

$$\hat{z}(t) = G(q^{-1})\hat{u}(t). \quad (\text{B.6})$$

Define the dummy error (for a fixed estimated set of parameters)

$$\epsilon(t) = -u(t) + \hat{u}(t) \quad (\text{B.7})$$

and the residual error

$$\nu(t) = -e(t) = -(-z(t) + \hat{z}(t)) = -G(q^{-1})\epsilon(t). \quad (\text{B.8})$$

Eq. (B.4) can be rewritten as

$$\begin{aligned} u(t+1) &= -(A_Q S_0)^* \hat{u}(t) + A_Q R_0 \hat{y}(t+1) + B_Q [B_M^* \hat{u}(t) - A_M \hat{y}(t+1)] - \\ &\quad - (A_Q S_0)^* [u(t) - \hat{u}(t)] + A_Q R_0 [y(t+1) - \hat{y}(t+1)] + \\ &\quad + B_Q [B_M^* (u(t) - \hat{u}(t)) - A_M (y(t+1) - \hat{y}(t+1))]. \end{aligned} \quad (\text{B.9})$$

Taking into consideration eqs. (3.20) and (B.3)

$$\begin{aligned} B_Q [B_M^* (u(t) - \hat{u}(t)) - A_M (y(t+1) - \hat{y}(t+1))] &= \\ = -B_Q \left[B_M^* \epsilon(t) - A_M \frac{B_M^*}{A_M} \epsilon(t) \right] &= 0 \end{aligned} \quad (\text{B.10})$$

and subtracting eq. (B.9) from (B.5) one obtains

$$\begin{aligned} \epsilon(t+1) &= -((-A_Q + \hat{A}_Q) S_0)^* \hat{u}(t) + (-A_Q + \hat{A}_Q) R_0 \hat{y}(t+1) + \\ &\quad + (-B_Q + \hat{B}_Q) [B_M^* \hat{u}(t) - A_M \hat{y}(t+1)] - \\ &\quad - (A_Q S_0)^* \epsilon(t) + A_Q R_0 \frac{B_M^*}{A_M} \epsilon(t). \end{aligned} \quad (\text{B.11})$$

Passing the terms in $\epsilon(t)$ on the left hand side, it results

$$\begin{aligned} \left[1 + q^{-1} \left(\frac{A_M (A_Q S_0)^* - A_Q R_0 B_M^*}{A_M} \right) \right] \epsilon(t+1) &= \frac{A_Q P_0}{A_M} \epsilon(t+1) = \\ &= (-A_Q^* + \hat{A}_Q^*) [-S_0 \hat{u}(t) + R_0 \hat{y}(t)] \\ &\quad + (-B_Q + \hat{B}_Q) [B_M \hat{u}(t+1) - A_M \hat{y}(t+1)]. \end{aligned} \quad (\text{B.12})$$

Using eqs. (B.8) and (5.14)

$$\nu(t+1) = \frac{A_M(q^{-1})G(q^{-1})}{A_Q(q^{-1})P_0(q^{-1})} (\theta - \hat{\theta})^T \phi(t), \quad (\text{B.13})$$

which corresponds to eq. (5.12) and thus ends the proof. \square

B.2 Proof of Lemma 5.4.1

Proof. Using Theorem 3.2 from [Landau et al., 2011g], under the condition (5.35), (5.30) and (5.32) hold.

However, in order to show that $\nu^0(t+1)$ goes to zero, one has to show first that the components of the observation vector are bounded. The result (5.32) suggests to use the Goodwin's "bounded growth" lemma ([Landau et al., 2001b] and Lemma 11.1 in [Landau et al., 2011g]). Provided that one has

$$|\psi^T(t)F(t)\psi(t)|^{\frac{1}{2}} \leq C_1 + C_2 \cdot \max_{0 \leq k \leq t+1} |\nu^0(k)| \quad (\text{B.14})$$

$$0 < C_1 < \infty, \quad 0 < C_2 < \infty, \quad F(t) > 0,$$

$\|\psi(t)\|$ will be bounded. So it will be shown that (B.14) holds. This will be proved for Algorithm *I* (for Algorithms *II* and *III*, the proof is similar).

From (3.36) one has

$$-\hat{z}(t) = \nu(t) + x(t). \quad (\text{B.15})$$

Since $x(t)$ is bounded (output of an asymptotically stable system with bounded input), one has

$$\begin{aligned} |\hat{u}_f(t)| = |G\hat{u}(t)| = |\hat{z}(t)| &\leq C_3 + C_4 \cdot \max_{0 \leq k \leq t+1} |\nu(k)| \\ &\leq C'_3 + C'_4 \cdot \max_{0 \leq k \leq t+1} |\nu^0(k)| \end{aligned} \quad (\text{B.16})$$

$$0 < C_3, C_4, C'_3, C'_4 < \infty \quad (\text{B.17})$$

since $|\nu(t)| \leq |\nu^0(t)|$ for all t . Filtering both sides of eq. (3.20) by $G(q^{-1})$, one gets in the adaptive case

$$\hat{y}_f(t) = G \cdot w(t) + \frac{B_M}{A_M} \hat{u}_f(t). \quad (\text{B.18})$$

Since A_G and A_M are Hurwitz polynomials and $w(t)$ is bounded, it results that

$$|\hat{y}_f(t)| \leq C_5 + C_6 \cdot \max_{0 \leq k \leq t+1} |\nu^0(k)|; \quad 0 < C_5, C_6 < \infty. \quad (\text{B.19})$$

Using Eqs. (5.14a), (5.14b), (5.22), (B.17) and (B.19), one can conclude that

$$|\alpha_f(t)| \leq C_7 + C_8 \cdot \max_{0 \leq k \leq t+1} |\nu^0(k)| \quad (\text{B.20})$$

and

$$|\beta_f(t)| \leq C_9 + C_{10} \cdot \max_{0 \leq k \leq t+1} |\nu^0(k)|. \quad (\text{B.21})$$

Therefore, (B.14) holds, which implies that $\psi(t)$ is bounded and one can conclude that (5.34) also holds. End of the proof. \square

B.3 Changes to Lemma 5.3.1 when hypothesis H2 is not satisfied

When hypothesis H2 is not satisfied ($\hat{A}_M \neq A_M$ and $\hat{B}_M \neq B_M$), hypotheses H3 and H4 become:

H3) There exists a central feedforward compensator N_0 (R_0 , S_0) which stabilizes the inner positive feedback loop formed by N_0 and M and a $QIIR$ filter (B_Q , A_Q) such that the characteristic polynomial of the closed loop

$$P = A_Q P_0 - B_Q (A_M \hat{B}_M - \hat{A}_M B_M) \quad (\text{B.22})$$

is a Hurwitz polynomial.

H4) Perfect matching condition - There exists a value of the Q parameters such that

$$\frac{G \cdot A_M (R_0 A_Q - \hat{A}_M B_Q)}{A_Q P_0 - B_Q (A_M \hat{B}_M - \hat{A}_M B_M)} = -D. \quad (\text{B.23})$$

Lemma B.3.1. *Under the hypotheses H1, H3 - H6 for the system described by equations (3.2) - (3.34) (with $K \equiv 0$) using an estimated IIR Youla-Kučera parameterized feedforward compensator with constant parameters $\hat{\theta}$, one has*

$$\nu(t+1) = \frac{A_M G}{A_Q P_0 - B_Q (A_M \hat{B}_M - \hat{A}_M B_M)} [\theta - \hat{\theta}]^T \phi(t), \quad (\text{B.24})$$

where $\phi(t)$, $\alpha(t+1)$, and $\beta(t)$ are given by eqs. (5.13), (5.14a), and (5.14b) respectively.

Proof. Using hypotheses H2 and H4 (perfect matching condition), one can construct an equivalent closed loop system for the primary path as in Figure B.2.

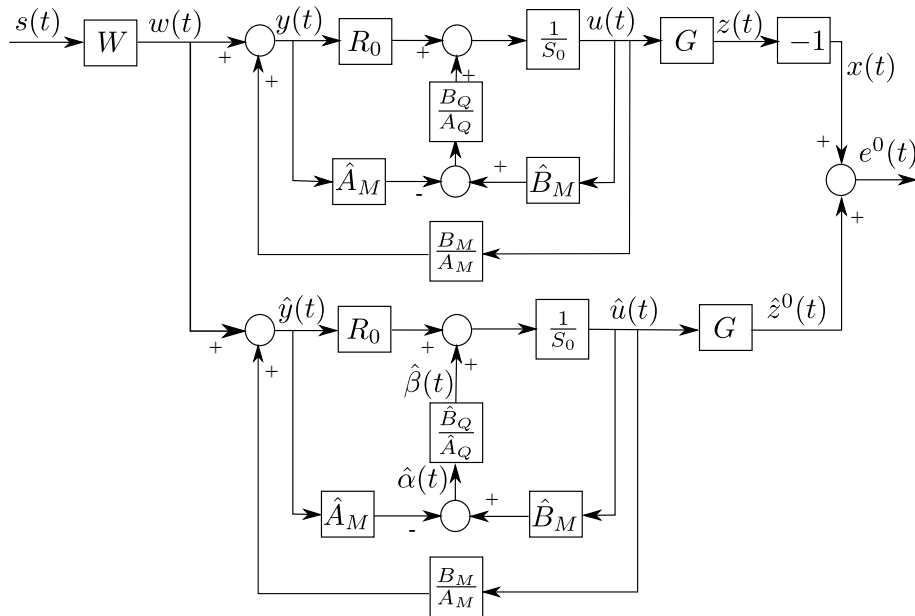


Figure B.2: Equivalent system representation for Youla-Kučera parameterized feedforward compensators in the absence of hypothesis H2.

Considering a $Q(q^{-1})$ filter as in eq. (5.3), the polynomial $S(q^{-1})$ given in eq. (3.13) can be rewritten as

$$S(q^{-1}) = 1 + q^{-1} S^* = 1 + q^{-1} ((A_Q S_0)^* - B_Q \hat{B}_M^*). \quad (\text{B.25})$$

Under hypothesis *H4*, the output of the primary path can be expressed as

$$x(t) = -z(t) = -G(q^{-1})u(t) \quad (\text{B.26})$$

and the input of the Youla-Kučera scheme as

$$y(t+1) = w(t+1) + \frac{B_M}{A_M}u(t+1), \quad (\text{B.27})$$

where $u(t)$ is a dummy variable given by

$$\begin{aligned} u(t+1) &= -S^*u(t) + Ry(t+1) \\ &= -((A_Q S_0)^* - B_Q \hat{B}_M^*)u(t) + (A_Q R_0 - B_Q \hat{A}_M)y(t+1) \\ &= -(A_Q S_0)^*u(t) + A_Q R_0 y(t+1) + B_Q (\hat{B}_M^* u(t) - \hat{A}_M y(t+1)). \end{aligned} \quad (\text{B.28})$$

Similarly, the output of the adaptive feedforward filter (for a **fixed** \hat{Q}) is given by

$$\hat{u}(t+1) = -(\hat{A}_Q S_0)^* \hat{u}(t) + \hat{A}_Q R_0 \hat{y}(t+1) + \hat{B}_Q (\hat{B}_M^* \hat{u}(t) - \hat{A}_M \hat{y}(t+1)). \quad (\text{B.29})$$

The output of the secondary path is

$$\hat{z}(t) = G(q^{-1})\hat{u}(t). \quad (\text{B.30})$$

Define the dummy error (for a fixed estimated set of parameters)

$$\epsilon(t) = -u(t) + \hat{u}(t) \quad (\text{B.31})$$

and the residual error

$$\nu(t) = -e(t) = -(-z(t) + \hat{z}(t)) = -G(q^{-1})\epsilon(t). \quad (\text{B.32})$$

Eq. (B.28) can be rewritten as

$$\begin{aligned} u(t+1) &= -(A_Q S_0)^* \hat{u}(t) + A_Q R_0 \hat{y}(t+1) + B_Q [\hat{B}_M^* \hat{u}(t) - \hat{A}_M \hat{y}(t+1)] - \\ &\quad - (A_Q S_0)^* [u(t) - \hat{u}(t)] + A_Q R_0 [y(t+1) - \hat{y}(t+1)] + \\ &\quad + B_Q [\hat{B}_M^* (u(t) - \hat{u}(t)) - \hat{A}_M (y(t+1) - \hat{y}(t+1))]. \end{aligned} \quad (\text{B.33})$$

Taking into consideration eqs. (3.20), (B.27)

$$\begin{aligned} B_Q [\hat{B}_M^* (u(t) - \hat{u}(t)) - \hat{A}_M (y(t+1) - \hat{y}(t+1))] &= \\ = -B_Q \left[\hat{B}_M^* \epsilon(t) - \hat{A}_M \frac{B_M^*}{A_M} \epsilon(t) \right] &= -B_Q \frac{A_M \hat{B}_M^* - \hat{A}_M B_M^*}{A_M} \epsilon(t) \neq 0 \end{aligned} \quad (\text{B.34})$$

and subtracting eq. (B.33) from (B.29) one obtains

$$\begin{aligned} \epsilon(t+1) &= -((-A_Q + \hat{A}_Q) S_0)^* \hat{u}(t) + (-A_Q + \hat{A}_Q) R_0 \hat{y}(t+1) + \\ &\quad + (-B_Q + \hat{B}_Q) [\hat{B}_M^* \hat{u}(t) - \hat{A}_M \hat{y}(t+1)] - \\ &\quad - (A_Q S_0)^* \epsilon(t) + A_Q R_0 \frac{B_M^*}{A_M} \epsilon(t) + B_Q \frac{A_M \hat{B}_M^* - \hat{A}_M B_M^*}{A_M} \epsilon(t). \end{aligned} \quad (\text{B.35})$$

Passing the terms in $\epsilon(t)$ on the left hand side, it results

$$\begin{aligned} & \left[1 + q^{-1} \left(\frac{A_M(A_Q S_0)^* - A_Q R_0 B_M^*}{A_M} \right) - q^{-1} B_Q \frac{A_M \hat{B}_M^* - \hat{A}_M B_M^*}{A_M} \right] \epsilon(t+1) = \\ & = \frac{A_Q P_0 - B_Q(A_M \hat{B}_M - \hat{A}_M B_M)}{A_M} \epsilon(t+1) = (-A_Q^* + \hat{A}_Q^*)[-S_0 \hat{u}(t) + R_0 \hat{y}(t)] + \\ & \quad + (-B_Q + \hat{B}_Q)[B_M \hat{u}(t+1) - A_M \hat{y}(t+1)]. \quad (\text{B.36}) \end{aligned}$$

Using eqs. (B.32) and (5.14)

$$\nu(t+1) = \frac{A_M(q^{-1})G(q^{-1})}{A_Q(q^{-1})P_0(q^{-1}) - B_Q(A_M \hat{B}_M - \hat{A}_M B_M)} (\theta - \hat{\theta})^T \phi(t), \quad (\text{B.37})$$

which corresponds to eq. (B.24) and thus ends the proof. \square

B.4 Changes to the stability condition when hypothesis H2 is not satisfied

The effects brought by the violation of hypothesis H2 upon the adaptation algorithms are discussed in this section.

Remark: Suppression of this hypothesis does not influence the implementation of the algorithms, which remains unchanged (the filter L has been given in Section 5.3).

The elimination of hypothesis H2 influences the stability condition for the adaptation algorithms. In this context, the transfer function $H(q^{-1})$, given by eq. (5.29), becomes, for Algorithm *IIa*,

$$H = A_M \frac{G}{\hat{G}} \cdot \frac{1}{A_Q(A_M S_0 - B_M R_0) - B_Q(A_M \hat{B}_M - \hat{A}_M B_M)} \quad (\text{B.38})$$

for Algorithm *IIb*,

$$H = \frac{A_M}{\hat{A}_M} \cdot \frac{G}{\hat{G}} \cdot \frac{\hat{A}_M S_0 - \hat{B}_M R_0}{A_Q(A_M S_0 - B_M R_0) - B_Q(A_M \hat{B}_M - \hat{A}_M B_M)} \quad (\text{B.39})$$

and, for Algorithm *III*,

$$H = \frac{A_M}{\hat{A}_M} \cdot \frac{G}{\hat{G}} \cdot \frac{\hat{A}_Q (\hat{A}_M S_0 - \hat{B}_M R_0)}{A_Q(A_M S_0 - B_M R_0) - B_Q(A_M \hat{B}_M - \hat{A}_M B_M)}. \quad (\text{B.40})$$

Similar stability and convergence results are obtained under the perfect matching condition (hypothesis H4). The strictly positive realness of the transfer function

$$H'(z^{-1}) = H(z^{-1}) - \frac{\lambda_2}{2} \quad (\text{B.41})$$

has to be checked, where $H(z^{-1})$ is now computed, for Algorithms *IIa*, *IIb*, and *III*, as shown in eqs. B.38, B.39, and B.40.

An analysis of the bias distribution in the absence of hypothesis H2 shows that eq. (5.44) becomes

$$\hat{\theta}^* = \arg \min_{\hat{\theta}} \int_{-\pi}^{\pi} \left[\left| G A_M^2 \right|^2 \left| \frac{S_0 \hat{A}_M - R_0 \hat{B}_M}{\hat{A}_Q P_0 - \hat{B}_Q (A_M \hat{B}_M - \hat{A}_M B_M)} \cdot \frac{\hat{A}_Q B_Q - A_Q \hat{B}_Q}{A_Q P_0 - B_Q (A_M \hat{B}_M - \hat{A}_M B_M)} \right|^2 \phi_w(\omega) + \phi_n(\omega) \right] d\omega, \quad (\text{B.42})$$

which, if particularized for $\hat{A}_M \equiv A_M$ and $\hat{B}_M \equiv B_M$, gives the result obtained in eq. (5.45).

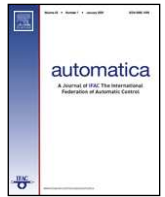
APPENDIX C

ADAPTIVE FEEDFORWARD COMPENSATION ALGORITHMS FOR ACTIVE VIBRATION CONTROL WITH MECHANICAL COUPLING

Authors: Ioan Doré Landau, Marouane Alma, and Tudor-Bogdan Airimițoiaie

Journal: Automatica 47 (2011) 2185–2196

Type of submission: Regular paper



Adaptive feedforward compensation algorithms for active vibration control with mechanical coupling[☆]

Ioan Doré Landau¹, Marouane Alma, Tudor-Bogdan Airimitoie

Control System Department of GIPSA-Lab, BP 46 St Martin d'Hères, 38402, France

ARTICLE INFO

Article history:

Received 13 April 2010
 Received in revised form
 12 January 2011
 Accepted 15 April 2011
 Available online 1 September 2011

Keywords:

Active vibration control
 Adaptive feedforward compensation
 Adaptive control
 Identification in closed loop
 Parameter estimation

ABSTRACT

Adaptive feedforward broadband vibration (or noise) compensation is currently used when a correlated measurement with the disturbance (an image of the disturbance) is available. However in most of the systems there is a "positive" mechanical feedback coupling between the compensator system and the measurement of the image of the disturbance. This may lead to the instability of the system. The paper proposes new algorithms taking into account this coupling effect and provides the corresponding analysis. The algorithms have been applied to an active vibration control (AVC) system and real time results are presented. A theoretical and experimental comparison with some existing algorithms is also provided.

© 2011 Elsevier Ltd. All rights reserved.

1. Introduction

Adaptive feedforward broadband vibration (or noise) compensation is currently used in ANC (Active Noise Control) and AVC (Active Vibration Control) when a correlated measurement with the disturbance (an image of the disturbance) is available (Elliott & Nelson, 1994; Elliott & Sutton, 1996; Kuo & Morgan, 1999; Zeng & de Callafon, 2006). From the user's point of view and taking into account the type of operation of adaptive disturbance compensation systems, one has to consider two modes of operation of the adaptive schemes:

- *Adaptive* operation. The adaptation is performed continuously with a non vanishing adaptation gain.
- *Self-tuning* operation. The adaptation procedure starts either on demand or when the performance is unsatisfactory. A vanishing adaptation gain is used.

At the end of the nineties it was pointed out that in many systems there is a "positive" feedback coupling between the

compensator system and the measurement of the image of the disturbance. The positive feedback may destabilize the system. The system is no longer a pure feedforward compensator. Different solutions have been proposed to overcome this problem (Hu & Linn, 2000; Jacobson, Johnson, Mc Cormick, & Sethares, 2001; Kuo & Morgan, 1999, 1996; Zeng & de Callafon, 2006).

One of the solutions to overcome this problem (Kuo & Morgan, 1999) is to try to compensate for the positive feedback (Fraanje, Verhaegen, & Doelman, 1999; Kuo & Morgan, 1999). However since the compensation can not be perfect, the potential instability of the system still exists (Bai & Lin, 1997; Wang & Ren, 1999).

Another approach discussed in the literature is the analysis in this new context of existing algorithms for adaptive feedforward compensation developed for the case without feedback. An attempt is made in Wang and Ren (1999) where the asymptotic convergence in a stochastic environment of the so called "Filtered-U LMS" (FULMS) algorithm is discussed. Further results on the same direction can be found in Fraanje et al. (1999). The authors use Ljung's ODE method (Ljung & Söderström, 1983) for the case of a scalar vanishing adaptation gain. Unfortunately this is not enough because nothing is said about the stability of the system with respect to initial conditions and when a non vanishing adaptation gain is used (to keep adaptation capabilities). The authors assume that the positive feedback does not destabilize the system.

A stability approach for developing appropriate adaptive algorithms in the context of internal positive feedback is discussed in Jacobson et al. (2001). Unfortunately the results are obtained in the context of very particular assumptions upon the system,

[☆] This paper was not presented at any IFAC meeting. This paper was recommended for publication in revised form by Associate Editor Andrea Serrani under the direction of Editor Miroslav Krstic.

E-mail addresses: ioan-dore.landau@gipsa-lab.grenoble-inp.fr (I.D. Landau), marouane.alma@gipsa-lab.grenoble-inp.fr (M. Alma), tudor-bogdan.airimitoie@gipsa-lab.grenoble-inp.fr (T.-B. Airimitoie).

¹ Tel.: +33 4 7682 6391; fax: +33 4 7682 6382.

namely that the transfer function of the physical compensator system (called “secondary path” – see Section 2) is strictly positive real, that the feedback path and the primary path (the transfer between the disturbance and the residual error) can be described by FIR (finite impulse response) models. Only the case of constant scalar adaption gain is considered. Convergence analysis in the stochastic case with a vanishing adaption gain is not provided.

An interesting approach is adopted in Zeng and de Callafon (2006) using a Youla–Kucera parametrization (Q – parametrization) of the feedforward compensator. A fixed stabilizing feedforward filter is first designed and a recursive self-tuning procedure for estimating the Q filter is implemented using input–output data acquired without the compensator. Details are not given concerning a possible adaptive operation in the presence of the feedforward compensator. A stability analysis of the self-tuning algorithm is not provided.

The problem of the internal positive feedback can be properly addressed in the context of H_∞ or H_2 model based design. This approach has been considered in Bai and Lin (1997), Rotunno and de Callafon (1999) and Alma, Martinez, Landau, and Buche (2011). However the resulting compensator does not have adaptation capabilities and its performance is not necessarily very good. Provided that the high dimension of the resulting compensator can be reduced, it may constitute an “initial” value for the parameters of an adaptive or self-tuning feedforward compensator. In Bai and Lin (1997) it is shown experimentally that the results obtained with the H_∞ approach are better than those obtained using the very popular FULMS adaptation algorithm (for a disturbance with known spectral characteristics). A similar comparison done experimentally in this paper confirms this fact. However this is no more true when comparing the H_∞ design with the adaptive algorithms introduced in the present paper (see Section 7).

It is important to remark that all these contributions (except Alma et al., 2011) have been done in the context of active noise control. While the algorithms for active noise control can be used in active vibration control, one has to take into account the specificity of these latter systems which feature many low damped vibration modes (resonance) and low damped complex zeros (anti-resonance).

The main contributions of the present paper are:

- Development of new real time recursive adaptation algorithms for active vibration control systems with mechanical coupling.
- Stability analysis (in a deterministic context) and convergence analysis (in a stochastic context) of the algorithms.
- Application of the algorithms to an active vibration control system (most of the available control literature deal only with active noise control).
- Comparison of the new algorithms with existing algorithms (both theoretically and experimentally).

While the algorithms have been developed in the context of AVC, they are certainly applicable to ANC systems with acoustic coupling.

The paper is organized as follows. The AVC system on which the algorithms will be tested is presented in Section 2. The system representation and feedforward compensator structure are given in Section 3. The algorithm for adaptive feedforward compensation will be developed in Section 4 and analysed in Section 5. Section 6 will present a comparison with other algorithms. Section 7 will present experimental results obtained on the active vibration control system with the algorithms introduced in this paper as well as with two other adaptive algorithms given in the literature.

2. An active vibration control system using an inertial actuator

Figs. 1 and 2 represent an AVC system using a correlated measurement with the disturbance and an inertial actuator for

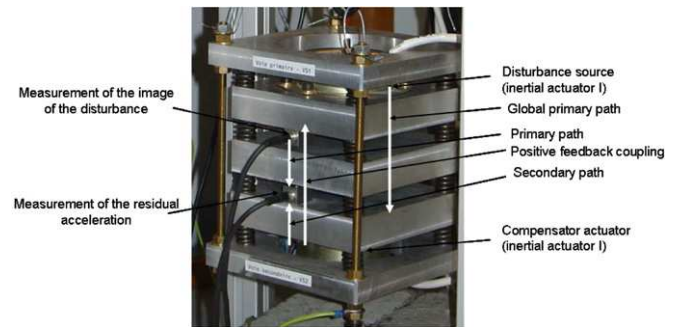


Fig. 1. An AVC system using a feedforward compensation – photo.

reducing the residual acceleration. The structure is representative for a number of situations encountered in practice.

The system consists of three mobile metallic plates (M1, M2, M3) connected by springs. The first and the third plates are also connected by springs to the rigid part of the system formed by two other metallic plates connected themselves rigidly. The upper and lower mobile plates (M1 and M3) are equipped with inertial actuators. The one on the top serves as disturbance generator (inertial actuator 1 in Fig. 2), the one at the bottom serves for disturbance compensation (inertial actuator 2 in Fig. 2). The system is equipped with a measure of the residual acceleration (on plate M3) and a measure of the image of the disturbance made by an accelerometer posed on plate M1. The path between the disturbance (in this case, generated by the inertial actuator on top of the structure), and the residual acceleration is called the *global primary path*. The path between the measure of the image of the disturbance and the residual acceleration (in open loop) is called the *primary path* and the path between the inertial actuator for compensation and the residual acceleration is called the *secondary path*. When the compensator system is active, the actuator acts upon the residual acceleration, but also upon the measurement of the image of the disturbance (a positive feedback). The measured quantity $\hat{u}(t)$ will be the sum of the correlated disturbance measurement $d(t)$ obtained in the absence of the feedforward compensation (see Fig. 3(a)) and of the effect of the actuator used for compensation.

The disturbance is the position of the mobile part of the inertial actuator (see Figs. 1 and 2) located on top of the structure. The input to the compensator system is the position of the mobile part of the inertial actuator located on the bottom of the structure.

The input to the inertial actuators being a position, the global primary path, the secondary path and the positive feedback path have a double differentiator behavior.

The corresponding block diagrams in open loop operation and with the compensator system are shown in Fig. 3(a) and (b), respectively. In Fig. 3(b), $\hat{u}(t)$ denotes the effective output provided by the measurement device and which will serve as input to the adaptive feedforward filter \hat{N} . The output of this filter denoted by $\hat{y}(t)$ is applied to the actuator through an amplifier. The transfer function G (the secondary path) characterizes the dynamics from the output of the filter \hat{N} to the residual acceleration measurement (amplifier + actuator + dynamics of the mechanical system). The transfer function D between $d(t)$ and the measurement of the residual acceleration (in open loop operation) characterizes the primary path.

The coupling between the output of the filter and the measurement $\hat{u}(t)$ through the compensator actuator is denoted by M . As indicated in Fig. 3(b) this coupling is a “positive” feedback. This unwanted coupling raises problems in practice (source of instabilities) and makes the analysis of adaptive (estimation) algorithms more difficult.

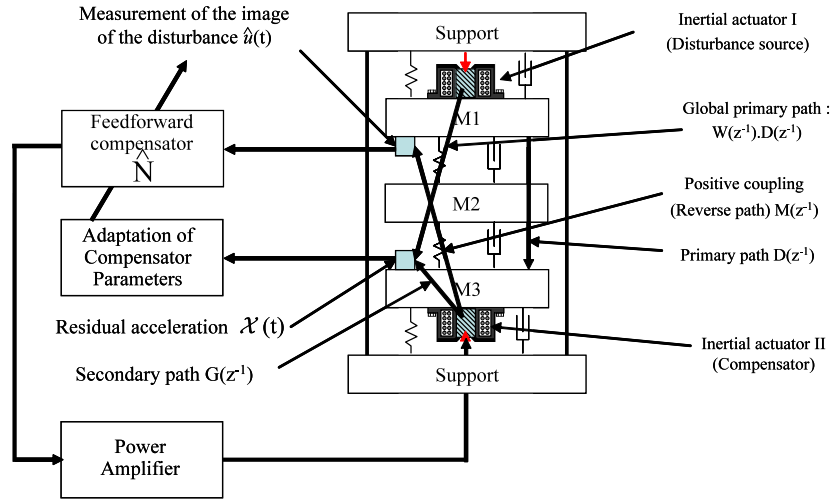


Fig. 2. An AVC system using a feedforward compensation – scheme.

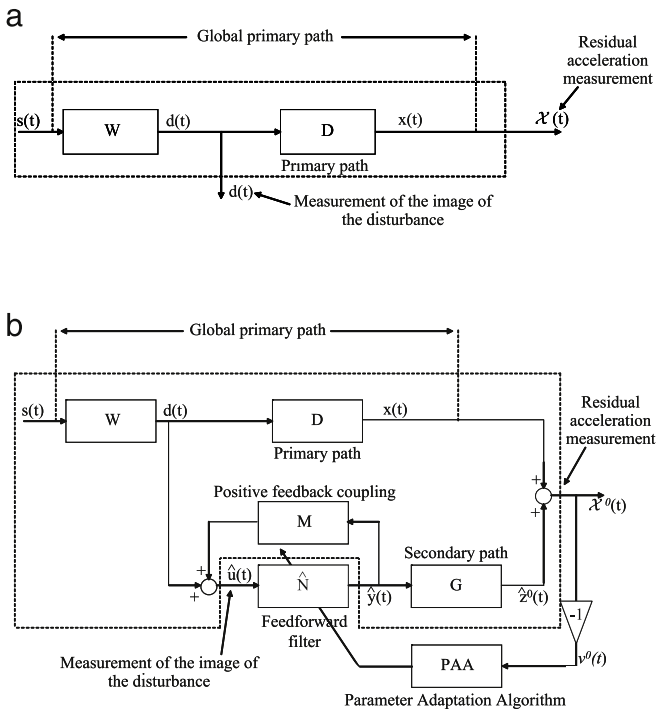


Fig. 3. Feedforward AVC: in open loop (a) and with adaptive feedforward compensator (b).

At this stage it is important to make the following remarks, when the feedforward filter is absent (open loop operation):

- very reliable models for the secondary path and the “positive” feedback path can be identified by applying appropriate excitation on the actuator.
- An estimation of the primary path transfer function can be obtained using the measured $d(t)$ as input and $\chi(t)$ as output (the compensator actuator being at rest).

The objective is to develop stable recursive algorithms for online estimation and adaptation of the parameters of the feedforward filter compensator (which will be denoted \hat{N}) such that the measured residual error (acceleration or force in AVC, noise in ANC) be minimized in the sense of a certain criterion. This has to be done for broadband disturbances $d(t)$ (or $s(t)$) with

unknown and variable spectral characteristics and an unknown primary path model.²

3. Basic equations and notations

The description of the various blocks will be made with respect to Fig. 3.

The primary path is characterized by the asymptotically stable transfer operator³:

$$D(q^{-1}) = \frac{B_D(q^{-1})}{A_D(q^{-1})} \quad (1)$$

where

$$B_D(q^{-1}) = b_1^D q^{-1} + \dots + b_{n_{BD}}^D q^{-n_{BD}} \quad (2)$$

$$A_D(q^{-1}) = 1 + a_1^D q^{-1} + \dots + a_{n_{AD}}^D q^{-n_{AD}}. \quad (3)$$

The unmeasurable value of the output of the primary path (when the compensation is active) is denoted $x(t)$.

The secondary path is characterized by the asymptotically stable transfer operator:

$$G(q^{-1}) = \frac{B_G(q^{-1})}{A_G(q^{-1})} \quad (4)$$

where:

$$B_G(q^{-1}) = b_1^G q^{-1} + \dots + b_{n_{BG}}^G q^{-n_{BG}} = q^{-1} B_G^*(q^{-1}) \quad (5)$$

$$A_G(q^{-1}) = 1 + a_1^G q^{-1} + \dots + a_{n_{AG}}^G q^{-n_{AG}}. \quad (6)$$

The positive feedback coupling is characterized by the asymptotically stable transfer operator:

$$M(q^{-1}) = \frac{B_M(q^{-1})}{A_M(q^{-1})} \quad (7)$$

² Variations of the unknown model W , the transfer function between the disturbance $s(t)$ and $d(t)$ are equivalent to variations of the spectral characteristics of $s(t)$.

³ The complex variable z^{-1} will be used for characterizing the system's behavior in the frequency domain and the delay operator q^{-1} will be used for describing the system's behavior in the time domain.

where:

$$B_M(q^{-1}) = b_1^M q^{-1} + \dots + b_{n_{B_M}}^M q^{-n_{B_M}} = q^{-1} B_M^*(q^{-1}) \quad (8)$$

$$A_M(q^{-1}) = 1 + a_1^M q^{-1} + \dots + a_{n_{A_M}}^M q^{-n_{A_M}}. \quad (9)$$

Both B_G and B_M have a one step discretization delay. The identified models of the secondary path and of the positive feedback coupling will be denoted \hat{G} and \hat{M} , respectively.

The optimal feedforward filter (unknown) is defined by:

$$N(q^{-1}) = \frac{R(q^{-1})}{S(q^{-1})} \quad (10)$$

where:

$$R(q^{-1}) = r_0 + r_1 q^{-1} + \dots + r_{n_R} q^{-n_R} \quad (11)$$

$$S(q^{-1}) = 1 + s_1 q^{-1} + \dots + s_{n_S} q^{-n_S} = 1 + q^{-1} S^*(q^{-1}). \quad (12)$$

The estimated filter is denoted by $\hat{N}(q^{-1})$ or $\hat{N}(\hat{\theta}, q^{-1})$ when it is a linear filter with constant coefficients or $\hat{N}(t, q^{-1})$ during estimation (adaptation) of its parameters.

The input of the feedforward filter is denoted by $\hat{u}(t)$ and it corresponds to the measurement provided by the primary transducer (force or acceleration transducer in AVC or a microphone in ANC). In the absence of the compensation loop (open loop operation) $\hat{u}(t) = d(t)$. The “a posteriori” output of the feedforward filter (which is the control signal applied to the secondary path) is denoted by $\hat{y}(t+1) = \hat{y}(t+1 | \hat{\theta}(t+1))$. The “a priori” output of the estimated feedforward filter is given by:

$$\begin{aligned} \hat{y}^0(t+1) &= \hat{y}(t+1 | \hat{\theta}(t)) \\ &= -\hat{S}^*(t, q^{-1}) \hat{y}(t) + \hat{R}(t, q^{-1}) \hat{u}(t+1) \\ &= \hat{\theta}^T(t) \phi(t) = [\hat{\theta}_S^T(t), \hat{\theta}_R^T(t)] \begin{bmatrix} \phi_y(t) \\ \phi_u(t) \end{bmatrix} \end{aligned} \quad (13)$$

where

$$\hat{\theta}^T(t) = [\hat{s}_1(t) \dots \hat{s}_{n_S}(t), \hat{r}_0(t) \dots \hat{r}_{n_R}(t)] = [\hat{\theta}_S^T(t), \hat{\theta}_R^T(t)] \quad (14)$$

$$\begin{aligned} \phi^T(t) &= [-\hat{y}(t) \dots -\hat{y}(t-n_S+1), \hat{u}(t+1), \\ &\quad \hat{u}(t) \dots \hat{u}(t-n_R+1)] \\ &= [\phi_y^T(t), \phi_u^T(t)] \end{aligned} \quad (15)$$

and $\hat{y}(t)$, $\hat{y}(t-1) \dots$ are the “a posteriori” outputs of the feedforward filter generated by:

$$\hat{y}(t+1) = \hat{y}(t+1 | \hat{\theta}(t+1)) = \hat{\theta}^T(t+1) \phi(t) \quad (16)$$

while $\hat{u}(t+1)$, $\hat{u}(t) \dots$ are the measurements provided by the primary transducer.⁴ The unmeasurable “a priori” output of the secondary path will be denoted $\hat{z}^0(t+1)$.

$$\hat{z}^0(t+1) = \hat{z}(t+1 | \hat{\theta}(t)) = \frac{B_G^*(q^{-1})}{A_G(q^{-1})} \hat{y}(t). \quad (17)$$

The “a posteriori” unmeasurable value of the output of the secondary path is denoted by:

$$\hat{z}(t+1) = \hat{z}(t+1 | \hat{\theta}(t+1)). \quad (18)$$

The measured primary signal (called also reference) satisfies the following equation:

$$\hat{u}(t+1) = d(t+1) + \frac{B_M^*(q^{-1})}{A_M(q^{-1})} \hat{y}(t). \quad (19)$$

The measured residual error satisfies the following equation:

$$\chi^0(t+1) = \chi(t+1 | \hat{\theta}(t)) = \hat{z}^0(t+1) + x(t+1). \quad (20)$$

The “a priori” adaptation error is defined as:

$$v^0(t+1) = -\chi^0(t+1) = -x(t+1) - \hat{z}^0(t+1). \quad (21)$$

The “a posteriori” adaptation (residual) error (which is computed) will be given by:

$$v(t+1) = v(t+1 | \hat{\theta}(t+1)) = -x(t+1) - \hat{z}(t+1). \quad (22)$$

When using an estimated filter \hat{N} with constant parameters: $\hat{y}^0(t) = \hat{y}(t)$, $\hat{z}^0(t) = \hat{z}(t)$ and $v^0(t) = v(t)$.

4. Development of the algorithms

The algorithms for adaptive feedforward compensation will be developed under the following hypotheses:

(1) H1 – The signal $d(t)$ is bounded i.e.

$$|d(t)| \leq \alpha \quad \forall t \quad (0 \leq \alpha < \infty) \quad (23)$$

(which is equivalently to say that $s(t)$ is bounded and $W(q^{-1})$ in Fig. 3 is asymptotically stable).

(2) H2 – Perfect matching condition. There exists a filter $N(q^{-1})$ of finite dimension such that⁵:

$$D = -\frac{N}{(1-NM)} G \quad (24)$$

and the characteristic polynomial of the “internal” feedback loop:

$$P(z^{-1}) = A_M(z^{-1})S(z^{-1}) - B_M(z^{-1})R(z^{-1}) \quad (25)$$

is a Hurwitz polynomial.

(3) H3 – The effect of the measurement noise upon the measured residual error is neglected (deterministic context).

(4) H4 – The primary path model $D(z^{-1})$ is unknown and constant.

Once the algorithms will be developed under these hypotheses, hypotheses (2) and (3) will be removed and the algorithms will be analyzed in this modified context.

A first step in the development of the algorithms is to establish a relation between the errors on the estimation of the parameters of the feedforward filter and the measured residual acceleration. This is summarized in the following lemma.

Lemma 4.1. *Under hypotheses H1 through H4, for the system described by Eqs. (1) through (22) using a feedforward compensator \hat{N} with constant parameters, one has:*

$$v(t+1) = \frac{A_M(q^{-1})G(q^{-1})}{P(q^{-1})} [\theta - \hat{\theta}]^T \phi(t) \quad (26)$$

where

$$\theta^T = [s_1, \dots, s_{n_S}, r_0, r_1, \dots, r_{n_R}] = [\theta_S^T, \theta_R^T] \quad (27)$$

is the vector of parameters of the optimal filter N assuring perfect matching

$$\hat{\theta}^T = [\hat{s}_1 \dots \hat{s}_{n_S}, \hat{r}_0 \dots \hat{r}_{n_R}] = [\hat{\theta}_S^T, \hat{\theta}_R^T] \quad (28)$$

is the vector of constant estimated parameters of \hat{N} and $\phi(t)$ and $\hat{u}(t+1)$ are given by (15) and (19).

The proof of this lemma is given in Appendix A.

⁴ $\hat{u}(t+1)$ is available before adaptation of parameters starts at $t+1$.

⁵ In many cases, the argument q^{-1} or z^{-1} will be dropped out.

Filtering the vector $\phi(t)$ through an asymptotically stable filter $L(q^{-1}) = \frac{B_L}{A_L}$, Eq. (26) for $\hat{\theta} = \text{constant}$ becomes:

$$v(t+1) = \frac{A_M(q^{-1})G(q^{-1})}{P(q^{-1})L(q^{-1})} [\theta - \hat{\theta}]^T \phi_f(t) \quad (29)$$

with:

$$\phi_f(t) = L(q^{-1})\phi(t). \quad (30)$$

Eq. (29) will be used to develop the adaptation algorithms neglecting for the moment the non-commutativity of the operators when $\hat{\theta}$ is time varying (however an exact algorithm can be derived in such cases – see Landau, Lozano, and Saad (1997)).

Replacing the fixed estimated parameters by the current estimated parameters, Eq. (29) becomes the equation or the a-posteriori residual error $v(t+1)$ (which is computed):

$$v(t+1) = \frac{A_M(q^{-1})G(q^{-1})}{P(q^{-1})L(q^{-1})} [\theta - \hat{\theta}(t+1)]^T \phi_f(t). \quad (31)$$

Eq. (31) has the standard form for an a-posteriori adaptation error (Landau et al., 1997), which immediately suggests to use the following parameter adaptation algorithm:

$$\hat{\theta}(t+1) = \hat{\theta}(t) + F(t)\psi(t)v(t+1); \quad (32)$$

$$v(t+1) = \frac{v^0(t+1)}{1 + \psi^T(t)F(t)\psi(t)}; \quad (33)$$

$$F(t+1) = \frac{1}{\lambda_1(t)} \left[F(t) - \frac{F(t)\psi(t)\psi^T(t)F(t)}{\lambda_1(t) + \psi^T(t)F(t)\psi(t)} \right] \quad (34)$$

$$1 \geq \lambda_1(t) > 0; \quad 0 \leq \lambda_2(t) < 2; \quad F(0) > 0 \quad (35)$$

$$\psi(t) = \phi_f(t) \quad (36)$$

where $\lambda_1(t)$ and $\lambda_2(t)$ allow to obtain various profiles for the matrix adaptation gain $F(t)$ (see Section 7 and Landau et al., 1997). By taking $\lambda_2(t) \equiv 0$ and $\lambda_1(t) \equiv 1$, one gets a constant adaptation gain matrix (and choosing $F = \gamma I$, $\gamma > 0$ one gets a scalar adaptation gain).

Three choices for the filter L will be considered, leading to three different algorithms: Algorithm I: $L = G$.

Algorithm II: $L = \hat{G}$.

Algorithm III:

$$L = \frac{\hat{A}_M \hat{G}}{\hat{P}} \quad (37)$$

where:

$$\hat{P} = \hat{A}_M \hat{S} - \hat{B}_M \hat{R} \quad (38)$$

is an estimation of the characteristic polynomial of the internal feedback loop computed on the basis of available estimates of the parameters of the filter \hat{N} .

For Algorithm III several options for updating \hat{P} can be considered:

- Run Algorithm II for a certain time to get estimates of \hat{R} and \hat{S} .
- Run a simulation (using the identified models).
- Update \hat{P} at each sampling instant or from time to time using Algorithm III (after a short initialization horizon using Algorithm II).

The following procedure is applied at each sampling time for adaptive or self-tuning operation:

- (1) Get the measured image of the disturbance $\hat{u}(t+1)$, the measured residual error $\chi^0(t+1)$ and compute $v^0(t+1) = -\chi^0(t+1)$
- (2) Compute $\phi(t)$ and $\phi_f(t)$ using (15) and (30)

- (3) Estimate the parameter vector $\hat{\theta}(t+1)$ using the parametric adaptation algorithm (32) through (36).
- (4) Compute (using (16)) and apply the control.

5. Analysis of the algorithms

5.1. The deterministic case – perfect matching

For algorithms I–III the equation for the a-posteriori adaptation error has the form:

$$v(t+1) = H(q^{-1})[\theta - \hat{\theta}(t+1)]^T \psi(t) \quad (39)$$

where:

$$H(q^{-1}) = \frac{A_M(q^{-1})G(q^{-1})}{P(q^{-1})L(q^{-1})}, \quad \psi = \phi_f. \quad (40)$$

Neglecting the non-commutativity of time varying operators, one has the following result.

Lemma 5.1. Assuming that Eq. (39) represents the evolution of the a posteriori adaptation error and that the parameter adaptation algorithm (32) through (36) is used, one has:

$$\lim_{t \rightarrow \infty} v(t+1) = 0 \quad (41)$$

$$\lim_{t \rightarrow \infty} \frac{[v^0(t+1)]^2}{1 + \psi^T(t)F(t)\psi(t)} = 0 \quad (42)$$

$$\|\psi(t)\| \text{ is bounded} \quad (43)$$

$$\lim_{t \rightarrow \infty} v^0(t+1) = 0 \quad (44)$$

for any initial conditions $\hat{\theta}(0)$, $v^0(0)$, $F(0)$, provided that:

$$H'(z^{-1}) = H(z^{-1}) - \frac{\lambda_2}{2}, \quad \max_t [\lambda_2(t)] \leq \lambda_2 < 2 \quad (45)$$

is a strictly positive real transfer function.

Proof. Using Theorem 3.3.2 from Landau et al. (1997), under the condition (45), (41) and (42) hold.

However in order to show that $v^0(t+1)$ goes to zero one has to show first that the components of the observation vector are bounded. The result (42) suggests to use Goodwin's "bounded growth" lemma (Landau, Karimi, and Constantinescu (2001a) and lemma 11.2.1 in Landau et al. (1997)).

Provided that one has:

$$|\psi^T(t)F(t)\psi(t)|^{\frac{1}{2}} \leq C_1 + C_2 \cdot \max_{0 \leq k \leq t+1} |v^0(k)| \quad (46)$$

$$0 < C_1 < \infty \quad 0 < C_2 < \infty \quad F(t) > 0$$

$\|\psi(t)\|$ will be bounded. So it will be shown that (46) holds for Algorithm I (for algorithms II and III the proof is similar). From (22) one has:

$$-\hat{z}(t) = v(t) + x(t). \quad (47)$$

Since $x(t)$ is bounded (output of an asymptotically stable system with bounded input), one has:

$$\begin{aligned} |-\hat{y}_f(t)| &= | -G\hat{y}(t) | = | -\hat{z}(t) | \leq C_3 + C_4 \cdot \max_{0 \leq k \leq t+1} |v(k)| \\ &\leq C'_3 + C'_4 \cdot \max_{0 \leq k \leq t+1} |v^0(k)| \end{aligned} \quad (48)$$

$$0 < C_3, C_4, C'_3, C'_4 < \infty \quad (49)$$

since $|v(t)| \leq |v^0(t)|$ for all t . Filtering both sides of Eq. (19) by $G(q^{-1})$ one gets in the adaptive case:

$$\hat{u}_f(t) = \frac{B_G}{A_G} d(t) + \frac{B_M}{A_M} \hat{y}_f(t). \quad (50)$$

Since A_G and A_M are Hurwitz polynomials and $d(t)$ is bounded, it results that:

$$|\hat{u}_j(t)| \leq C_5 + C_6 \cdot \max_{0 \leq k \leq t+1} |v^0(k)|; \quad 0 < C_5, C_6 < \infty. \quad (51)$$

Therefore (46) holds, which implies that $\psi(t)$ is bounded and one can conclude that (44) also holds. End of the proof. \square

It is interesting to remark that for Algorithm III taking into account Eq. (37), the stability condition is that:

$$\frac{A_M}{\hat{A}_M} \cdot \frac{\hat{P}}{P} \cdot \frac{G}{\hat{G}} - \frac{\lambda_2}{2} \quad (52)$$

should be a strictly positive real transfer function. However this condition can be re-written for $\lambda_2 = 1$ as (Ljung, 1977; Ljung & Söderström, 1983):

$$\left| \left(\frac{A_M}{\hat{A}_M} \cdot \frac{\hat{P}}{P} \cdot \frac{G}{\hat{G}} \right)^{-1} - 1 \right| < 1 \quad (53)$$

for all ω . This roughly means that it always holds provided that the estimates of A_M , P , and G are close to the true values (i.e. $H(e^{j\omega})$ in this case is close to a unit transfer function).

5.2. The stochastic case – perfect matching

There are two sources of measurement noise, one acting on the primary transducer which gives the correlated measurement with the disturbance and the second acting on the measurement of the residual error (force, acceleration). For the primary transducer the effect of the measurement noise is negligible since the signal to noise ratio is very high. The situation is different for the residual error where the effect of the noise can not be neglected.

In the presence of the measurement noise (w), the equation of the a-posteriori residual error becomes:

$$v(t+1) = H(q^{-1})[\theta - \hat{\theta}(t+1)]^T \psi(t) + w(t+1). \quad (54)$$

The O.D.E. method (Ljung, 1977; Ljung & Söderström, 1983) can be used to analyze the asymptotic behavior of the algorithm in the presence of noise. Taking into account the form of Eq. (54), one can directly use Theorem 4.2.1 of Landau et al. (1997) or Theorem B1 of Landau and Karimi (1997).

The following assumptions will be made:

- (1) $\lambda_1(t) = 1$ and $\lambda_2(t) = \lambda_2 > 0$
- (2) $\hat{\theta}(t)$ generated by the algorithm belongs infinitely often to the domain D_S :

$$D_S \triangleq \{\hat{\theta} : \hat{P}(z^{-1}) = 0 \Rightarrow |z| < 1\}$$

for which stationary processes:

$$\psi(t, \hat{\theta}) \triangleq \psi(t)|_{\hat{\theta}(t)=\hat{\theta}=\text{const}}$$

$$\chi(t, \hat{\theta}) = \chi(t)|_{\hat{\theta}(t)=\hat{\theta}=\text{const}}$$

can be defined.

- (3) $w(t)$ is a zero mean stochastic process with finite moments and is independent of the sequence $d(t)$.

From (54) for $\hat{\theta}(t) = \hat{\theta}$, one gets:

$$v(t+1, \hat{\theta}) = H(q^{-1})[\theta - \hat{\theta}]^T \psi(t, \hat{\theta}) + w(t+1, \hat{\theta}). \quad (55)$$

Since $\psi(t, \hat{\theta})$ depends upon $d(t)$ one concludes that $\psi(t, \hat{\theta})$ and $w(t+1, \hat{\theta})$ are independent. Therefore using Theorem 4.2.1 from Landau et al. (1997) it results that if:

$$H'(z^{-1}) = \frac{A_M(z^{-1})G(z^{-1})}{P(z^{-1})L(z^{-1})} - \frac{\lambda_2}{2} \quad (56)$$

is a strictly positive real transfer function, one has: $\text{Prob}\{\lim_{t \rightarrow \infty} \hat{\theta}(t) \in D_C\} = 1$ where: $D_C = \{\hat{\theta} : \psi^T(t, \hat{\theta})(\theta - \hat{\theta}) = 0\}$.

If furthermore $\psi^T(t, \hat{\theta})(\theta - \hat{\theta}) = 0$ has a unique solution (richness condition), the condition that $H'(z^{-1})$ be strictly positive real implies that: $\text{Prob}\{\lim_{t \rightarrow \infty} \hat{\theta}(t) = \theta\} = 1$.

5.3. The case of non-perfect matching

If $\hat{N}(t, q^{-1})$ does not have the appropriate dimension there is no chance to satisfy the perfect matching condition.

Two questions are of interest in this case:

- (1) The boundedness of the residual error
- (2) The bias distribution in the frequency domain.

5.3.1. Boundedness of the residual error

For analyzing the boundedness of the residual error, results from Landau and Karimi (1997); Landau et al. (2001a), can be used. The following assumptions are made:

- (1) There exists a reduced order filter \hat{N} characterized by the unknown polynomials \hat{S} (of order n_S) and \hat{R} (of order n_R), for which the closed loop formed by \hat{N} and M is asymptotically stable. i.e. $A_M \hat{S} - B_M \hat{R}$ is a Hurwitz polynomial.
- (2) The output of the optimal filter satisfying the matching condition can be expressed as:

$$\hat{y}(t+1) = -[\hat{S}^*(q^{-1})\hat{y}(t) - \hat{R}(q^{-1})\hat{u}(t+1) + \eta(t+1)] \quad (57)$$

where $\eta(t+1)$ is a norm bounded signal.

Using the results of Landau and Karimi (1997) (Theorem 4.1 pp. 1505–1506) and assuming that $d(t)$ is norm bounded, it can be shown that all the signals are norm bounded under the passivity condition (45), where P is computed now with the reduced order estimated filter.

5.3.2. Bias distribution

Using Parseval's relation, the asymptotic bias distribution of the estimated parameters in the frequency domain can be obtained starting from the expression of $v(t)$, by taking into account that the algorithm minimizes (almost) a criterion of the form $\lim_{N \rightarrow \infty} \frac{1}{N} \sum_{t=1}^N v^2(t)$.

The bias distribution (for Algorithm III) will be given by:

$$\hat{\theta}^* = \arg \min_{\hat{\theta}} \int_{-\pi}^{\pi} \left[\left| D(j\omega) - \frac{\hat{N}(j\omega)G(j\omega)}{1 - \hat{N}(j\omega)M(j\omega)} \right|^2 \phi_d(\omega) + \phi_w(\omega) \right] d\omega \quad (58)$$

where ϕ_d and ϕ_w are the spectral densities of the disturbance $d(t)$ and of the measurement noise. Taking into account Eq. (24), one obtains:

$$\hat{\theta}^* = \arg \min_{\hat{\theta}} \int_{-\pi}^{\pi} [|S_{NM}|^2 |N - \hat{N}|^2 |S_{NM}|^2 |G|^2 \phi_d(\omega) + \phi_w(\omega)] d\omega \quad (59)$$

where S_{NM} and S_{NM} are the output sensitivity functions of the internal closed loop for N and respectively \hat{N} : $S_{NM} = \frac{1}{1-NM}$; $S_{NM} = \frac{1}{1-\hat{N}M}$.

From (58) and (59) one concludes that a good approximation of N will be obtained in the frequency region where ϕ_d is significant and where G has a high gain (usually G should have high gain in the frequency region where ϕ_d is significant in order to counteract the effect of $d(t)$). However the quality of the estimated \hat{N} will be affected also by the output sensitivity functions of the internal closed loop $N - M$.

5.4. Relaxing the positive real condition

It is possible to relax the strictly positive real (S.P.R.) conditions taking into account that:

- (1) The disturbance (input to the system) is a broadband signal.
- (2) Most of the adaptation algorithms work with a low adaptation gain.

Under these two assumptions, the behavior of the algorithm can be well described by the “averaging theory” developed in Anderson et al. (1986) and Ljung and Söderström (1983) (see also Landau et al., 1997).

When using the averaging approach, the basic assumption of a slow adaptation holds for small adaptation gains (constant and scalar in Anderson et al. (1986) i.e. $\lambda_2(t) \equiv 0$, $\lambda_1(t) = 1$; matrix and time decreasing asymptotically in Ljung and Söderström (1983) and Landau et al. (1997) i.e. $\lim_{t \rightarrow \infty} \lambda_1(t) = 1$, $\lambda_2(t) = \lambda_2 > 0$ or scalar and time decreasing).

In the context of averaging, the basic condition for stability is that:

$$\lim_{N \rightarrow \infty} \frac{1}{N} \sum_{t=1}^N \psi(t) H'(q^{-1}) \psi^T(t) = \frac{1}{2} \int_{-\pi}^{\pi} \psi(e^{j\omega}) [H'(e^{j\omega}) + H'(e^{-j\omega})] \psi^T(e^{-j\omega}) d\omega > 0 \quad (60)$$

be a positive definite matrix ($\psi(e^{j\omega})$ is the Fourier transform of $\psi(t)$).

One can view (60) as the weighted energy of the observation vector ψ . Of course the S.P.R. sufficient condition upon $H'(z^{-1})$ (see Eq. (45)) allows to satisfy this condition. However in the averaging context it is only necessary that (60) is true which allows that H' be non positive real in a limited frequency band. Expression (60) can be re-written as follows:

$$\begin{aligned} & \int_{-\pi}^{\pi} \psi(e^{j\omega}) [H' + H'^*] \psi^T(e^{-j\omega}) d\omega \\ &= \sum_{i=1}^r \int_{\alpha_i}^{\alpha_i + \Delta_i} \psi(e^{j\omega}) [H' + H'^*] \psi^T(e^{-j\omega}) d\omega \\ & \quad - \sum_{j=1}^p \int_{\beta_j}^{\beta_j + \Delta_j} \psi(e^{j\omega}) [\bar{H}' + \bar{H}'^*] \psi^T(e^{-j\omega}) d\omega > 0 \end{aligned} \quad (61)$$

where H' is strictly positive real in the frequency intervals $[\alpha_i, \alpha_i + \Delta_i]$ and $\bar{H}' = -H'$ is positive real in the frequencies intervals $[\beta_j, \beta_j + \Delta_j]$ (H'^* denotes the complex conjugate of H'). The conclusion is that H' does not need to be S.P.R. It is enough that the “positive” weighted energy exceeds the “negative” weighted energy. This explains why algorithms I and II will work in practice in most of the cases. It is however important to remark that if the disturbance is a single sinusoid (which violates the hypothesis of broadband disturbance) located in the frequency region where H' is not S.P.R, the algorithm may diverge (see Anderson et al., 1986; Ljung & Söderström, 1983).

Without doubt, the best approach for relaxing the S.P.R. conditions, is to use Algorithm III (given in Eq. (37)) instead of Algorithm II. This is motivated by Eqs. (52) and (53). As it will be shown experimentally, this algorithm gives the best results.

6. Comparison with other algorithms

The algorithms developed in this paper with matrix and scalar adaptation gain for IIR feedforward compensators will be compared with the algorithm of Jacobson et al. (2001) and the FULMS (Wang & Ren, 1999) algorithm. These two references

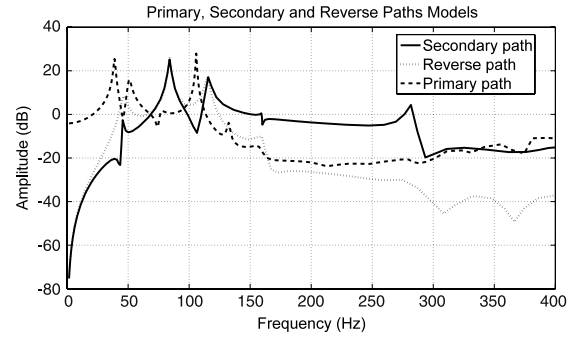


Fig. 4. Frequency characteristics of the primary, secondary and reverse paths.

consider the same type of compensator and take into account the internal positive feedback.⁶

Table 1 summarizes the structure of the algorithms, the stability and convergence conditions as well as the hypotheses upon the structure of the system. The notations adopted in this paper were used to describe the other algorithms. A table in Appendix B gives the equivalence of the notations between the present paper and the notations used in Jacobson et al. (2001) and Wang and Ren (1999). It was not possible to give in Table 1 all the options for the adaptation gain. However basic characteristics for adaptive operation (non vanishing adaptation gain) and self-tuning operation (vanishing adaptation gain) have been provided.⁷

7. Experimental results

A detailed view of the mechanical structure used for the experiments has been given in Fig. 1 and the description of the system has been given in Section 2.

7.1. System identification

The models of the plant may be obtained by parametric system identification with the same methodology used for an active suspension in Landau et al. (2001a) and Landau, Constantinescu, Loubat, Rey, and Franco (2001b).

The secondary path between the control signal $\hat{y}(t)$ and the output $\chi(t)$ has been identified in the absence of the feedforward compensator. The excitation signal was a PRBS generated with a shift register with $N = 10$ and a frequency divider of $p = 4$. The estimated orders of the model are $n_{B_C} = 15$, $n_{A_C} = 13$. The best results in terms of model validation were obtained with the *Recursive Extended Least Square* method. The frequency characteristic of the secondary path is shown in Fig. 4 (solid). There are several very low damped vibration modes in the secondary path. The first vibration mode is at 46.56 Hz with a damping of 0.013, the second at 83.9 Hz with a damping of 0.011, the third one at 116 Hz with a damping of 0.014. There is also a pair of low damped complex zeros at 108 Hz with a damping of 0.021. There are two zeros on the unit circle corresponding to the double differentiator behavior.

The reverse path $M(q^{-1})$ has been identified in the absence of the feedforward compensator with the same PRBS excitation ($N = 10$ and a frequency divider of $p = 4$) applied at $\hat{y}(t)$ and measuring the output signal of the primary transducer $\hat{u}(t)$. The estimated orders of the model are $n_{B_M} = 15$, $n_{A_M} = 13$. The frequency characteristic of the reverse path is presented in Fig. 4

⁶ Algorithms dedicated to FIR feedforward compensators have not been considered because they are particular cases of the algorithms for IIR compensators.

⁷ Convergence analysis can be applied only for vanishing adaptation gains.

Table 1
Comparison of algorithms for adaptive feedforward compensation in AVC with mechanical coupling.

	Paper (matrix gain)	Paper (scalar gain)	Jacobson–Johnson (scalar gain)	FULMS (scalar gain)
$\hat{\theta}(t+1) =$	$\hat{\theta}(t) + F(t)\psi(t) \frac{v^0(t+1)}{1+\psi^T(t)F(t)\psi(t)}$	$\hat{\theta}(t) + \gamma(t)\psi(t) \frac{v^0(t+1)}{1+\gamma(t)\psi^T(t)\psi(t)}$	$\hat{\theta}(t) + \mu\gamma\psi(t) \frac{v^0(t+1)}{1+\gamma\psi^T(t)\psi(t)}$	$\hat{\theta}(t) + \gamma(t)\psi(t-1)v^0(t)$
Adapt. gain	$F(t+1)^{-1} = \lambda_1(t)F(t) + \lambda_2(t)\psi(t)\psi^T(t)$ $0 \leq \lambda_1(t) < 1$, $0 \leq \lambda_2(t) < 2$, $F(0) > 0$	$\gamma(t) > 0$	$\gamma > 0$, $0 < \mu \leq 1$	$\gamma(t) > 0$
Adaptive	Decr. gain and const. trace	$\gamma(t) = \gamma = const$	$\gamma > 0$	$\gamma(t) = \gamma = const$
Self tuning	$\lambda_2 = const$, $\lim_{t \rightarrow \infty} \lambda_1(t) = 1$	$\sum_{t=1}^{\infty} \gamma(t) = \infty$, $\lim_{t \rightarrow \infty} \gamma(t) = 0$	Does not apply	$\sum_{t=1}^{\infty} \gamma(t) = \infty$, $\lim_{t \rightarrow \infty} \gamma(t) = 0$
$\phi^T(t) =$	$[-\hat{y}(t), \dots, \hat{u}(t+1), \dots]$	$[-\hat{y}(t), \dots, \hat{u}(t+1), \dots]$	$[-\hat{y}(t), \dots, \hat{u}(t+1), \dots]$	$[-\hat{y}(t), \dots, \hat{u}(t+1), \dots]$
$\psi(t) =$	$L\phi(t)L_2 = \hat{G}$; $L_3 = \frac{\hat{A}_M}{P}\hat{G}\hat{P} = \hat{A}_M\hat{S} - \hat{B}_M\hat{R}$	$L\phi(t)L_2 = \hat{G}$; $L_3 = \frac{\hat{A}_M}{P}\hat{G}\hat{P} = \hat{A}_M\hat{S} - \hat{B}_M\hat{R}$	$\phi(t)$	$L\phi(t)L = \hat{G}$
$G = \frac{B_G}{A_G}$	$B_G = b_{1G}z^{-1} + b_{2G}z^{-2} + \dots$ $A_G = 1 + a_{1G}z^{-1} + a_{2G}z^{-2} + \dots$	$B_G = b_{1G}z^{-1} + b_{2G}z^{-2} + \dots$ $A_G = 1 + a_{1G}z^{-1} + \dots$	$B_G = 1$, $A_G = 1$ or $G = SPR$	$B_G = b_{1G}z^{-1} + b_{2G}z^{-2} + \dots$ $A_G = 1 + a_{1G}z^{-1} + \dots$
$M = \frac{B_M}{A_M}$	$B_M = b_{1M}z^{-1} + b_{2M}z^{-2} + \dots$ $A_M = 1 + a_{1M}z^{-1} + a_{2M}z^{-2} + \dots$	$B_M = b_{1M}z^{-1} + b_{2M}z^{-2} + \dots$ $A_M = 1 + a_{1M}z^{-1} + \dots$	$B_M = b_{1M}z^{-1} + b_{2M}z^{-2} + \dots$ $A_M = 1$	$B_M = b_{1M}z^{-1} + b_{2M}z^{-2} + \dots$ $A_M = 1$
$D = \frac{B_D}{A_D}$	$B_D = b_{1D}z^{-1} + b_{2D}z^{-2} + \dots$ $A_D = 1 + a_{1D}z^{-1} + a_{2D}z^{-2} + \dots$	$B_D = b_{1D}z^{-1} + b_{2D}z^{-2} + \dots$ $A_D = 1 + a_{1D}z^{-1} + \dots$	$B_D = b_{1D}z^{-1} + b_{2D}z^{-2} + \dots$ $A_D = 1$	$B_D = b_{1D}z^{-1} + b_{2D}z^{-2} + \dots$ $A_D = 1 + a_{1D}z^{-1} + \dots$
Stability Condition	$\frac{A_M G}{P L} - \frac{\lambda}{2} = SPR$ $\lambda = \max \lambda_2(t)$	$\frac{A_M G}{P L} = SPR$	$G = SPR$	Unknown
Conv. Condition	$\frac{A_M G}{P L} - \frac{\lambda}{2} = SPR$ $\lambda = \lambda_2$	$\frac{A_M G}{P L} = SPR$	Does not Apply	$\frac{G}{P G} = SPR$

(dotted). There are several very low damped vibration modes at 46.20 Hz with a damping of 0.045, at 83.9 Hz with a damping of 0.01, at 115 Hz with a damping of 0.014 and some additional modes in high frequencies. There are two zeros on the unit circle corresponding to the double differentiator behavior.

The primary path has been identified in the absence of the feedforward compensator using $d(t)$ as an input and measuring $\chi(t)$. The disturbance $s(t)$ was a PRBS sequence ($N = 10$, frequency divider $p = 2$). The estimated orders of the model are $n_{B_D} = 26$, $n_{A_D} = 26$. The frequency characteristic is presented in Fig. 4 (dashed) and may serve for simulations and detailed performance evaluation. Note that the primary path features a strong resonance at 108 Hz, exactly where the secondary path has a pair of low damped complex zeros (almost no gain). Therefore one can not expect good attenuation around this frequency.

7.2. Broadband disturbance rejection using matrix adaptation gain

The performance of the system for rejecting broadband disturbances will be illustrated using the adaptive feedforward scheme. The adaptive filter structure for most of the experiments has been $n_R = 9$, $n_S = 10$ (total of 20 parameters) and this complexity does not allow to verify the “perfect matching condition” (not enough parameters). The influence of the number of parameters upon the performance of the system has been also investigated (up to 40 parameters).

A PRBS excitation on the global primary path will be considered as the disturbance. The corresponding spectral densities of $d(t)$ in open loop and of $\hat{u}(t)$ when feedforward compensation is active are shown in Fig. 5 (the effect of the mechanical feedback is significant).

For the *adaptive* operation, algorithms II and III have been used with decreasing adaptation gain ($\lambda_1(t) = 1$, $\lambda_2(t) = 1$)

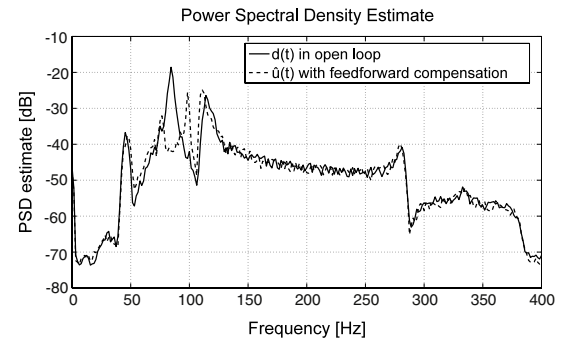


Fig. 5. Spectral densities of the image of the disturbance in open loop $d(t)$ and in feedforward compensation scheme $\hat{u}(t)$ (experimental).

combined with a *constant trace* adaptation gain.⁸ Once the trace of the adaptation gain is below a given value, one switches to the constant trace gain updating. The trace of the adaptation gain $F(t)$ is kept constant by modifying appropriately $\lambda_1(t)$ for a fixed ratio $\alpha = \lambda_1(t)/\lambda_2(t)$. The corresponding formula is:

$$\begin{aligned} \text{tr}F(t+1) &= \frac{1}{\lambda_1(t)} \text{tr} \left[F(t) - \frac{F(t)\psi(t)\psi^T(t)F(t)}{\alpha + \psi^T(t)F(t)\psi(t)} \right] \\ &= \text{tr}F(t). \end{aligned} \quad (62)$$

The advantage of the *constant trace* gain updating is that the adaptation moves in an optimal direction (least squares) but the size of the step does not go to zero. For details see Landau and Zito (2005) and Landau et al. (1997).

⁸ Almost similar results are obtained if instead of the “decreasing adaptation gain” one uses adaptation gain updating with variable forgetting factor $\lambda_1(t)$ (the variable forgetting factor tends towards 1).

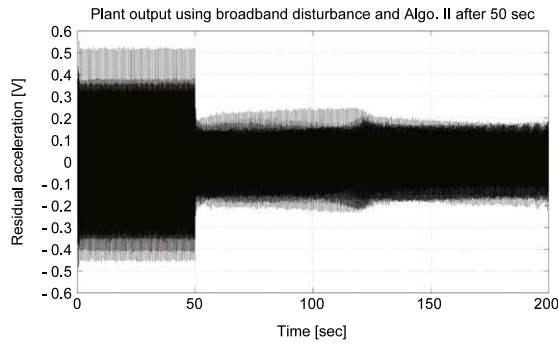


Fig. 6. Real time results obtained with Algorithm II using matrix adaptation gain.

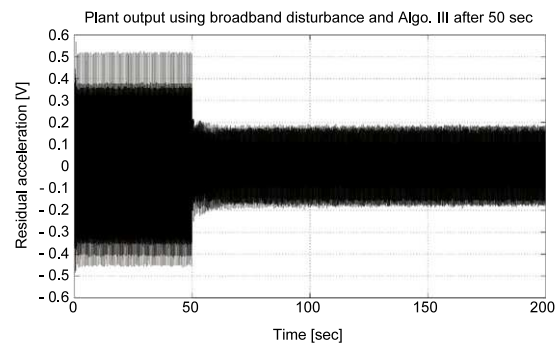


Fig. 7. Real time results obtained with Algorithm III using matrix adaptation gain.

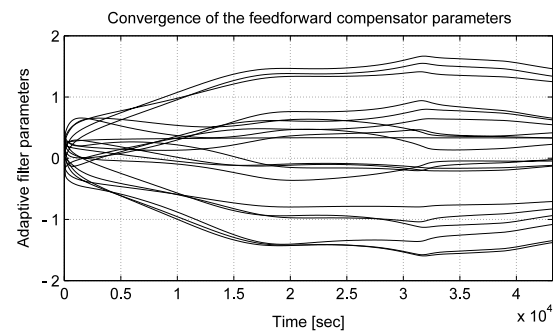


Fig. 8. Evolution of the feedforward compensator parameters for Algorithm III using matrix adaptation gain (experimental).

The experiments have been carried on by first applying the disturbance and then starting the adaptive feedforward compensation after 50 s. Time domain results obtained in open loop and with adaptive feedforward compensation algorithms II and III on the AVC system are shown in Figs. 6 and 7, respectively. The filter for Algorithm III has been computed based on the parameter estimates obtained with Algorithm II at $t = 3600$ s (almost the same results are obtained if the initialization horizon is of the order of 200 s). The initial trace of the matrix adaptation gain for 20 parameters was 10 and the constant trace has been fixed at 0.2. As it can be seen the transient duration for Algorithm II is approximately 75 s while for Algorithm III it is approximately 12 s.

The variance of the residual force without the feedforward compensator is: $\text{var}(\chi(t) = x(t)) = 0.0354$. With adaptive feedforward compensation Algorithm II, the variance is: $\text{var}(\chi(t)) = 0.0058$ (evaluated after 175 s, when the transient is finished). This corresponds to a global attenuation of 15.68 dB. Using Algorithm III the variance of the residual acceleration is: $\text{var}(\chi(t)) = 0.0054$. This corresponds to a global attenuation of 16.23 dB, which is an improvement with respect to Algorithm II. The convergence of the parameters is much slower (but this does not have an impact on the

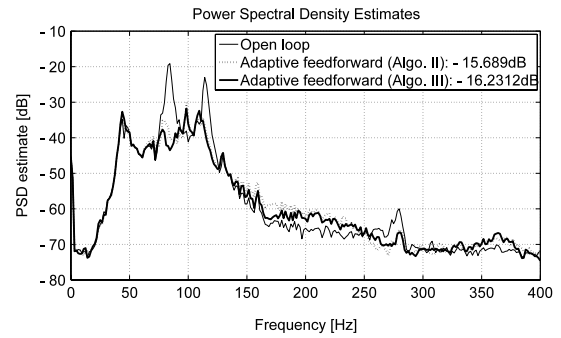


Fig. 9. Power spectral densities of the residual acceleration in open loop and with adaptive feedforward compensation (experimental).

Table 2

Influence of the number of parameters upon the global attenuation.

Number of parameters	20	32	40
Global attenuation (db)	16.23	16.49	16.89

performance). This is illustrated in Fig. 8. The experiment has been carried out over 12 h using Algorithm III. Fig. 9 shows the power spectral densities of the residual acceleration measured on the AVC in open loop (without compensator) and using adaptive feedforward compensation (after the adaptation transient i.e. 175 s). The corresponding global attenuations are also given. Algorithm III performs slightly better than Algorithm II. The influence of the number of parameters upon the performance of the system is summarized in Table 2 for the case of Algorithm III. The global attenuation is slightly improved when the number of parameters of the compensator is augmented over 20 (the PSD are almost the same).

To test the adaptive capabilities of the algorithms, a sinusoidal disturbance has been added at 1500 s (adaptation algorithm III with constant trace set at 1). Fig. 10 shows the time domain results in the case when the adaptation is stopped prior to the application of the sinusoidal disturbance (upper diagram) and when the adaptation is active (lower diagram). The duration of the transient is approximately 25 s. Fig. 11 shows the evolution of the parameters when the sinusoidal disturbance is applied. The power spectral densities when adaptation is stopped prior to the application of the sinusoidal disturbance and when adaptation is active are shown in Fig. 12. One can remark a strong attenuation of the sinusoidal disturbance (larger than 35 dB) without affecting other frequencies (similar results are obtained with Algorithm II).

7.3. Broadband disturbance rejection using scalar adaptation gain

Experiments have been carried out under the same protocol using the algorithms with scalar adaptation gain given in column 2 (introduced in this paper), 3 (Jacobson et al., 2001) and 4 (Wang & Ren, 1999) of Table 1. The algorithm of Jacobson–Johnson (column 3) was unstable even for very low adaptation gain. The explanation is clear. It does not use filtering at least by \bar{G} and since G is not positive real (in particular in the frequency zone where most of the energy of the disturbance is concentrated) the instability is not surprising. To make a fair comparison the same adaptation gain has been used for the algorithms given in columns 2 and 4 of Table 1. Since the FULMS is very sensitive to the value of the adaptation gain (becomes easily unstable and the transients are very bad) a value for the adaptation gain of 0.001 has been chosen (for a higher value FULMS is unstable). This value corresponds to a trace of a diagonal matrix adaptation gain of 0.02 when using a compensator filter with 20 parameters.

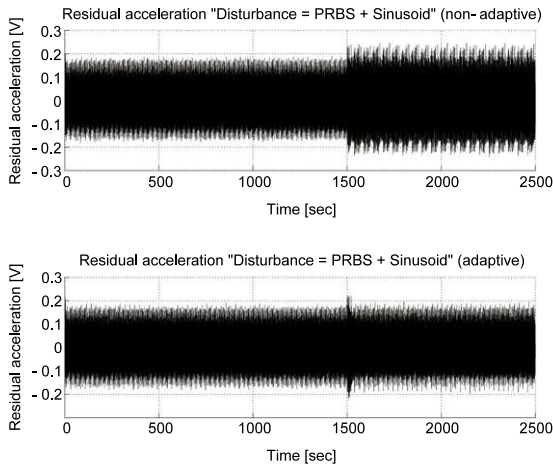


Fig. 10. Real time results for rejection of an additional sinusoidal disturbance. Upper diagram: adaptation stopped prior application of the disturbance. Lower diagram: adaptation is active.

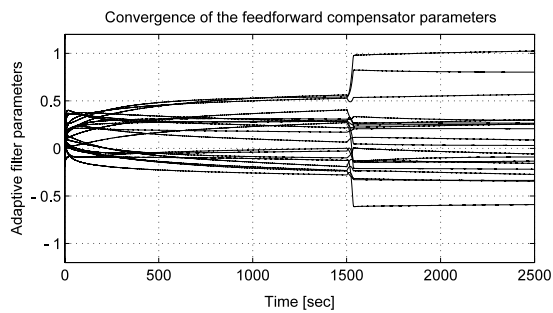


Fig. 11. Evolution of the compensator parameters when a sinusoidal disturbance is added (experimental).

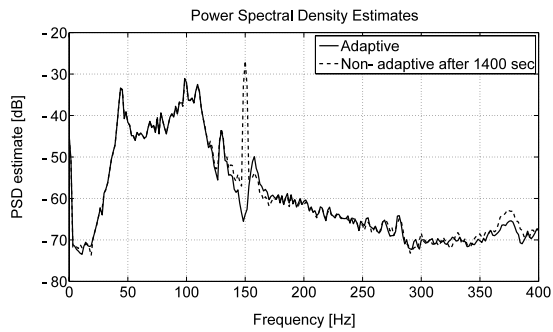


Fig. 12. Power spectral densities of the residual acceleration when an additional sinusoidal disturbance is added (Disturbance = PRBS + sinusoid).

Fig. 13 shows the adaptation transient for the FULMS algorithm. The maximum value is unacceptable in practice (one can not tolerate an overshoot over 30% of the uncompensated residual acceleration). Fig. 14 shows the adaptation transient for the scalar version of Algorithm III, which is surprisingly good. Almost same transient behavior is obtained with the scalar version of Algorithm II. Figs. 15 and 16 show the evolution of the parameters for the FULMS algorithm and the scalar version of Algorithm III. One can see jumps in the evolution of the parameters for the FULMS algorithms and instabilities occur on a long run. For Algorithm III, evolution of the parameters is smooth and no instabilities occur in a long run (12 h). Comparing Figs. 16 and 8 one can see that the convergence point in the parameter space is not the same. Either the algorithm with scalar gain has not yet converged or there are several local minima in the case of a compensator with not enough parameters for satisfying the perfect matching condition.

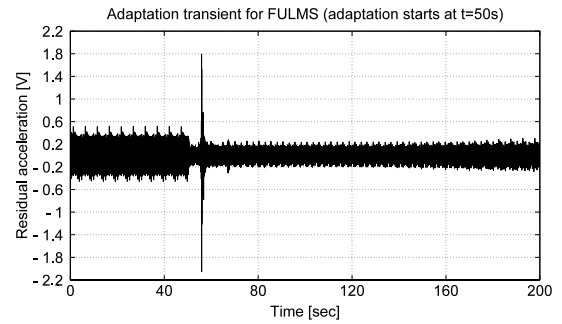


Fig. 13. Real time results obtained with FULMS algorithm.

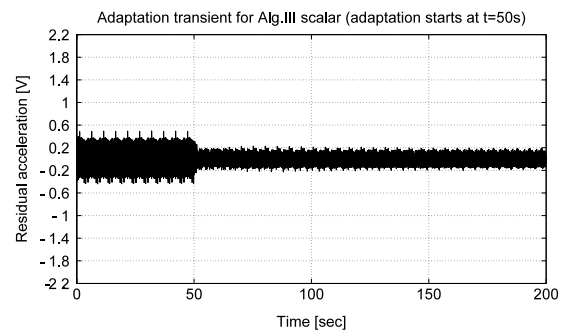


Fig. 14. Real time results obtained with Algorithm III using scalar adaptation gain.

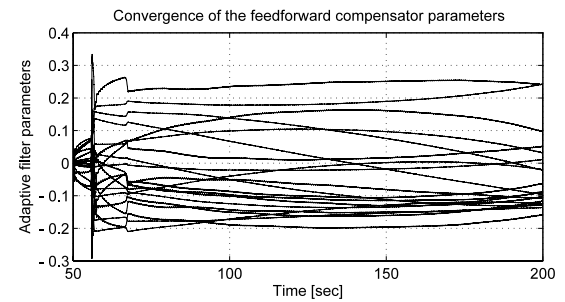


Fig. 15. Evolution of the feedforward compensator parameters (experimental) – Algorithm FULMS.

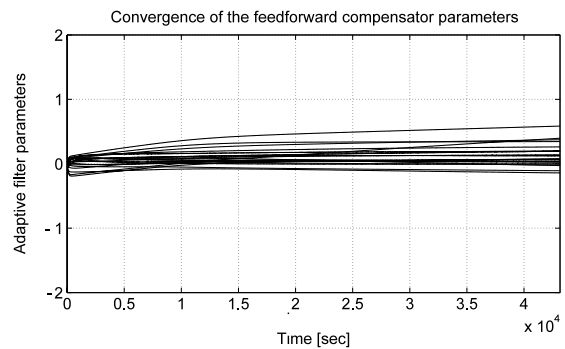


Fig. 16. Evolution of the feedforward compensator parameters (experimental) – Algorithm III using scalar adaptation gain.

The performances in the frequency domain are summarized in Fig. 17 where the power spectral densities and the global attenuation provided by the algorithms with scalar adaptation gain are shown. In Fig. 17 the performances of a H_∞ compensator designed in Alma et al. (2011) are also given (initial complexity: 70 parameters, reduced to 40 without loss of performance). The H_∞ design provides better performance than the FULMS but less good performance than algorithms II and III in their scalar or matrix

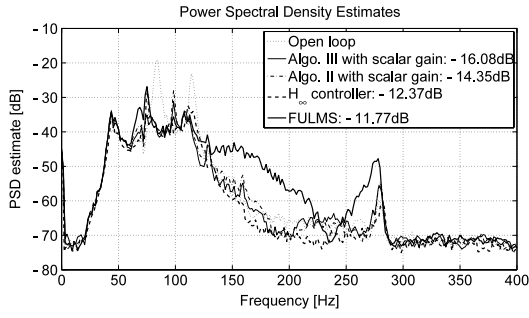


Fig. 17. Spectral densities of the residual acceleration in open loop and with adaptive feedforward compensation using scalar adaptation gain or H_∞ compensator.

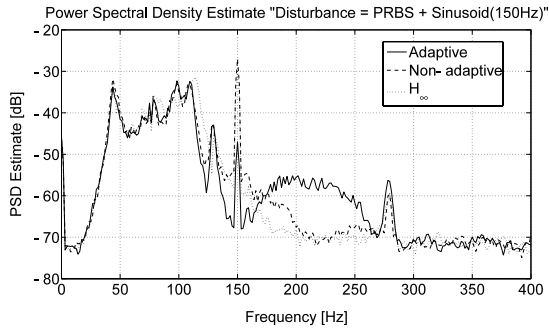


Fig. 18. Spectral densities of the residual acceleration in open loop and with adaptive feedforward compensation using scalar adaptation gain (Disturbance = PRBS + sinusoid) (experimental).

version (despite that the number of filter parameters is divided by 2).

Adaptation capabilities have been tested by adding a sinusoidal disturbance like for the case of matrix adaptation gain. The FULMS has been destabilized by the application of the sinusoidal disturbance. Fig. 18 shows the power spectral densities of the residual acceleration when the adaptation is stopped before the sinusoidal disturbance is applied, when the adaptation is active and when the H_∞ compensator (not designed for this supplementary disturbance) is used. The performance of the adaptation algorithm III with scalar gain is inferior compared with the case of matrix adaptation gain (see Fig. 12). The sinusoidal disturbance is attenuated in the scalar case by 20 dB while the attenuation is over 35 dB with a matrix adaptation gain. In addition the performance is degraded in the frequency region 170–270 Hz which does not occur when using a matrix adaptation gain. The H_∞ compensator does very little attenuation of the sinusoidal disturbance (2.6 dB). It does not have “adaptation capabilities”.

8. Concluding remarks

The paper has presented several new algorithms for adaptive feedforward compensation in AVC systems taking into account the existence of an inherent internal positive feedback coupling.

Theoretical analysis has pointed out the presence of a sufficient condition for stability involving a positive real condition on a certain transfer function. This condition can be relaxed by taking into account the nature of the disturbance (broadband) or by an appropriate filtering of the regressor vector.

Real time results obtained on an active vibration control system have shown the feasibility and good performance of the proposed algorithms. The algorithms have been compared theoretically and experimentally with two other algorithms for which an analysis in the context of the internal positive feedback is available as well as

with an H_∞ controller. It will be interesting to test the proposed algorithms on ANC systems.

Subjects for further research may include: (1) initialization procedures using model based designed feedforward compensators, (2) imposing constraints on the poles of the internal positive feedback loop.

Appendix A. Proof of Lemma 4.1

Proof. Under the assumption H2 (perfect matching condition) the output of the primary path can be expressed as: equation

$$x(t) = -G(q^{-1})y(t) \quad (63)$$

where $y(t)$ is a dummy variable given by:

$$\begin{aligned} y(t+1) &= -S^*(q^{-1})y(t) + R(q^{-1})u(t+1) \\ &= \theta^T \varphi(t) = [\theta_S^T, \theta_R^T] \begin{bmatrix} \varphi_y(t) \\ \varphi_u(t) \end{bmatrix} \end{aligned} \quad (64)$$

where:

$$\theta^T = [s_1, \dots, s_{n_S}, r_0, r_1, \dots, r_{n_R}] = [\theta_S^T, \theta_R^T] \quad (65)$$

$$\begin{aligned} \varphi^T(t) &= [-y(t) \dots -y(t-n_S+1), u(t+1) \dots u(t-n_R+1)] \\ &= [\varphi_y^T(t), \varphi_u^T(t)] \end{aligned} \quad (66)$$

and $u(t)$ is given by:

$$u(t+1) = d(t+1) + \frac{B_M^*(q^{-1})}{A_M(q^{-1})}y(t). \quad (67)$$

For a fixed value of the parameter vector $\hat{\theta}$ characterizing the estimated filter $\hat{N}(q^{-1})$ of same dimension as the optimal filter $N(q^{-1})$, the output of the secondary path can be expressed by (in this case $\hat{z}(t) = z^0(t)$ and $\hat{y}(t) = y^0(t)$):

$$\hat{z}(t) = G(q^{-1})\hat{y}(t) \quad (68)$$

where:

$$\hat{y}(t+1) = \hat{\theta}^T \phi(t). \quad (69)$$

The key observation is that the dummy variable $y(t+1)$ can be expressed as:

$$\begin{aligned} y(t+1) &= \theta^T \phi(t) + \theta^T [\varphi(t) - \phi(t)] \\ &= \theta^T \phi(t) + \theta_S^T [\varphi_y - \phi_y] + \theta_R^T [\varphi_u - \phi_u]. \end{aligned} \quad (70)$$

Define the dummy error (for a fixed vector $\hat{\theta}$)

$$\varepsilon(t+1) = y(t+1) - \hat{y}(t+1) \quad (71)$$

and the adaptation error becomes:

$$v(t+1) = -x(t) - \hat{z}(t) = G(q^{-1})\varepsilon(t+1). \quad (72)$$

It results from (70) by taking into account the expressions of $u(t)$ and $\hat{u}(t)$ given by (19) and (67) that:

$$y(t+1) = \theta^T \phi(t) - \left(S^*(q^{-1}) - \frac{R(q^{-1})B_M^*(q^{-1})}{A_M(q^{-1})} \right) \varepsilon(t). \quad (73)$$

Using Eqs. (69) and (71), one gets (after passing all terms in ε on the left hand side):

$$\varepsilon(t+1) = \frac{A_M(q^{-1})}{P(q^{-1})} [\theta - \hat{\theta}]^T \phi(t). \quad (74)$$

Taking now into account Eq. (72) one obtains Eq. (26). End of the proof. \square

Table 3
Present notations compared to those of Jacobson et al. (2001) and Wang and Ren (1999).

Present paper	In Jacobson et al. (2001)	In Wang and Ren (1999)
t	k	k
D	P	G
G	C	P
B_M	F	F
A_M	1	1
N	W	C
R	$b_0 + b_1 q^{-1} + \dots$	A
S	$1 - a_1 q^{-1} - \dots$	B
d	s	x
\hat{y}	\hat{y}	u
\hat{u}	u	$x + Fu$
γ	$\frac{1}{s}$	γ
ϕ	ϕ	ϕ
$\psi = L\phi$	ϕ	$\hat{P}\phi$
F	$\frac{1}{s}I$	γI

Appendix B. Equivalence of notations

See Table 3.

References

- Alma, M., Martinez, J. J., Landau, I. D., & Buche, G. (2011). Design and tuning of reduced order H -infinity feedforward compensators for active vibration control. *Control Systems Technology, IEEE Transactions on*, *PP*(99), 1–8. doi:10.1109/TCST.2011.2119485.
- Anderson, B. D. O., Bitmead, R. R., Johnson, C. R., Kokotovic, P. V., Kosut, R. L., Mareels, I. M. Y., et al. (1986). *Stability of adaptive systems*. Cambridge Massachusetts, London, England: M.I.T Press.
- Bai, M. R., & Lin, H. H. (1997). Comparison of active noise control structures in the presence of acoustical feedback by using the Hinf synthesis technique. *Journal of Sound and Vibration*, *206*, 453–471.
- Elliott, S. J., & Nelson, P. A. (1994). Active noise control. *Noise/News International*, (June), 75–98.
- Elliott, S. J., & Sutton, T. J. (1996). Performance of feedforward and feedback systems for active control. *IEEE Transactions on Speech and Audio Processing*, *4*(3), 214–223.
- Fraanje, R., Verhaegen, M., & Doelman, N. (1999). Convergence analysis of the filtered-u lms algorithm for active noise control in case perfect cancellation is not possible. *Signal Processing*, *73*, 255–266.
- Hu, J., & Linn, J. F. (2000). Feedforward active noise controller design in ducts without independent noise source measurements. *IEEE Transactions on Control System Technology*, *8*(3), 443–455.
- Jacobson, C. A., Johnson, C. R., Mc Cormick, D. C., & Sethares, W. A. (2001). Stability of active noise control algorithms. *IEEE Signal Processing Letters*, *8*(3), 74–76.
- Kuo, M. S., & Morgan, D. R. (1999). Active noise control: a tutorial review. *Proceedings of the IEEE*, *87*, 943–973.
- Kuo, M. S., & Morgan, D. R. (1996). *Active noise control systems-algorithms and DSP implementation*. New York: Wiley.
- Landau, I. D., Constantinescu, A., Loubat, P., Rey, D., & Franco, A. (2001). A methodology for the design of feedback active vibration control systems. In *Proceedings of the European control conference 2001. Porto, Portugal*.
- Landau, I. D., & Karimi, A. (1997). Recursive algorithms for identification in closed loop. a unified approach and evaluation. *Automatica*, *33*(8), 1499–1523.
- Landau, I. D., Karimi, A., & Constantinescu, A. (2001). Direct controller order reduction by identification in closed loop. *Automatica*, *37*(11), 1689–1702.
- Landau, I. D., Lozano, R., & Saad, M. M. (1997). *Adaptive control*. London: Springer.
- Landau, I. D., & Zito, G. (2005). *Digital control systems – design, identification and implementation*. London: Springer.
- Ljung, L. (1977). On positive real transfer functions and the convergence of some recursive schemes. *IEEE Trans. on Automatic Control*, *AC-22*, 539–551.
- Ljung, L., & Söderström, T. (1983). *Theory and practice of recursive identification*. Cambridge Massachusetts, London, England: M.I.T Press.
- Rotunno, M., & de Callafon, R. A. (1999). Design of model-based feedforward compensators for vibration compensation in a flexible structure. *Internal report*. Dept. of mechanical and aerospace engineering, University of California, San Diego.
- Wang, A. K., & Ren, W. (1999). Convergence analysis of the filtered-u algorithm for active noise control. *Signal Processing*, *73*, 255–266.
- Zeng, J., & de Callafon, R. A. (2006). Recursive filter estimation for feedforward noise cancellation with acoustic coupling. *Journal of Sound and Vibration*, *291*, 1061–1079.



Ioan Doré Landau is Emeritus Research Director at C.N.R.S. (National Center for Scientific Research) since September 2003 and continues to collaborate with the GIPSA-LAB(CNRS/INPG), Control Department in Grenoble. His research interests encompass theory and applications in system identification, adaptive control, robust digital control and nonlinear systems. He has authored and co-authored over 200 papers on these subjects. He is the author and co-author of several books including: *Adaptive Control – The Model Reference Approach* (Dekker 1979), *System Identification and Control Design* (Hermès 1993, Prentice Hall 1990), *Digital Control Systems* (Springer 2005, Hermès-Lavoisier, 2002) and co-author of the books *Adaptive Control – Theory and Practice* (in Japanese-Ohm 1981) (with Tomizuka) and *Adaptive Control* (Springer 1997) (with Lozano and M'Saad). Dr. Landau received the *Rufus Oldenburger Medal 2000* from the American Society of Mechanical Engineers. He is “*Doctor Honoris Causa*” of the Université Catholique de Louvain-la-Neuve (2003). He was appointed as an “*IFAC Fellow*” in 2007. He received the Great Gold Medal at the Invention Exhibition, Vienna (1968), the *CNRS Silver Medal* (1982) and the *Price Monpetit* from the French Academy of Science (1990).



Marouane Alma was born in Azzaba, Algeria, in 1984. He received an Automatic control Engineering Degree from the National Polytechnic School of Algiers in 2006, a Master's Degree in 2007 from the Polytechnic Institute of Grenoble. He has been a Ph.D. student since October 2007 in Gipsa-lab, Grenoble University, and a teaching assistant at Ecole Nationale Supérieure de l'Energie, l'Eau et l'Environnement since September 2010. His current research interests include system identification, robust and adaptive control for active vibration control systems.



Tudor-Bogdan Airimioaie was born in Suceava, Romania, in 1983. He received an Automatic Control Engineering Degree from the University “Politehnica” of Bucharest, Romania in 2008. He is now working on his Ph.D. degree in a joint project between the Control System Department of GIPSA-Lab, University of Grenoble, France and the University “Politehnica” of Bucharest, Romania where he is a teaching assistant since October 2008. His main research interests include system identification and adaptive and robust control techniques for active vibration control systems.

APPENDIX D

ADAPTIVE FEEDFORWARD COMPENSATION ALGORITHMS FOR AVC SYSTEMS IN THE PRESENCE OF A FEEDBACK CONTROLLER

Authors: Marouane Alma, Ioan Doré Landau, and Tudor-Bogdan Airimițoaie

Journal: Automatica 48 (2012) 982–985

Type of submission: Technical communique



Technical communique

Adaptive feedforward compensation algorithms for AVC systems in the presence of a feedback controller[☆]

Marouane Alma, Ioan Doré Landau¹, Tudor-Bogdan Airimitoiaie

GIPSA-LAB, Department of Automatic Control, ENSIEG BP 46, 38402 Saint-Martin d'Hères, France

ARTICLE INFO

Article history:

Received 27 June 2011

Received in revised form

12 October 2011

Accepted 29 December 2011

Available online 14 March 2012

Keywords:

Active vibration control

Adaptive feedforward compensation

Feedback control

Adaptive control

Parameter estimation

ABSTRACT

In Jacobson, Johnson, Mc Cormick, and Sethares (2001) and Landau, Alma, and Airimitoiaie (2011) adaptation algorithms taking into account the “positive” feedback coupling arising in most of the active noise and vibration control systems have been proposed and analyzed. The stability of the system requires satisfaction of a positive real condition through an appropriate filtering of the regressor vector. It is shown in this note that the presence in addition of a feedback controller on one hand strongly influences the positive real conditions for stability and the structure of the filter to be used in the algorithm and on the other hand improves significantly the performance of the system. Experimental results obtained on an active vibration control (AVC) system clearly illustrate the benefit of using a hybrid adaptive feedforward + feedback approach.

© 2012 Elsevier Ltd. All rights reserved.

1. Introduction

Adaptive feedforward for broadband disturbance compensation is widely used when a well correlated signal with the disturbance (image of the disturbance) is available (Elliott & Nelson, 1994; Elliott & Sutton, 1996; Kuo & Morgan, 1999; Zeng & de Callafon, 2006). However in many systems there is a positive (mechanical or acoustical) coupling between the feedforward compensation system and the measurement of the disturbance.

In Jacobson et al. (2001) and Landau et al. (2011) adaptation algorithms taking into account this “positive” feedback have been proposed and analyzed. The stability of the system requires satisfaction of a positive real condition through an appropriate filtering of the regressor vector. The objective of this note is to show theoretically and experimentally what the impact of using a feedback compensator in addition to an adaptive feedforward filter as discussed in Landau et al. (2011) is.

A combination of adaptive feedforward + fixed feedback disturbance compensation has already been discussed since it is expected to improve the performance of active noise control

[☆] The material in this paper was not presented at any conference. This paper was recommended for publication in revised form by Associate Editor A. Pedro Aguiar under the direction of Editor André L. Tits.

E-mail addresses: marouane.alma@gipsa-lab.grenoble-inp.fr (M. Alma), ioan-dore.landau@gipsa-lab.grenoble-inp.fr (I.D. Landau), a_tudor_b@yahoo.com (T.-B. Airimitoiaie).

¹ Tel.: +33 4 7682 6391; fax: +33 4 7682 6382.

(ANC) and active vibration control (AVC) systems. See for example De Callafon (2010), Ray, Solbeck, Streeter, and Collier (2006), Esmailzadeh, Alasty, and Ohadi (2002). However the influence of the feedback upon the stability of the adaptive feedforward algorithms has not been examined.

The main contributions of the present paper are:

- Establishing the influence of the feedback control loop upon the stability conditions for adaptive feedforward compensation (with and without internal positive coupling)
- Showing the improvement of the global attenuation w.r.t results obtained with adaptive feedforward compensation (Landau et al., 2011).

2. Basic equations and notations

The block diagram associated with an AVC system using a hybrid (feedback + adaptive feedforward) control is shown in Fig. 1.

The description, equations and notations of the various blocs and transfer functions have been presented in detail in Landau et al. (2011) Eqs. (1)–(12). $D = \frac{B_D}{A_D}$, $G = \frac{B_G}{A_G}$, $M = \frac{B_M}{A_M}$ represent the transfer operators associated with the primary, secondary and reverse paths (all asymptotically stable). The feedforward compensator is $\hat{N} = \frac{\hat{R}}{\hat{S}}$ with:

$$\hat{R}(q^{-1}) = \hat{r}_0 + \hat{r}_1 q^{-1} + \dots + \hat{r}_{n_R} q^{-n_R}, \quad (1)$$

$$\hat{S}(q^{-1}) = 1 + \hat{s}_1 q^{-1} + \dots + \hat{s}_{n_S} q^{-n_S} = 1 + q^{-1} \hat{S}^*(q^{-1}). \quad (2)$$

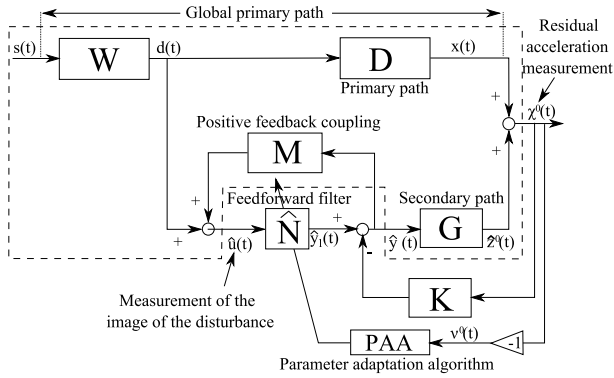


Fig. 1. Feedforward AVC with fixed feedback controller (K) and adaptive feedforward compensator (\hat{N}).

The signal $s(t)$ is the external disturbance source, $d(t)$ is the correlated disturbance measurement (in the absence of the compensation) and $\hat{u}(t)$ is the measured primary signal which is the sum of $d(t)$ and of the effect of the actuator used for compensation.

The fixed feedback controller K , is characterized by the stable transfer function:

$$K(q^{-1}) = \frac{B_K(q^{-1})}{A_K(q^{-1})} = \frac{b_0^K + b_1^K q^{-1} + \dots + b_{n_{B_K}}^K q^{-n_{B_K}}}{1 + a_1^K q^{-1} + \dots + a_{n_{A_K}}^K q^{-n_{A_K}}}. \quad (3)$$

The “a posteriori” output of the feedforward filter is denoted by: $\hat{y}_1(t+1) = \hat{y}_1(t+1|\hat{\theta}(t+1))$.

The “a priori” output of the estimated feedforward filter is given by:

$$\begin{aligned} \hat{y}_1^0(t+1) &= \hat{y}_1(t+1|\hat{\theta}(t)) \\ &= \hat{\theta}^T(t)\phi(t) = \begin{bmatrix} \hat{\theta}_S^T(t), \hat{\theta}_R^T(t) \end{bmatrix} \begin{bmatrix} \phi_{y_1}(t) \\ \phi_u(t) \end{bmatrix} \end{aligned} \quad (4)$$

where

$$\begin{aligned} \hat{\theta}^T(t) &= [\hat{s}_1(t) \dots \hat{s}_{n_S}(t), \hat{r}_0(t) \dots \hat{r}_{n_R}(t)] = [\hat{\theta}_S^T(t), \hat{\theta}_R^T(t)] \quad (5) \\ \phi^T(t) &= [-\hat{y}_1(t) \dots -\hat{y}_1(t-n_S+1), \hat{u}(t+1), \\ &\quad \hat{u}(t) \dots \hat{u}(t-n_R+1)] \\ &= [\phi_{y_1}^T(t), \phi_u^T(t)] \end{aligned} \quad (6)$$

and $\hat{y}_1(t), \hat{y}_1(t-1) \dots$ are the “a posteriori” outputs of the feedforward filter generated by:

$$\hat{y}_1(t+1) = \hat{y}_1(t+1|\hat{\theta}(t+1)) = \hat{\theta}^T(t+1)\phi(t) \quad (7)$$

while $\hat{u}(t+1), \hat{u}(t) \dots$ are the measurements provided by the primary transducer.²

The control signal applied to the secondary path is given by

$$\hat{y}(t+1) = \hat{y}_1(t+1) - \frac{B_K}{A_K} \chi^0(t+1) \quad (8)$$

where $\chi^0(t+1)$ is the measured residual acceleration.

3. Development of the algorithms

The algorithms for adaptive feedforward compensation in the presence of a feedback controller will be developed under the hypotheses H1, H3 and H4 from Landau et al. (2011) and new hypothesis H2:

H2-Perfect matching condition. There exists a filter $N(q^{-1})$ of finite dimension such that³:

$$\frac{N}{(1-NM)}G = -D \quad (9)$$

and the characteristic polynomials (i) of the “internal” positive coupling loop:

$$P = A_M S - B_M R \quad (10)$$

(ii) of the closed loop ($G - K$):

$$P_{cl} = A_C A_K + B_C B_K \quad (11)$$

and of the coupled feedforward–feedback loop:

$$P_{fb-ff} = A_M S [A_C A_K + B_C B_K] - B_M R A_K A_C \quad (12)$$

are Hurwitz polynomials.

A first step in the development of the algorithms is to establish a relation between the errors on the estimation of the parameters of the feedforward filter and the measured residual acceleration. This is summarized in the following lemma.

Lemma 3.1. Under hypotheses H1–H4, for the system described in Section 2, using a feedforward compensator \hat{N} with constant parameters and a feedback controller K , one has:

$$v(t+1) = -\chi(t+1) = \frac{A_M A_C A_K G}{P_{fb-ff}} [\theta - \hat{\theta}]^T \phi(t) \quad (13)$$

where

$$\theta^T = [s_1, \dots, s_{n_S}, r_0, r_1, \dots, r_{n_R}] = [\theta_S^T, \theta_R^T] \quad (14)$$

is the vector of parameters of the optimal filter N assuring perfect matching

$$\hat{\theta}^T = [\hat{s}_1 \dots \hat{s}_{n_S}, \hat{r}_0 \dots \hat{r}_{n_R}] = [\hat{\theta}_S^T, \hat{\theta}_R^T] \quad (15)$$

is the vector of constant estimated parameters of \hat{N}

$$\begin{aligned} \phi^T(t) &= [-\hat{y}_1(t) \dots -\hat{y}_1(t-n_S+1), \\ &\quad \hat{u}(t+1), \hat{u}(t) \dots \hat{u}(t-n_R+1)] \\ &= [\phi_{y_1}^T(t), \phi_u^T(t)] \end{aligned} \quad (16)$$

and $\hat{u}(t+1)$ is given by⁴:

$$\hat{u}(t+1) = d(t+1) + \frac{B_M^*}{A_M} \hat{y}(t). \quad (17)$$

The proof is given in the Appendix.

Corollary 1. For $B_K = 0$ (absence of the feedback controller), the error equation for pure feedforward compensation given in Landau et al. (2011), is obtained.

Corollary 2. For $B_M = 0$ (absence of the mechanical coupling), the error equation is given by:

$$v(t+1) = \frac{B_C A_K}{P_{cl} S} [\theta - \hat{\theta}]^T \phi(t) = \frac{G_{cl}}{S} [\theta - \hat{\theta}]^T \phi(t) \quad (18)$$

where: G_{cl} is the closed loop transfer function (G, K) defined by: $G_{cl} = \frac{B_C A_K}{P_{cl}}$.

² $\hat{u}(t+1)$ is available before the adaptation of parameters starts at $t+1$.

³ In many cases, the argument q^{-1} or z^{-1} will be dropped out.

⁴ $B(q^{-1}) = q^{-1} B^*(q^{-1})$.

Filtering the vector $\phi(t)$ through an asymptotically stable filter $L(q^{-1}) = \frac{\hat{B}_L}{\hat{A}_L}$, Eq. (13) for $\hat{\theta} = \text{constant}$ becomes:

$$v(t+1) = \frac{A_M A_G A_K G}{P_{fb-ff} L} [\theta - \hat{\theta}]^T \phi_f(t) \quad (19)$$

$$\phi_f(t) = L(q^{-1})\phi(t). \quad (20)$$

Eq. (19) will be used to develop the adaptation algorithms neglecting the non-commutativity of the operators when $\hat{\theta}$ is time varying (however an exact algorithm can be derived in such cases - see Landau, Lozano, and M'Saad (2011)).

Replacing the fixed estimated parameters by the current estimated parameters, Eq. (19) becomes the equation of the a posteriori residual (adaptation) error $v(t+1)$ (which is computed):

$$v(t+1/\hat{\theta}(t+1)) = \frac{A_M A_G A_K G}{P_{fb-ff} L} G[\theta - \hat{\theta}(t+1)]^T \phi_f(t). \quad (21)$$

Eq. (21) has the standard form for an a posteriori adaptation error (Landau et al., 2011), which immediately suggests to use the following parameter adaptation algorithm (the same as in Landau et al. (2011)):

$$\hat{\theta}(t+1) = \hat{\theta}(t) + F(t)\psi(t)v(t+1); \quad (22)$$

$$v(t+1) = \frac{v^0(t+1)}{1 + \psi^T(t)F(t)\psi(t)}; \quad (23)$$

$$F(t+1) = \frac{1}{\lambda_1(t)} \left[F(t) - \frac{F(t)\psi(t)\psi^T(t)F(t)}{\lambda_2(t) + \psi^T(t)F(t)\psi(t)} \right] \quad (24)$$

$$1 \geq \lambda_1(t) > 0; \quad 0 \leq \lambda_2(t) < 2; \quad F(0) > 0 \quad (25)$$

$$\psi(t) = \phi_f(t) \quad (26)$$

where $\lambda_1(t)$ and $\lambda_2(t)$ allow to obtain various profiles for the matrix adaptation gain $F(t)$ (see Section 4 and Landau et al. (2011)).

Three choices for the filter L will be considered, leading to three different algorithms:

Algorithm I: $L = G$

Algorithm II: $L = \hat{G}$

Algorithm III: $L = \frac{\hat{A}_M \hat{A}_G A_K \hat{G}}{P_{fb-ff}}$

where:

$$\hat{P}_{fb-ff} = \hat{A}_M \hat{S} [\hat{A}_G A_K + \hat{B}_G B_K] - \hat{B}_M \hat{R} A_K \hat{A}_G \quad (27)$$

is an estimation of the characteristic polynomial of the coupled feedforward–feedback loop computed on the basis of available estimates of the parameters of the filter \hat{N} and estimated models $\hat{G} = \frac{\hat{B}_G}{\hat{A}_G}$ and $\hat{M} = \frac{\hat{B}_M}{\hat{A}_M}$. For Algorithm III several options for updating \hat{P}_{fb-ff} can be considered:

- Run Algorithm II for a certain time to get estimates of \hat{R} and \hat{S} and compute \hat{P}_{fb-ff}
- Update \hat{P}_{fb-ff} at each sampling instant or from time to time using Algorithm III (after a short initialization horizon using Algorithm II).

3.1. Analysis of the algorithms

For Algorithms I, II and III the equation for the a posteriori adaptation error has the form⁵:

$$v(t+1) = H(q^{-1})[\theta - \hat{\theta}(t+1)]^T \psi(t) \quad (28)$$

⁵ The argument $\hat{\theta}(t+1)$ has been dropped out.

where:

$$H(q^{-1}) = \frac{A_M A_G A_K G}{P_{fb-ff} L}, \quad \psi = \phi_f. \quad (29)$$

Neglecting the non-commutativity of time varying operators, one has the following result:

Lemma 3.2. Assuming that Eq. (28) represents the evolution of the a posteriori adaptation error and that the parameter adaptation algorithm (22) through (26) is used, one has:

$$\lim_{t \rightarrow \infty} v(t+1) = 0 \quad (30)$$

$$\lim_{t \rightarrow \infty} \frac{[v^0(t+1)]^2}{1 + \psi^T(t)F(t)\psi(t)} = 0 \quad (31)$$

$$\|\psi(t)\| \text{ is bounded} \quad (32)$$

$$\lim_{t \rightarrow \infty} v^0(t+1) = 0 \quad (33)$$

for any initial conditions $\hat{\theta}(0)$, $v^0(0)$, $F(0)$, provided that:

$$H'(z^{-1}) = H(z^{-1}) - \frac{\lambda_2}{2}, \quad \max_t [\lambda_2(t)] \leq \lambda_2 < 2 \quad (34)$$

is a strictly positive real (SPR) transfer function.

The proof is similar to that given in Landau et al. (2011) for $B_K = 0$ and $A_K = 1$ (absence of the feedback controller) and it is omitted.

4. Experimental results

The same AVC system as in Landau et al. (2011) has been used.

4.1. Design of the feedback controller

The objective of the feedback controller K is to reduce the disturbance effect on the residual acceleration $\chi(t)$ where the secondary path G has enough gain, without using the disturbance correlated measurement $\hat{u}(t)$.

4.2. Broadband disturbance rejection

The adaptive feedforward filter structure for most of the experiments has been $n_R = 9$, $n_S = 10$ (total of 20 parameters) and this complexity does not allow to verify the “perfect matching condition” (which requires more than 40 parameters). A pseudo-random binary sequence (PRBS) excitation on the global primary path will be considered as the disturbance. For the adaptive operation the Algorithms II and III have been used with decreasing adaptation gain ($\lambda_1(t) = 1$, $\lambda_2(t) = 1$) combined with a constant trace adaptation gain.

The experiments have been carried on by first applying the disturbance in open loop during 50 s and after that closing the loop with the hybrid adaptive feedforward–feedback algorithms. Time domain results obtained in open loop and with hybrid control (using Algorithm III) on the AVC system are shown in Fig. 2. The initial trace of the matrix adaptation gain was 10 and the constant trace has been fixed at 0.2.

Table 1 summarizes the global attenuation results for various configurations. Clearly, the hybrid adaptive feedforward–feedback scheme brings a significant improvement in performance with respect to adaptive feedforward compensation alone. Comparing with the results of Landau et al. (2011), (Table 2) one can conclude that in terms of performance and complexity it is more interesting to add a linear feedback than augmenting the number of parameters of the adaptive feedforward filter beyond a certain value.

Table 1
Global attenuation for various configurations.

	No feedback no feedforward	Feedback only	Adaptive feedforward	Feedback & Ad. feedforward
Variance	0.0354	0.0067	0.0054	0.0033
Normalized var.	1	0.1892	0.1525	0.0932
Atten. (dB)	0	−14.40	−16.23	−20.53

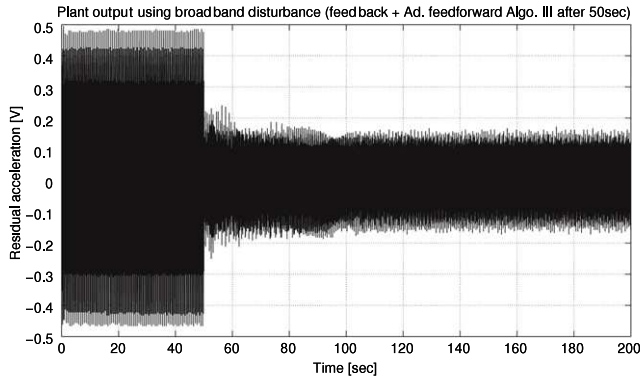


Fig. 2. Real time results obtained with feedback controller and adaptive feedforward Algorithm III.

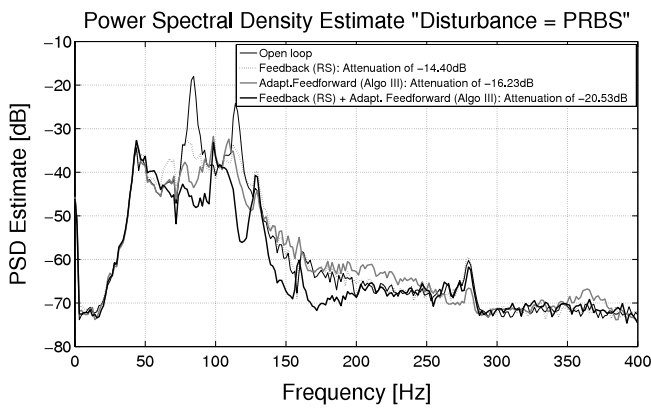


Fig. 3. Power spectral densities of the residual acceleration (disturbance = PRBS).

Fig. 3 shows a comparison of the power spectral densities for adaptive feedforward alone with 20 parameters (Algorithm III), feedback controller alone, and the hybrid “feedback-adaptive feedforward” scheme with 20 parameters (Algorithm III).

5. Conclusions

The theoretical analysis presented in this note has pointed out the interaction between the feedback and the stability conditions for adaptive feedforward compensation. Experimental results on an AVC system featuring an internal “positive” coupling have illustrated the improvement in the performance provided by the hybrid approach.

Appendix. Proof of Lemma 3.1

For a fixed value of the parameter vector $\hat{\theta}$ characterizing the estimated filter $\hat{N}(q^{-1})$ of same dimension as the optimal filter $N(q^{-1})$, the output of the secondary path can be expressed by (in this case $\hat{z}(t) = \hat{z}^0(t)$, $\hat{y}(t) = \hat{y}^0(t)$ and $\chi(t) = \chi^0(t)$):

$$\hat{z}(t) = G\hat{y}(t) \quad (35)$$

with:

$$\hat{y}(t) = \hat{y}_1(t) - \frac{B_K}{A_K} \chi(t) = \hat{y}_1(t) + \frac{B_K}{A_K} v(t) \quad (36)$$

where:

$$\hat{y}_1(t+1) = \hat{\theta}^T \phi(t). \quad (37)$$

The key observation is that using Eqs. (63) through (67) from Landau et al. (2011) the dummy variable $y(t+1)$ can be expressed as:

$$y(t+1) = \theta^T \phi(t) - S^*[y(t) - \hat{y}_1(t)] + R[u(t+1) - \hat{u}(t+1)]. \quad (38)$$

Define the dummy error (for a fixed vector $\hat{\theta}$)

$$\varepsilon(t+1) = y(t+1) - \hat{y}_1(t+1) - K_G \varepsilon(t) \quad (39)$$

and the residual error becomes:

$$v(t+1) = -x(t+1) - \hat{z}(t+1) = G\varepsilon(t+1). \quad (40)$$

By taking into account the Eqs. (36) and (40), $y(t+1)$ becomes:

$$y(t+1) = \theta^T \phi(t) - S^* \left[y(t) - \hat{y}(t) + \frac{B_K B_G}{A_K A_G} \varepsilon(t) \right] + R[u(t+1) - \hat{u}(t+1)]. \quad (41)$$

It results from (41) by taking into account the expressions of $u(t)$ and $\hat{u}(t)$ given by (67) of Landau et al. (2011) and (17) that:

$$y(t+1) = \theta^T \phi(t) - \left[S^* \left(1 + \frac{B_K B_G}{A_K A_G} \right) - \frac{R(q^{-1}) B_M^*}{A_M} \right] \varepsilon(t). \quad (42)$$

Using Eqs. (36) and (39), one gets (after passing all terms in ε on the left hand side):

$$\varepsilon(t+1) = \frac{A_M A_G A_K}{P_{fb-ff}} [\theta - \hat{\theta}]^T \phi(t). \quad (43)$$

Taking now into account Eq. (40) one obtains Eq. (13). End of the proof.

References

- De Callafon, R. (2010). Active noise control method and apparatus including feedforward and feedback controller (7688984 B2).
- Elliott, S. J., & Nelson, P. A. (1994). Active noise control. *Noise/News International*, 75–98.
- Elliott, S. J., & Sutton, T. J. (1996). Performance of feedforward and feedback systems for active control. *IEEE Transactions on Speech and Audio Processing*, 4(3), 214–223.
- Esmailzadeh, E., Alasty, A., & Ohadi, A. R. (2002). Hybrid active noise control of a one-dimensional acoustic duct. *Journal of Vibration and Acoustics*, 124(1), 10–18.
- Jacobson, C. A., Johnson, C. R., Mc Cormick, D. C., & Sethares, W. A. (2001). Stability of active noise control algorithms. *IEEE Signal Processing Letters*, 8(3), 74–76.
- Kuo, M. S., & Morgan, D. R. (1999). Active noise control: a tutorial review. *Proceedings of the IEEE*, 87, 943–973.
- Landau, I. D., Alma, M., & Airimitoie, T. B. (2011). Adaptive feedforward compensation algorithms for active vibration control with mechanical coupling. *Automatica*, 47(10), 2185–2196.
- Landau, I. D., Lozano, R., & M'Saad, M. (2011). *Adaptive control* (2nd ed.). London: Springer.
- Ray, L. R., Solbeck, J. A., Streeter, A. D., & Collier, R. D. (2006). Hybrid feedforward-feedback active noise reduction for hearing protection and communication. *The Journal of the Acoustical Society of America*, 120(4), 2026–2036.
- Zeng, J., & de Callafon, R. A. (2006). Recursive filter estimation for feedforward noise cancellation with acoustic coupling. *Journal of Sound and Vibration*, 291, 1061–1079.

APPENDIX E

IIR YOULA-KUCERA PARAMETERIZED ADAPTIVE FEEDFORWARD COMPENSATORS FOR ACTIVE VIBRATION CONTROL WITH MECHANICAL COUPLING

Authors: Ioan Doré Landau, Tudor-Bogdan Airimițoiaie, and Marouane Alma

Journal: IEEE Transactions on Control Systems Technology

Type of submission: Regular paper

Status: Accepted for publication

IIR Youla-Kucera parameterized adaptive feedforward compensators for active vibration control with mechanical coupling

Ioan Doré Landau, Tudor-Bogdan Airimîtoaic, and Marouane Alma

Abstract—Adaptive feedforward broadband vibration (or noise) compensation requires a reliable correlated measurement with the disturbance (an image of the disturbance). The reliability of this measurement is compromised in most of the systems by a "positive" internal feedback coupling between the compensator system and the correlated measurement of the disturbance. The system may become unstable if the adaptation algorithms do not take into account this positive feedback. Instead of using classical IIR or FIR feedforward compensators, the present paper proposes and analyses an IIR Youla - Kucera parametrization of the feedforward compensator. A model based central IIR stabilizing compensator is used and its performance is enhanced by the adaptation of the parameters (Q-parameters) of an IIR Youla-Kucera filter. Adaptation algorithms assuring the stability of the system in the presence of the positive internal feedback are provided. Their performances are evaluated experimentally on an active vibration control (AVC) system. Theoretical and experimental comparisons with FIR Youla-Kucera parameterized feedforward compensators and IIR feedforward compensators are provided.

Index Terms—active vibration control, adaptive feedforward compensation, adaptive control, Youla-Kucera parametrization, parameter estimation.

LIST OF ACRONYMS

ANC - Active noise control system
 AVC - Active vibration control system
 FIRYK - Youla-Kucera parameterized IIR adaptive feedforward compensator using a FIR Youla-Kucera filter
 IIR - IIR adaptive feedforward compensator
 IIRYK - Youla-Kucera parameterized IIR adaptive feedforward compensator using an IIR Youla-Kucera filter
 PAA - Parameter adaptation algorithm
 PRBS - Pseudo random binary sequence
 QFIR - Youla-Kucera FIR filter
 QIIR - Youla-Kucera IIR filter
 SPR - Strictly positive real (transfer function)

I. INTRODUCTION

A preliminary version of this paper has been presented at the CDC/ECC 2011, Orlando, USA. The authors are with the Control System Department of GIPSA-Lab, St. Martin d'Hères, 38402 FRANCE, emails: ([Ioan-Dore.Landau, Tudor-Bogdan.Airimitoaic, Marouane.Alma]@gipsa-lab.grenoble-inp.fr).

Tudor-Bogdan Airimîtoaic is also with the Faculty of Automatic Control and Computers, University "Politehnica" of Bucharest, Bucharest, 060042 ROMANIA.

ADAPTIVE feedforward broadband vibration (or noise) compensation requires a reliable correlated measurement with the disturbance (an image of the disturbance) ([1], [2], [3], [4]). The reliability of this measurement is compromised in most of the systems by a "positive" internal feedback coupling between the compensator system and the correlated measurement of the disturbance. The system may become unstable if the adaptation algorithms do not take into account this positive feedback ([2], [4], [5], [6]). One of the solutions to overcome this problem ([3]) is to try to compensate the positive feedback ([3], [7]). However, since the compensation can not be perfect, the potential instability of the system still exists ([8], [9]).

In the context of this inherent "positive" feedback, the adaptive feedforward compensator should minimize the effect of the disturbance while simultaneously assuring the stability of the internal positive feedback loop.

However this problem can be formulated as a standard feedback control problem using the 2x2 generalized plant representation [10]. The inputs are the disturbance and the input to the compensator system (the control) and the outputs are the residual acceleration (force, noise) which is the performance variable and the effective measurement of the disturbance. The problem is now to design a feedback compensator (from the measurement of the disturbance to the input of the compensator system) which minimizes the residual acceleration and stabilizes the system ([11], [12]). From a control perspective, the compensator filter appears as a feedback controller while in all the literature dedicated to active vibration (or noise) control the term "feedforward compensator" is used. The term "feedforward" is justified by the fact that the information upon the disturbance is taken "upstream" while for a "feedback compensator" is taken "downstream" by measuring its effect (upon the residual acceleration)¹.

An approach discussed in the literature is the analysis in this new context of existing algorithms for adaptive feedforward compensation developed for the case without internal coupling. An attempt is made in [8] where the asymptotic convergence in a stochastic environment of the so called "Filtered-U LMS" (FULMS) algorithm is discussed. Further results on the same direction can be found in [7]. The authors use the Ljung's ODE method ([13]) for the case of a scalar vanishing adaptation gain. Unfortunately this is not enough

¹For a coherent presentation with related contributions in the field of active vibration (noise) control, the terminology of the field will be used throughout the paper

because nothing is said about the stability of the system with respect to initial conditions and when a non vanishing adaptation gain is used (to keep adaptation capabilities). The authors assume that the positive feedback does not destabilize the system.

A stability approach for developing appropriate adaptive algorithms in the context of internal positive feedback is discussed in [6] and [14]. Reference [14] provides also an experimental comparison of various algorithms for IIR adaptive compensators in the presence of the internal positive feedback.

In [4], the idea of using an Youla-Kucera parametrization² of the feedforward compensator is illustrated in the context of ANC. Based on the identification of the system, a stabilizing Youla-Kucera controller using an orthonormal basis filter is designed. The Youla-Kucera parameters weighting the orthonormal basis filters are then updated by using a two time scale indirect procedure: (1) estimation of the Q-filter's parameters over a certain horizon, (2) updating of the controller. No stability proof for the tuning procedure is provided.

In [15] an algorithm for adapting the Q parameters of a FIR Youla-Kucera (subsequently called QFIR) parameterized feedforward compensator has been proposed, analyzed and tested experimentally on an AVC system. While the central stabilizing compensator has an IIR structure, the Youla-Kucera filter has a FIR structure.

In the control literature the use of Youla-Kucera type controllers has been extensively discussed. See [16], [17]. Reference [17] gives an extensive coverage of the subject. Related references are also [18], [19]³.

The objectives of this paper are:

- to develop, to analyze, and to evaluate experimentally new recursive algorithms for online estimation and adaptation of the Q-parameters of IIR Youla-Kucera (subsequently called QIIR) parameterized feedforward compensators for broadband disturbances with unknown and variable spectral characteristics;
- to evaluate comparatively these algorithms with respect to existing algorithms from theoretical, implementation, and experimental points of view.

The main contributions of this paper with respect to [4] and [15] are:

- the development of new real time recursive adaptation algorithms for the Q-parameters of IIR Youla-Kucera feedforward compensators and the analysis of the stability of the resulting system;
- the algorithms presented in [15] for FIR Youla-Kucera adaptive feedforward compensators are particular cases of those introduced in this paper;
- application of the algorithms to an AVC system;
- experimental comparison with adaptive IIR feedforward compensators and with adaptive FIR Youla-Kucera parametrization;

²Throughout the paper the *Youla-Kucera parametrization* will also be called *Q* (or *YK*) -*parametrization*.

³To the knowledge of the authors the specific problem considered in this paper is not covered in the existing literature.

- significant reduction of the number of parameters to be adapted for the same level of performance when using adaptive IIR Youla-Kucera feedforward compensators instead of adaptive FIR Youla-Kucera feedforward compensators.

In the context of this paper it is assumed that:

- the characteristics of the wide band disturbance acting on the system are unknown and they may vary;
- the internal positive feedback can not be neglected;
- the dynamic models of the AVC are constant and a good estimation of these models is available (these models can be estimated from experimental data).

From the user point of view and taking into account the type of operation of adaptive disturbance compensation systems, one has to consider two modes of operation of the adaptive schemes:

- *Adaptive* operation. The adaptation is performed continuously with a non vanishing adaptation gain.
- *Self-tuning* operation. The adaptation procedure starts either on demand or when the performance is unsatisfactory. A vanishing adaptation gain is used.

From an implementation point of view the paper will explore the comparative performances of adaptation algorithms with matrix adaptation gain and with scalar adaptation gain. While the algorithms have been developed and tested in the context of AVC, the results are certainly applicable to ANC systems since they feature the same type of internal positive feedback.

The paper is organized as follows. The AVC system (featuring an internal positive mechanical coupling) on which the algorithms will be tested, is presented in section II. The system representation and the IIR Youla-Kucera feedforward compensator structure are given in section III. The algorithms for adaptive feedforward compensation will be developed in section IV and analyzed in section V. Section VI will present experimental results obtained on the AVC system with the algorithms introduced in this paper as well as an experimental comparison with those given in [14], [15]. Section VII will summarize the comparison with other algorithms.

II. AN ACTIVE VIBRATION CONTROL SYSTEM USING AN INERTIAL ACTUATOR

Figures 1 and 2 show an AVC system using a correlated measurement with the disturbance and an inertial actuator for reducing the residual acceleration. The corresponding block diagrams in open loop operation and with the compensator system are shown in Figures 3(a) and 3(b), respectively. The structure is representative for a number of situations encountered in practice (see [12]). It consists on five metal plates (in dural of 1.8 Kg each one) connected by springs. The uppermost and lowermost ones are rigidly jointed together by four screws. The middle three plates will be labeled for easier referencing M1, M2 and M3 (see figure 2). M1 and M3 are equipped with inertial actuators. The one on M1 serves as disturbance generator (inertial actuator I in figure 2), the one at the bottom serves for disturbance compensation (inertial actuator II in figure 2). Inertial actuators use a similar

principle as loudspeakers (see [20], [21]). The correlated measurement with the disturbance (image of the disturbance) is obtained from an accelerometer which is positioned on plate M1. Another sensor of the same type is positioned on plate M3 and serves for measuring the residual acceleration (see figure 2). The objective is to minimize the residual acceleration measured on plate M3.

When the compensator system is active, the actuator acts upon the residual acceleration, but also upon the measurement of the image of the disturbance through the *reverse path* (a positive feedback coupling). The measured quantity $\hat{y}(t)$ will be the sum of the correlated disturbance measurement $w(t)$ obtained in the absence of the feedforward compensation (see figure 3(a)) and of the effect of the actuator used for compensation. The disturbance is the position of the mobile part of the inertial actuator (see figures 1 and 2) located on top of the structure. The input to the compensator system is the position of the mobile part of the inertial actuator located on the bottom of the structure. The input to the inertial actuators being a position, the global primary path, the secondary path, and the reverse path have a double differentiator behavior. Similar internal positive feedback coupling occur also in feedforward ANC ([4], [6]).

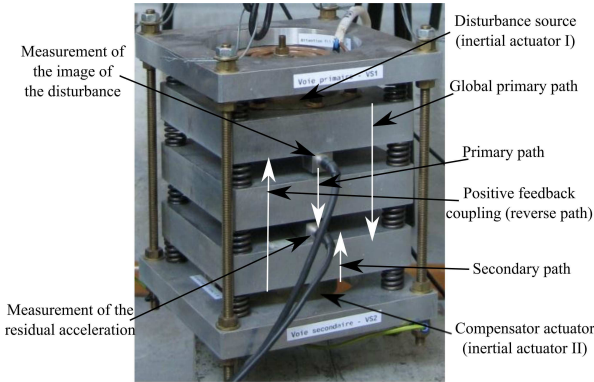


Fig. 1. An AVC system using a feedforward compensation - photo.

In figure 3(b), $\hat{y}(t)$ denotes the effective output provided by the measurement device and which will serve as input to the adaptive feedforward filter \hat{N} . The output of this filter denoted by $\hat{u}(t)$ is applied to the actuator through an amplifier. The transfer function G (the secondary path) characterizes

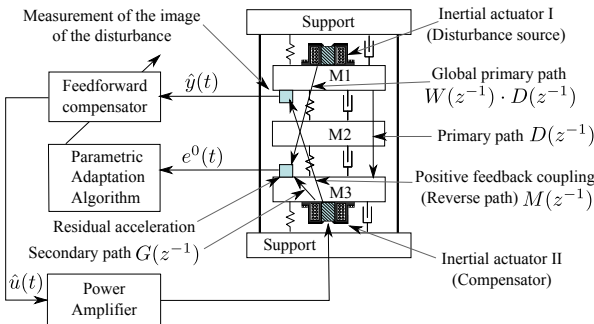


Fig. 2. An AVC system using a feedforward compensation - schema.

the dynamics from the output of the filter \hat{N} to the residual acceleration measurement (amplifier + actuator + dynamics of the mechanical system). The transfer function D between $w(t)$ and the measurement of the residual acceleration (in open loop operation) characterizes the primary path.

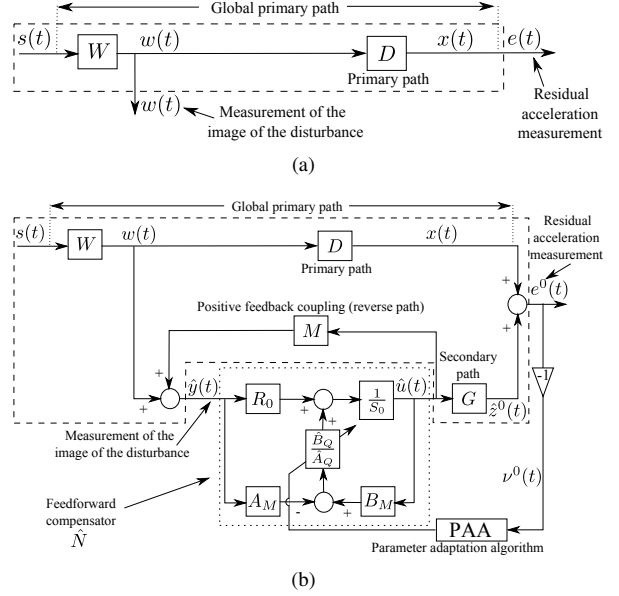


Fig. 3. Feedforward AVC: in open loop (a) and with adaptive feedforward compensator (b).

The coupling between the output of the filter and the measurement $\hat{y}(t)$ through the compensator actuator is denoted by M . As indicated in figure 3(b) this coupling is a "positive" feedback. This unwanted coupling raises problems in practice (source of instabilities) and makes the analysis of adaptive (estimation) algorithms more difficult. The system shown in figure 3(b) can be represented in the standard feedback form shown in Figure 4 (for details see Section III).

At this stage it is important to make the following remarks, when the feedforward filter is absent (open loop operation):

- very reliable models for the secondary path and the "positive" feedback path can be identified by applying appropriate excitation on the actuator used for compensation;
- an initial estimation of the primary path transfer function can be obtained using the measured $w(t)$ as input and $e(t)$ as output (the compensator actuator being at rest);
- the design of a fixed model based stabilizing feedforward compensator requires the knowledge of the reverse path model only;
- the adaptation algorithms do not use information upon the primary path whose characteristics may be unknown or subject to change;
- the knowledge of the disturbance characteristics and of the primary path model in addition of the secondary and reverse paths models is mandatory for the design of an optimal fixed model based feedforward compensator ([11], [12]).

The objective is to develop stable recursive algorithms for adaptation of the parameters of the feedforward filter com-

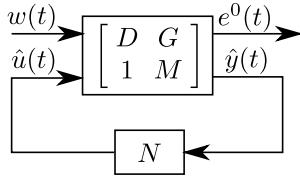


Fig. 4. Feedback representation of the system shown in Figure 3(b).

pensator such that the measured residual error (acceleration or force in AVC, noise in ANC) be minimized in the sense of a certain criterion while simultaneously assuring the stability of the internal positive feedback loop. This has to be done for broadband disturbances $w(t)$ (or $s(t)$) with unknown and variable spectral characteristics and an unknown primary path model⁴.

III. BASIC EQUATIONS AND NOTATIONS

The block diagrams associated with an AVC system are shown in fig. 3 in open loop (3(a)) and when an IIR (Infinite Impulse Response) Youla-Kucera compensator is active (3(b)).

The primary (D), secondary (G), and reverse (positive coupling) (M) paths represented in fig. 3(b) are characterized by the asymptotically stable transfer operators:

$$X(q^{-1}) = \frac{B_X(q^{-1})}{A_X(q^{-1})} = \frac{b_1^X q^{-1} + \dots + b_{n_{B_X}}^X q^{-n_{B_X}}}{1 + a_1^X q^{-1} + \dots + a_{n_{A_X}}^X q^{-n_{A_X}}}, \quad (1)$$

with $B_X = q^{-1}B_X^*$ for any $X \in \{D, G, M\}$. $\hat{G} = \frac{\hat{B}_G}{\hat{A}_G}$, $\hat{M} = \frac{\hat{B}_M}{\hat{A}_M}$, and $\hat{D} = \frac{\hat{B}_D}{\hat{A}_D}$ denote the identified (estimated) models of G , M , and D .

The equations associated with the feedback system representation shown in figure 4 are:

$$\begin{bmatrix} e^0(t) \\ \hat{y}(t) \end{bmatrix} = \begin{bmatrix} P_{11} & P_{12} \\ P_{21} & P_{22} \end{bmatrix} \begin{bmatrix} w(t) \\ \hat{u}(t) \end{bmatrix} = \begin{bmatrix} D & G \\ 1 & M \end{bmatrix} \begin{bmatrix} w(t) \\ \hat{u}(t) \end{bmatrix}, \quad (2)$$

where $e^0(t)$ is the performance variable to be minimized (residual acceleration), $\hat{y}(t)$ is the measured variable (image of the disturbance), $w(t)$ is the disturbance ($w(t) = W(q^{-1})s(t)$), and $\hat{u}(t)$ is the control input⁵.

The optimal IIR feedforward compensator which will minimize the residual acceleration can be written, using the Youla-Kucera parametrization, as

$$N(q^{-1}) = \frac{R(q^{-1})}{S(q^{-1})} = \frac{A_Q(q^{-1})R_0(q^{-1}) - B_Q(q^{-1})A_M(q^{-1})}{A_Q(q^{-1})S_0(q^{-1}) - B_Q(q^{-1})B_M(q^{-1})} \quad (3)$$

where the optimal polynomial $Q(q^{-1})$ has an IIR structure

$$Q(q^{-1}) = \frac{B_Q(q^{-1})}{A_Q(q^{-1})} = \frac{b_0^Q + b_1^Q q^{-1} + \dots + b_{n_{B_Q}}^Q q^{-n_{B_Q}}}{1 + a_1^Q q^{-1} + \dots + a_{n_{A_Q}}^Q q^{-n_{A_Q}}} \quad (4)$$

⁴Variations of the unknown model W , the transfer function between the disturbance $s(t)$ and $w(t)$ are equivalent to variations of the spectral characteristics of $s(t)$.

⁵If $w(t)$ is not measured $P_{21} = 0$. If there is no internal positive coupling $M = 0$.

and $R_0(q^{-1})$, $S_0(q^{-1}) = 1 + q^{-1}S_0^*(q^{-1})$ are the polynomials of the central (stabilizing) filter and $A_M(q^{-1})$, $B_M(q^{-1})$ are given in (1)⁶.

The estimated QIIR filter is denoted by $\hat{Q}(q^{-1})$ or $\hat{Q}(\hat{\theta}, q^{-1})$ when it is a linear filter with constant coefficients or $\hat{Q}(t, q^{-1})$ during estimation (adaptation). The vector of parameters of the optimal QIIR filter assuring perfect matching will be denoted by

$$\theta^T = [b_0^Q, \dots, b_{n_{B_Q}}^Q, a_1^Q, \dots, a_{n_{A_Q}}^Q] = [\theta_{B_Q}^T, \theta_{A_Q}^T]. \quad (5)$$

The vector of parameters for the estimated \hat{Q} IIR filter

$$\hat{Q}(q^{-1}) = \frac{\hat{B}_Q(q^{-1})}{\hat{A}_Q(q^{-1})} = \frac{\hat{b}_0^Q + \hat{b}_1^Q q^{-1} + \dots + \hat{b}_{n_{B_Q}}^Q q^{-n_{B_Q}}}{1 + \hat{a}_1^Q q^{-1} + \dots + \hat{a}_{n_{A_Q}}^Q q^{-n_{A_Q}}} \quad (6)$$

is denoted by

$$\hat{\theta}^T = [\hat{b}_0^Q, \dots, \hat{b}_{n_{B_Q}}^Q, \hat{a}_1^Q, \dots, \hat{a}_{n_{A_Q}}^Q] = [\hat{\theta}_{B_Q}^T, \hat{\theta}_{A_Q}^T]. \quad (7)$$

The input of the feedforward filter (called also reference) is denoted by $\hat{y}(t)$ and it corresponds to the measurement provided by the primary transducer (force or acceleration transducer in AVC or a microphone in ANC). In the absence of the compensation loop (open loop operation) $\hat{y}(t) = w(t)$. The output of the feedforward compensator (which is the control signal applied to the secondary path) is denoted by $\hat{u}(t+1) = \hat{u}(t+1/\hat{\theta}(t+1))$ (a posteriori output)⁷.

The "a priori" output of the estimated feedforward compensator using an YKIIR parametrization for the case of time varying parameter estimates is given by (using eq. (3))

$$\begin{aligned} \hat{u}^0(t+1) &= \hat{u}(t+1/\hat{\theta}(t)) = -\hat{S}^*(t, q^{-1})\hat{u}(t) + \hat{R}(t, q^{-1})\hat{y}(t+1) \\ &= -(\hat{A}_Q(t, q^{-1})S_0)^*\hat{u}(t) + \hat{A}_Q(t, q^{-1})R_0\hat{y}(t+1) \\ &\quad + \hat{B}_Q(t, q^{-1})(B_M^*\hat{u}(t) - A_M\hat{y}(t+1)), \end{aligned} \quad (8)$$

where

$$\begin{aligned} \hat{u}(t+1) &= -(\hat{A}_Q(t+1, q^{-1})S_0)^*\hat{u}(t) + \hat{A}_Q(t+1, q^{-1})R_0\hat{y}(t+1) \\ &\quad + \hat{B}_Q(t+1, q^{-1})(B_M^*\hat{u}(t) - A_M\hat{y}(t+1)). \end{aligned} \quad (9)$$

It should be observed that eqs. (3), (4), (8), and (9) can be easily particularized for the case of a FIR Youla-Kucera parametrization by taking $\hat{A}_Q(t, q^{-1}) \equiv 1$.

The measured input to the feedforward filter can also be written as

$$\hat{y}(t+1) = w(t+1) + \frac{B_M^*(q^{-1})}{A_M(q^{-1})}\hat{u}(t). \quad (10)$$

The unmeasurable value of the output of the primary path (when the compensation is active) is denoted $x(t)$. The "a priori" output of the secondary path will be denoted $\hat{z}^0(t+1) = \hat{z}(t+1/\hat{\theta}(t))$ while its input is $\hat{u}(t)$. One has

$$\hat{z}^0(t+1) = \frac{B_G^*(q^{-1})}{A_G(q^{-1})}\hat{u}(t) = \frac{B_G^*(q^{-1})}{A_G(q^{-1})}\hat{u}(t/\hat{\theta}(t)), \quad (11)$$

⁶The following notation for polynomials will be used throughout this paper: $A(q^{-1}) = a_0 + \sum_{i=1}^{n_A} a_i q^{-i} = a_0 + q^{-1}A^*(q^{-1})$.

⁷In adaptive control and estimation the predicted output at $t+1$ can be computed either on the basis of the previous parameter estimates (a priori) or on the basis of the current parameter estimates (a posteriori).

where $\hat{\theta}(t)$ is the vector of estimated parameters given in (7). The measured residual acceleration (or force) satisfies the following equation

$$e^0(t+1) = x(t+1) + \hat{z}^0(t+1). \quad (12)$$

The "a priori" adaptation error is defined as

$$\nu^0(t+1) = \nu(t+1/\hat{\theta}(t)) = -e^0(t+1) = -x(t+1) - \hat{z}^0(t+1). \quad (13)$$

The "a posteriori" unmeasurable (but computable) adaptation error is given by

$$\nu(t+1) = \nu(t+1/\hat{\theta}(t+1)) = -e(t+1) = -x(t+1) - \hat{z}(t+1). \quad (14)$$

where the "a posteriori" value of the output of the secondary path $\hat{z}(t+1)$ (dummy variable) is given by

$$\hat{z}(t+1) = \hat{z}(t+1/\hat{\theta}(t+1)) = \frac{B_G^*(q^{-1})}{A_G(q^{-1})} \hat{u}(t/\hat{\theta}(t+1)). \quad (15)$$

For compensators with constant parameters $\nu^0(t) = \nu(t)$, $e^0(t) = e(t)$, $\hat{z}^0(t) = \hat{z}(t)$, $\hat{u}^0(t) = \hat{u}(t)$.

The objective is to develop stable recursive algorithms for adaptation of the parameters of the Q filter such that the measured residual error (acceleration or force in AVC, noise in ANC) be minimized in the sense of a certain criterion. This has to be done for broadband disturbances $w(t)$ (or $s(t)$) with unknown and variable spectral characteristics and an unknown primary path model.

IV. DEVELOPMENT OF THE ALGORITHMS

The algorithm for adaptive feedforward YKIIR compensators will be developed under the following hypotheses:

- 1) H1 - The signal $w(t)$ is bounded (which is equivalently to say that $s(t)$ is bounded and $W(q^{-1})$ in figure 3 is asymptotically stable).
- 2) H2 - There exists a central feedforward compensator N_0 (R_0 , S_0) which stabilizes the inner positive feedback loop formed by N_0 and M and the characteristic polynomial of the closed loop⁸

$$P_0(z^{-1}) = A_M(z^{-1})S_0(z^{-1}) - B_M(z^{-1})R_0(z^{-1})$$

is a Hurwitz polynomial.

- 3) H3 - (Perfect matching condition) There exists a value of the Q parameters such that

$$\frac{G \cdot A_M(R_0 A_Q - A_M B_Q)}{A_Q(A_M S_0 - B_M R_0)} = -D. \quad (16)$$

- 4) H4 - The effect of the measurement noise upon the measurement of the residual acceleration is neglected (deterministic context).

Once the algorithm will be developed under these hypotheses, H3 and H4 will be removed and the algorithm will be analyzed in this modified context.

A first step in the development of the algorithms is to establish for a fixed estimated compensator a relation between

the error on the Q-parameters (with respect to the optimal values) and the adaptation error ν . This is summarized in the following Lemma.

Lemma 4.1: Under the hypothesis H1 through H4 for the system described by equations (1) through (15) using an estimated IIR Youla-Kucera parameterized feedforward compensator with constant parameters one has:

$$\nu(t+1/\hat{\theta}) = \frac{A_M(q^{-1})G(q^{-1})}{A_Q(q^{-1})P_0(q^{-1})} [\theta - \hat{\theta}]^T \phi(t), \quad (17)$$

with $\phi(t)$ given by:

$$\phi^T(t) = [\alpha(t+1), \alpha(t), \dots, \alpha(t-n_{B_Q}+1), \\ -\beta(t), -\beta(t-1), \dots, -\beta(t-n_{A_Q})]. \quad (18)$$

where:

$$\alpha(t+1) = B_M \hat{u}(t+1) - A_M \hat{y}(t+1) = \\ = B_M^* \hat{u}(t) - A_M \hat{y}(t+1) \quad (19a)$$

$$\beta(t) = S_0 \hat{u}(t) - R_0 \hat{y}(t). \quad (19b)$$

The proof of this lemma is given in Appendix A.

Corollary 4.1: Under the hypothesis H1 through H4 for the system described by equations (1) through (15) using an estimated FIR Youla-Kucera parameterized feedforward compensator with constant parameters one has:

$$\nu(t+1/\hat{\theta}) = \frac{A_M(q^{-1})G(q^{-1})}{P_0(q^{-1})} [\theta - \hat{\theta}]^T \phi(t), \quad (20)$$

where

$$\theta^T = [b_0^Q, \dots, b_{n_{B_Q}}^Q] = [\theta_{B_Q}^T] \quad (21)$$

is the vector of parameters of the optimal QFIR filter assuring perfect matching,

$$\hat{\theta}^T = [\hat{b}_0^Q, \dots, \hat{b}_{n_{B_Q}}^Q] = [\hat{\theta}_{B_Q}^T] \quad (22)$$

is the vector of parameters for the estimated \hat{Q} FIR filter

$$\hat{Q}(q^{-1}) = \hat{B}_Q(q^{-1}) = \hat{b}_0^Q + \hat{b}_1^Q q^{-1} + \dots + \hat{b}_{n_{B_Q}}^Q q^{-n_{B_Q}}, \quad (23)$$

and $\phi^T(t)$ is given by:

$$\phi^T(t) = [\alpha(t+1), \alpha(t), \dots, \alpha(t-n_{B_Q}+1)], \quad (24)$$

where $\alpha(t+1)$ is given in eq. (19a).

Proof: This result is straightforwardly obtained by making $\hat{A}_Q(q^{-1}) = 1$ and $A_Q(q^{-1}) = 1$ in Lemma 4.1. ■

Throughout the remainder of this section and the next one, unless stated differently, the Youla-Kucera parametrization having an QIIR filter will be discussed. It should be observed that in most of the cases results for QFIR-polynomials can be obtained by imposing $A_Q(q^{-1}) = 1$ and $\hat{A}_Q(q^{-1}) = 1$.

As it will be shown later on, it is convenient for assuring the stability of the system to filter the observation vector $\phi(t)$. Filtering the vector $\phi(t)$ through an asymptotically stable filter $L(q^{-1}) = \frac{B_L}{A_L}$, equation (17) for $\hat{\theta} = constant$ becomes

$$\nu(t+1/\hat{\theta}) = \frac{A_M(q^{-1})G(q^{-1})}{A_Q(q^{-1})P_0(q^{-1})L(q^{-1})} [\theta - \hat{\theta}]^T \phi_f(t) \quad (25)$$

⁸The parenthesis (q^{-1}) will be omitted in some of the following equations to make them more compact.

with

$$\begin{aligned} \phi_f(t) = L(q^{-1})\phi(t) = & [\alpha_f(t+1), \dots, \alpha_f(t-n_{B_Q}+1), \\ & \beta_f(t), \beta_f(t-1), \dots, \beta_f(t-n_{A_Q})] \end{aligned} \quad (26)$$

where

$$\begin{aligned} \alpha_f(t+1) &= L(q^{-1})\alpha(t+1) \\ \beta_f(t) &= L(q^{-1})\beta(t). \end{aligned} \quad (27)$$

Equation (25) will be used to develop the adaptation algorithms. When the parameters of \hat{Q} evolve over time and neglecting the non-commutativity of the time varying operators (which implies slow adaptation (see [22]), i.e., a limited value for the adaptation gain), equation (25) transforms into⁹

$$\nu(t+1)\hat{\theta}(t+1) = \frac{A_M(q^{-1})G(q^{-1})}{A_Q(q^{-1})P_0(q^{-1})L(q^{-1})}[\theta - \hat{\theta}(t+1)]^T \phi_f(t). \quad (28)$$

Equation (28) has the standard form for an a-posteriori adaptation error ([23]), which immediately suggests to use the following PAA:

$$\hat{\theta}(t+1) = \hat{\theta}(t) + F(t)\psi(t)\nu(t+1); \quad (29a)$$

$$\nu(t+1) = \frac{\nu^0(t+1)}{1 + \psi^T(t)F(t)\psi(t)}; \quad (29b)$$

$$F(t+1) = \frac{1}{\lambda_1(t)} \left[F(t) - \frac{F(t)\psi(t)\psi^T(t)F(t)}{\frac{\lambda_1(t)}{\lambda_2(t)} + \psi^T(t)F(t)\psi(t)} \right] \quad (29c)$$

$$1 \geq \lambda_1(t) > 0; 0 \leq \lambda_2(t) < 2; F(0) > 0 \quad (29d)$$

$$\psi(t) = \phi_f(t), \quad (29e)$$

where $\lambda_1(t)$ and $\lambda_2(t)$ allow to obtain various profiles for the matrix adaptation gain $F(t)$ (see section VI and [23]). By taking $\lambda_2(t) \equiv 0$ and $\lambda_1(t) \equiv 1$, one gets a constant adaptation gain matrix (and choosing $F = \gamma I$, $\gamma > 0$ one gets a scalar adaptation gain).

Several choices for the filter L will be considered, leading to different algorithms:

$$\text{Algorithm I} \quad L = G$$

$$\text{Algorithm IIa} \quad L = \hat{G}$$

$$\text{Algorithm IIb} \quad L = \frac{\hat{A}_M}{\hat{P}_0} \hat{G}$$

Algorithm III

$$L = \frac{\hat{A}_M}{\hat{P}} \hat{G} \quad (30)$$

with

$$\hat{P} = \hat{A}_Q(\hat{A}_M S_0 - \hat{B}_M R_0) = \hat{A}_Q \hat{P}_0, \quad (31)$$

where \hat{A}_Q is an estimation of the denominator of the ideal QIIR filter computed on the basis of available estimates of the parameters of the filter \hat{Q} . For the Algorithm III several options for updating \hat{A}_Q can be considered:

- Run Algorithm IIa or IIb for a certain time to get an estimate of \hat{A}_Q
- Run a simulation (using the identified models)
- Update \hat{A}_Q at each sampling instant or from time to time using Algorithm III (after a short initialization horizon using Algorithm IIa or IIb)

⁹However, exact algorithms can be developed taking into account the non-commutativity of the time varying operators - see [23].

The following procedure is applied at each sampling time for *adaptive* or *self-tuning* operation:

- 1) Get the measured image of the disturbance $\hat{y}(t+1)$, the measured residual error $e^0(t+1)$ and compute $\nu^0(t+1) = -e^0(t+1)$.
- 2) Compute $\phi(t)$ and $\phi_f(t)$ using (18) and (26).
- 3) Estimate the parameter vector $\hat{\theta}(t+1)$ using the parametric adaptation algorithm (29a) through (29e).
- 4) Compute (using (9)) and apply the control.

V. ANALYSIS OF THE ALGORITHMS

A. The Deterministic Case - Perfect Matching

For algorithms I, IIa, IIb and III the equation for the a-posteriori adaptation error has the form:

$$\nu(t+1) = H(q^{-1})[\theta - \hat{\theta}(t+1)]^T \psi(t), \quad (32)$$

where

$$H(q^{-1}) = \frac{A_M(q^{-1})G(q^{-1})}{A_Q(q^{-1})P_0(q^{-1})L(q^{-1})}, \psi = \phi_f. \quad (33)$$

Neglecting the non-commutativity of time varying operators, one has the following result:

Lemma 5.1: Assuming that eq. (32) represents the evolution of the a posteriori adaptation error when using an IIR Youla-Kucera adaptive feedforward compensator and that the PAA (29a) through (29e) is used, one has:

$$\lim_{t \rightarrow \infty} \nu(t+1) = 0 \quad (34)$$

$$\lim_{t \rightarrow \infty} \psi(t)[\theta - \hat{\theta}(t+1)] = 0 \quad (35)$$

$$\lim_{t \rightarrow \infty} \frac{[\nu^0(t+1)]^2}{1 + \psi(t)^T F(t) \psi(t)} = 0 \quad (36)$$

$$\|\psi(t)\| \text{ is bounded} \quad (37)$$

$$\lim_{t \rightarrow \infty} \nu^0(t+1) = 0 \quad (38)$$

for any initial conditions $\hat{\theta}(0)$, $\nu^0(0)$, $F(0)$, provided that

$$H'(z^{-1}) = H(z^{-1}) - \frac{\lambda_2}{2}, \max_t [\lambda_2(t)] \leq \lambda_2 < 2 \quad (39)$$

is a SPR transfer function.

The proof of this lemma is given in Appendix B. This result can be particularized for the case of FIR Youla-Kucera adaptive compensators by using the following corollary:

Corollary 5.1: Assuming that eq. (32) represents the evolution of the a posteriori adaptation error for FIR Youla - Kucera adaptive feedforward compensators, where

$$H(q^{-1}) = \frac{A_M(q^{-1})G(q^{-1})}{P_0(q^{-1})L(q^{-1})}, \psi = \phi_f, \quad (40)$$

$$\phi_f(t) = L(q^{-1})\phi(t) = [\alpha_f(t+1), \dots, \alpha_f(t-n_{B_Q}+1)],$$

and that the PAA (29a) through (29e) is used with $\hat{\theta}(t)$ given by (22), then (34) through (38) hold for any initial conditions $\hat{\theta}(0)$, $\nu^0(0)$, $F(0)$, provided that

$$H'(z^{-1}) = H(z^{-1}) - \frac{\lambda_2}{2}, \max_t [\lambda_2(t)] \leq \lambda_2 < 2 \quad (41)$$

is a SPR transfer function.

The proof is similar to that of Lemma 5.1 and will be omitted.

Remark 1: Using Algorithm III and taking into account eq. (30), the stability condition for $\lambda_2 = 1$ can be transformed into ([13], [24]):

$$\left| \left(\frac{A_M}{\hat{A}_M} \cdot \frac{\hat{A}_Q}{A_Q} \cdot \frac{\hat{P}_0}{P_0} \cdot \frac{G}{\hat{G}} \right)^{-1} - 1 \right| < 1 \quad (42)$$

for all ω . This roughly means that it always holds provided that the estimates of A_M , A_Q , P_0 , and G are close to the true values (i.e. $H(e^{-j\omega})$ in this case is close to a unit transfer function).

Remark 2: For the case of constant adaptation gain ($F = \alpha I = \text{const.}$) and using Algorithm III, eq. (29a) can be viewed as an approximation of the gradient algorithm. For constant adaptation gain $\lambda_2(t) \equiv 0$ and the strict positive realness on $H'(z^{-1})$ implies at all the frequencies

$$-90^\circ < \angle \frac{A_M(e^{-j\omega})G(e^{-j\omega})}{A_Q(e^{-j\omega})P_0(e^{-j\omega})} - \angle \frac{\hat{A}_M(e^{-j\omega})\hat{G}(e^{-j\omega})}{\hat{A}_Q(e^{-j\omega})\hat{P}_0(e^{-j\omega})} < 90^\circ. \quad (43)$$

Therefore the interpretation of the SPR condition of Lemma 5.1 is that the angle between the direction of adaptation and the direction of the inverse of the true gradient (not computable) should be less than 90° . For time-varying adaptation gains the condition is sharper since in this case $\text{Re}\{H(e^{-j\omega})\}$ should be larger than $\frac{\lambda_2}{2}$ at all frequencies.

Remark 3: Eq. (35) indicates that the estimated parameters of the feedforward compensator converge toward the domain $D_C = \{\hat{\theta} : \psi^T(t, \hat{\theta})(\theta - \hat{\theta}) = 0\}$. If furthermore $\psi^T(t, \hat{\theta})(\theta - \hat{\theta}) = 0$ has a unique solution (richness condition), then $\lim_{t \rightarrow \infty} \hat{\theta}(t) = \theta$.

Remark 4: The poles of the estimated Q filter (the roots of \hat{A}_Q), which are also poles of the internal positive closed loop, will be asymptotically inside the unit circle, if the SPR condition is satisfied. However, transiently they may be outside the unit circle. It is possible to force these poles to remain inside of the unit circle during transient using adaptive algorithms with projection (see [23]). However, the SPR condition remains the same.

B. The Stochastic Case - Perfect Matching

There are two sources of measurement noise, one acting on the primary transducer which gives the correlated measurement with the disturbance and the second acting on the measurement of the residual error (force, acceleration). For the primary transducer the effect of the measurement noise is negligible since the signal to noise ratio is very high. The situation is different for the residual error where the effect of the noise can not be neglected.

In the presence of the measurement noise ($n(t)$), the equation of the a-posteriori residual error becomes

$$\nu(t+1) = H(q^{-1})[\theta - \hat{\theta}(t+1)]^T \psi(t) + n(t+1). \quad (44)$$

In this context, we should analyze the asymptotic behavior of the adaptation algorithms (i.e., the convergence points in the parameter space). The O.D.E. method [13], [24] can be used

to analyse the asymptotic behavior of the algorithm in the presence of noise. Taking into account the form of equation (44), one can directly use Theorem 4.1 of [23] or Theorem B1 of [25].

The following assumptions will be made:

- 1) $\lambda_1(t) = 1$ and $\lambda_2(t) = \lambda_2 > 0$ (decreasing adaptation gain)
- 2) $\hat{\theta}(t)$ generated by the algorithm belongs infinitely often to the domain D_S :

$$D_S \triangleq \{\hat{\theta} : \hat{P}(z^{-1}) = 0 \Rightarrow |z| < 1\}$$

for which stationary processes:

$$\psi(t, \hat{\theta}) \triangleq \psi(t)|_{\hat{\theta}(t)=\hat{\theta}=\text{const}}$$

$$e(t, \hat{\theta}) = e(t)|_{\hat{\theta}(t)=\hat{\theta}=\text{const}}$$

can be defined.

- 3) $n(t)$ is a zero mean stochastic process with finite moments and independent of the sequence $d(t)$.

From (44) for $\hat{\theta}(t) = \hat{\theta}$, one gets

$$\nu(t+1, \hat{\theta}) = H(q^{-1})[\theta - \hat{\theta}]^T \psi(t, \hat{\theta}) + n(t+1). \quad (45)$$

Since $\psi(t, \hat{\theta})$ depends upon $w(t)$ only, one concludes that $\psi(t, \hat{\theta})$ and $n(t+1)$ are independent. Therefore using Theorem 4.1 from [23] it results that if

$$H'(z^{-1}) = \frac{A_M(z^{-1})G(z^{-1})}{A_Q(z^{-1})P_0(z^{-1})L(z^{-1})} - \frac{\lambda_2}{2} \quad (46)$$

is a SPR transfer function, one has $\text{Prob}\{\lim_{t \rightarrow \infty} \hat{\theta}(t) \in D_C\} = 1$.

If furthermore $\psi^T(t, \hat{\theta})(\theta - \hat{\theta}) = 0$ has a unique solution (richness condition), then $\text{Prob}\{\lim_{t \rightarrow \infty} \hat{\theta}(t) = \theta\} = 1$. Therefore one can say that the parameters of the estimated feedforward compensator will converge to the same value as for the case without noise.

C. The Case of Non-Perfect Matching

If $\hat{Q}(t, q^{-1})$ does not have the appropriate dimension there is no chance to satisfy the perfect matching condition. Two questions are of interest in this case:

- 1) The boundedness of the residual error;
- 2) The bias distribution in the frequency domain.

1) *Boundedness of the residual error:* For analyzing the boundedness of the residual error, results from [25], [26], can be used. The following assumptions are made:

- 1) There exists a reduced order filter \hat{N} characterized by the unknown polynomials \hat{A}_Q (of order n_{A_Q}) and \hat{B}_Q (of order n_{B_Q}) as described in eq. (3), for which the closed loop formed by \hat{N} and M is asymptotically stable, i.e. $\hat{A}_Q(A_M S_0 - B_M R_0)$ is a Hurwitz polynomial;
- 2) The output of the optimal filter satisfying the matching condition can be expressed as:

$$\hat{u}(t+1) = -[\hat{S}^*(q^{-1})\hat{u}(t) - \hat{R}(q^{-1})\hat{y}(t+1) + \eta(t+1)] \quad (47)$$

where $\eta(t+1)$ is a norm bounded signal.

Using the results of [25] (Theorem 4.1 pp. 1505-1506) and assuming that $w(t)$ is norm bounded, it can be shown that all the signals are norm bounded under the passivity condition (39), where P is computed now with the reduced order estimated filter.

2) *Bias distribution*: Using the Parseval's relation, the asymptotic bias distribution of the estimated parameters in the frequency domain can be obtained starting from the expression of $\nu(t)$, by taking into account that the algorithm minimizes (almost) a criterion of the form $\lim_{N \rightarrow \infty} \frac{1}{N} \sum_{t=1}^N \nu^2(t)$. Using eq. (16), the bias distribution (for algorithm *III*) will be given by

$$\hat{\theta}^* = \arg \min_{\hat{\theta}} \int_{-\pi}^{\pi} \left[|D(e^{-j\omega}) + \frac{\hat{N}(e^{-j\omega})G(e^{-j\omega})}{1 - \hat{N}(e^{-j\omega})M(e^{-j\omega})}|^2 \phi_w(\omega) + \phi_n(\omega) \right] d\omega \quad (48)$$

where ϕ_w and ϕ_n are the spectral densities of the disturbance $w(t)$ and of the measurement noise. Taking into account equation (16), one obtains

$$\hat{\theta}^* = \arg \min_{\hat{\theta}} \int_{-\pi}^{\pi} \left[\left| \frac{GA_M^2}{P_0} \right|^2 \frac{B_Q}{A_Q} - \frac{\hat{B}_Q}{\hat{A}_Q} \right]^2 \phi_w(\omega) + \phi_n(\omega) \right] d\omega. \quad (49)$$

From (49) one concludes that a good approximation of Q filter will be obtained in the frequency region where ϕ_w is significant and where G has a high gain (usually G should have high gain in the frequency region where ϕ_w is significant in order to counteract the effect of $w(t)$). However the quality of the estimated \hat{Q} filter will be affected also by the transfer function $\frac{A_M^2}{P_0}$.

D. Relaxing the Positive Real Condition

It is possible to relax the SPR conditions taking into account that:

- 1) The disturbance (input to the system) is a broadband signal;
- 2) Most of the adaptation algorithms work with a low adaptation gain.

Under these two assumptions, the behavior of the algorithm can be well described by the "averaging theory" developed in [22] and [13] (see also [23]).

When using the averaging approach, the basic assumption of a slow adaptation holds for small adaptation gains (constant and scalar in [22] i.e. $\lambda_2(t) \equiv 0, \lambda_1(t) = 1$; matrix and time decreasing asymptotically in [13], [23] i.e. $\lim_{t \rightarrow \infty} \lambda_1(t) = 1, \lambda_2(t) = \lambda_2 > 0$).

In the context of averaging, the basic condition for stability is that:

$$\lim_{N \rightarrow \infty} \frac{1}{N} \sum_{t=1}^N \psi(t) H'(q^{-1}) \psi^T(t) = \frac{1}{2} \int_{-\pi}^{\pi} \Psi(e^{j\omega}) [H'(e^{j\omega}) + H'(e^{-j\omega})] \Psi^T(e^{-j\omega}) d\omega > 0 \quad (50)$$

be a positive definite matrix ($\Psi(e^{j\omega})$ is the Fourier transform of $\psi(t)$).

One can view (50) as the weighted energy of the observation vector ψ . Of course the SPR sufficient condition upon $H'(z^{-1})$ (see Equation 39) allows to satisfy this condition. However in the averaging context it is only needed that (50) is true which allows that H' be non positive real in a limited frequency band. Expression (50) can be re-written as follows ([14]):

$$\int_{-\pi}^{\pi} \psi(e^{j\omega}) [H' + H'^*] \psi^T(e^{-j\omega}) d\omega = \sum_{i=1}^r \int_{\alpha_i}^{\alpha_i + \Delta_i} \psi(e^{j\omega}) [H' + H'^*] \psi^T(e^{-j\omega}) d\omega - \sum_{j=1}^p \int_{\beta_j}^{\beta_j + \Delta_j} \psi(e^{j\omega}) [\bar{H}' + \bar{H}'^*] \psi^T(e^{-j\omega}) d\omega > 0 \quad (51)$$

where H' is SPR in the frequency intervals $[\alpha_i, \alpha_i + \Delta_i]$ and $\bar{H}' = -H'$ is positive real in the frequencies intervals $[\beta_j, \beta_j + \Delta_j]$ (H'^* denotes the complex conjugate of H'). The conclusion is that H' does not need to be SPR. It is enough that the "positive" weighted energy exceeds the "negative" weighted energy. This explains why algorithms *I*, *IIa* and *IIb* will work in practice in most of the cases. It is however important to remark that if the disturbance is a single sinusoid (which violates the hypothesis of broadband disturbance) located in the frequency region where H' is not SPR, the algorithm may diverge (see [13], [22]). It was observed that despite satisfaction of condition (51) which will assure the stability of the system, attenuation is not very good in the frequency regions where the positive real condition (41) is violated.

Without doubt, the best approach for relaxing the SPR conditions is to use algorithm *III* (given in eq. (30)) instead of algorithm *IIa* or *IIb*. This is motivated by eq. (42). As it will be shown experimentally, this algorithm gives the best results.

E. Summary of the algorithms

Table I summarizes the structure of the algorithms and the stability and convergence conditions for the algorithms developed in this paper with matrix and scalar adaptation gain for IIR Youla-Kucera feedforward compensators, for FIR Youla-Kucera feedforward compensators ([15]) and for IIR adaptive feedforward compensators introduced in [14]. These two references take also into account the internal positive feedback. Concerning algorithms for IIR adaptive feedforward compensators, the algorithms introduced in [6] and the FULMS algorithms ([8]) can be viewed as particular cases of those introduced in [14].

It was not possible to give in table I all the options for the adaptation gain. However basic characteristics for adaptive operation (non vanishing adaptation gain) and self-tuning operation (vanishing adaptation gain) have been provided¹⁰.

VI. EXPERIMENTAL RESULTS

The detailed description of the system used for the experiments has been given in section II and a photo of the mechanical structure is shown in figure 1.

¹⁰Convergence analysis can be applied only for vanishing adaptation gains.

TABLE I
 COMPARISON OF ALGORITHMS FOR ADAPTIVE FEEDFORWARD COMPENSATION IN AVC WITH MECHANICAL COUPLING

	YKIIR	YKFIR	[14]	YKIIR	YKFIR	[14]
	Matrix gain			Scalar gain		
$\hat{\theta}(t+1) =$	$\hat{\theta}(t) + F(t)\psi(t) \frac{\nu^0(t+1)}{1+\psi^T(t)F(t)\psi(t)}$			$\hat{\theta}(t) + \gamma(t)\psi(t) \frac{\nu^0(t+1)}{1+\gamma(t)\psi^T(t)\psi(t)}$		
Adapt. gain	$F(t+1)^{-1} = \lambda_1(t)F(t) + \lambda_2(t)\psi(t)\psi^T(t)$ $0 \leq \lambda_1(t) < 1, 0 \leq \lambda_2(t) < 2, F(0) > 0$			$\gamma(t) > 0$		
Adaptive	Decr. gain and const. trace			$\gamma(t) = \gamma = const$		
Self tuning	$\lambda_2 = const., \lim_{t \rightarrow \infty} \lambda_1(t) = 1$			$\sum_{t=1}^{\infty} \gamma(t) = \infty, \lim_{t \rightarrow \infty} \gamma(t) = 0$		
$\hat{\theta}(t) =$	$[\hat{b}_0^Q, \dots, \hat{a}_1^Q, \dots]$	$[\hat{b}_0^Q, \dots]$	$[-\hat{s}_1(t), \dots, \hat{r}_0(t), \dots]$	$[\hat{b}_0^Q, \dots, \hat{a}_1^Q, \dots]$	$[\hat{b}_0^Q, \dots]$	$[-\hat{s}_1(t), \dots, \hat{r}_0(t), \dots]$
$\phi^T(t) =$	$[\alpha(t+1), \dots, \beta(t), \dots]$ $\alpha(t) = B_M \hat{u}(t) - A_M \hat{y}(t)$ $\beta(t) = R_0 \hat{y}(t) - S_0 \hat{u}(t)$	$[\alpha(t+1), \dots]$ $\alpha(t) = B_M \hat{u}(t)$ $-A_M \hat{y}(t)$	$[-\hat{u}(t), \dots]$ $\hat{y}(t+1), \dots]$	$[\alpha(t+1), \dots, \beta(t), \dots]$ $\alpha(t) = B_M \hat{u}(t) - A_M \hat{y}(t)$ $\beta(t) = R_0 \hat{y}(t) - S_0 \hat{u}(t)$	$[\alpha(t+1), \dots]$ $\alpha(t) = B_M \hat{u}(t)$ $-A_M \hat{y}(t)$	$[-\hat{u}(t), \dots]$ $\hat{y}(t+1), \dots]$
$\hat{P} =$	$\hat{A}_Q(\hat{A}_M S_0 - \hat{B}_M R_0)$	$\hat{A}_M S_0 - \hat{B}_M R_0$	$\hat{A}_M \hat{S} - \hat{B}_M \hat{R}$	$\hat{A}_Q(\hat{A}_M S_0 - \hat{B}_M R_0)$	$\hat{A}_M S_0 - \hat{B}_M R_0$	$\hat{A}_M \hat{S} - \hat{B}_M \hat{R}$
$\hat{P} =$	$\hat{A}_Q(\hat{A}_M S_0 - \hat{B}_M R_0)$	$\hat{A}_M S_0 - \hat{B}_M R_0$	$\hat{A}_M \hat{S} - \hat{B}_M \hat{R}$	$\hat{A}_Q(\hat{A}_M S_0 - \hat{B}_M R_0)$	$\hat{A}_M S_0 - \hat{B}_M R_0$	$\hat{A}_M \hat{S} - \hat{B}_M \hat{R}$
$\psi(t) =$	$L\phi(t); L_2 = \hat{G}; L_3 = \frac{\hat{A}_M}{\hat{P}} \hat{G}$			$L\phi(t); L_2 = \hat{G}; L_3 = \frac{\hat{A}_M}{\hat{P}} \hat{G}$		
Stability condition	$\frac{\hat{A}_M \hat{G}}{\hat{P} L} - \frac{\lambda}{2} = SPR \quad (\lambda = \max \lambda_2(t))$			$\frac{\hat{A}_M \hat{G}}{\hat{P} L} = SPR$		
Conv. condition	$\frac{\hat{A}_M \hat{G}}{\hat{P} L} - \frac{\lambda}{2} = SPR \quad (\lambda = \lambda_2)$			$\frac{\hat{A}_M \hat{G}}{\hat{P} L} = SPR$		

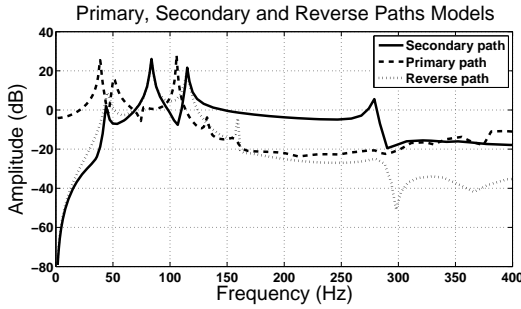


Fig. 5. Frequency characteristics of the primary, secondary and reverse paths

A. System identification

The methodology used for parametric identification of the mechanical structure's paths is similar to that of [14], [26], [27]. The sampling frequency is 800Hz .

The secondary and reverse paths have been identified in the absence of the feedforward compensator (see figure 3(b)) using as excitation signal a PRBS generated by a 10 bit shift register and a frequency divider $p = 4$ applied at the input of the amplifier feeding the inertial actuator used for compensation¹¹ (see figures 1 and 2). For the secondary path, $G(q^{-1})$, the output is the residual acceleration measurement, $e(t)$. For the reverse path, $M(q^{-1})$, the output is the signal delivered by the primary transducer (accelerometer) $\hat{y}(t)$.

The estimated orders of the model for the secondary path are $n_{B_G} = 14, n_{A_G} = 14$. The best results, in terms of validation, have been obtained with the *Recursive Extended Least Square* method. The frequency characteristic of the secondary path is shown in figure 5, solid line. It features several very low damped vibration modes. The first vibration mode is at 44Hz

¹¹It was first verified with $p = 2$ that there are no significant dynamics around 200Hz and then $p = 4$ has been chosen in order to enhance the power spectral density of the excitation in low frequencies while keeping a reasonable length for the experiment.

with a damping of 0.0212, the second at 83.8Hz with a damping of 0.00961, the third one at 115Hz with a damping of 0.00694. There is also a pair of low damped complex zeros at 108Hz with a damping of 0.021. As a consequence of the double differentiator behavior, a double zero at $z = 1$ is also present.

For the reverse path $M(q^{-1})$, the model's complexity has been estimated to be $n_{B_M} = 13, n_{A_M} = 13$. The frequency characteristic of the reverse path is shown in figure 5 (dotted line). There are several very low damped vibration modes at 45.1Hz with a damping of 0.0331, at 83.6Hz with a damping of 0.00967, at 115Hz with a damping of 0.0107 and some additional modes in high frequencies. There are two zeros on the unit circle corresponding to the double differentiator behavior. The gain of the reverse path is of the same order of magnitude as the gain of the secondary path up to 150Hz , indicating a strong feedback in this frequency zone.

The primary path has been identified in the absence of the feedforward compensator using $w(t)$ as an input and measuring $e(t)$. The disturbance $s(t)$ was a PRBS sequence ($N=10$, frequency divider $p=2$). The estimated orders of the model are $n_{B_D} = 26, n_{A_D} = 26$. The frequency characteristic is presented in figure 5 (dashed line) and may serve for simulations and detailed performance evaluation. Note that the primary path features a strong resonance at 108Hz , exactly where the secondary path has a pair of low damped complex zeros (almost no gain). Therefore one can not expect good attenuation around this frequency.

B. The central controllers and comparison objectives

Two central controllers have been used to test IIRYK adaptive feedforward compensators. The first (PP) has been designed using a pole placement method adapted for the case of positive feedback systems. Its main objective is to stabilize the internal positive feedback loop. The end result was a controller of orders $n_{R_0} = 15$ and $n_{S_0} = 17$. The second

(H_∞) is a reduced order H_∞ controller with $n_{R_0} = 19$ and $n_{S_0} = 20$ from [11]¹². For the design of the H_∞ controller, the knowledge of the primary path is mandatory (which is not necessary for the PP controller). Figure 6 shows a comparison of the performances obtained with these controllers. One observes that H_∞ already provides a good attenuation (14.70 dB)¹³.

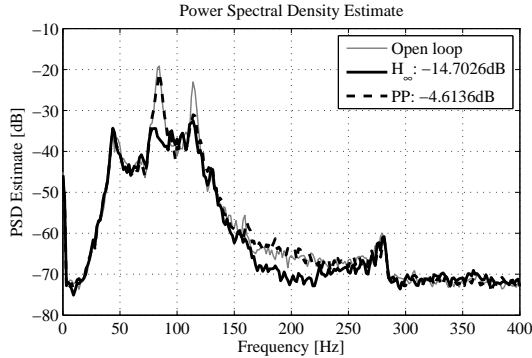


Fig. 6. Spectral densities of residual acceleration for the two central controllers (experimental)

C. Broadband disturbance rejection using matrix adaptation gain

Broadband disturbance rejection capabilities using the two Youla-Kucera parametrizations with IIR and FIR filters described in column 2 and 3 of table I are evaluated in this subsection and some observations regarding how they compare to the algorithm of column 4 (see also [14]) are made. For most of the experiments, the complexity of the IIRYK filter was $n_{B_Q} = 3$ and $n_{A_Q} = 8$, therefore having 12 parameters in the adaptation algorithm according to eq. (4). For the FIRYK parametrization, an adaptive filter of order $n_Q = 31$ (32 parameters) has been used. These values do not allow for the “perfect matching condition” to be verified.

A PRBS excitation on the global primary path is considered as the disturbance.

Two modes of operation can be considered, depending on the particular choices taken in eq. (29c):

- For adaptive operation, Algorithms *IIa* and *III* have been used with *decreasing adaptation gain* ($\lambda_1(t) = 1$, $\lambda_2(t) = 1$) combined with a *constant trace* adaptation gain. When the trace of the adaptation matrix is below a given value, the constant trace gain updating modifies the values of $\lambda_1(t)$ and $\lambda_2(t)$ so that the trace of F is kept constant. This assures the evolution of the PAA in the optimal direction but the step size does not go to zero, therefore maintaining adaptation capabilities for eventual changes in disturbance or variations of the primary path model.
- In self-tuning operation, a decreasing adaptation gain $F(t)$ is used and the step size goes to zero. Then, if

¹²The orders of the initial H_∞ controller were: $n_{R_{H_\infty}} = 70$ and $n_{S_{H_\infty}} = 70$.

¹³The same central controllers have been used in [15] for evaluating FIRYK feedforward adaptive compensators.

a degradation of the performance is observed, as a consequence of a change of the disturbance characteristics, the PAA is re-started.

The parametric adaptation algorithms have been implemented using the UD factorization [23]¹⁴. For reason of space only the experimental results in adaptive operation will be presented. For IIRYK the adaptation has been done starting with an initial gain of 0.02 (initial trace = initial gain \times number of adjustable parameters, thus 0.24) and using a constant trace of 0.02. For FIRYK an initial gain of 0.05 (initial trace $0.05 \times 32 = 1.6$) and constant trace 0.1 have been used.

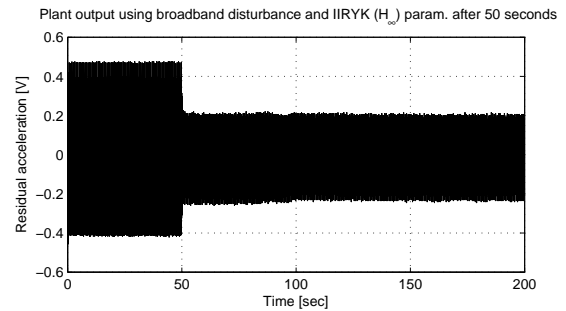


Fig. 7. Real time residual acceleration obtained with the IIR Youla-Kucera parametrization ($n_{B_Q} = 3$, $n_{A_Q} = 8$) using Algorithm *IIa* with matrix adaptation gain and the H_∞ central controller.

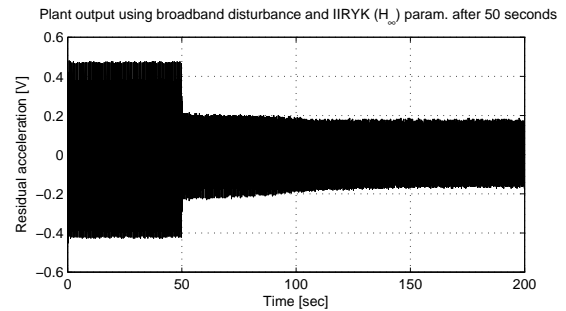


Fig. 8. Real time residual acceleration obtained with the IIR Youla-Kucera parametrization ($n_{B_Q} = 3$, $n_{A_Q} = 8$) using Algorithm *III* with matrix adaptation gain and the H_∞ central controller.

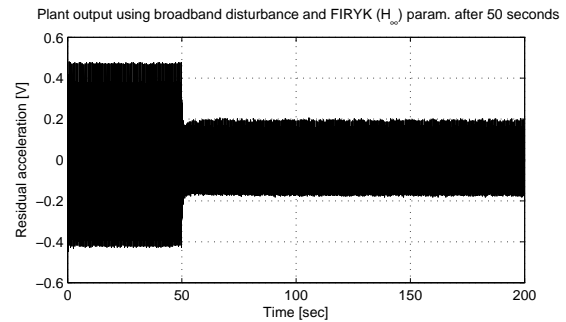


Fig. 9. Real time results obtained with the FIR Youla-Kucera parametrization ($n_Q = 31$) using Algorithm *III* with matrix adaptation gain and the H_∞ central controller.

¹⁴An array implementation as in [28] can be also considered.

The experiments have been carried out by first applying the disturbance and then starting the adaptive feedforward compensation after 50 seconds using the FIR or the IIR Youla-Kucera parametrization. If not otherwise specified, the results which will be presented have been obtained with the H_∞ central controller. In the case of the IIRYK parametrization using Algorithm *III*, the filtering by the denominator of the QIR filter used in equation (31) is done adaptively by using the last stable estimation of $A_Q(q^{-1})$. Time domain results using IIRYK with Algorithms *IIa* and *III* are shown in figures 7 and 8 respectively. It can be seen that Algorithm *III* provides a better performance than Algorithm *IIa* and this can be explained by a better approximation of the positive real condition (see discussion in subsection V-D). Figure 9 shows the evolution of the residual acceleration with the FIRYK adaptive compensator using Algorithm *III* of [15]. The final attenuation given by IIRYK using Algorithm *III* (16.21dB) is better than that provided by IIRYK using Algorithm *IIa* (13.37dB) and slightly better than that provided by using FIRYK with Algorithm *III* (16.17dB) which uses significantly more adjustable parameters (32 instead of 12). However the adaptation transient is slightly more rapid for FIRYK.

The power spectral density of the residual acceleration (after adaptation transient is finished) for the considered algorithms are shown in fig. 10.

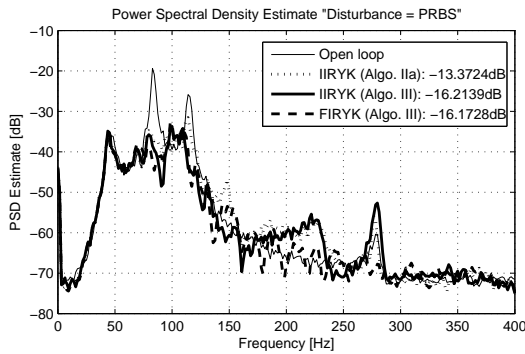


Fig. 10. Power spectral densities of the residual acceleration in open loop, with IIRYK ($n_{BQ} = 3$, $n_{AQ} = 8$) and with FIRYK ($n_Q = 31$) using the H_∞ central controller (experimental).

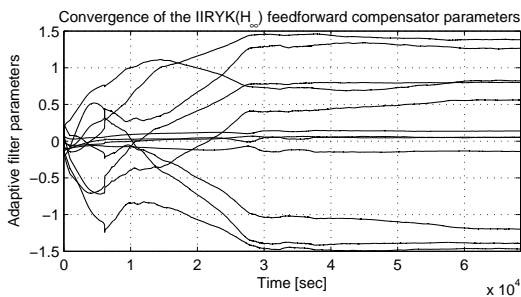


Fig. 11. Evolution of the IIRYK parameters ($n_{BQ} = 3$, $n_{AQ} = 8$ and H_∞ central controller) for Algorithm *III* using matrix adaptation gain (experimental).

Figure 11 shows the convergence of the parameters for the IIRYK feedforward adaptive compensator using Algorithm

III. The experiment has been carried out over an horizon of 13 hours. Parameters take approximatively 8 hours to almost settle. However this does not affect the performance (the transient duration on the residual acceleration for Algorithm *III* is about 50 s).

An evaluation of the influence of the number of parameters upon the global attenuation of the IIRYK parametrization is shown in table II. The results are grouped on two lines corresponding to the two central controllers used, and the given attenuations are measured in dB. The column headers give the number of numerator coefficients followed by the number of denominator coefficients. It can be observed that a larger order of the denominator is better than a larger order of the numerator.

Total no. param.	0	8	12			16		
No. param. of num/den	0/0	4/4	8/4	4/8	6/6	10/6	6/10	8/8
H_∞ (db)	14.7	15.96	15.56	16.21	16.31	15.67	16.5	16.47
PP (db)	4.61	15.52	16.25	16.02	16.24	15.57	15.72	16.21

TABLE II
INFLUENCE OF THE NUMBER OF THE IIRYK PARAMETERS UPON THE GLOBAL ATTENUATION

A similar analysis for the FIRYK feedforward adaptive compensators is given in table III. Comparing the two tables one can say that a reduction of adjustable parameters by a factor of (at least) 2 is obtained in the case of IIRYK with respect to FIRYK for approximatively same level of performance (compare IIRYK with 8 parameters with the FIRYK with 16 and the IIRYK with 6/6 parameters with the FIRYK with 32 parameters). It can be noticed that the IIRYK is less sensitive that FIRYK with respect to the performances of the model based central controller. Table III gives also comparative results for the IIR adaptive feedforward compensators. The IIRYK structure seems to allows a slight reduction of the number of parameters with respect to the IIR structure for the same level of performance (compare the results of IIRYK with 16 adjustable parameters (6/10) with the IIR using 20 adjustable parameters).

No. param.	0	8	16	20	32	40
H_∞ (db)	14.7	15.4	15.6	-	16.17	16.03
PP (db)	4.61	14.69	15.89	-	15.7	15.33
IIR (db)	-	-	-	16.23	16.49	16.89

TABLE III
INFLUENCE OF THE NUMBER OF PARAMETERS UPON THE GLOBAL ATTENUATION FOR THE FIRYK PARAMETRIZATION (LINES 2 AND 3) AND FOR THE IIR ADAPTIVE FILTER (LINE 4)

To verify the adaptive capabilities of the two parametrizations, a narrow band disturbance has been added after 1400 seconds of experimentation. This has been realized by using a sinusoidal signal of 150 Hz. Power spectral density estimates are shown in fig. 12 for the IIRYK parametrization and in fig. 13 for the FIRYK parametrization. Better results are obtained with the IIRYK parametrization and they are comparable with those obtained for IIR adaptive feedforward compensators. See [14, Fig. 12].

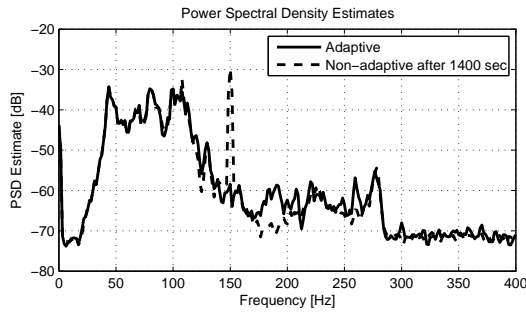


Fig. 12. Power spectral densities of the residual acceleration when an additional sinusoidal disturbance is added (Disturbance = PRBS + sinusoid) and the IIRYK parametrization is used.

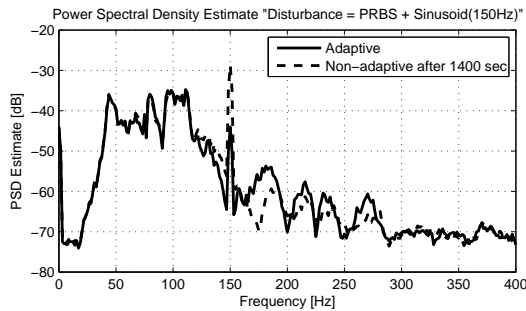


Fig. 13. Power spectral densities of the residual acceleration when an additional sinusoidal disturbance is added (Disturbance = PRBS + sinusoid) and the FIRYK parametrization is used.

D. Broadband disturbance rejection using scalar adaptation gain

The scalar adaptation gain algorithms of columns 5 and 6 from table I have been also tested on the AVC system.

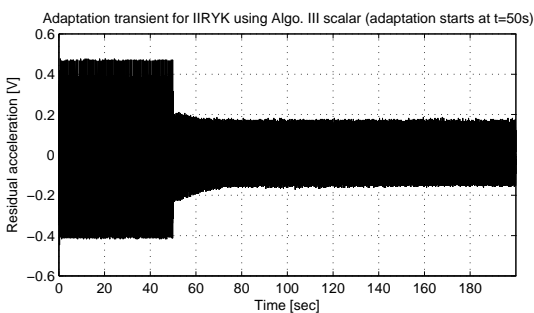


Fig. 14. Real time residual acceleration obtained with the IIR Youla-Kucera parametrization ($n_{B_Q} = 3$, $n_{A_Q} = 8$) using Algorithm III with scalar adaptation gain and the H_∞ central controller.

In the *adaptation* regime, as opposed to the matrix cases, a constant adaptation gain of 0.001 has been used for both parametrizations, as in [14] (see also table I). This corresponds to a constant trace of 0.012 for the IIRYK and 0.032 for the FIRYK (taking into account the number of adapted parameters). Figure 14 shows the adaptation transient for the scalar version of the IIRYK parametrization using Algorithm III. Surprisingly, the performances are close to those obtained with a matrix adaptation gain. (a similar observation has been made in [14, Fig. 14]. Figure 15 shows the adaptation

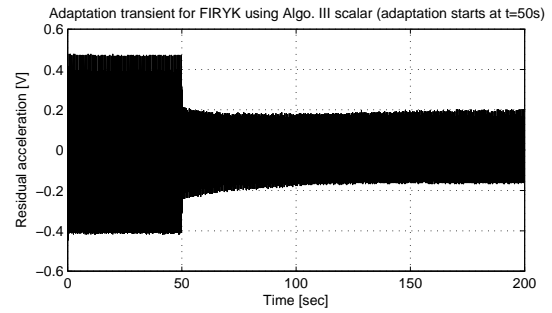


Fig. 15. Real time residual acceleration obtained with the FIR Youla-Kucera parametrization ($n_Q = 31$) using Algorithm III with scalar adaptation gain and the H_∞ central controller.

transient for the FIRYK parametrization using a scalar adaptation gain. It can be seen that the transient performances are a little better for the IIRYK. In fig. 16, power spectral densities and the corresponding global attenuations are given for both parametrizations. It can be observed that IIRYK parametrization with 12 adjustable parameters gives a slightly better attenuation (additional 0.5 dB) with respect to a FIRYK parametrization with 32 parameters.

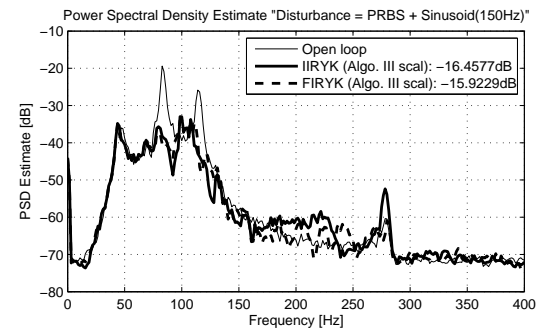


Fig. 16. Power spectral densities of the residual acceleration in open loop, with IIRYK ($n_{B_Q} = 3$, $n_{A_Q} = 8$) and with FIRYK ($n_Q = 31$) using scalar adaptation gain and the H_∞ central controller (experimental).

VII. COMPARISON WITH OTHER ALGORITHMS

The algorithms developed in this paper with matrix and scalar adaptation gains for IIR Youla-Kucera feedforward compensators have been compared with the FIR Youla-Kucera parameterized feedforward compensators from [15] and the direct IIR adaptive algorithm of [14] (see Table I). This section summarizes the observations made in Subsection V-E and in Section VI based on experimental results.

Remark 1 - The number of adjustable parameters. The main advantage of the IIRYK adaptive feedforward compensators introduced in this paper compared with FIRYK adaptive compensators is that they require a significantly lower number of adjustable parameters for a given level of performance (a reduction by a factor of 2 in the application presented). This is without doubt a major practical advantage in terms of implementation complexity. A slight reduction of the number of adjustable parameters is also obtained with respect to IIR adaptive feedforward compensators.

Remark 2 - The poles of the internal positive closed loop. For IIR adaptive feedforward compensators provided that the SPR condition for stability is satisfied, the poles of the internal "positive" loop will be asymptotically stable but they can be very close to the unit circle. For FIRYK, the poles of the internal positive feedback loop are assigned by the central stabilizing controller and they remain unchanged under the effect of adaptation. For IIRYK, part of the poles of the internal positive feedback loop are assigned by the central stabilizing controller but there are additional poles corresponding to \hat{A}_Q . These poles will be inside the unit circle if the positive real condition for stability is satisfied but they can be very close to the unit circle (at least theoretically). However if one likes to impose that these poles lie inside a circle of a certain radius, this can be easily achieved by using parameter adaptation algorithms with "projections" ([23], [29]).

Remark 3 - Implementation of the filter for Algorithm III. For IIRYK adaptive compensator one has to run first algorithm *IIa* or *IIb* over a short horizon in order to get an estimate of \hat{A}_Q for implementing the appropriate filter. A similar procedure has to be used also for IIR adaptive compensators (See [14]). For the IIRYK the filter can be continuously improved by updating at each step the estimation of \hat{A}_Q in the filter. Such a procedure is more difficult to apply to the IIR structure since the estimated closed loop poles have to be computed at each step based on current estimates of the feedforward compensator's parameters and the knowledge of the reverse path $M(q^{-1})$. For FIRYK this initialization procedure is not necessary since the poles of the internal positive feedback loop remain unchanged under the effect of adaptation and a good estimation is provided by the knowledge of the central stabilizing compensator and of the model of the reverse path.

Remark 4 - Initial model based design compensator. Since the system as well as the initial characteristics of the disturbance can be identified, a model based design of an initial feedforward compensator can be done. For a FIRYK or an IIRYK adaptive feedforward compensator, any model based designed compensator can be used as the central controller (no matter what is its dimension). Its performances will be enhanced by the adaptation of the Q-parameters. However, for IIR adaptive feedforward compensators the initial model based designed compensator should have the same structure (number of parameters) as the adaptive structure.

Remark 5 - Influence of the initial stabilizing controller. The performances of IIRYK adaptive compensator are less sensitive than those of FIRYK adaptive compensator with respect to the performances of the initial model based stabilizing controller (at least for a reduced number of adjustable parameters).

VIII. CONCLUDING REMARKS

The paper has presented an adaptive IIR Youla-Kucera parameterized feedforward compensator built around a stabilizing filter for the internal "positive" feedback loop occurring in AVC and ANC systems. Experimental results on an AVC system featuring an internal "positive" feedback have

illustrated the potential of the approach. It has been shown that the use of the IIR Youla-Kucera filters allows to reduce significantly the number of parameters to be adapted with respect to the FIR Youla-Kucera filters for the same level of performance.

APPENDIX A PROOF OF LEMMA 4.1

Proof: Using hypothesis H3, one can construct an equivalent closed loop system for the primary path as in figure 17.

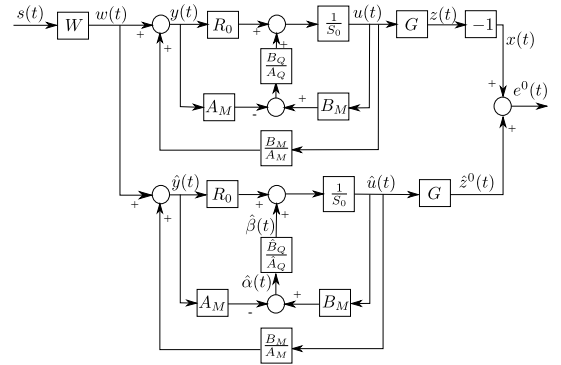


Fig. 17. Equivalent system representation

Considering a $Q(q^{-1})$ filter as in eq. (4), the polynomial $S(q^{-1})$ given in eq. (3) can be rewritten as

$$S(q^{-1}) = 1 + q^{-1}S^* = 1 + q^{-1}((A_Q S_0)^* - B_Q B_M^*). \quad (52)$$

Under hypothesis 3 (perfect matching condition) the output of the primary path can be expressed as

$$x(t) = -z(t) = -G(q^{-1})u(t) \quad (53)$$

and the input to the Youla-Kucera schema as

$$y(t+1) = w(t+1) + \frac{B_M}{A_M}u(t+1) \quad (54)$$

where $u(t)$ is a dummy variable given by

$$\begin{aligned} u(t+1) &= -S^*u(t) + Ry(t+1) \\ &= -((A_Q S_0)^* - B_Q B_M^*)u(t) + (A_Q R_0 - B_Q A_M)y(t+1) \\ &= -(A_Q S_0)^*u(t) + A_Q R_0 y(t+1) \\ &\quad + B_Q (B_M^* u(t) - A_M y(t+1)). \end{aligned} \quad (55)$$

Similarly, the output of the adaptive feedforward filter (for a fixed \hat{Q}) is given by

$$\begin{aligned} \hat{u}(t+1) &= -(\hat{A}_Q S_0)^* \hat{u}(t) + \hat{A}_Q R_0 \hat{y}(t+1) \\ &\quad + \hat{B}_Q (B_M^* \hat{u}(t) - A_M \hat{y}(t+1)). \end{aligned} \quad (56)$$

The output of the secondary path is

$$\hat{z}(t) = G(q^{-1})\hat{u}(t). \quad (57)$$

Define the dummy error (for a fixed estimated set of parameters)

$$\epsilon(t) = -u(t) + \hat{u}(t) \quad (58)$$

and the residual error

$$\nu(t) = -e(t) = -(-z(t) + \hat{z}(t)) = -G(q^{-1})\epsilon(t). \quad (59)$$

Equation (55) can be rewritten as

$$\begin{aligned} u(t+1) = & -(A_Q S_0)^* \hat{u}(t) + A_Q R_0 \hat{y}(t+1) + B_Q (B_M^* \hat{u}(t) \\ & - A_M \hat{y}(t+1)) - (A_Q S_0)^* (u(t) - \hat{u}(t)) + A_Q R_0 (y(t+1) \\ & - \hat{y}(t+1)) + B_Q [B_M^* (u(t) - \hat{u}(t)) - A_M (y(t+1) - \hat{y}(t+1))]. \end{aligned} \quad (60)$$

Taking into consideration eqs. (10), (54)

$$\begin{aligned} B_Q [B_M^* (u(t) - \hat{u}(t)) - A_M (y(t+1) - \hat{y}(t+1))] = \\ = B_Q \left[B_M^* \epsilon(t) - A_M \frac{B_M^*}{A_M} \epsilon(t) \right] = 0 \end{aligned} \quad (61)$$

and subtracting equation (56), from (60) one obtains

$$\begin{aligned} \epsilon(t+1) = & -((-A_Q + \hat{A}_Q) S_0)^* \hat{u}(t) + (-A_Q + \hat{A}_Q) R_0 \hat{y}(t+1) \\ & + (-B_Q + \hat{B}_Q) [B_M^* \hat{u}(t) - A_M \hat{y}(t+1)] \\ & - (A_Q S_0)^* \epsilon(t) + A_Q R_0 \frac{B_M^*}{A_M} \epsilon(t). \end{aligned} \quad (62)$$

Passing the terms in $\epsilon(t)$ on the left hand side, one gets:

$$\begin{aligned} \left[1 + q^{-1} \left(\frac{A_M (A_Q S_0)^* - A_Q R_0 B_M^*}{A_M} \right) \right] \epsilon(t+1) = \frac{A_Q P_0}{A_M} \epsilon(t+1) \\ = (-A_Q^* + \hat{A}_Q^*) [-S_0 \hat{u}(t) + R_0 \hat{y}(t)] \\ + (-B_Q + \hat{B}_Q) [B_M \hat{u}(t+1) - A_M \hat{y}(t+1)] \end{aligned} \quad (63)$$

Using eqs. (59) and (19) one gets:

$$\nu(t+1) = \frac{A_M (q^{-1}) G(q^{-1})}{A_Q (q^{-1}) P_0 (q^{-1})} (\theta - \hat{\theta})^T \phi(t), \quad (64)$$

which corresponds to eq. (17) and this ends the proof. ■

APPENDIX B PROOF OF LEMMA 5.1

Proof: Using Theorem 3.2 from [23], under the condition (39), (34), (35) and (36) hold.

However in order to show that $\nu^0(t+1)$ goes to zero one has to show first that the components of the observation vector are bounded. The result (36) suggests to use the Goodwin's "bounded growth" lemma ([26] and Lemma 11.1 in [23]). Provided that one has:

$$|\psi^T(t) F(t) \psi(t)|^{\frac{1}{2}} \leq C_1 + C_2 \cdot \max_{0 \leq k \leq t+1} |\nu^0(k)| \quad (65)$$

$$0 < C_1 < \infty, \quad 0 < C_2 < \infty, \quad F(t) > 0,$$

$\|\psi(t)\|$ will be bounded. So it will be shown that (65) holds. This will be proved for algorithm I (for algorithms II and III the proof is similar).

From (14) one has

$$-\hat{z}(t) = \nu(t) + x(t). \quad (66)$$

Since $x(t)$ is bounded (output of an asymptotically stable system with bounded input), one has

$$\begin{aligned} |\hat{u}_f(t)| = |G \hat{u}(t)| = |\hat{z}(t)| \leq C_3 + C_4 \cdot \max_{0 \leq k \leq t+1} |\nu(k)| \\ \leq C_3' + C_4' \cdot \max_{0 \leq k \leq t+1} |\nu^0(k)| \end{aligned} \quad (67)$$

$$0 < C_3, C_4, C_3', C_4' < \infty \quad (68)$$

since $|\nu(t)| \leq |\nu^0(t)|$ for all t . Filtering both sides of equation (10) by $G(q^{-1})$ one gets in the adaptive case:

$$\hat{y}_f(t) = G \cdot w(t) + \frac{B_M}{A_M} \cdot \hat{u}_f(t) \quad (69)$$

Since A_G and A_M are Hurwitz polynomials and $d(t)$ is bounded, it results that

$$|\hat{y}_f(t)| \leq C_5 + C_6 \cdot \max_{0 \leq k \leq t+1} |\nu^0(k)|; \quad 0 < C_5, C_6 < \infty \quad (70)$$

Using equations (19a), (19b), (27), (68) and (70) one can conclude that

$$|\alpha_f(t)| \leq C_7 + C_8 \cdot \max_{0 \leq k \leq t+1} |\nu^0(k)| \quad (71)$$

and

$$|\beta_f(t)| \leq C_9 + C_{10} \cdot \max_{0 \leq k \leq t+1} |\nu^0(k)| \quad (72)$$

Therefore (65) holds, which implies that $\psi(t)$ is bounded and one can conclude that (38) also holds. End of the proof. ■

REFERENCES

- [1] S. Elliott and P. Nelson, "Active noise control," *Noise / News International*, pp. 75–98, June 1994.
- [2] S. Elliott and T. Sutton, "Performance of feedforward and feedback systems for active control," *IEEE Transactions on Speech and Audio Processing*, vol. 4, no. 3, pp. 214–223, May 1996.
- [3] M. Kuo and D. Morgan, "Active noise control: A tutorial review," *Proceedings of the IEEE*, vol. 87, pp. 943–973, 1999.
- [4] J. Zeng and R. de Callafon, "Recursive filter estimation for feedforward noise cancellation with acoustic coupling," *Journal of sound and vibration*, vol. 291, pp. 1061–1079, 2006.
- [5] J. Hu and J. Linn, "Feedforward active noise controller design in ducts without independent noise source measurements," *IEEE transactions on control system technology*, vol. 8, no. 3, pp. 443–455, 2000.
- [6] C. Jacobson, C. Johnson, D. M. Cormick, and W. Sethares, "Stability of active noise control algorithms," *IEEE Signal Processing letters*, vol. 8, no. 3, pp. 74–76, 2001.
- [7] R. Fraanje, M. Verhaegen, and N. Doelman, "Convergence analysis of the filtered-u lms algorithm for active noise control in case perfect cancellation is not possible," *Signal Processing*, vol. 73, pp. 255–266, 1999.
- [8] A. Wang and W. Ren, "Convergence analysis of the filtered-u algorithm for active noise control," *Signal Processing*, vol. 73, pp. 255–266, 1999.
- [9] M. Bai and H.H.Lin, "Comparison of active noise control structures in the presence of acoustical feedback by using the hinf synthesis technique," *J. of Sound and Vibration*, vol. 206, pp. 453–471, 1997.
- [10] K. Zhou, J. C. Doyle, and K. Glover, *Robust and optimal control*. Upper Saddle River, New Jersey: Prentice Hall, 1996.
- [11] M. Alma, J. Martinez, I. Landau, and G. Buche, "Design and tuning of reduced order h-infinity feedforward compensators for active vibration control," *Control Systems Technology, IEEE Transactions on*, vol. 20, no. 2, pp. 554–561, march 2012.
- [12] M. Rotunno and R. de Callafon, "Design of model-based feedforward compensators for vibration compensation in a flexible structure," in *Proceedings of the 17th ASME Biennial Conference on Mechanical Vibration and Noise, Las Vegas, NV, USA, 1999*.
- [13] L. Ljung and T. Söderström, *Theory and practice of recursive identification*. Cambridge Massachusetts, London, England: The M.I.T Press, 1983.
- [14] I. Landau, M. Alma, and T. Airimițoiaie, "Adaptive feedforward compensation algorithms for active vibration control with mechanical coupling," *Automatica*, vol. 47, no. 10, pp. 2185–2196, 2011.
- [15] I. Landau, T. Airimițoiaie, and M. Alma, "A youla-kucera parametrized adaptive feedforward compensator for active vibration control," in *Proceedings of the 18th IFAC World Congress, Milano, Italy, 2011*.
- [16] B. Anderson, "From Youla-Kucera to identification, adaptive and non-linear control," *Automatica*, vol. 34, pp. 1485–1506, 1998.
- [17] T. Tay, I. Mareels, and J. Moore, *High Performance Control*. Boston: Birkhäuser, 1997.

- [18] R. A. de Callafon and C. E. Kinney, "Robust estimation and adaptive controller tuning for variance minimization in servo systems," *Journal of Advanced Mechanical Design, Systems, and Manufacturing*, vol. 4, no. 1, pp. 130–142, 2010.
- [19] M. Ficocelli and F. Ben Amara, "Adaptive regulation of mimo linear systems against unknown sinusoidal exogenous inputs," *International Journal of Adaptive Control and Signal Processing*, vol. 23, no. 6, pp. 581–603, 2009.
- [20] T. Marcos, "The straight attraction," *Motion control*, vol. 13, pp. 29–33, 2000.
- [21] I. Landau, M. Alma, J. Martinez, and G. Buche, "Adaptive suppression of multiple time-varying unknown vibrations using an inertial actuator," *Control Systems Technology, IEEE Transactions on*, vol. 19, no. 6, pp. 1327–1338, nov. 2011.
- [22] B. Anderson, R. Bitmead, C. Johnson, P. Kokotovic, R. Kosut, I. Mareels, L. Praly, and B. Riedle, *Stability of adaptive systems*. Cambridge Massachusetts, London, England: The M.I.T Press, 1986.
- [23] I. D. Landau, R. Lozano, M. M'Saad, and A. Karimi, *Adaptive control*, 2nd ed. London: Springer, 2011.
- [24] L. Ljung, "On positive real transfer functions and the convergence of some recursive schemes," *IEEE Trans. on Automatic Control*, vol. AC-22, pp. 539–551, 1977.
- [25] I. Landau and A. Karimi, "Recursive algorithms for identification in closed loop. a unified approach and evaluation," *Automatica*, vol. 33, no. 8, pp. 1499–1523, 1997.
- [26] I. Landau, A. Karimi, and A. Constantinescu, "Direct controller order reduction by identification in closed loop," *Automatica*, vol. 37, no. 11, pp. 1689–1702, 2001.
- [27] I. Landau, A. Constantinescu, P. Loubat, D. Rey, and A. Franco, "A methodology for the design of feedback active vibration control systems," in *Proceedings of the European Control Conference 2001, Porto, Portugal*, 2001.
- [28] A. Montazeri and J. Poshtan, "A computationally efficient adaptive iir solution to active noise and vibration control systems," *IEEE Trans. on Automatic Control*, vol. AC-55, pp. 2671 – 2676, 2010.
- [29] G. Goodwin and K. Sin, *Adaptive Filtering Prediction and Control*. N. J.: Prentice Hall, 1984.

APPENDIX F

A YOULA-KUCERA PARAMETRIZED ADAPTIVE FEEDFORWARD COMPENSATOR FOR ACTIVE VIBRATION CONTROL WITH MECHANICAL COUPLING

Authors: Ioan Doré Landau, Tudor-Bogdan Airimițoaie, and Marouane Alma

Journal: Automatica

Type of submission: Brief paper

Status: Accepted for publication

A Youla-Kucera parametrized adaptive feedforward compensator for active vibration control with mechanical coupling[☆]

Ioan Doré Landau^{a,*}, Tudor-Bogdan Airimioaie^{a,b}, Marouane Alma^a

^aControl system department of Gipsa-lab, St Martin d'Hères, 38402 FRANCE

^bFaculty of Automatic Control and Computers, University "Politehnica", Bucharest, 060042 ROMANIA

Abstract

Most of the adaptive feedforward vibration (or noise) compensation systems feature an internal "positive feedback" coupling between the compensator system and the correlated disturbance measurement which serves as reference. This may lead to the instability of the system. Instead of the standard IIR structure for the adaptive feedforward compensator, the paper proposes a Youla-Kucera parametrization of the adaptive compensator. The central compensator assures the stability of the system and its performances are enhanced in real time by the direct adaptation of the Youla-Kucera parameters. Theoretical and experimental comparison with recent results obtained using an IIR adaptive feedforward compensators are provided.

Keywords: active vibration control, adaptive feedforward compensation, adaptive control, Youla-Kucera parametrization, parameter estimation.

1. Introduction

When a correlated measurement with the disturbance is available, adaptive feedforward compensation of broadband vibrations or noise can be considered (Elliott & Nelson, 1994; Kuo & Morgan, 1996; Jacobson et al., 2001; Zeng & de Callafon, 2006). However in many AVC (Active Vibration Control) or ANC (Active Noise Control) systems there is a "positive" feedback coupling between the compensator system and the correlated measurement of the disturbance which serves as reference (Jacobson et al., 2001; Zeng & de Callafon, 2006; Hu & Linn, 2000). The positive feedback may destabilize the system. The disturbance is assumed to be unknown and with variable spectral characteristics, but the dynamic models of the AVC and ANC are supposed to be constant and known (these models can be identified).

In Jacobson et al. (2001) and Landau et al. (2011a), algorithms for adapting an IIR feedforward compensator in real time taking into account the presence of the internal positive feedback have been proposed, analyzed and evaluated. In Zeng & de Callafon (2006), the idea of using a Youla-Kucera parametrization¹ of the feedforward compensator is illustrated in the context of active noise control. Based on the identification of the system, a stabilizing YK controller is designed. The YK parameters are then updated by using a two time scale indirect procedure: (1) estimation of the Q-filter's parameters over a certain horizon, (2) updating of the controller.

The main contributions of the present paper with respect to Zeng & de Callafon (2006) and Landau et al. (2011a) are:

1. the development of a direct real time recursive adaptation algorithm for the Q-parameters of a Youla-Kucera parameterized feedforward filter and the analysis of the stability of the resulting system;
2. possibility to assign the poles of the internal positive closed loop (not possible in Landau et al. (2011a));
3. easier satisfaction of the positive real condition for stability and convergence;
4. application of the algorithm to an active vibration control system (in Zeng & de Callafon (2006) an active noise control system is considered) and comparative evaluation with the results given in Landau et al. (2011a).

While the paper is developed in the context of AVC, the results are certainly applicable to ANC systems.

The paper is organized as follows. The system structure is presented in section 2. The algorithm for adaptive feedforward compensation will be developed in section 3 and analysed in section 4. In section 5 the AVC system used for real time experiments is briefly presented. Experimental results obtained on the AVC system are shown in section 6.

2. Basic equations and notations

The block diagrams associated with an AVC system are shown in fig.1 in open loop (1(a)) and when the Youla-Kucera compensator is active (1(b)). For adaptive IIR feedforward compensators see Landau et al. (2011a). $s(t)$ is the disturbance and $d(t)$ is the correlated measurement with the disturbance. The primary (D), secondary (G) and reverse (positive coupling)

[☆]The preliminary version of the paper has been accepted at the IFAC World Congress 2011.

*Corresponding author. Tel. +33-4-7682-6391. Fax +33-4-7682-6382. E-mail Ioan-Dore.Landau@gipsa-lab.grenoble-inp.fr.

¹Throughout the paper the *Youla-Kucera parametrization* will also be called *Q* (or *YK*) -*parametrization*.

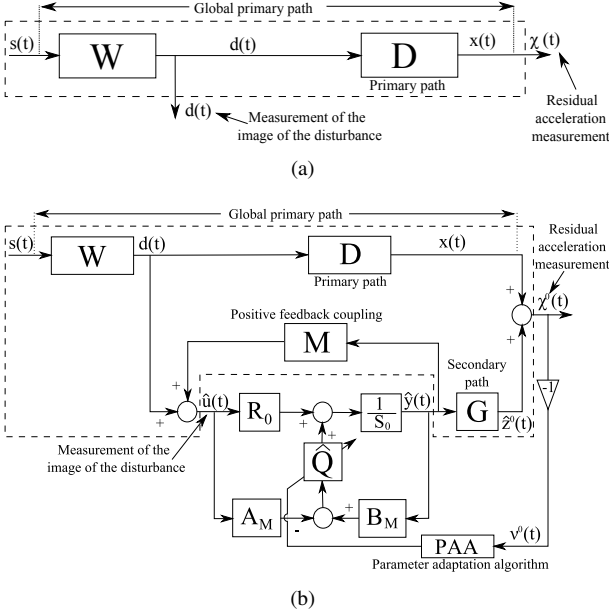


Figure 1: Feedforward AVC: in open loop (a) and with adaptive feedforward compensator (b)

(M) paths represented in (1(b)) are respectively characterized by the asymptotically stable transfer operators:

$$D(q^{-1}) = \frac{B_D(q^{-1})}{A_D(q^{-1})} = \frac{b_1^D q^{-1} + \dots + b_{n_{BD}}^D q^{-n_{BD}}}{1 + a_1^D q^{-1} + \dots + a_{n_{AD}}^D q^{-n_{AD}}}, \quad (1)$$

$$G(q^{-1}) = \frac{B_G(q^{-1})}{A_G(q^{-1})} = \frac{b_1^G q^{-1} + \dots + b_{n_{BG}}^G q^{-n_{BG}}}{1 + a_1^G q^{-1} + \dots + a_{n_{AG}}^G q^{-n_{AG}}}, \quad (2)$$

$$M(q^{-1}) = \frac{B_M(q^{-1})}{A_M(q^{-1})} = \frac{b_1^M q^{-1} + \dots + b_{n_{BM}}^M q^{-n_{BM}}}{1 + a_1^M q^{-1} + \dots + a_{n_{AM}}^M q^{-n_{AM}}}, \quad (3)$$

with $B_x = q^{-1} B_x^*$ for any $x \in \{D, G, M\}$. \hat{G} , \hat{M} and \hat{D} denote the identified (estimated) models of G , M and D . The optimal IIR feedforward compensator which will minimize the residual acceleration can be written, using the Youla-Kucera parametrization (Q-parametrization), as

$$N(q^{-1}) = \frac{R(q^{-1})}{S(q^{-1})} = \frac{R_0(q^{-1}) - A_M(q^{-1})Q(q^{-1})}{S_0(q^{-1}) - B_M(q^{-1})Q(q^{-1})} \quad (4)$$

where the optimal polynomial $Q(q^{-1})$ has a FIR structure:

$$Q(q^{-1}) = q_0 + q_1 q^{-1} + \dots + q_{n_Q} q^{-n_Q}. \quad (5)$$

and $R_0(q^{-1})$, $S_0(q^{-1}) = 1 + q^{-1} S_0^*(q^{-1})$ are the polynomials of the central (stabilizing) filter and $A_M(q^{-1})$, $B_M(q^{-1})$ are given in (3).

The estimated Q polynomial is denoted² by $\hat{Q}(q^{-1})$ or $\hat{Q}(\hat{\theta}, q^{-1})$ when it is a linear filter with constant coefficients or $\hat{Q}(t, q^{-1})$ during estimation (adaptation).

²The complex variable z^{-1} will be used for characterizing the system's behavior in the frequency domain and the delay operator q^{-1} will be used for describing the system's behavior in the time domain.

The input of the feedforward filter (called also reference) is denoted by $\hat{u}(t)$ and it corresponds to the measurement provided by the primary transducer (force or acceleration transducer in AVC or a microphone in ANC). In the absence of the compensation loop (open loop operation) $\hat{u}(t) = d(t)$. The output of the feedforward filter (which is the control signal applied to the secondary path) is denoted by $\hat{y}(t) = \hat{y}(t+1|\hat{\theta}(t+1))$ (a posteriori output). The a priori output $\hat{y}^0(t+1) = \hat{y}(t+1|\hat{\theta}(t))$ is given by:

$$\hat{y}^0(t+1) = -S_0^* \hat{y}(t) + R_0 \hat{u}(t+1) + \hat{Q}(t, q^{-1}) [B_M^* \hat{y}(t) - A_M \hat{u}(t+1)], \quad (6)$$

where $\hat{y}(t)$, $\hat{y}(t-1)$, ... are the "a posteriori" outputs of the feedforward filter generated by

$$\hat{y}(t+1) = -S_0^* \hat{y}(t) + R_0 \hat{u}(t+1) + \hat{Q}(t+1, q^{-1}) [B_M^* \hat{y}(t) - A_M \hat{u}(t+1)]. \quad (7)$$

The measured input to the feedforward filter satisfies the following equation (when feedforward compensation is active)

$$\hat{u}(t+1) = d(t+1) + \frac{B_M^*(q^{-1})}{A_M(q^{-1})} \hat{y}(t). \quad (8)$$

The unmeasurable value of the output of the primary path is denoted $x(t)$. The unmeasurable "a priori" output of the secondary path will be denoted $\hat{z}^0(t+1)$.

$$\hat{z}^0(t+1) = \hat{z}(t+1|\hat{\theta}(t)) = \frac{B_G^*(q^{-1})}{A_G(q^{-1})} \hat{y}(t) \quad (9)$$

The "a posteriori" unmeasurable value of the output of the secondary path is denoted by:

$$\hat{z}(t+1) = \hat{z}(t+1|\hat{\theta}(t+1)) \quad (10)$$

The a priori adaptation error is defined as:

$$v^0(t+1) = v(t+1|\hat{\theta}(t)) = -\chi^0(t+1) = -x(t+1) - \hat{z}^0(t+1) \quad (11)$$

where $\chi^0(t+1)$ is the measured residual acceleration. The "a posteriori" adaptation error (computed) will be given by:

$$v(t+1) = v(t+1|\hat{\theta}(t+1)) = -x(t+1) - \hat{z}(t+1). \quad (12)$$

When using an estimated filter \hat{N} with constant parameters: $\hat{y}^0(t) = \hat{y}(t)$, $\hat{z}^0(t) = \hat{z}(t)$ and $v^0(t) = v(t)$.

The objective is to develop stable recursive algorithms for adaptation of the parameters of the Q filter such that the measured residual error (acceleration or force in AVC, noise in ANC) be minimized in the sense of a certain criterion. This has to be done for broadband disturbances $d(t)$ (or $s(t)$) with unknown and variable spectral characteristics and an unknown primary path model.

3. Algorithm development

The algorithm for adaptive feedforward compensation will be developed under the following hypotheses:

1. The signal $d(t)$ is bounded (which is equivalent to say that $s(t)$ is bounded and $W(q^{-1})$ in figure 1 is asymptotically stable).

2. It exists a central feedforward compensator N_0 (R_0 , S_0) which stabilizes the inner positive feedback loop formed by N_0 and M such that its characteristic polynomial³

$$P_0(z^{-1}) = A_M(z^{-1})S_0(z^{-1}) - B_M(z^{-1})R_0(z^{-1}) \quad (13)$$

is a Hurwitz polynomial.

3. (Perfect matching condition) It exists a value of the Q parameters such that

$$\frac{G \cdot A_M(R_0 - A_M Q)}{A_M S_0 - B_M R_0} = -D. \quad (14)$$

4. The effect of the measurement noise upon the measurement of the residual acceleration is neglected (deterministic context).

Once the algorithm will be developed under these hypotheses, hypotheses 3 and 4 are removed and the algorithm can be analyzed in this modified context.

A first step in the development of the algorithms is to establish for a fixed estimated compensator a relation between the error on the Q -parameters (with respect to the optimal values) and the adaptation error v . This is summarized in the following Lemma.

Lemma 1. *Under the hypothesis 1, 2, 3 and 4 for the system described by eqs. (1) through (12), using a Q -parameterized feedforward compensator with constant parameters, one has:*

$$v(t+1/\hat{\theta}) = \frac{A_M(q^{-1})G(q^{-1})}{P_0(q^{-1})} [\theta - \hat{\theta}]^T \phi(t), \quad (15)$$

where θ , $\hat{\theta}$ and ϕ are given respectively by:

$$\theta^T = [q_0, q_1, q_2, \dots, q_{n_Q}] \quad (16a)$$

$$\hat{\theta}^T = [\hat{q}_0, \hat{q}_1, \hat{q}_2, \dots, \hat{q}_{n_Q}] \quad (16b)$$

$$\phi^T(t) = [\alpha(t+1), \alpha(t), \dots, \alpha(t-n_Q+1)]. \quad (16c)$$

$$\begin{aligned} \alpha(t+1) &= B_M \hat{y}(t+1) - A_M \hat{u}(t+1) \\ &= B_M^* \hat{y}(t) - A_M \hat{u}(t+1) \end{aligned} \quad (16d)$$

q_i are the coefficients of the optimal Q -filter and \hat{q}_i are the coefficients of the fixed estimated \hat{Q} -filter.

For a proof, see Appendix A.

Filtering the vector ϕ by an asymptotically stable filter $L(q^{-1})$, eq. (15) becomes

$$v(t+1/\hat{\theta}) = \frac{A_M(q^{-1})G(q^{-1})}{P_0(q^{-1})L(q^{-1})} [\theta - \hat{\theta}]^T \phi_f(t) \quad (17)$$

with

$$\begin{aligned} \phi_f(t) &= L(q^{-1})\phi(t) \\ &= [\alpha_f(t+1), \alpha_f(t), \dots, \alpha_f(t-n_{Q+1})], \end{aligned} \quad (18)$$

³The parenthesis (q^{-1}) will be omitted in some of the following equations to make them more compact.

	Present paper (Fix IIR + Adaptive YKFIR)	Landau et al. (2011a) (Adaptive IIR)
$\hat{\theta}(t+1) =$	$\hat{\theta}(t) + F(t)\psi(t) \frac{v^0(t+1)}{1 + \psi^T(t)F(t)\psi(t)}$	
Adapt. gain	$F(t+1)^{-1} = \lambda_1(t)F(t) + \lambda_2(t)\psi(t)\psi^T(t)$ $0 \leq \lambda_1(t) < 1, 0 \leq \lambda_2(t) < 2, F(0) > 0$	
Adaptive	Decr. gain and const. trace	
Self tuning	$\lambda_2 = const., \lim_{t \rightarrow \infty} \lambda_1(t) = 1$	
$\hat{\theta}(t) =$	$[\hat{q}_0(t), \hat{q}_1(t), \dots]$	$[-\hat{s}_1(t), \dots, \hat{r}_0(t), \dots]$
$\phi^T(t) =$	$[\alpha(t+1), \alpha(t), \dots]$ $\alpha(t) = B_M \hat{y}(t) - A_M \hat{u}(t)$	$[-\hat{y}(t), \dots, \hat{u}(t+1), \dots]$
$\hat{P} =$	$\hat{A}_M S_0 - \hat{B}_M R_0$	$\hat{A}_M \hat{S} - \hat{B}_M \hat{R}$
$P =$	$A_M S_0 - B_M R_0$	$A_M \hat{S} - B_M \hat{R}$
$\psi(t) =$	$L\phi(t); L_2 = \hat{G}; L_3 = \frac{\hat{A}_M}{\hat{P}} \hat{G}$	
Stability condition	$\frac{A_M G}{PL} - \frac{\lambda}{2} = SPR \quad (\lambda = \max \lambda_2(t))$	
Conv. condition	$\frac{A_M G}{PL} - \frac{\lambda}{2} = SPR \quad (\lambda = \lambda_2)$	

Table 1: Algorithms for adaptive feedforward compensation in AVC with mechanical coupling (YK parametrization and IIR parametrization)

where

$$\alpha_f(t+1) = L(q^{-1})\alpha(t+1). \quad (19)$$

Eq. (17) will be used to develop the adaptation algorithms.

When the parameters of \hat{Q} evolve over time and neglecting the non-commutativity of the time varying operators (which implies slow adaptation (Anderson et al., 1986) i.e., a limited value for the adaptation gain), equation (17) transforms into⁴

$$v(t+1/\hat{\theta}(t+1)) = \frac{A_M(q^{-1})G(q^{-1})}{P_0(q^{-1})L(q^{-1})} [\theta - \hat{\theta}(t+1)]^T \phi_f(t). \quad (20)$$

Eq. (20) has the standard form of an "a posteriori adaption error equation" (Landau et al., 2011b), which immediately suggests to use the following parameter adaptation algorithm:

$$\hat{\theta}(t+1) = \hat{\theta}(t) + F(t)\psi(t)v(t+1) \quad (21a)$$

$$v(t+1) = \frac{v^0(t+1)}{1 + \psi^T(t)F(t)\psi(t)} \quad (21b)$$

$$F(t+1) = \frac{1}{\lambda_1(t)} \left[F(t) - \frac{F(t)\psi(t)\psi^T(t)F(t)}{\lambda_1(t) + \psi^T(t)F(t)\psi(t)} \right] \quad (21c)$$

$$1 \geq \lambda_1(t) > 0; 0 \leq \lambda_2(t) < 2; F(0) = \alpha I; \alpha_{max} > \alpha > 0 \quad (21d)$$

$$\psi(t) = \phi_f(t) \quad (21e)$$

where $\lambda_1(t)$ and $\lambda_2(t)$ allow to obtain various profiles for the adaptation gain $F(t)$ (see Landau et al. (2011b)).

⁴However, exact algorithms can be developed taking into account the non-commutativity of the time varying operators - see Landau et al. (2011b)

Three choices for the filter L will be considered:

Algorithm I $L = G$
 Algorithm II $L = \hat{G}$
 Algorithm III

$$L = \frac{\hat{A}_M}{\hat{P}_0} \hat{G} \quad (22)$$

where

$$\hat{P}_0 = \hat{A}_M S_0 - \hat{B}_M R_0. \quad (23)$$

A comparison with algorithms for IIR adaptive compensators (Landau et al., 2011a) is summarized in Table 1. For the IIR one adapts the filter parameters while for YK parametrized filters one adapts the parameters of the Q filter. For IIR, the regressor vector is constituted by filtered inputs and outputs while for YK parametrization, the components of the regressor vector are filtered linear combinations of input and outputs weighted by the parameters of the reverse path model.

4. Analysis of the algorithms

4.1. The deterministic case - perfect matching

Equation (20) for the a posteriori adaptation error has the form:

$$v(t+1) = H(q^{-1})[\theta - \hat{\theta}(t+1)]^T \psi(t), \quad (24)$$

where

$$H(q^{-1}) = \frac{A_M(q^{-1})G(q^{-1})}{P_0(q^{-1})L(q^{-1})}, \quad \psi = \phi_f. \quad (25)$$

One has the following result:

Lemma 2. Assuming that eq. (24) represents the evolution of the a posteriori adaptation error and that the parameter adaptation algorithm (21a) through (21e) is used one has:

$$\lim_{t \rightarrow \infty} v(t+1) = 0 \quad (26)$$

$$\lim_{t \rightarrow \infty} \frac{[v^0(t+1)]^2}{1 + \psi(t)^T F(t) \psi(t)} = 0 \quad (27)$$

$$\|\psi(t)\| \text{ is bounded} \quad (28)$$

$$\lim_{t \rightarrow \infty} v^0(t+1) = 0 \quad (29)$$

for any initial conditions $\hat{\theta}(0), v(0)$ if:

$$H'(z^{-1}) = H(z^{-1}) - \frac{\lambda_2}{2}, \quad \max_t [\lambda_2(t)] \leq \lambda_2 < 2 \quad (30)$$

is a strictly positive real (SPR) transfer function.

Proof: The proof is similar to that of (Landau et al., 2011a, Lemma 5.1) and is omitted.

The analysis in the presence of a measurement noise and when the perfect model matching does not hold can be carried on in a similar way as in Landau et al. (2011a) and it is omitted.

Remark 1: For algorithm III, the stability condition (30) for $\lambda_2 = 1$ can be transformed into (Ljung & Söderström, 1983)

$$\left| \left(\frac{A_M(e^{-j\omega})}{\hat{A}_M(e^{-j\omega})} \cdot \frac{\hat{P}_0(e^{-j\omega})}{P_0(e^{-j\omega})} \cdot \frac{G(e^{-j\omega})}{\hat{G}(e^{-j\omega})} \right)^{-1} - 1 \right| < 1 \quad (31)$$

for all ω , which is always true provided that the initial estimates of M and G are close to the true values (the differences between P_0 and \hat{P}_0 depend only upon the estimation errors of \hat{M}).

Remark 2: Consider eq. (15) for the case of time varying parameter $\hat{\theta}$. Neglecting the non-commutativity of time varying operators it can be written as:

$$v(t+1|\hat{\theta}(t+1)) = [\theta - \hat{\theta}(t+1)]^T \phi_f'(t) \quad (32)$$

$$\phi_f'(t) = \frac{A_M(q^{-1})G(q^{-1})}{P_0(q^{-1})} \phi(t) \quad (33)$$

If one would like to minimize a one step ahead quadratic criterion $J(t+1) = v^2(t+1)$ using the gradient technique (Landau et al., 2011b) one gets

$$\frac{1}{2} \frac{\partial J(t+1)}{\partial \hat{\theta}(t+1)} = -\phi_f'(t)v(t+1) \quad (34)$$

Using algorithm III, eq. (21a) can be viewed as an approximation of the gradient ($F = \alpha I = \text{const.}$ for the gradient technique). For constant adaptation gain $\lambda_2(t) \equiv 0$ and the strict positive realness on $H'(z^{-1})$ implies at all the frequencies:

$$-90^\circ < \angle \frac{A_M(e^{-j\omega})G(e^{-j\omega})}{P_0(e^{-j\omega})} - \angle \frac{\hat{A}_M(e^{-j\omega})\hat{G}(e^{-j\omega})}{\hat{P}_0(e^{-j\omega})} < 90^\circ \quad (35)$$

Therefore the interpretation of the SPR condition of Lemma 2 is that the angle between the direction of adaptation and the direction of the inverse of the true gradient should be less than 90° . For time-varying adaptation gains the condition is sharper since in this case $\text{Re}\{H(e^{-j\omega})\}$ should be larger than $\frac{\lambda_2}{2}$ at all frequencies.

Remark 3: The asymptotic bias distribution when perfect matching condition is not satisfied is given by (see Landau et al. (2011a) for the computation method):

$$\hat{\theta}^* = \arg \min_{\hat{\theta}} \int_{-\pi}^{\pi} \left[\left| \frac{G(j\omega)A_M^2(j\omega)}{P_0(j\omega)} \right|^2 |Q(j\omega) - \hat{Q}(j\omega)|^2 \phi_d(\omega) + \phi_w(\omega) \right] d\omega \quad (36)$$

where ϕ_d and ϕ_w are the spectral densities of $d(t)$ and of the measurement noise. From (36) one concludes that a good approximation of Q corresponding to the perfect matching will be obtained in the frequency region where ϕ_d is significant and where G has a high gain (usually G should have high gain in the frequency region where ϕ_d is significant in order to counteract the effect of $d(t)$). The quality of the estimated \hat{Q} will be affected also by A_M^2/P_0 .

Remark 4: In the case where some of the zeros of G are outside the unit circle, the use of Lemma 2 requires that the estimated unstable zeros be equal to the true unstable zeros and in addition that the minimal order transfer function H' be SPR. Extensive simulations have shown however that it is enough that real and estimated unstable zeros be sufficiently close in order that the phase condition associated to the positivity of the real part of H' is satisfied (even if H' in this case can not be SPR).

4.2. Comparison with IIR adaptive feedforward compensators

Lets focus now on the differences between the IIR adaptive compensator given in Landau et al. (2011a) and the YK adaptive compensator.

Remark 1: For IIR adaptive compensators, provided that the SPR condition is satisfied, the poles of the internal "positive" loop will be asymptotically stable but they can be very close to the unit circle (they can be inside of a circle of radius 0.99999...). This may induce some numerical problems in practice (when using truncation or fixed point arithmetic).

Remark 2: The central YK controller allows to assign the poles of the internal closed loop. Therefore one can impose that all the poles of the internal loop be inside of a circle of radius $1 - \delta$, $\delta > 0$ (δ takes care of the numerical approximations).

Remark 3: If a model based initial IIR compensator is available, it can not in general be used to initialize the parameters of the IIR adaptive compensator since often the number of parameters of the fixed compensator is higher than the number of parameters of the adaptive IIR compensator. The situation is different for YK adaptive compensator where any initial stabilizing compensator can be used whatever its complexity is.

Remark 4: For YK adaptive compensators the filters for Algorithm III can be directly implemented since the estimated closed loop poles are defined by the central controller and \hat{M} . For IIR adaptive compensators there is a need for an initialization horizon using Algorithm II followed by the real time computation of the estimated closed loop poles using \hat{N} and \hat{M} .

5. An active vibration control system using an inertial actuator

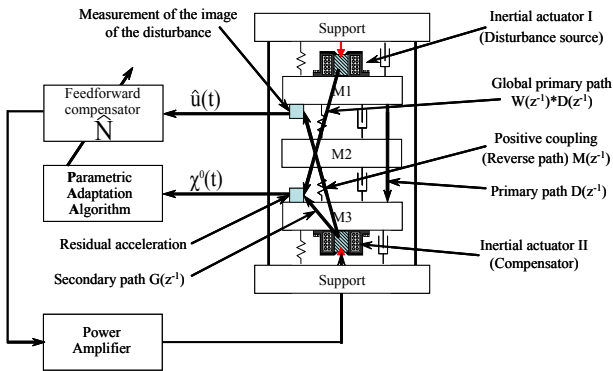


Figure 2: An AVC system using a feedforward compensation - scheme

Figure 2 represents an AVC system using a measurement of the image of the disturbance and an inertial actuator for reducing the residual acceleration which has been used for real time experiments. The system is composed of three metal plates interconnected by springs. The one on top (M1) is equipped with an inertial actuator which generates the disturbance $s(t)$ (figure 1). Another inertial actuator is located below plate M3 and is used for disturbance rejection. Two accelerometers positioned as in figure 2 measure the image of the disturbance and the residual acceleration $\chi^0(t)$. The corresponding block diagrams in open loop operation and with the compensator system are shown in figures 1(a) and 1(b). The procedure for identifying the various models has been described in Landau et al. (2011a). Their frequency characteristics are shown in

figure 3. The model orders for the secondary path (solid line) and the reverse path (dotted line) have been estimated to be: $n_{B_G} = 17$, $n_{A_G} = 15$ and $n_{B_M} = 16$, $n_{A_M} = 16$ respectively. The primary path model has been used only for simulations.

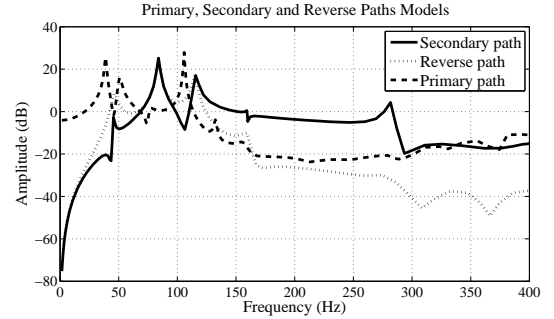


Figure 3: Frequency characteristics of the primary, secondary and reverse paths (identified models)

6. Experimental results

6.1. The central controllers

Two central controllers have been used to test this approach. The first (PP) has been designed using pole placement method. Its main objective is to stabilize the internal positive feedback loop. The end result was a controller of orders $n_{R_0} = 15$ and $n_{S_0} = 17$. The second controller is a reduced order H_∞ controller with $n_{R_0} = 19$ and $n_{S_0} = 20$ from Alma et al. (2011)⁵.

6.2. Experimental results - Broadband disturbance rejection

The broadband disturbance is a PRBS applied on the inertial actuator on top of the system. Its effect in the absence of the compensation system can be viewed in figures 4 and 5 (open loop power spectral density). Preliminary simulation studies

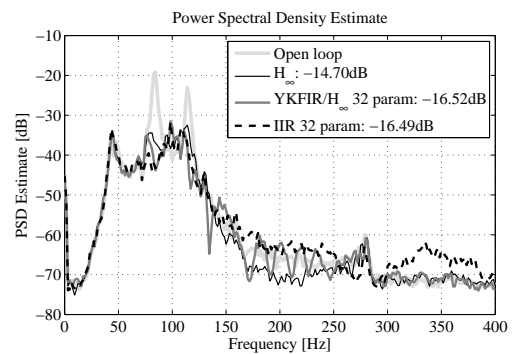


Figure 4: Experimental spectral densities of the residual acceleration (H_∞)

have confirmed the theoretical expectations that algorithm III gives better results than algorithm II. Subsequently only the algorithm III has been considered in the experiments. The power spectral densities obtained with the two central controllers without and with adaptation (32 parameters) are shown in figures 4

⁵The orders of the initial H_∞ controller were: $n_{R_{H_\infty}} = 70$ and $n_{S_{H_\infty}} = 70$

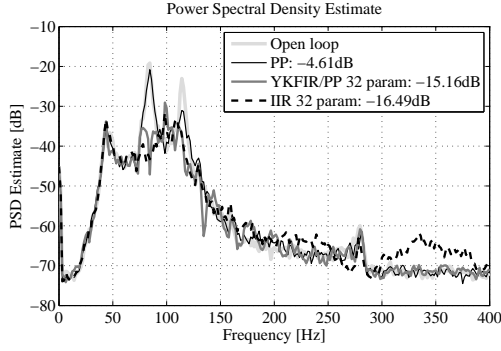


Figure 5: Experimental spectral densities of the residual acceleration (PP)

No. of param.	0	8	20	32	40
YK with H_∞	14.70 dB	16.24 dB	16.76 dB	16.52 dB	16.04 dB
YK with PP	4.61 dB	14.26 dB	14.49 dB	15.16 dB	15.56 dB
IIR	-	16.14 dB	16.23 dB	16.49 dB	16.89 dB

Table 2: Influence of the number of parameters upon the global attenuation (experimental).

and 5. On both figures, the spectral density obtained using the IIR adaptive filter (Landau et al., 2011a), with 32 parameters, is also shown for comparison. Table 2 summarizes the global attenuation results obtained with the two central controllers for various number of parameters of the Q polynomial. The last line give the results for the IIR adaptive feedforward filter used in Landau et al. (2011a). In the column "0", the attenuations obtained for each structure, in the absence of the adapted filters, are given. For the YK parametrization, this corresponds to the use of the fixed central controller. For the IIR filter, this corresponds to open loop operation. For YK parametrized feedforward compensator the performance depends upon the central controller. For a well designed central controller, the performances are close to those of the IIR adaptive compensator.

7. Conclusions

FIR Youla Kucera parametrized adaptive feedforward compensators and IIR adaptive feedforward compensators provide close performances. However from a practical point of view the YK adaptive feedforward compensator seems more interesting in terms of initialization, assignment of the inner closed loop poles and implementation of the filters required by the positive real condition for stability and convergence.

Appendix A. Proof of Lemma 1

Under the assumption 3 (perfect matching condition) the output of the primary path can be expressed as

$$x(t) = -G(q^{-1})y(t), \quad (\text{A.1})$$

where $y(t)$ is a dummy variable given by

$$y(t+1) = -S_0^*y(t) + R_0u(t+1) + Q[B_M^*y(t) - A_Mu(t+1)] \quad (\text{A.2})$$

with

$$u(t+1) = d(t+1) + \frac{B_M^*}{A_M}y(t). \quad (\text{A.3})$$

The output of the adaptive feedforward filter (for a fixed \hat{Q}) is given by (7), where one replaces $\hat{Q}(t+1, q^{-1})$ with $\hat{Q}(q^{-1})$. The output of the secondary path is

$$\hat{z}(t) = G(q^{-1})\hat{y}(t). \quad (\text{A.4})$$

Define the dummy error (for a fixed estimated set of parameters)

$$\varepsilon(t) = y(t) - \hat{y}(t) \quad (\text{A.5})$$

and the residual adaptation error becomes:

$$v(t) = -\chi(t) = -x(t) - \hat{z}(t) = G(q^{-1})\varepsilon(t). \quad (\text{A.6})$$

Equation (A.2) can be rewritten as

$$\begin{aligned} y(t+1) = & -S_0^*\hat{y}(t) + R_0\hat{u}(t+1) + Q[B_M^*\hat{y}(t) - A_M\hat{u}(t+1)] \\ & - S_0^*[y(t) - \hat{y}(t)] + R_0[u(t+1) - \hat{u}(t+1)] \\ & + Q[B_M^*(y(t) - \hat{y}(t)) - A_M(u(t+1) - \hat{u}(t+1))]. \end{aligned} \quad (\text{A.7})$$

Using (8) and (A.3) it results that

$$Q[B_M^*(y(t) - \hat{y}(t)) - A_M(u(t+1) - \hat{u}(t+1))] = 0 \quad (\text{A.8})$$

From equations (7) and (A.7) one obtains

$$\varepsilon(t+1) = -S_0^*\varepsilon(t) + \frac{R_0B_M^*}{A_M}\varepsilon(t) + (Q - \hat{Q})[B_M^*\hat{y}(t) - A_M\hat{u}(t+1)]. \quad (\text{A.9})$$

Passing the terms in $\varepsilon(t)$ on the left hand side and taking into account eqs. (16d) and (A.6), one gets:

$$v(t+1) = \frac{A_M(q^{-1})G(q^{-1})}{P_0(q^{-1})}(Q - \hat{Q})\alpha(t+1), \quad (\text{A.10})$$

Using eqs. (16a), (16b) and (16c), eq. (A.10) can be rewritten as eq. (15) which ends the proof.

References

- Alma, M., Martinez, J. J., Landau, I. D., & Buche, G. (2011). Design and tuning of reduced order h-infinity feedforward compensators for active vibration control. *Control Systems Technology, IEEE Transactions on, PP*, 1–8. DOI: 10.1109/TCST.2011.2119485.
- Anderson, B., Bitmead, R., Johnson, C., Kokotovic, P., Kosut, R., Mareels, I., Praly, L., & Riedle, B. (1986). *Stability of adaptive systems*. Cambridge Massachusetts, London, England: The M.I.T Press.
- Elliott, S., & Nelson, P. (1994). Active noise control. *Noise / News International*, (pp. 75–98).
- Hu, J., & Linn, J. (2000). Feedforward active noise controller design in ducts without independent noise source measurements. *Control Systems Technology, IEEE Transactions on*, 8, 443–455.
- Jacobson, C., Johnson, C., Cormick, D. M., & Sethares, W. (2001). Stability of active noise control algorithms. *IEEE Signal Processing letters*, 8, 74–76.
- Kuo, M., & Morgan, D. (1996). *Active noise control systems- Algorithms and DSP implementation*. New York,: Wiley.
- Landau, I., Alma, M., & Airimiñoaie, T. (2011a). Adaptive feedforward compensation algorithms for active vibration control with mechanical coupling. *Automatica*, 47, 2185 – 2196.
- Landau, I. D., Lozano, R., M'Saad, M., & Karimi, A. (2011b). *Adaptive control*. (2nd ed.). London: Springer.
- Ljung, L., & Söderström, T. (1983). *Theory and practice of recursive identification*. Cambridge Massachusetts, London, England: The M.I.T Press.
- Zeng, J., & de Callafon, R. (2006). Recursive filter estimation for feedforward noise cancellation with acoustic coupling. *Journal of sound and vibration*, 291, 1061–1079.

BIBLIOGRAPHY

- [Airimițoaie et al., 2011] Airimițoaie, T., Landau, I., Dugard, L., and Popescu, D. (2011). Identification of mechanical structures in the presence of narrow band disturbances - application to an active suspension. In *The 19th Mediterranean Conference on Control and Automation (MED)*, pages 904 – 909, Corfu, Greece.
- [Airimițoaie et al., 2009] Airimițoaie, T., Popescu, D., and Dimon, C. (2009). Advanced control and optimization for thermo-energetic installations. In *5th International Symposium on Applied Computational Intelligence and Informatics*, pages 83 – 88, Timișoara, România.
- [Alma, 2011] Alma, M. (2011). *Rejet adaptatif de perturbations en contrôle actif de vibrations*. PhD thesis, Université de Grenoble.
- [Alma et al., 2011] Alma, M., Landau, I., Martinez, J., and Airimițoaie, T. (2011). Hybrid adaptive feedforward-feedback compensation algorithms for active vibration control systems. 50th IEEE Conference on Decision and Control and European Control Conference.
- [Alma et al., 2012a] Alma, M., Landau, I. D., and Airimitoaie, T.-B. (2012a). Adaptive feedforward compensation algorithms for avc systems in the presence of a feedback controller. *Automatica*, 48(5):982 – 985.
- [Alma et al., 2012b] Alma, M., Martinez, J., Landau, I., and Buche, G. (2012b). Design and tuning of reduced order h-infinity feedforward compensators for active vibration control. *Control Systems Technology, IEEE Transactions on*, 20(2):554 – 561.
- [Amara et al., 1999a] Amara, F. B., Kabamba, P., and Ulsoy, A. (1999a). Adaptive sinusoidal disturbance rejection in linear discrete-time systems - Part I: Theory. *Journal of Dynamic Systems Measurement and Control*, 121:648–654.
- [Amara et al., 1999b] Amara, F. B., Kabamba, P., and Ulsoy, A. (1999b). Adaptive sinusoidal disturbance rejection in linear discrete-time systems - Part II: Experiments. *Journal of Dynamic Systems Measurement and Control*, 121:655–659.
- [Anderson, 1998] Anderson, B. (1998). From Youla-Kucera to identification, adaptive and nonlinear control. *Automatica*, 34:1485–1506.
- [Anderson et al., 1986] Anderson, B., Bitmead, R., Johnson, C., Kokotovic, P., Kosut, R., Mareels, I., Praly, L., and Riedle, B. (1986). *Stability of adaptive systems*. The M.I.T Press, Cambridge Massachusetts , London, England.
- [Åström and Murray, 2008] Åström, K. and Murray, R. (2008). *Feedback Systems: An Introduction for Scientists and Engineers*. Princeton University Press.

- [Bai and H.H.Lin, 1997] Bai, M. and H.H.Lin (1997). Comparison of active noise control structures in the presence of acoustical feedback by using the hinf synthesis technique. *J. of Sound and Vibration*, 206:453–471.
- [Bengtsson, 1977] Bengtsson, G. (1977). Output regulation and internal models—a frequency domain approach. *Automatica*, 13(4):333 – 345.
- [Beranek and Ver, 1992] Beranek, L. and Ver, I. (1992). *Noise and Vibration Control Engineering: Principles and Applications*. Wiley, New York.
- [Bierman, 1977] Bierman, G. (1977). *Factorization methods for discrete sequential estimation*. Academic Press, New York.
- [Billoud, 2001] Billoud, D. G. (2001). Ll-6508 active control at lord corporation – a reality by dr. guy billoud, lord corporation active control at lord corporation – a reality.
- [Bodson, 2005] Bodson, M. (2005). Rejection of periodic disturbances of unknown and time-varying frequency. *Int. J. of Adapt. Contr. and Sign. Proc.*, 19:67–88.
- [Bodson and Douglas, 1997] Bodson, M. and Douglas, S. (1997). Adaptive algorithms for the rejection of sinusoidal disturbances with unknown frequency. *Automatica*, 33:2213–2221.
- [Burges, 1981] Burges, J. (1981). Active adaptive sound control in a duct: A computer simulation. *J. Acoust. Soc. Am.*, 70:715–726.
- [Chen et al., 1992] Chen, B.-S., Yang, T.-Y., and Lin, B.-H. (1992). Adaptive notch filter by direct frequency estimation. *Signal Processing*, 27(2):161 – 176.
- [Chen and Tomizuka, 2012] Chen, X. and Tomizuka, M. (2012). A minimum parameter adaptive approach for rejecting multiple narrow-band disturbances with application to hard disk drives. *Control Systems Technology, IEEE Transactions on*, 20(2):408 –415.
- [Coanda, 1930] Coanda, H. (1930). Procédé de protection control le bruit. French Patent FR 722.274.
- [Crawford and Stewart, 1997] Crawford, D. and Stewart, R. (1997). Adaptive iir filtered-v algorithms for active noise control. *J. Acoust. Soc. Am.*, 101(4).
- [de Callafon and Kinney, 2010] de Callafon, R. A. and Kinney, C. E. (2010). Robust estimation and adaptive controller tuning for variance minimization in servo systems. *Journal of Advanced Mechanical Design, Systems, and Manufacturing*, 4(1):130–142.
- [Ding, 2003] Ding, Z. (2003). Global stabilization and disturbance suppression of a class of nonlinear systems with uncertain internal model. *Automatica*, 39(3):471 – 479.
- [Elliott, 2001] Elliott, S. (2001). *Signal processing for active control*. Academic Press.
- [Elliott and Nelson, 1993] Elliott, S. and Nelson, P. (1993). Active noise control. *Signal Processing Magazine, IEEE*, 10(4):12 –35.
- [Elliott and Nelson, 1994] Elliott, S. and Nelson, P. (1994). Active noise control. *Noise / News International*, pages 75–98.

- [Elliott and Sutton, 1996] Elliott, S. and Sutton, T. (1996). Performance of feedforward and feedback systems for active control. *Speech and Audio Processing, IEEE Transactions on*, 4(3):214–223.
- [Eriksson et al., 1987] Eriksson, L., Allie, M., and Greiner, R. (1987). The selection and application of an iir adaptive filter for use in active sound attenuation. *Acoustics, Speech and Signal Processing, IEEE Transactions on*, 35(4):433–437.
- [Esmailzadeh et al., 2002] Esmailzadeh, E., Alasty, A., and Ohadi, A. (2002). Hybrid active noise control of a one-dimensional acoustic duct. *Journal of vibration and acoustics*, 124(1):10–18.
- [Feintuch, 1976] Feintuch, P. (1976). An adaptive recursive lms filter. *Proceedings of the IEEE*, 64(11):1622–1624.
- [Ficocelli and Ben Amara, 2009] Ficocelli, M. and Ben Amara, F. (2009). Adaptive regulation of mimo linear systems against unknown sinusoidal exogenous inputs. *International Journal of Adaptive Control and Signal Processing*, 23(6):581–603.
- [Fleming et al., 2007] Fleming, A., Niederberger, D., Moheimani, S., and Morari, M. (2007). Control of resonant acoustic sound fields by electrical shunting of a loudspeaker. *Control Systems Technology, IEEE Transactions on*, 15(4):689–703.
- [Fraanje et al., 1999] Fraanje, R., Verhaegen, M., and Doelman, N. (1999). Convergence analysis of the filtered-u lms algorithm for active noise control in case perfect cancellation is not possible. *Signal Processing*, 73:255–266.
- [Francis and Wonham, 1976] Francis, B. and Wonham, W. (1976). The internal model principle of control theory. *Automatica*, 12(5):457–465.
- [Fuller et al., 1997] Fuller, C., Elliott, S., and Nelson, P. (1997). *Active Control of Vibration*. Academic Press, New York.
- [Fuller and von Flotow, 1995] Fuller, C. and von Flotow, A. (1995). Active control of sound and vibration. *Control Systems, IEEE*, 15(6):9–19.
- [Goodwin and Sin, 1984] Goodwin, G. and Sin, K. (1984). *Adaptive Filtering Prediction and Control*. Prentice Hall, N. J.
- [Gouraud et al., 1997] Gouraud, T., Guglielmi, M., and Auger, F. (1997). Design of robust and frequency adaptive controllers for harmonic disturbance rejection in a single-phase power network. *Proceedings of the European Control Conference, Bruxelles*.
- [Guicking, 2007] Guicking, D. (2007). Active control of sound and vibration history – fundamentals – state of the art. Festschrift DPI, 1–32, Herausgeber (ed.), Universitätsverlag Göttingen 2007.
- [Heuberger et al., 1995] Heuberger, P., Van den Hof, P., and Bosgra, O. (1995). A generalized orthonormal basis for linear dynamical systems. *Automatic Control, IEEE Transactions on*, 40(3):451–465.

- [Hillerstrom and Sternby, 1994] Hillerstrom, G. and Sternby, J. (1994). Rejection of periodic disturbances with unknown period - a frequency domain approach. *Proceedings of American Control Conference, Baltimore*, pages 1626–1631.
- [Hong and Bernstein, 1998] Hong, J. and Bernstein, D. (1998). Bode integral constraints, collocation, and spillover in active noise and vibration control. *Control Systems Technology, IEEE Transactions on*, 6(1):111–120.
- [Huang and Messner, 1998] Huang, Y. and Messner, W. (1998). A novel disturbance observer design for magnetic hard drive servo system with a rotary actuator. *Magnetics, IEEE Transactions on*, 34(4):1892–1894.
- [Jacobson et al., 2001] Jacobson, C., Johnson, C.R., J., McCormick, D., and Sethares, W. (2001). Stability of active noise control algorithms. *Signal Processing Letters, IEEE*, 8(3):74–76.
- [Johnson, 1976] Johnson, C. (1976). Theory of disturbance-accomodating controllers. In *Control and Dynamical Systems* (C. T. Leondes, Ed.). Vol. 12, pp. 387-489.
- [Johnson, 1979] Johnson, C., J. (1979). A convergence proof for a hyperstable adaptive recursive filter (corresp.). *Information Theory, IEEE Transactions on*, 25(6):745–749.
- [Kuo and Morgan, 1999] Kuo, S. and Morgan, D. (1999). Active noise control: a tutorial review. *Proceedings of the IEEE*, 87(6):943–973.
- [Landau, 1976] Landau, I. (1976). Unbiased recursive identification using model reference adaptive techniques. *Automatic Control, IEEE Transactions on*, 21(2):194–202.
- [Landau, 1979] Landau, I. (1979). *Adaptive control — the model reference approach*. Marcel Dekker, New York.
- [Landau, 1980] Landau, I. (1980). An extension of a stability theorem applicable to adaptive control. *Automatic Control, IEEE Transactions on*, 25(4):814–817.
- [Landau et al., 2011a] Landau, I., Airimițoaie, T., and Alma, M. (2011a). Comparison of two approaches for adaptive feedforward compensation in active vibration control with mechanical coupling. In *The 19th Mediterranean Conference on Control and Automation (MED)*, pages 207–212, Corfu, Greece.
- [Landau et al., 2011b] Landau, I., Airimițoaie, T., and Alma, M. (2011b). An iir youla-kučera parametrized adaptive feedforward compensator for active vibration control with mechanical coupling. In *Proceedings of the 50th IEEE Conference on Decision and Control, Atlanta, USA*.
- [Landau et al., 2011c] Landau, I., Airimițoaie, T., and Alma, M. (2011c). A youla-kučera parametrized adaptive feedforward compensator for active vibration control. In *Proceedings of the 18th IFAC World Congress, Milano, Italy*.
- [Landau et al., 2012a] Landau, I., Airimițoaie, T., and Alma, M. (2012a). Iir youla-kučera parametrized adaptive feedforward compensators for active vibration control with mechanical coupling. *Control Systems Technology, IEEE Transactions on*. accepted for publication.

- [Landau et al., 2012b] Landau, I., Airimițoiaie, T., and Alma, M. (2012b). A youla-kučera parametrized adaptive feedforward compensator for active vibration control with mechanical coupling. *Automatica*. accepted for publication.
- [Landau et al., 2011d] Landau, I., Alma, M., and Airimițoiaie, T. (2011d). Adaptive feedforward compensation algorithms for active vibration control with mechanical coupling. *Automatica*, 47(10):2185 – 2196.
- [Landau et al., 2011e] Landau, I., Alma, M., Martinez, J., and Buche, G. (2011e). Adaptive suppression of multiple time-varying unknown vibrations using an inertial actuator. *Control Systems Technology, IEEE Transactions on*, 19(6):1327 –1338.
- [Landau et al., 2001a] Landau, I., Constantinescu, A., Loubat, P., Rey, D., and Franco, A. (2001a). A methodology for the design of feedback active vibration control systems. In *Proceedings of the European Control Conference, Porto, Portugal*, pages 1571–1576.
- [Landau et al., 2005] Landau, I., Constantinescu, A., and Rey, D. (2005). Adaptive narrow band disturbance rejection applied to an active suspension - an internal model principle approach. *Automatica*, 41(4):563–574.
- [Landau and Karimi, 1997] Landau, I. and Karimi, A. (1997). Recursive algorithms for identification in closed loop. a unified approach and evaluation. *Automatica*, 33(8):1499–1523.
- [Landau et al., 2001b] Landau, I., Karimi, A., and Constantinescu, A. (2001b). Direct controller order reduction by identification in closed loop. *Automatica*, 37:1689–1702.
- [Landau and Silveira, 1979] Landau, I. and Silveira, H. (1979). A stability theorem with applications to adaptive control. *Automatic Control, IEEE Transactions on*, 24(2):305 – 312.
- [Landau and Zito, 2005] Landau, I. and Zito, G. (2005). *Digital Control Systems - Design, Identification and Implementation*. Springer, London.
- [Landau et al., 2011f] Landau, I. D., Alma, M., Constantinescu, A., Martinez, J. J., and Noë, M. (2011f). Adaptive regulation—rejection of unknown multiple narrow band disturbances (a review on algorithms and applications). *Control Engineering Practice*, 19(10):1168 – 1181.
- [Landau et al., 2011g] Landau, I. D., Lozano, R., M’Saad, M., and Karimi, A. (2011g). *Adaptive control*. Springer, London, 2nd edition.
- [Larimore et al., 1980] Larimore, M., Treichler, J., and Johnson, C., J. (1980). Sharf: An algorithm for adapting iir digital filters. *Acoustics, Speech and Signal Processing, IEEE Transactions on*, 28(4):428 – 440.
- [Li, 1997] Li, G. (1997). A stable and efficient adaptive notch filter for direct frequency estimation. *Signal Processing, IEEE Transactions on*, 45(8):2001 –2009.
- [Ljung, 1977a] Ljung, L. (1977a). Analysis of recursive stochastic algorithms. *Automatic Control, IEEE Transactions on*, 22(4):551 – 575.

- [Ljung, 1977b] Ljung, L. (1977b). On positive real transfer functions and the convergence of some recursive schemes. *IEEE Trans. on Automatic Control*, AC-22:539–551.
- [Ljung and Söderström, 1983] Ljung, L. and Söderström, T. (1983). *Theory and practice of recursive identification*. The M.I.T Press, Cambridge Massachusetts, London, England.
- [Lueg, 1934] Lueg, P. (1934). Process of silencing sound oscillations. US Patent 2,043,416.
- [Marcos, 2000] Marcos, T. (2000). The straight attraction. *Motion control*, 13:29–33.
- [Marino et al., 2003] Marino, R., Santosuosso, G., and Tomei, P. (2003). Robust adaptive compensation of biased sinusoidal disturbances with unknown frequency. *Automatica*, 39:1755–1761.
- [Marino and Tomei, 2007] Marino, R. and Tomei, P. (2007). Output regulation for linear minimum phase systems with unknown order exosystem. *Automatic Control, IEEE Transactions on*, 52(10):2000–2005.
- [Montazeri and Poshtan, 2010] Montazeri, A. and Poshtan, J. (2010). A computationally efficient adaptive iir solution to active noise and vibration control systems. *IEEE Trans. on Automatic Control*, AC-55:2671 – 2676.
- [Montazeri and Poshtan, 2011] Montazeri, A. and Poshtan, J. (2011). A new adaptive recursive rls-based fast-array iir filter for active noise and vibration control systems. *Signal Processing*, 91(1):98 – 113.
- [Mosquera et al., 1999] Mosquera, C., Gomez, J., Perez, F., and Sobreira, M. (1999). Adaptive iir filters for active noise control. In *Sound and Vibration, Sixth International Congress on ICSV '99.*, pages 1571 – 1582.
- [M'Sirdi et al., 1988] M'Sirdi, N., Tjokronegoro, H., and Landau, I. (1988). An rml algorithm for retrieval of sinusoids with cascaded notch filters. In *Acoustics, Speech, and Signal Processing, 1988. ICASSP-88., 1988 International Conference on*, pages 2484–2487 vol.4.
- [Nakao et al., 1987] Nakao, M., Ohnishi, K., and Miyachi, K. (1987). A robust decentralized joint control based on interference estimation. In *Robotics and Automation. Proceedings. 1987 IEEE International Conference on*, volume 4, pages 326 – 331.
- [Nehorai, 1985] Nehorai, A. (1985). A minimal parameter adaptive notch filter with constrained poles and zeros. *IEEE Trans. Acoust., Speech, Signal Processing*, ASSP-33:983–996.
- [Nelson and Elliott, 1993] Nelson, P. and Elliott, S. (1993). *Active Control of Sound*. Academic Press.
- [Olson and May, 1953] Olson, H. F. and May, E. G. (1953). Electronic sound absorber. *The Journal of the Acoustical Society of America*, 25(6):1130–1136.
- [Popov, 1960] Popov, V. (1960). Criterii de stabilitate pentru sistemele automate conținând elemente neunivoce, probleme de automatizare. *Publishing House of the Romanian Academy*, pages 143–151.

- [Popov, 1963] Popov, V. (1963). Solution of a new stability problem for controlled systems. *Automatic Remote Control*, 24(1):1–23.
- [Popov, 1966] Popov, V. (1966). *Hiperstabilitatea Sistemelor Automate*. Editura Academiei Republicii Socialiste România.
- [Popov, 1973] Popov, V. (1973). *Hyperstability of Control Systems*. Springer-Verlag, trans. edition.
- [Procházka and Landau, 2003] Procházka, H. and Landau, I. D. (2003). Pole placement with sensitivity function shaping using 2nd order digital notch filters. *Automatica*, 39(6):1103 – 1107.
- [Rao and Kung, 1984] Rao, D. and Kung, S.-Y. (1984). Adaptive notch filtering for the retrieval of sinusoids in noise. *Acoustics, Speech and Signal Processing, IEEE Transactions on*, 32(4):791 – 802.
- [Ray et al., 2006] Ray, L., Solbeck, J., Streeter, A., and Collier, R. (2006). Hybrid feedforward-feedback active noise reduction for hearing protection and communication. *The Journal of the Acoustical Society of America*, 120(4):2026–2036.
- [Rotunno and de Callafon, 2003] Rotunno, M. and de Callafon, R. (2003). Design of model-based feedforward compensators for vibration compensation in a flexible structure. Internal report, Dept. of Mechanical and Aerospace Engineering. University of California, San Diego.
- [Serrani, 2006] Serrani, A. (2006). Rejection of harmonic disturbances at the controller input via hybrid adaptive external models. *Automatica*, 42(11):1977 – 1985.
- [Snyder, 1994] Snyder, S. (1994). Active control using iir filters—a second look. In *Acoustics, Speech, and Signal Processing, 1994. ICASSP-94., 1994 IEEE International Conference on*, volume ii, pages II/241 –II/244 vol.2.
- [Snyder, 2000] Snyder, S. D. (2000). *Active Noise Control Primer*. Springer Verlag.
- [Stoica and Nehorai, 1988] Stoica, P. and Nehorai, A. (1988). Performance analysis of an adaptive notch filter with constrained poles and zeros. *IEEE Trans. Acoust., Speech, Signal Processing*, 36(6):911 – 919.
- [Sun and Chen, 2002] Sun, X. and Chen, D.-S. (2002). A new infinite impulse response filter-based adaptive algorithm for active noise control. *Journal of Sound and Vibration*, 258(2):385 – 397.
- [Sun and Meng, 2004] Sun, X. and Meng, G. (2004). Steiglitz–mcbride type adaptive iir algorithm for active noise control. *Journal of Sound and Vibration*, 273(1-2):441 – 450.
- [Tay et al., 1997] Tay, T. T., Mareels, I. M. Y., and Moore, J. B. (1997). *High Performance Control*. Birkhäuser Boston.
- [Tichavský and Nehorai, 1997] Tichavský, P. and Nehorai, A. (1997). Comparative study of four adaptive frequency trackers. *Automatic Control, IEEE Transactions on*, 45(6):1473 – 1484.

- [Tomizuka, 1982] Tomizuka, M. (1982). Parallel mras without compensation block. *Automatic Control, IEEE Transactions on*, 27(2):505 – 506.
- [Treichler et al., 1978] Treichler, J., Larimore, M., and Johnson, C., J. (1978). Simple adaptive iir filtering. In *Acoustics, Speech, and Signal Processing, IEEE International Conference on ICASSP '78.*, volume 3, pages 118 – 122.
- [Tsyppkin, 1997] Tsyppkin, Y. (1997). Stochastic discrete systems with internal models. *Journal of Automation and Information Sciences*, 29(4&5):156–161.
- [Valentinotti, 2001] Valentinotti, S. (2001). *Adaptive Rejection of Unstable Disturbances: Application to a Fed-Batch Fermentation*. Thèse de doctorat, École Polytechnique Fédérale de Lausanne.
- [Valentinotti et al., 2003] Valentinotti, S., Srinivasan, B., Holmberg, U., Bonvin, D., Cannizzaro, C., Rhiel, M., and von Stockar, U. (2003). Optimal operation of fed-batch fermentations via adaptive control of overflow metabolite. *Control Engineering Practice*, 11(6):665 – 674.
- [Wang and Ren, 2003] Wang, A. and Ren, W. (2003). Convergence analysis of the filtered-u algorithm for active noise control. *Signal Processing*, 83:1239–1254.
- [Widrow, 1971] Widrow, B. (1971). Adaptive filters. In Kalman, R. and DeClaris, H., editors, *Aspects of Network and System Theory*. Holt, Rinehart and Winston.
- [Widrow et al., 1975] Widrow, B., Glover, J.R., J., McCool, J., Kaunitz, J., Williams, C., Hearn, R., Zeidler, J., Eugene Dong, J., and Goodlin, R. (1975). Adaptive noise cancelling: Principles and applications. *Proceedings of the IEEE*, 63(12):1692 – 1716.
- [Widrow et al., 1981] Widrow, B., Shur, D., and Shaffer, S. (1981). On adaptive inverse control. In *Proc. 15th Asilomar Conf. Circuits, Systems and Computers*, Pacific Grove, CA, USA.
- [Zeng and de Callafon, 2006] Zeng, J. and de Callafon, R. (2006). Recursive filter estimation for feedforward noise cancellation with acoustic coupling. *Journal of Sound and Vibration*, 291(3-5):1061 – 1079.
- [Zhou et al., 1996] Zhou, K., Doyle, J. C., and Glover, K. (1996). *Robust and optimal control*. Prentice Hall, Upper Saddle River, New Jersey.